IMMUNOMODULATORY FUNCTIONS OF FIBROBLAST-LIKE SYNOVIOCYTES IN JOINT INFLAMMATION AND DESTRUCTION DURING RHEUMATOID ARTHRITIS

EDITED BY: Hanshi Xu, David Fox and Song Guo Zheng
PUBLISHED IN: Frontiers in Immunology

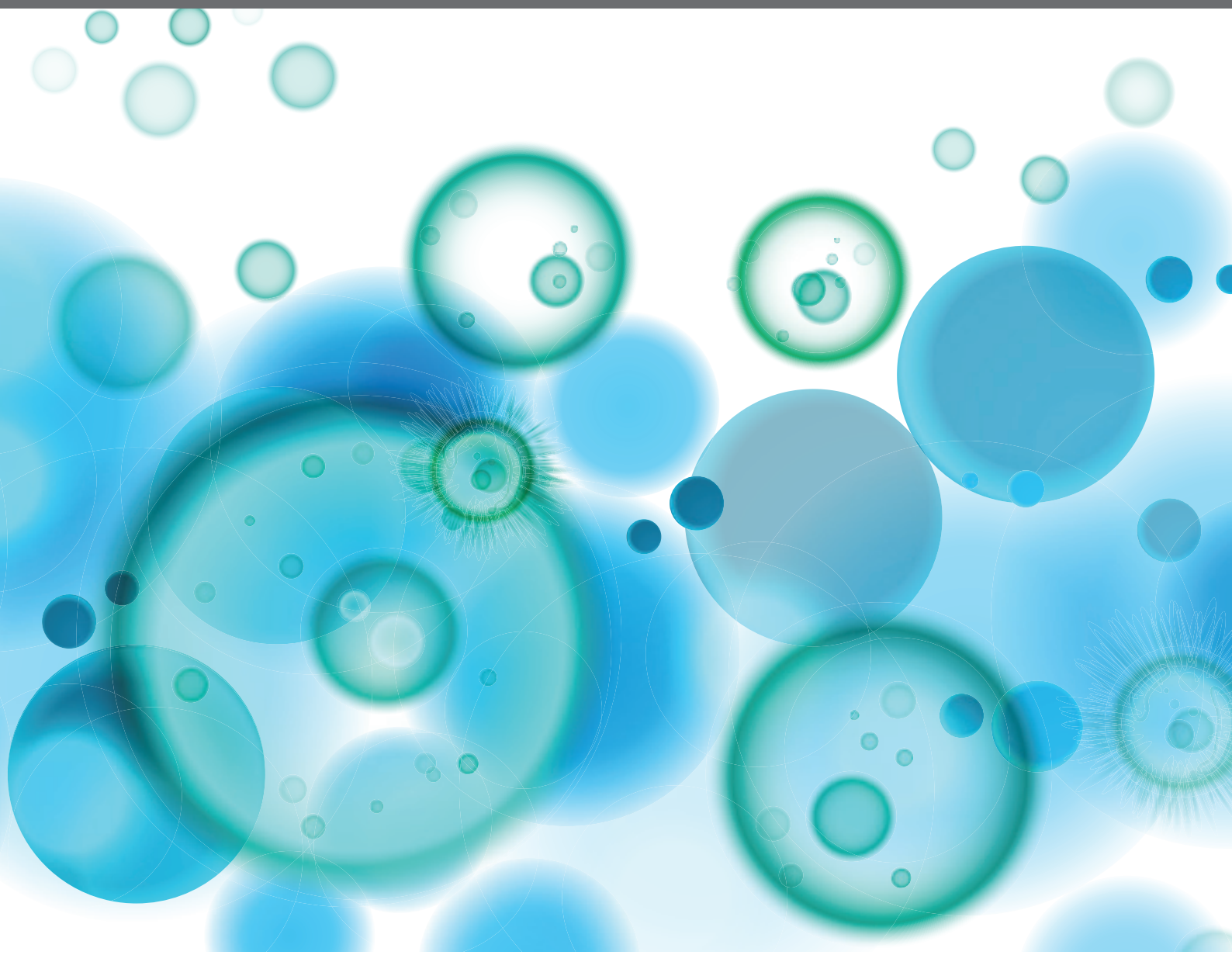

frontiers Research Topics

frontiers

ISSN 1664-8714
ISBN 978-2-88963-823-9
DOI 10.3389/978-2-88963-823-9

About Frontiers

Frontiers is more than just an open-access publisher of scholarly articles: it is a pioneering approach to the world of academia, radically improving the way scholarly research is managed. The grand vision of Frontiers is a world where all people have an equal opportunity to seek, share and generate knowledge. Frontiers provides immediate and permanent online open access to all its publications, but this alone is not enough to realize our grand goals.

Frontiers Journal Series

The Frontiers Journal Series is a multi-tier and interdisciplinary set of open-access, online journals, promising a paradigm shift from the current review, selection and dissemination processes in academic publishing. All Frontiers journals are driven by researchers for researchers; therefore, they constitute a service to the scholarly community. At the same time, the Frontiers Journal Series operates on a revolutionary invention, the tiered publishing system, initially addressing specific communities of scholars, and gradually climbing up to broader public understanding, thus serving the interests of the lay society, too.

Dedication to Quality

Each Frontiers article is a landmark of the highest quality, thanks to genuinely collaborative interactions between authors and review editors, who include some of the world's best academicians. Research must be certified by peers before entering a stream of knowledge that may eventually reach the public - and shape society; therefore, Frontiers only applies the most rigorous and unbiased reviews.
Frontiers revolutionizes research publishing by freely delivering the most outstanding research, evaluated with no bias from both the academic and social point of view. By applying the most advanced information technologies, Frontiers is catapulting scholarly publishing into a new generation.

What are Frontiers Research Topics?

Frontiers Research Topics are very popular trademarks of the Frontiers Journals Series: they are collections of at least ten articles, all centered on a particular subject. With their unique mix of varied contributions from Original Research to Review Articles, Frontiers Research Topics unify the most influential researchers, the latest key findings and historical advances in a hot research area! Find out more on how to host your own Frontiers Research Topic or contribute to one as an author by contacting the Frontiers Editorial Office: researchtopics@frontiersin.org

IMMUNOMODULATORY FUNCTIONS OF FIBROBLAST-LIKE SYNOVIOCYTES IN JOINT INFLAMMATION AND DESTRUCTION DURING RHEUMATOID ARTHRITIS

Topic Editors:
Hanshi Xu, First Affiliated Hospital of Sun Yat-Sen University, China
David Fox, University of Michigan, United States
Song Guo Zheng, The Ohio State University, United States

Citation: Xu, H., Fox, D., Zheng, S. G., eds. (2020). Immunomodulatory Functions of Fibroblast-like Synoviocytes in Joint Inflammation and Destruction During Rheumatoid Arthritis. Lausanne: Frontiers Media SA.
doi: 10.3389/978-2-88963-823-9

Table of Contents

frontiers in Immunology

EDITORIAL
published: 20 May 2020
doi: 10.3389/fimmu.2020.00955

Editorial: Immunomodulatory Functions of Fibroblast-like Synoviocytes in Joint Inflammation and Destruction during Rheumatoid Arthritis

Hanshi Xu[1]*, *Song Guo Zheng*[2]* and *David Fox*[3]*

[1] Department of Rheumatology and Immunology, The First Affiliated Hospital, Sun Yat-sen University, Guangzhou, China, [2] Department of Internal Medicine, The Ohio State University Wexner Medical Center and College of Medicine, Columbus, OH, United States, [3] Division of Rheumatology, Clinical Autoimmunity Center of Excellence, University of Michigan Medical School, Ann Arbor, MI, United States

Keywords: rheumatoid arthritis, synoviocyte, inflammation, aggressor, immunomodulatory functions

OPEN ACCESS

Edited by:
Carlo Riccardi,
University of Perugia, Italy

Reviewed by:
Guenter Steiner,
Medical University of Vienna, Austria
Erika H. Noss,
University of Washington, United States

***Correspondence:**
Hanshi Xu
xuhanshi@mail.sysu.edu.cn
Song Guo Zheng
SongGuo.Zheng@osumc.edu
David Fox
dfox@med.umich.edu

Specialty section:
This article was submitted to Autoimmune and Autoinflammatory Disorders, a section of the journal Frontiers in Immunology

Received: *28 March 2020*
Accepted: *23 April 2020*
Published: *20 May 2020*

Citation:
Xu H, Zheng SG and Fox D (2020) Editorial: Immunomodulatory Functions of Fibroblast-like Synoviocytes in Joint Inflammation and Destruction during Rheumatoid Arthritis. Front. Immunol. 11:955. doi: 10.3389/fimmu.2020.00955

Editorial on the Research Topic

Immunomodulatory Functions of Fibroblast-like Synoviocytes in Joint Inflammation and Destruction during Rheumatoid Arthritis

Rheumatoid Arthritis (RA) is a common rheumatic disorder characterized by persistent synovial inflammation and destruction of joints. Fibroblast-like synoviocytes (FLSs) exhibit critical immunomodulatory functions through secretion of inflammatory cytokines and through direct interactions with several synovial-infiltrated immune cell types (1, 2). RA FLSs also display surprisingly aggressive behavior (3), metabolic changes (4, 5), and epigenetic alterations (6, 7). More interestingly, recent studies have identified and described the biological functions of distinct subclasses of RA FLSs, for instance, $FAP\alpha^{+}THY1^{-}$ fibroblasts are responsible for bone and cartilage damage, whereas $FAP\alpha^{+}$ $THY1^{+}$ fibroblasts mediate synovial inflammation (8). Another study indicates that $THY1^{+}HLA\text{-}DRA^{hi}$ fibroblasts contribute to IL-6 expression (9). Increasing evidence suggests that targeting activated FLS may be a novel therapeutic strategy for attenuating RA joint damage (3). This Research Topic brings together original and review articles that explore the immunomodulatory functions of FLS in joint inflammation and destruction in RA.

Bergström et al. conducted a detailed study showing that the autoimmune regulator gene *AIRE* is a cytokine-induced RA risk gene in RA FLS. AIRE is expressed by activated FLS in synovial tissue from RA patients. AIRE does not induce tissue restricted antigens (TRAs) in RA FLS, but augments tumor necrosis factor and interleukin-1β-induced pro-inflammatory response by promoting the transcription of a set of genes associated with systemic autoimmune disease and annotated as interferon-γ regulated genes. These data provide a novel pathological mechanism for association of AIRE with RA.

Yan et al. determined the role of long non-coding RNAs (lncRNAs) HIX003209 in pathogenesis of RA. HIX003209 expression is significantly increased in the peripheral blood mononuclear cells (PBMCs) from RA patients, and is involved in TLR4-mediated inflammation via targeting miR-6089 and thereby releasing regulation of the TLR4/NF-kB pathway in macrophages. Understanding the role of lncRNAs in RA pathogenesis may help to develop innovative therapeutic approaches in the future.

Two groups explored the effects of compounds from phytomedicine on joint damage in RA animal models through their regulation of RA FLS behavior. Wu et al. demonstrated that treatment with Kirenol, a diterpenoid extracted from the Chinese herbal medicine *Siegesbeckiae*, inhibited the migration, invasion, and IL-6 secretion of RA FLS *in vitro*, and improved synovial hyperplasia and cartilage erosion in a collagen-induced arthritis (CIA) mouse model *in vivo*. Du et al. presented that treatment with 3 3-Diindolylmethane (DIM), a main product of the acid-catalyzed oligomerization of indole-3-carbinol from cruciferous vegetables, not only suppressed proliferation, invasion, and inflammatory response of RA-FLS by inhibiting activation of p38, JNK/MAPK, and AKT/mTOR pathways, but also attenuated severity of knee arthritis in f AIA mice. In addition, a cannabinoid receptor 2 (CB2) selective agonist JWH-015 exhibited anti-inflammatory action in human RA FLS by utilizing glucocorticoid receptors. JWH-015 administration inhibited bone destruction in the rat AIA model of RA. These findings may provide an opportunity to develop molecules of similar structure as non-opioid analgesic and bone protective agents in RA.

Diller et al. showed that JAK inhibitors, including tofacitinib, baricitinib, filgotinib, and peficitinib, suppressed the inflammatory responses induced by oncostatin M and by trans-signaling of IL-6 in RA FLS. Indeed, IL-6 and TNF-α play an important role in the pathogenesis of RA (10). Interestingly, only peficitinib reduced the IL-1β-induced inflammatory response and proliferation of RA FLS *in vitro* at concentrations close to reported Cmax values of well-tolerated doses *in vivo*. Peficitinib also significantly inhibited RA FLS migration. This study indicates a possible advantage of peficitinib through targeting of RA FLS, which could result in higher response rates *in vivo* compared to other JAKi.

Finally, the review by de Oliveira et al. discussed glucose metabolism of fibroblast-like synoviocytes as a potential therapeutic target in RA. Key rate-limiting glycolytic enzymes, including hexokinase 2 (HK2) and 6-phosphofructo-2-kinase/fructose-2, 6-biphosphatase (PFKFB) enzymes, play important roles in regulating inflammation and aggressive behavior of RA FLS. Glycolytic inhibitors can inhibit FLS aggressive behavior *in vitro* and attenuate bone and cartilage damage in murine models of RA. Therefore, agents that interfere with certain critical steps of glycolysis may be novel therapeutics, independent of systemic immunosuppression, and suitable for combination therapy in RA.

The articles included in this Research Topic illustrate the complex immunomodulatory functions of FLS in the pathogenesis of RA, and envisage development of potential therapeutic agents for RA by targeting RA FLS. We believe that more detailed understanding of the mechanisms that underlie immunomodulatory functions of FLS will provide novel targets for RA treatment.

AUTHOR CONTRIBUTIONS

All authors listed have made a substantial, direct and intellectual contribution to the work, and approved it for publication.

REFERENCES

1. Bi X, Guo XH, Mo BY, Wang ML, Luo XQ, Chen YX, et al. LncRNA PICSAR promotes cell proliferation, migration and invasion of fibroblast-like synoviocytes by sponging miRNA-4701-5p in rheumatoid arthritis. *EBiomedicine.* (2019) 50:408–20. doi: 10.1016/j.ebiom.2019.11.024
2. Liu Y, Pan YF, Xue YQ, Fang LK, Guo XH, Guo X, et al. uPAR promotes tumor-like biologic behaviors of fibroblast-like synoviocytes through PI3K/Akt signaling pathway in patients with rheumatoid arthritis. *Cell Mol Immunol.* (2018) 15:171–81. doi: 10.1038/cmi.2016.60
3. Bottini N, Firestein GS. Duality of fibroblast-like synoviocytes in RA: passive responders and imprinted aggressors. *Nat Rev Rheumatol.* (2013) 9:24–33. doi: 10.1038/nrrheum.2012.190
4. McGarry T, Fearon U. Cell metabolism as a potentially targetable pathway in RA. *Nat Rev Rheumatol.* (2019) 15:70–2. doi: 10.1038/s41584-018-0148-8
5. Zou Y, Zeng S, Huang M, Qiu Q, Xiao Y, Shi M, et al. Inhibition of 6-phosphofructo-2-kinase suppresses fibroblast-like synoviocytes-mediated synovial inflammation and joint destruction in rheumatoid arthritis. *Br J Pharmacol.* (2017) 174:893–908. doi: 10.1111/bph.13762
6. Zou Y, Xu S, Xiao Y, Qiu Q, Shi M, Wang J, et al. Long noncoding RNA LERFS negatively regulates rheumatoid synovial aggression and proliferation. *J Clin Invest.* (2018) 128:4510–24. doi: 10.1172/JCI97965
7. Mo BY, Guo XH, Yang MR, Liu F, Bi X, Liu Y, et al. Long non-coding RNA GAPLINC promotes tumor-like biologic behaviors of fibroblast-like synoviocytes as MicroRNA sponging in rheumatoid arthritis patients. *Front Immunol.* (2018) 9:702. doi: 10.3389/fimmu.2018.00702
8. Croft AP, Campos J, Jansen K, Turner JD, Marshall J, Attar M, et al. Distinct fibroblast subsets drive inflammation and damage in arthritis *Nature*. (2019) 570:246–51. doi: 10.1038/s41586-019-1263-7
9. Zhang F, Wei K, Slowikowski K, Fonseka CY, Rao DA, Kelly S, et al. Defining inflammatory cell states in rheumatoid arthritis joint synovial tissues by integrating single-cell transcriptomics and mass cytometry. *Nat Immunol.* (2019) 20:928–42. doi: 10.1038/s41590-019-0378-1
10. Luo Y, Zheng SG. Hall of fame among pro-inflammatory cytokines: interleukin-6 gene and its transcriptional regulation mechanisms. *Front Immunol.* (2016) 7:604. doi: 10.3389/fimmu.2016.00604

Conflict of Interest: The authors declare that the research was conducted in the absence of any commercial or financial relationships that could be construed as a potential conflict of interest.

frontiers in Immunology

ORIGINAL RESEARCH
published: 26 March 2019
doi: 10.3389/fimmu.2019.00541

Targeting Activated Synovial Fibroblasts in Rheumatoid Arthritis by Peficitinib

*Magnus Diller[1], Rebecca Hasseli[1], Marie-Lisa Hülser[1], Iris Aykara[1], Klaus Frommer[1], Stefan Rehart[2], Ulf Müller-Ladner[1] and Elena Neumann[1]**

[1] Department of Rheumatology and Clinical Immunology, Campus Kerckhoff, Justus-Liebig-University Giessen, Giessen, Germany, [2] Department of Orthopedics and Trauma Surgery, Agaplesion Markus Hospital, Frankfurt, Germany

Background: Synovial fibroblasts (SF) play a major role in the pathogenesis of rheumatoid arthritis (RA) and develop an aggressive phenotype destroying cartilage and bone, thus termed RASF. JAK inhibitors have shown to be an efficient therapeutic option in RA treatment, but less is known about the effect of JAK inhibitors on activated RASF. The aim of the study was to examine the effects of JAK inhibitors on activated RASF.

Methods: Synovium of RA patients was obtained during knee replacement surgeries. Synoviocytes were isolated and pretreated with JAK inhibitors. Pro-inflammatory cytokines and matrix degrading proteinases were measured by ELISA in supernatant after stimulation with oncostatin M or IL-1β. The proliferation of RASF was measured by BrdU incorporation. Cell culture inserts were used to evaluate cell migration. For adhesion assays, RASF were seeded in culture plates. Then, plates were extensively shaken and adherent RASF quantified. Cell viability, cytotoxicity and apoptosis were measured using the ApoTox-Glo^{TM} Triplex and the CellTox^{TM} Green Cytotoxicity Assay.

Results: Tofacitinib and baricitinib decreased the IL-6 release of RASF stimulated with oncostatin M. JAK inhibition attenuated the IL-6 release of IL-1β activated and with soluble IL-6 receptor treated RASF. In contrast, only peficitinib and filgotinib decreased the IL-6 release of RASF activated with IL-1β. Peficitinib decreased also the MMP-3, CXCL8, and CXCL1 release at 5 μM. Moreover, peficitinib was the only JAK inhibitor suppressing proliferation of activated RASF at 1 μM. Peficitinib further decreased the migration of RASF without being cytotoxic or pro-apoptotic and without altering cell adhesion.

Conclusions: JAK inhibitors effectively suppress the inflammatory response induced by oncostatin M and by transsignaling of IL-6 in RASF. Only peficitinib modulated the IL-1β-induced response of RASF and their proliferation *in vitro* at concentrations close to reported Cmax values of well tolerated doses *in vivo*. In contrast to filgotinib, peficitinib also highly suppressed RASF migration showing the potential of peficitinib to target RASF.

Keywords: JAK inhibition, peficitinib, synovial fibroblast, rheumatoid arthritis, IL-1β

OPEN ACCESS

Edited by:
David Fox,
University of Michigan, United States

Reviewed by:
Pei-Suen Eliza Tsou,
University of Michigan, United States
Donghai Wang,
Duke University, United States

****Correspondence:***
Elena Neumann
e.neumann@kerckhoff-klinik.de

Specialty section:
This article was submitted to Autoimmune and Autoinflammatory Disorders, a section of the journal Frontiers in Immunology

Received: *05 December 2018*
Accepted: *27 February 2019*
Published: *26 March 2019*

Citation:
Diller M, Hasseli R, Hülser M-L, Aykara I, Frommer K, Rehart S, Müller-Ladner U and Neumann E (2019) Targeting Activated Synovial Fibroblasts in Rheumatoid Arthritis by Peficitinib. Front. Immunol. 10:541. doi: 10.3389/fimmu.2019.00541

INTRODUCTION

Rheumatoid arthritis (RA) is the most frequent disease among the inflammatory rheumatic diseases and affects approximately 0.41 to 0.54% of the adult population in the US (1). Currently, the pharmacological treatment options include conventional synthetic (cs), biological (b), and targeted synthetic (ts) DMARDs (disease-modifying antirheumatic drugs) (2). In 2012, tofacitinib was the first FDA approved Janus kinase inhibitor (JAKi) and the first tsDMARD for treatment of rheumatoid arthritis (RA) in the US. The approval of baricitinib followed in 2018. In the EU, baricitinib and tofacitinib were both approved for treatment of RA in 2017. In the past years, additional JAKi were developed. They differ mainly in the inhibition profile of the four isoforms JAK1, JAK2, JAK3, and TYK2. Filgotinib, inhibiting mainly JAK1/2 and the panJAKi peficitinib are currently examined in clinical trials. Both of the latter inhibitors are well tolerated and high C_{max} (maximum serum concentration) values above 1 μM could be reached in clinical studies (3, 4).

The effect of JAKi is mediated by suppression of the intracellular signaling of cytokines depending on JAK phosphorylation. IL-6, granulocyte-macrophage colony-stimulating factor (GM-CSF), and interferons (IFNs) are the most important representatives of these cytokines being involved in the pathogenesis of RA (5). Specifically activated lymphocytes are targeted by tofacitinib showing decreased proliferation and a suppressed production of IL-17 and IFNγ after treatment (6).

Synovial fibroblasts (RASF) play a major role in RA by contributing to the growing pannus in the inflammatory milieu of joints (7). Furthermore, they develop an aggressive phenotype, and are able to migrate to and invade into healthy cartilage (7, 8). Tofacitinib has shown to selectively block activated pathways dependent on the phosphorylation of JAKs, e.g., oncostatin M in RASF (9). However, RASF are mainly activated by the inflammatory milieu with IL-1β and TNF-α being central cytokines. Of note, JAKs are primarily not required for mediating the effects of IL-1β on gene expression of e.g., pro-inflammatory cytokines (10, 11). Nevertheless, TNF-α induces the production of pro-inflammatory cytokines elevating the pro-inflammatory response of RASF in an autocrine manner. These secondary effects of e.g., IFN could be suppressed by JAKi and therefore reduce the general pro-inflammatory response of TNF-α treated RASF (12). In contrast, tofacitinib did not affect the IL-6 and IL-8 release of IL-1β activated RASF (6). The effect of other JAKi has not yet been examined. Taken together, little is known about the impact especially of new developed JAKi (peficitinib, filgotinib) on the pro-inflammatory response of IL-1β activated RASF and on their proliferation. Therefore, the aim of the study was to compare the effect of different JAKi on pro-inflammatory response of activated RASF and further characterize the effect of the most effective inhibitors.

MATERIALS AND METHODS

Cells

Synovium of patients suffering from RA was obtained during knee replacement surgery (Agaplesion-Markus-Hospital, Frankfurt). All patients fulfilled the classification criteria of the American College of Rheumatology (13). This study was carried out in accordance with the recommendations of the ethic committee of the University of Giessen. All subjects gave written informed consent in accordance with the Declaration of Helsinki. The protocol was approved by the ethic committee of the University of Giessen. Synovium samples were digested (1 h at room temperature, dispase-II-solution, 0.1 ml/ml, PAN-Biotech, Aidenbach, Germany) (14) and passed through cell strainers. After centrifugation, cells were cultured in DMEM (GE Healthcare, Germany) containing 10% heat-inactivated fetal calf serum (FCS, Sigma-Aldrich, Taufkirchen, Germany), 1 U/ml penicillin/streptomycin (AppliChem, Darmstadt, Germany), and 1 mM HEPES (GE Healthcare) at 37°C and 10% CO_2 (14). Cells were passaged using trypsin/ EDTA (Capricorn, Ebsdorfergrund, Germany) for a maximum of passage 7 (15). Human umbilical vein endothelial cells (HUVEC) were cultured in Endothelial Cell Growth Medium 2 with recommended supplement mix (both PromoCell, Heidelberg, Germany) containing 1 U/ml penicillin/streptomycin and 1 mM HEPES at 37°C and 5% CO_2.

Stimulation of RASF

RASF were seeded into 6-well plates (1×10^5 cells/well) and pretreated with JAKi (Selleckchem, Houston, USA) for 2 h and then additionally stimulated with IL-1β (R&D systems, Wiesbaden, Germany) or oncostatin M (OSM, R&D systems) for the indicated time. Experiments with RASF stimulated with IL-1β and sIL-6R (R&D systems) were performed in 24-well plates (2×10^4 cells/well). Supernatants were collected, centrifuged at 10,600 × g for 10 min and stored at −20°C. Vehicle control containing 0.1% DMSO served as a control. Synthesis of pro-inflammatory cytokines, matrix degrading proteinases (MMP), and chemokines were measured by commercially available enzyme-linked immunosorbent assay (ELISA, R&D systems) according to manufacturer's protocol.

Migration Assay

To determine the impact of peficitinib on migration of RASF, 1×10^5 cells were seeded in Corning® Transwell® polycarbonate membrane cell culture inserts for 24-well plates (Corning, New York, USA) containing a final concentration of 2% FCS. The lower chamber contained 10% FCS as chemoattractant. The non-migrated cells on top of the membrane were removed by gently wiping the membrane with a cotton swab. The migrated cells on the bottom side were stained with 4′,6-diamidino-2-phenylindole (DAPI) and the number of RASF was counted in 5 representative areas of 3 wells (200x magnification).

Adhesion Assays

RASF were pretreated with peficitinib, filgotinib or DMSO 0.1% and additionally stimulated with IL-1β as described previously. The cells were detached with accutase (Capricorn), centrifuged and seeded in 24-well plates at 1×10^4 cells/well. After incubation for 1 h at 37°C, the plate was shaken for 5 min at full speed and the non-adherent or weakly attached cells were removed by washing with PBS. The procedure was repeated twice. The remaining attached RASF were stained with 0.1% crystal-violet

dye in methanol for 10 min and counted in 4 representative areas of 3 wells per cell population (50x magnification).

For the cell-to-cell binding assay HUVECs were seeded in 48-well plates and cultured as described above until the confluence reached 100%. RASF were pretreated with JAKi as described previously. In the last 30 min Calcein-AM (Thermo Fisher Scientific, Waltham, USA) was supplemented to the medium according to the manufacturer's instructions. Cells were detached with accutase, counted and 5×10^3 cells were seeded on top of the endothelial cell layer. After 30 min, plates were shaken for 5 min at full speed and the non-adherent or weakly attached cells were removed by washing with PBS. The procedure was repeated twice. Remaining cells were fixed with 4% formaldehyde and green fluorescent (Calcein-AM stained)

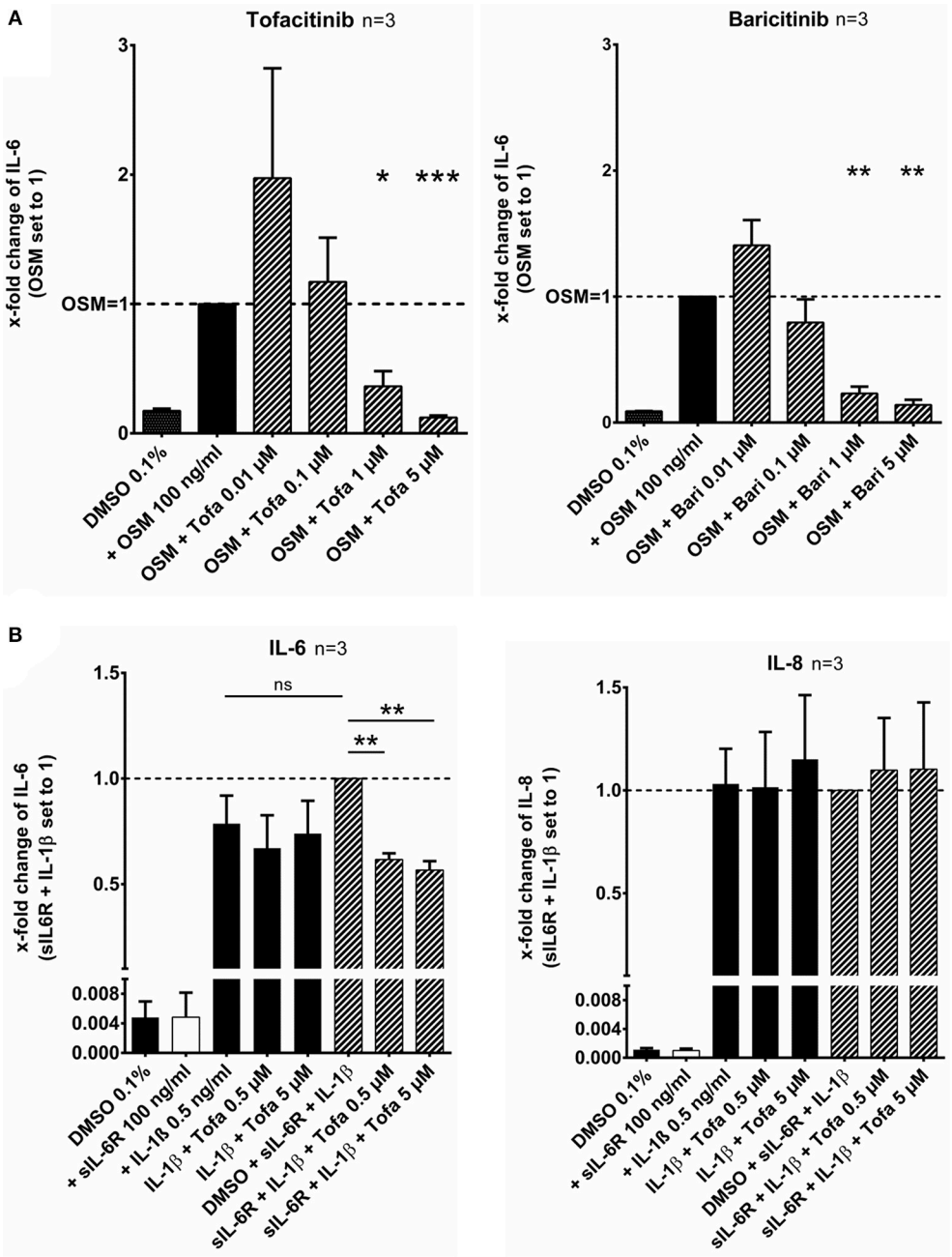

FIGURE 1 | Effect of tofacitinib and baricitinib on IL-6 dependent release of cytokines. **(A)** RASF were pretreated with JAKi or vehicle control (DMSO 0.1%) for 2 h and then additionally activated with OSM (100 ng/ml) for 24 h. The IL-6 release was decreased by tofacitinib or baricitinib confirming the inhibition of JAK dependent pathway. **(B)** The addition of sIL-6R to IL-1β stimulated RASF leads to an increase of IL-6 but not of IL-8 release. This increase could be blocked by tofacitinib. $^*p < 0.05$, $^{**}p < 0.01$, and $^{***}p < 0.001$ compared with OSM **(A)** or IL-1β and sIL6R **(B)** stimulated cells.

RASF were counted in 4 representative areas of 3 wells per cell population (50x magnification).

Proliferation Assay

RASF were seeded in 96-well plates at 3.5×10^3 cells/well overnight and then treated with JAKi or DMSO 0.1% with/without IL-1β for 24 h in the presence of 5-bromo-2′-deoxyuridine (BrdU). The BrdU incorporation indicating the proliferation of RASF was determined by a commercially available calorimetric BrdU cell proliferation assay kit (Merck, Darmstadt, Germany) according to manufacturer's protocol.

Measurement of Apoptosis, Viability, and Cytotoxicity

For measurement of changes in levels of apoptosis, viability, and cytotoxicity caused by peficitinib, RASF were seeded in 96-well plates at 3.5×10^3 cells/well overnight and then treated with peficitinib for 19 and 38 h. The ApoTox-Glo™ Triplex Assay (Promega, Madison, USA) was performed according to manufacturer's protocol. For the detection of cytotoxicity at multiple time points the CellTox™ Green Cytotoxicity Assay was used. The fluorescence (viability, cytotoxicity) and the luminescence (apoptosis) were measured as indicated by the manufacturer.

Statistics

All data are presented as arithmetic mean ± standard deviation (SD). For comparisons with a single control group, a one way ANOVA followed by Dunnett's *post-hoc* test was performed. The assessment of significance level for pair wise comparisons was calculated by a Student two-tailed *t*-test and Mann-Whitney-*U*-Test. $P < 0.05$ were considered significant. Statistical calculations and graphics were performed using GraphPad Prism.

RESULTS

Tofacitinib and Baricitinib Attenuated IL-6 and OSM Dependent IL-6 Release

RASF were pretreated with tofacitinib or baricitinib for 2 h and then additionally stimulated with the IL-6 like cytokine oncostatin M (OSM, 100 ng/ml) for 24 h (**Figure 1A**). Tofacitinib decreased the induced IL-6 release by 64% at 1 μM and by 88%

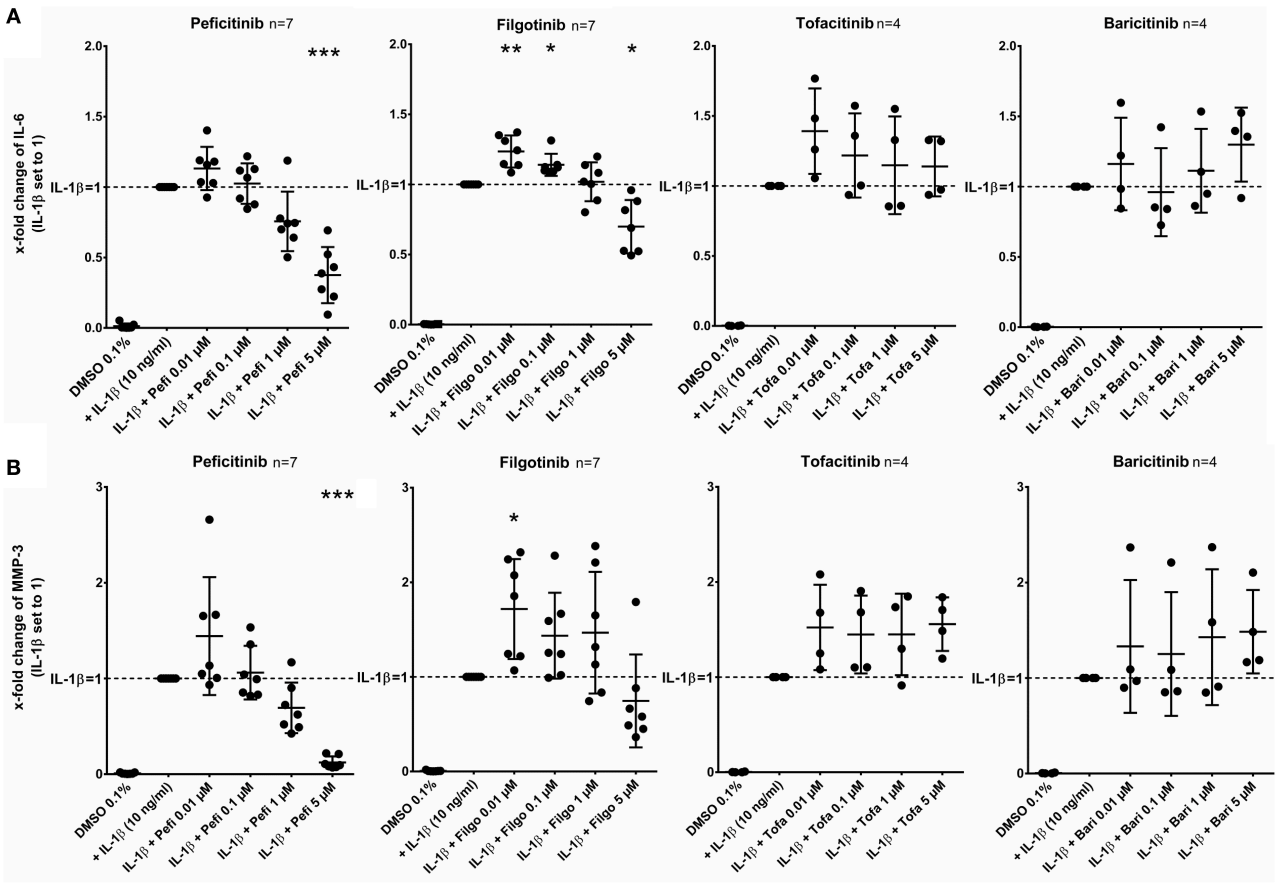

FIGURE 2 | Effect of JAKi on IL-6 and MMP-3 release of activated RASF by IL-1β. RASF were pretreated with JAKi or vehicle control (DMSO 0.1%) for 2 h and then additionally activated with IL-1β (10 ng/ml) for 17 h. The IL-6 and MMP-3 release was decreased by peficitinib at 1 and 5 μM, whereas filgotinib only decreased IL-6 levels at 5 μM. Tofacitinib and baricitinib did not attenuate the release of both proteins. *$p < 0.05$, **$p < 0.01$, and ***$p < 0.001$ compared with stimulated cells by IL-1β.

at 5 μM compared to OSM alone ($p < 0.05$, $p < 0.001$, $n = 3$, **Figure 1A**). Baricitinib at 1 and 5 μM also attenuated the IL-6 release by 77 and 86% (both $p > 0.05$, $n = 3$, **Figure 1A**). The combination of the soluble IL-6 receptor (sIL-6R) and IL-1β increased the IL-6 release by 21% (not significant) but not the IL-8 release in comparison to the stimulation with IL-1β alone (**Figure 1B**). The effect caused by sIL-6R was completely blocked by 0.5 or 5 μM tofacitinib (both $p < 0.01$).

Effect of JAKi on Cytokine and MMP Release of RASF Activated by IL-1β

After stimulation of RASF with IL-1β (10 ng/ml) for 17 h, peficitinib and filgotinib decreased the IL-6 release by 62% ($p < 0.001$) and by 30% at 5 μM ($p < 0.05$, $n = 7$). Peficitinib also attenuated the IL-6 release at 1 μM (24%, $n = 7$), but this observation did not reach the significance level due to high variability in responsiveness of RASF from

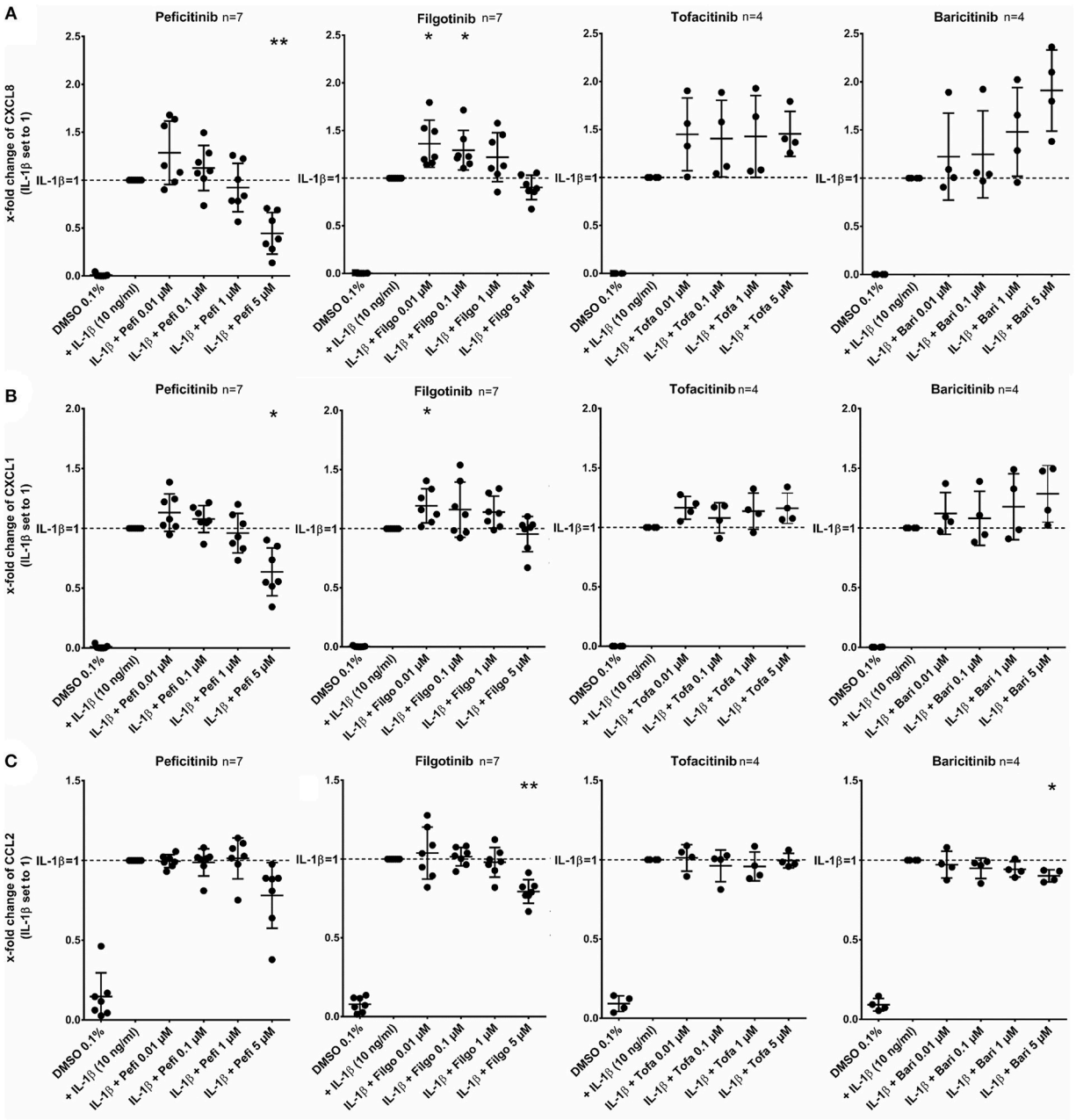

FIGURE 3 | Effect of JAKi on chemokine release of activated RASF by IL-1β. RASF were pretreated with JAKi or vehicle control (DMSO 0.1%) for 2 h and then additionally activated with IL-1β (10 ng/ml) for 17 h. Peficitinib at 5 μM decreased the release of CXCL8 **(A)** and CXCL1 **(B)**. CCL2 was attenuated significantly by filgotinib and baricitinib **(C)**. *$p < 0.05$ and **$p < 0.01$ compared with stimulated cells by IL-1β.

different patients. Filgotinib even slightly elevated IL-6 levels at 0.01 μM (24%, $p < 0.01$) and at 0.1 μM (14%, $p < 0.05$) (**Figure 2A**).

Peficitinib at 5 μM reduced the MMP-3 levels induced by IL-1β by 88% ($n = 7$, $p < 0.001$). At 1 μM, 6 of 7 patients showed a decrease (reduction by 31%, $n = 7$, not significant). The variability of MMP-3 levels was high after treatment with filgotinib and we could not observe a significant reduction (**Figure 2B**).

In contrast, tofacitinib and baricitinib did not decrease the IL-6 or MMP-3 release.

Effect of JAKi on Chemokine Release of RASF Activated by IL-1β

In contrast to other JAKi, only peficitinib at 5 μM decreased the release of CXCL8 (56%, $p < 0.01$) and CXCL1 (36%, $p < 0.05$). CCL2 was attenuated by peficitinib (22%) and by filgotinib (21%), whereas only the decrease of filgotinib was significant

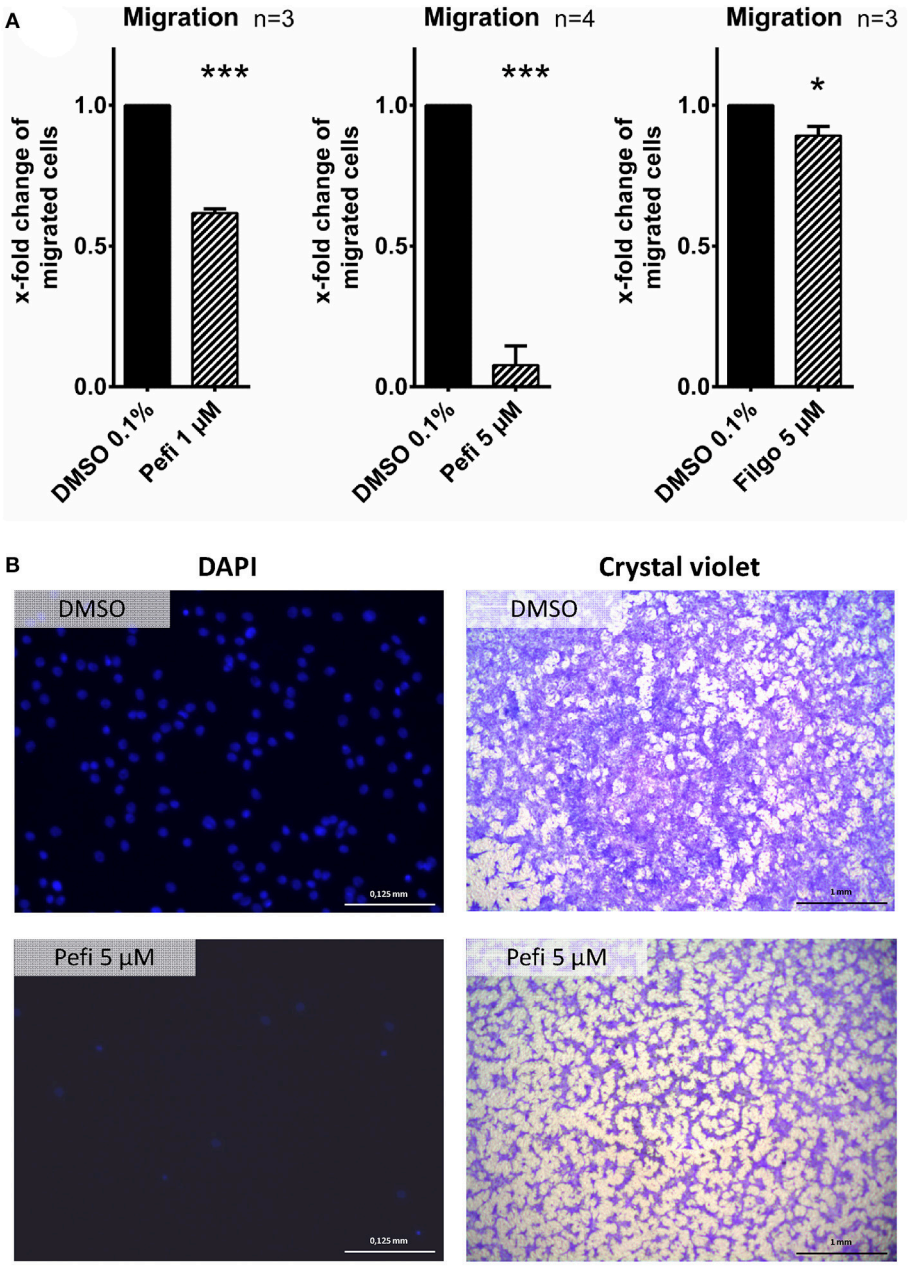

FIGURE 4 | Peficitinib and filgotinib attenuated migration of RASF. **(A)** The migration of RASF through a membrane (8 μM pores) toward a FCS gradient was reduced by pefictinib at 1 and 5 μM. **(B)** Representative crystal violet and DAPI staining of the bottom side of the inserts are shown. DAPI staining was used to quantify the migrated cells. *$p < 0.05$ and ***$p < 0.001$ compared with vehicle control.

($p < 0.01$). Baricitinib also attenuated the CCL2 release at 5 μM but compared to the other tested JAKi the effect was low (10%, $p < 0.05$) (**Figure 3**).

Peficitinib and Filgotinib Reduced Migration of RASF

The effect of peficitinib on migration of RASF toward a FCS gradient was studied by inserts containing membranes with 8 μm pores. Peficitinib decreased the number of migrated cells by 38% at 1 μM and by 92% at 5 μM (both $p < 0.001$, **Figure 4A**). In contrast, filgotinib only attenuated migration by 7% at 5 μM ($p < 0.05$, **Figure 4A**). DAPI staining was performed to count the migrated cells (**Figure 4B**). The effect on migration was not due to changed adhesion, because the short-term adhesion toward the plastic surface even of IL-1β activated RASF was not changed significantly by peficitinib or by filgotinib (**Figures 5A,B**). The adhesion on endothelial cells (HUVECs) was also not significantly affected by both JAKi (**Figures 5C,D**).

Effect of Different JAKi on Proliferation of RASF

Tofacitinib, baricitinib, and peficitinib at 5 μM decreased the proliferation rate studied by BrdU incorporation after 24 h compared to IL-1β (**Figure 6**). The strongest effect with a reduction of about 70% ($p < 0.001$, $n = 4$) was observed with peficitinib. Furthermore, only peficitinib attenuated the proliferation at 1 μM (23%, $p < 0.05$, $n = 4$). Interestingly, filgotinib did not change the proliferation of RASF.

Peficitinib Did Not Act Cytotoxic or Pro-apoptotic on RASF

The viability, activation of caspase 3/7 and the membrane integrity was measured to exclude toxic or pro-apoptotic effects

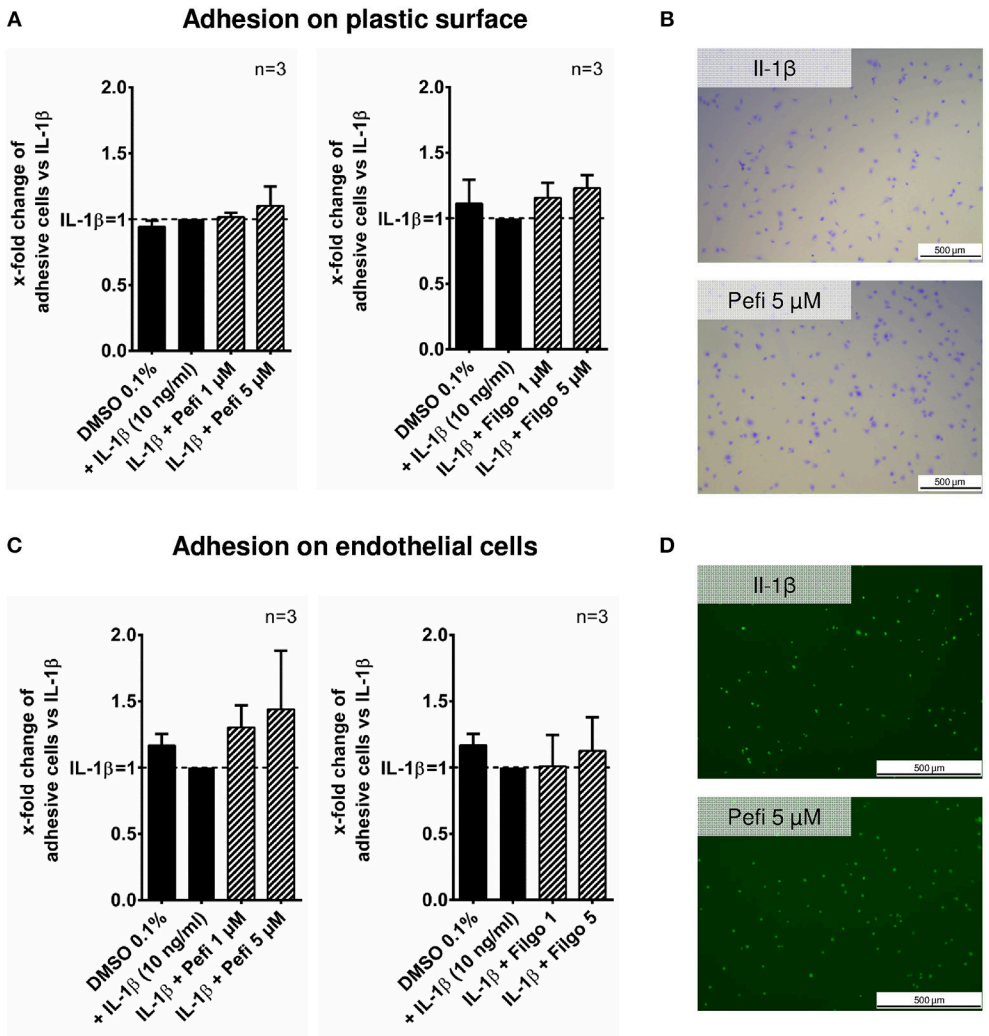

FIGURE 5 | Effect of different JAKi on proliferation of RASF. The adhesion of RASF on plastic surface **(A)** and on endothelial cells (HUVECs) **(C)** was not influenced by IL-1β and peficitinib or filgotinib at 1 and 5 μM. **(B)** Representative crystal violet staining is shown for adhesive cells on plastic surface. **(D)** Attached Calcein-AM stained RASF on endothelial cells were counted by fluorescence microscopy.

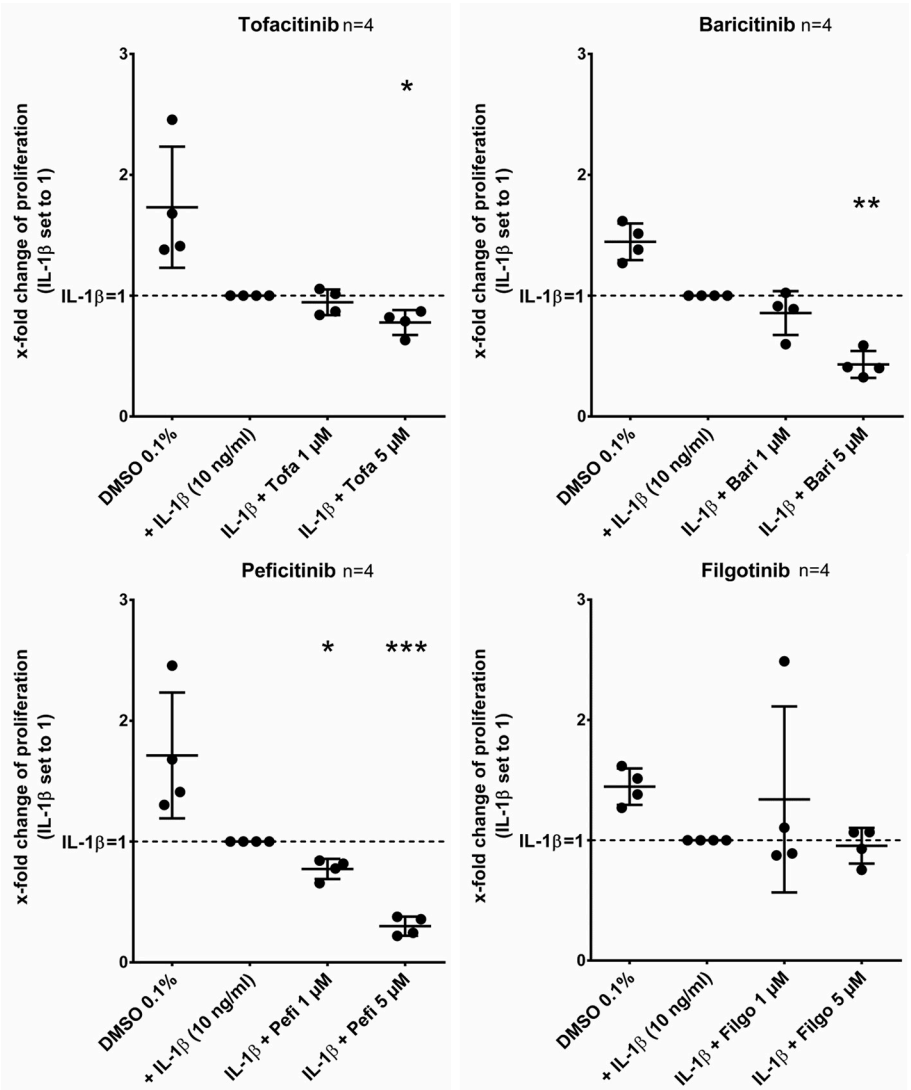

FIGURE 6 | Peficitinib did not influence the adhesion of activated RASF. Tofacitinib and baricitinib at 5 µM decreased proliferation of RASF activated by IL-1β, whereas filgotinib did not affect the proliferation. In contrast to the other JAKi, peficitinib inhibited proliferation of RASF at 1 µM. The proliferation was measured by BrdU-incorporation over 24 h. *$p < 0.05$, **$p < 0.01$, and ***$p < 0.001$ compared with activated RASF by IL-1β.

of peficitinib. The viability did not decrease after 19 h treatment of RASF with peficitinib at 1 and 5 µM in contrast to the staurosporin control (**Figure 7A**). After 38 h peficitinib at 5 µM induced a slight reduction of 13% ($p < 0.05$, $n = 4$). This effect was not caused by apoptosis after 19 or 38 h (**Figure 7B**) or cytotoxic effects between 4 and 48 h in contrast to the staurosporin control (**Figure 7C**).

DISCUSSION

In this study, all tested JAKi showed the ability to suppress the IL-6 and OSM mediated pro-inflammatory response in RASF. Furthermore, the panJAKi peficitinib was able to attenuate the broad pro-inflammatory response and the proliferation of IL-1β activated RASF.

First, we confirmed that tofacitinib is able to suppress the effects of the IL-6 like cytokine oncostatin M on IL-6 release. In contrast to findings of Migita et al. no reduction was observed in our study using 0.1 µM tofacitinib (9). This can be explained by differences in the experimental settings of both studies: We did not incubate the cells in serum-free medium and used higher concentrations of OSM (100 vs. 20 ng/ml). Additionally, we could show that baricitinib decreased OSM-mediated IL-6 release besides the known downregulation of CCL2 (16). RASF do not express the sIL-6R (17) and only transsignaling appears to play a role of mediating IL-6 effects in RASF (18, 19). Therefore, we additionally treated IL-1β activated RASF with sIL-6R, and indeed we could observe an increase of the IL-6 release. This increase could be fully blocked by treatment with tofacitinib even at 0.5 µM. These findings confirm that JAKi suppress

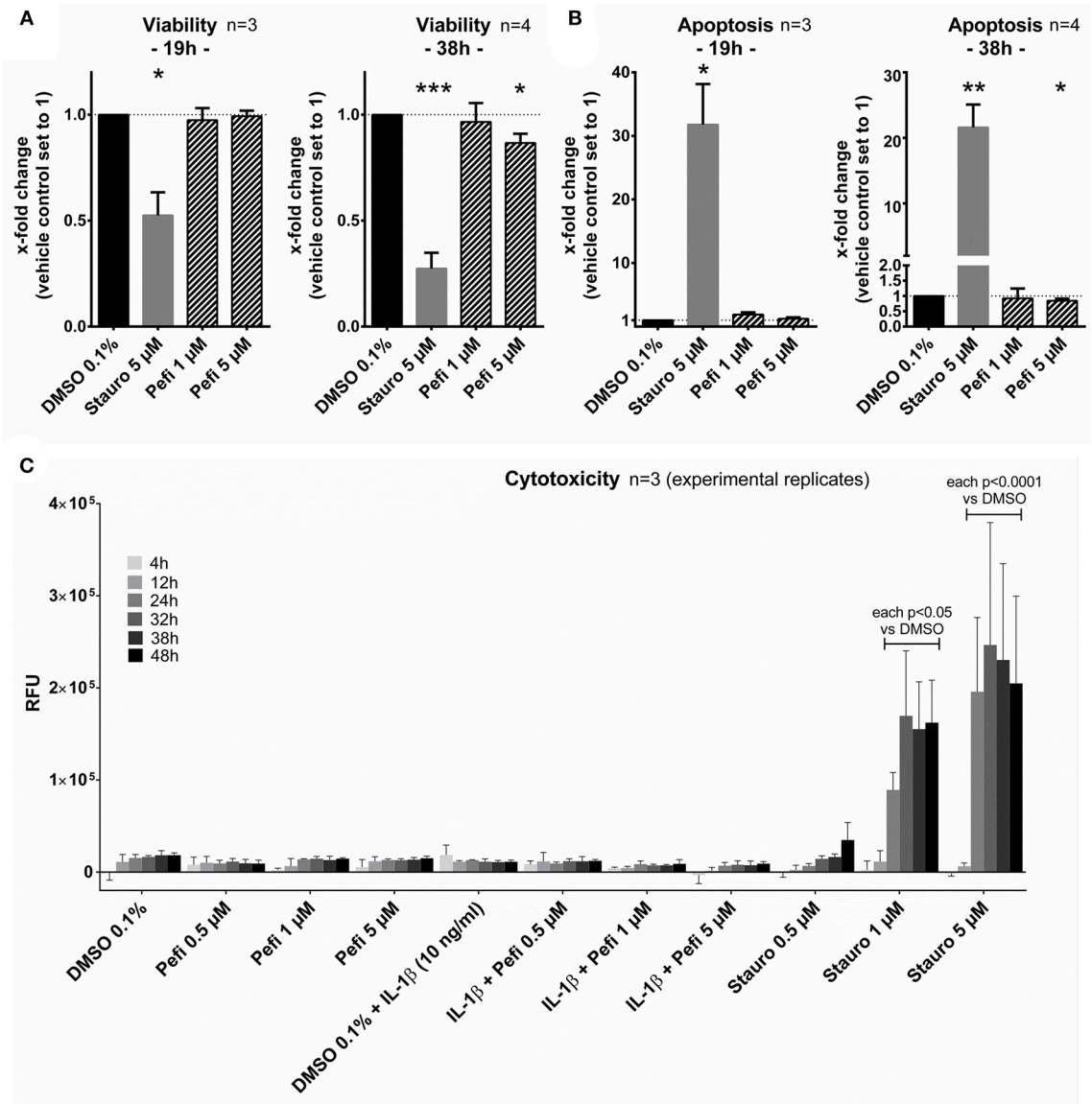

FIGURE 7 | Peficitinib did not act cytotoxic or pro-apoptotic on RASF. **(A)** The viability of RASF was not changed after treatment with peficitinib for 19 h. After 38 h the viability was slightly decreased by 5 μM peficitinib. **(B)** Even after 38 h, peficitinib did not affect the apoptosis rate of RASF measured by luciferase based detection of caspase-3/7 activation. **(C)** Peficitinib at 0.5, 1, and 5 μM alone or in combination with IL-1β did not induce cytotoxicity between 4 and 48 h. For all experiments staurosporin served as positive control. *$p < 0.05$, **$p < 0.01$ and ***$p < 0.001$ compared with vehicle control.

the JAK dependant signaling of the corresponding cytokines in RASF.

The effect of IL-6 and sIL-6R appears to be selective as the IL-1β induced IL-8 release could not be further increased by treatment with sIL-6R and not be blocked by JAKi. This finding is in line with data from Rosengren et al. showing that the TNF-α effect on IL-8 release was also not attenuated by JAK inhibition (12). However, in whole synovial tissue, the IL-8 levels were reduced in RA-patients treated with tofacitinib (20). This indicates that RASF are not the main producers of IL-8 in the synovial tissue or are affected by declining inflammatory mediators of other immune cells targeted by tofacitinib.

RASF cause a release of pro-inflammatory cytokines elevating the inflammatory response in an autocrine manner. This impact of secondary released mediators is known for the effect of TNF-α and IL-1β on IP-10 expression (12). Especially, type I interferons appear to mediate those secondary effects. Correspondingly, tofacitinib decreased the TNF-α induced release of CCL2 and IP-10 by suppression of JAK signaling (12). However, it has been also described that tofacitinib did not attenuate the IL-6 release of RASF stimulated with IL-1β (6). We confirmed this observation and could additionally show that baricitinib as well as tofacitinib did not suppress the IL-1β mediated IL-6, MMP3, CXCL8, and CXCL1 release. These data indicate that the

effects of JAK-dependant cytokines like IL-6 or OSM on IL-6, MMP3, CXCL8, and CXCL1 release appear to be negligible in the presence of high concentrations of IL-1β or in absence of sIL-6R. Against the background of the strong heterogenic distribution of sIL-6R levels with mean levels of 76 ng/ml in synovial fluid of RA patients (21), the treatment failure of some patients treated with JAKi could be explained by effects of remaining local high levels of IL-1β affecting RASF. Conversely, the successful treatment could partly be explained by suppressing transsignaling in RASF in the case of high sIL-6R levels and low IL-1β levels.

Of note, peficitinib and filgotinib were able to attenuate the IL-1β effect, but only above concentrations of 1 μM. Both inhibitors decreased the IL-6 release induced by IL-1β at 5 μM. Peficitinib also suppressed the IL-6 release at 1 μM in RASF from 6 to7 patients. Similar results for peficitinib were observed for the MMP-3 and CXCL1 release. In contrast, filgotinib did not affect the MMP-3 or CXCL1 levels but decreased CCL2 levels. Peficitinib was also the only JAKi decreasing the proliferation of IL-1β activated RASF at 1 μM. The effects of baricitinib and tofacitinib occurred even at 5 μM, but the C_{max} levels of both JAKi are below 200 nM after oral intake of approved doses (22, 23). In contrast, peficitinib is well tolerated by oral application of dosages up to 100 mg twice daily which cause serum levels up to 1.14 μM (373 ng/ml) (3). For filgotinib, C_{max} values up to 3.36 μM after application of 200 mg once daily were reached (4).

Additionally, peficitinib decreased impressively the migration of RASF even at 1 μM without affecting the adhesion. Taken together, peficitinib appears to be superior to other JAKi in decreasing the inflammatory response and the proliferation of RASF, although all JAKi effectively reduce the direct JAK-mediated signaling induced by OSM and IL-6/sIL-6. However, the effect of peficitinib occurs mainly at high concentrations and so we excluded possible pro-apoptotic and cytotoxic effects. The slightly decrease of viability observed after 38 h is not mediated by cytotoxicity or apoptosis and could be explained by decreased proliferation.

At concentrations higher than 1 μM, the used JAKi should inhibit JAK1, 2, and 3. For example, tofacitinib, and baricitinib at 1 μM were both able to inhibit sufficiently OSM-induced phosphorylation of JAK1, 2, and 3 (16). At concentrations of 1–5 μM used in our study, differences of JAKi in the ability to block different isoforms are not most likely to explain our observed differences. Filgotinib is described as a JAK1/2 inhibitor with comparable IC50 (inhibitory concentration 50%) values for JAK1/2 but even higher IC50 for the other JAKs in comparison to tofacitinib (24, 25). However, filgotinib slightly decreased the IL-6 release at 5 μM in contrast to tofacitinib. Furthermore, the nearly completely reduction of MMP-3 to baseline by peficitinib could not to be explained by blocking only secondary mediators. We therefore hypothesize that the effects of peficitinib and filgotinib at high concentrations are mediated by suppressing other kinases. Further, studies are required to examine the inhibition profile of JAKi in different human cell types at observed serum drug concentrations *in vivo*.

Our study indicates a possible advantage of peficitinib by targeting RASF *in vitro* and could result in higher response rates *in vivo* compared to other JAKi. Especially subgroups of patients suffering from severe synovial proliferations might benefit from higher dosages of peficitinib.

CONCLUSIONS

In conclusion, all JAKi tested suppressed the inflammatory response induced by OSM and by transsignaling of IL-6 in RASF. Only peficitinib was able to modulate the IL-1β induced response of RASF and their proliferation *in vitro* at concentrations which are close to reported C_{max} values of well tolerated doses *in vivo*, but the underlying mechanism remains unclear. Furthermore, peficitinib highly suppressed the migration of RASF showing the potential of peficitinib to target RASF.

DATA AVAILABILITY

The datasets generated for this study are available on request to the corresponding author.

AUTHOR CONTRIBUTIONS

MD, EN, KF, and UM-L designed the project. MD, IA, and M-LH were responsible for acquisition of data. MD, RH, KF, and EN analyzed and interpreted the data. SR collected the tissue samples and contributed to the project design. MD, RH, IA, EN, and UM-L contributed to drafting of the article. All authors contributed to manuscript revision, read, and approved the submitted version.

FUNDING

This work was supported by William G. Kerckhoff foundation. The funding body had no impact on the design of the study, collection, analysis, interpretation of data, or in writing the manuscript.

ACKNOWLEDGMENTS

We thank Mona Arnold and Carina Schreiyäck for excellent technical assistance.

REFERENCES

1. Hunter TM, Boytsov NN, Zhang X, Schroeder K, Michaud K, Araujo AB. Prevalence of rheumatoid arthritis in the United States adult population in healthcare claims databases, 2004–2014. *Rheumatol Int.* (2017) 37:1551–7. doi: 10.1007/s00296-017-3726-1
2. Smolen JS, Landewe R, Bijlsma J, Burmester G, Chatzidionysiou K, Dougados M, et al. EULAR recommendations for the management of rheumatoid arthritis with synthetic and biological disease-modifying

antirheumatic drugs: 2016 update. *Ann Rheum Dis.* (2017) 76:960–77. doi: 10.1136/annrheumdis-2016-210715
3. Cao YJ, Sawamoto T, Valluri U, Cho K, Lewand M, Swan S,et al. Pharmacokinetics, pharmacodynamics, and safety of ASP015K (Peficitinib), a new janus kinase inhibitor, in healthy subjects. *Clin Pharmacol Drug Dev.* (2016) 5:435–49. doi: 10.1002/cpdd.273
4. Vanhoutte F, Mazur M, Voloshyn O, Stanislavchuk M, Van der Aa A, Namour F, et al. Efficacy, safety, pharmacokinetics, and pharmacodynamics of filgotinib, a selective JAK-1 inhibitor, after short-term treatment of rheumatoid arthritis: results of two randomized phase IIa trials. *Arthritis Rheumatol.* (2017) 69:1949–59. doi: 10.1002/art.40186
5. Schwartz DM, Bonelli M, Gadina M, O'Shea JJ. Type I/II cytokines, JAKs, and new strategies for treating autoimmune diseases. *Nat Rev Rheumatol.* (2016) 12:25–36. doi: 10.1038/nrrheum.2015.167
6. Maeshima K, Yamaoka K, Kubo S, Nakano K, Iwata S, Saito K,et al. The JAK inhibitor tofacitinib regulates synovitis through inhibition of interferon-gamma and interleukin-17 production by human CD4+ T cells. *Arthritis Rheum.* (2012) 64:1790–8. doi: 10.1002/art.34329
7. Korb-Pap A, Bertrand J, Sherwood J, Pap T. Stable activation of fibroblasts in rheumatic arthritis-causes and consequences. *Rheumatology.* (2016) 55:ii64–7. doi: 10.1093/rheumatology/kew347
8. Lefevre S, Knedla A, Tennie C, Kampmann A, Wunrau C, Dinser R, et al. Synovial fibroblasts spread rheumatoid arthritis to unaffected joints. *Nat Med.* (2009) 15:1414–20. doi: 10.1038/nm.2050
9. Migita K, Komori A, Torigoshi T, Maeda Y, Izumi Y, Jiuchi Y, et al. CP690,550 inhibits oncostatin M-induced JAK/STAT signaling pathway in rheumatoid synoviocytes. *Arthritis Res Ther.* (2011) 13:R72. doi: 10.1186/ar3333
10. Miyazawa K, Mori A, Miyata H, Akahane M, Ajisawa Y, Okudaira. Regulation of interleukin-1beta-induced interleukin-6 gene expression in human fibroblast-like synoviocytes by p38 mitogen-activated protein kinase. *J Biol Chem.* (1998) 273:24832–8.
11. Miyazawa K, Mori A, Yamamoto K, Okudaira H. Transcriptional roles of CCAAT/enhancer binding protein-beta, nuclear factor-kappaB, and C-promoter binding factor 1 in interleukin (IL)-1beta-induced IL-6 synthesis by human rheumatoid fibroblast-like synoviocytes. *J Biol Chem.* (1998) 273:7620–7.
12. Rosengren S, Corr M, Firestein GS, Boyle DL. The JAK inhibitor CP-690,550 (tofacitinib) inhibits TNF-induced chemokine expression in fibroblast-like synoviocytes: autocrine role of type I interferon. *Ann Rheum Dis.* (2012) 71:440–7. doi: 10.1136/ard.2011.150284
13. Arnett FC, Edworthy SM, Bloch DA, McShane DJ, Fries JF, Cooper NS, et al. The American rheumatism association 1987 revised criteria for the classification of rheumatoid arthritis. *Arthritis Rheum.* (1988) 31:315–24.
14. Neumann E, Judex M, Kullmann F, Grifka J, Robbins PD, Pap T, et al. Inhibition of cartilage destruction by double gene transfer of IL-1Ra and IL-10 involves the activin pathway. *Gene Ther.* (2002) 9:1508–19. doi: 10.1038/sj.gt.3301811
15. Neumann E, Riepl B, Knedla A, Lefevre S, Tarner IH, Grifka J, et al. Cell culture and passaging alters gene expression pattern and proliferation rate in rheumatoid arthritis synovial fibroblasts. *Arthritis Res Ther.* (2010) 12:R83. doi: 10.1186/ar3010
16. Migita K, Izumi Y, Torigoshi T, Satomura K, Izumi M, Nishino Y, et al. Inhibition of Janus kinase/signal transducer and activator of transcription (JAK/STAT) signalling pathway in rheumatoid synovial fibroblasts using small molecule compounds. *Clin Exp Immunol.* (2013) 174:356–63. doi: 10.1111/cei.12190
17. Desgeorges A, Gabay C, Silacci P, Novick D, Roux-Lombard P, Grau G, et al. Concentrations and origins of soluble interleukin 6 receptor-alpha in serum and synovial fluid. *J Rheumatol.* (1997) 24:1510–6.
18. Hashizume M, Hayakawa N, Mihara M. IL-6 trans-signalling directly induces RANKL on fibroblast-like synovial cells and is involved in RANKL induction by TNF-alpha and IL-17. *Rheumatology.* (2008) 47:1635–40. doi: 10.1093/rheumatology/ken363
19. Mimata Y, Kamataki A, Oikawa S, Murakami K, Uzuki M, Shimamura T, et al. Interleukin-6 upregulates expression of ADAMTS-4 in fibroblast-like synoviocytes from patients with rheumatoid arthritis. *Int J Rheum Dis.* (2012) 15:36–44. doi: 10.1111/j.1756-185X.2011.01656.x
20. McGarry T, Orr C, Wade S, Biniecka M, Wade S, Gallagher L, et al. JAK-STAT blockade alters synovial bioenergetics, mitochondrial function and pro-inflammatory mediators in Rheumatoid arthritis. *Arthritis Rheumatol.* (2018) 70:1959–70. doi: 10.1002/art.40569
21. Uson J, Balsa A, Pascual-Salcedo D, Cabezas JA, Gonzalez-Tarrio JM, Martin-Mola E, et al. Soluble interleukin 6 (IL-6) receptor and IL-6 levels in serum and synovial fluid of patients with different arthropathies. *J Rheumatol.* (1997) 24:2069–75.
22. Lamba M, Wang R, Fletcher T, Alvey C, Kushner Jt, Stock TC. Extended-release once-daily formulation of tofacitinib: evaluation of pharmacokinetics compared with immediate-release tofacitinib and impact of food. *J Clin Pharmacol.* (2016) 56:1362–71. doi: 10.1002/jcph.734
23. Shi JG, Chen X, Lee F, Emm T, Scherle PA, Lo Y, et al. The pharmacokinetics, pharmacodynamics, and safety of baricitinib, an oral JAK 1/2 inhibitor, in healthy volunteers. *J Clin Pharmacol.* (2014) 54:1354–61. doi: 10.1002/jcph.354
24. Ito M, Yamazaki S, Yamagami K, Kuno M, Morita Y, Okuma K, et al. A novel JAK inhibitor, peficitinib, demonstrates potent efficacy in a rat adjuvant-induced arthritis model. *J Pharmacol Sci.* (2017) 133:25–33. doi: 10.1016/j.jphs.2016.12.001
25. Van Rompaey L, Galien R, van der Aar EM, Clement-Lacroix P, Nelles L, Smets B, et al. Preclinical characterization of GLPG0634, a selective inhibitor of JAK1, for the treatment of inflammatory diseases. *J Immunol.* (2013) 191:3568–77. doi: 10.4049/jimmunol.1201348

Conflict of Interest Statement: The authors declare that the research was conducted in the absence of any commercial or financial relationships that could be construed as a potential conflict of interest.

frontiers in Immunology

ORIGINAL RESEARCH
published: 08 May 2019
doi: 10.3389/fimmu.2019.01027

Cannabinoid Receptor 2 Agonist JWH-015 Inhibits Interleukin-1β-Induced Inflammation in Rheumatoid Arthritis Synovial Fibroblasts and in Adjuvant Induced Arthritis Rat via Glucocorticoid Receptor

Sabrina Fechtner[1†], Anil K. Singh[1†], Ila Srivastava[1], Christopher T. Szlenk[1], Tim R. Muench[2], Senthil Natesan[1] and Salahuddin Ahmed[1,3]*

[1] Department of Pharmaceutical Sciences, Washington State University College of Pharmacy and Pharmaceutical Sciences, Spokane, WA, United States, [2] Preclinical COE, ETHICON, Medical Device Business Services, Inc., DePuy Synthes, Somerville, NJ, United States, [3] Division of Rheumatology, University of Washington School of Medicine, Seattle, WA, United States

Management of pain in the treatment of rheumatoid arthritis (RA) is a priority that is not fully addressed by the conventional therapies. In the present study, we evaluated the efficacy of cannabinoid receptor 2 (CB2) agonist JWH-015 using RA synovial fibroblasts (RASFs) obtained from patients diagnosed with RA and in a rat adjuvant-induced arthritis (AIA) model of RA. Pretreatment of human RASFs with JWH-015 (10–20 μM) markedly inhibited the ability of pro-inflammatory cytokine interleukin-1β (IL-1β) to induce production of IL-6 and IL-8 and cellular expression of inflammatory cyclooxygenase-2 (COX-2). JWH-015 was effective in reducing IL-1β-induced phosphorylation of TAK1 ($Thr^{184/187}$) and JNK/SAPK in human RASFs. While the knockdown of CB2 in RASFs using siRNA method reduced IL-1β-induced inflammation, JWH-015 was still effective in eliciting its anti-inflammatory effects despite the absence of CB2, suggesting the role of non-canonical or an off-target receptor. Computational studies using molecular docking and molecular dynamics simulations showed that JWH-105 favorably binds to glucocorticoid receptor (GR) with the binding pose and interactions similar to its well-known ligand dexamethasone. Furthermore, knockdown of GR using siRNA abrogated JWH-015's ability to reduce IL-1β-induced IL-6 and IL-8 production. *In vivo*, administration of JWH-015 (5 mg/kg, daily i.p. for 7 days at the onset of arthritis) significantly ameliorated AIA in rats. Pain assessment studies using von Frey method showed a marked antinociception in AIA rats treated with JWH-015. In addition, JWH-015 treatment inhibited bone destruction as evident from micro-CT scanning and bone analysis on the harvested joints and modulated serum

OPEN ACCESS

Edited by:
Dirk Foell,
University Hospital Münster, Germany

Reviewed by:
Eugen Feist,
Charité Medical University of Berlin, Germany
Jessica Bertrand,
Universitätsklinikum Magdeburg, Germany

***Correspondence:**
Salahuddin Ahmed
salah.ahmed@wsu.edu

[†]These authors have contributed equally to this work

Specialty section:
This article was submitted to Autoimmune and Autoinflammatory Disorders, a section of the journal Frontiers in Immunology

Received: *14 January 2019*
Accepted: *23 April 2019*
Published: *08 May 2019*

Citation:
Fechtner S, Singh AK, Srivastava I, Szlenk CT, Muench TR, Natesan S and Ahmed S (2019) Cannabinoid Receptor 2 Agonist JWH-015 Inhibits Interleukin-1β-Induced Inflammation in Rheumatoid Arthritis Synovial Fibroblasts and in Adjuvant Induced Arthritis Rat via Glucocorticoid Receptor. Front. Immunol. 10:1027. doi: 10.3389/fimmu.2019.01027

RANKL and OPG levels. Overall, our findings suggest that CB2 agonist JWH-015 elicits anti-inflammatory effects partly through GR. This compound could further be tested as an adjunct therapy for the management of pain and tissue destruction as a non-opioid for RA.

Keywords: fibroblasts, endocannabinoids, bone degradation, inflammation, antinociception

INTRODUCTION

In 1990, cannabinoid receptor 1 (CB1) was identified as the receptor responsible for tetrahydrocannabinol carboxylic (THC) effects (1). Three years later cannabinoid receptor 2 (CB2) was identified and together these receptors comprise the endocannabinoid system (ECS). CB1 is mainly expressed in the central nervous system and is primarily responsible for the psychoactive effects of cannabinoids concomitant to the neuroprotective effects (2). CB2 is mainly expressed peripherally, with its highest expression on immune cells. It is thereby associated with the immune suppressive and anti-inflammatory effect of cannabinoids (2, 3). Since the discovery of these receptors, endogenous ligands of the ECS such as anandamide (AEA) and 2-arachidonoylglycerol (2-AG) have been identified, and their synthesis and metabolism have been characterized. In addition to the endogenous ligands, several exogenous ligands have been identified such as cannabidiol (CBD). Although these ligands activate the ECS, they lack specificity to one receptor or the other. Thus, as our understanding of the ECS grows, specific ligands of either CB1 or CB2 are needed to characterize each receptor separately.

To address this need, John W. Huffman synthesized several ligands termed JWH compounds. Each ligand has differing affinities to CB1 and CB2 that can be used to activate one specific receptor over the other (4, 5). Many JWH compounds are now commercially available and can be used to help distinguish the differential effects of CB1 and CB2 activation.

Rheumatoid arthritis (RA) is an autoimmune disease characterized by inflammation and joint degradation. RA synovial fibroblasts (RASFs) are considered to be the main perpetrators by responding to pro-inflammatory cytokines interleukin-1β (IL-1β) and tumor necrosis factor-α (TNF-α) by producing IL-6, IL-8, and prostaglandins that exacerbate inflammation. Current therapies are targeted mainly to alleviate symptoms (non-steroidal anti-inflammatory drugs, NSAIDs) and slow down disease progression (disease-modifying anti-rheumatic drugs, DMARDs). The main goal of RA therapy is to increase remission rate in patients and one way to do so is to provide pain relief. However, pain management therapies are some of the most needed and demanded. A recent survey of 1,004 RA patients in the U.S. showed that 80% of those patients still experience pain daily or multiple time a week. In addition, 74% of them wished their therapies worked better (6). Indeed, another study showed that disease activity score-28 (DAS-28) does not reflect a reduction in pain in RA patients on current treatment options (7).

Recent literature suggests that the ECS may reduce both pain and inflammation in RA (3, 8, 9). Both CB1 and CB2 expression have been characterized in RASFs, where CB2 is upregulated in synovial tissue and RASFs. Within the synovial fluid of RA patients, AEA and 2-AG are found in detectable levels; however, both are undetectable in healthy joints. However, the reason for CB2 upregulation and the effects of CB2-targeted therapies remains unknown. JWH-133 is a specific CB2 agonist which has over 200 times more affinity for CB2 than CB1. Interestingly, JWH-133 administration reduced osteoarthritis pain-related behavior in the monosodium iodate-induced OA rat model (10). A study done by Selvi et al., using non-specific agonist CP 55,940 observed IL-1β-induced IL-6 and IL-8 production was inhibited with this agonist, however cytokine levels were not changed using CB1 and CB2 antagonists suggesting the presence of another anti-inflammatory receptor (11).

Therefore, the present study was carried out to evaluate the efficacy of CB2 selective agonist JWH-015 in human RASFs and *in vivo* using a rat model of RA. Upon further analysis, we identified that JWH-015 utilizes glucocorticoid receptor to produce anti-inflammatory affects.

MATERIALS AND METHODS

Chemicals and Reagents

TRAF6, p-TAK$^{Thr184/187}$, p-IRAK4$^{Thr345/Ser346}$, IRAK4, p-P38, P38, p-JNK, JNK, p-ERK, ERK, GR, and NF-κBp65 antibodies were purchased from Cell Signaling Technologies (Danvers, MA) with respective catalog numbers 8028S, 90C7, D6D7, 4363, 4511S, 8690S, 9251S,9252T, 4370S, 4695S, 12041T, D14E12. p-TAK^{Ser439} was obtained from Abcam (Cat EPR2863). β-Actin and Lamin B antibodies were purchased from Santa Cruz Biotechnology (Santa Cruz, CA;, sc-47778, sc-6217). β-tubulin was purchased Sigma (St. Louis, MO cat# T8328). All antibodies were diluted in 5% BSA/TBS-T according to manufactures recommendation. JWH-015 was sourced from Tocris (Cat# 1341; ≥99% HPLC) and dissolved in DMSO at a stock concentration of 10 mM. For *in vivo* studies, JWH-015 was dissolved 3% DMSO/PBS.

Culturing of Human RASFs

Human RASFs were isolated from patients diagnosed with RA according to the American College of Rheumatology (ACR) guidelines (7 female, 2 male, average age 50 ± 16.9 years). Briefly, de-identified human RA synovial tissues were obtained from Cooperative Human Tissue Network (CTHN; Columbus, OH) and National Disease Research Interchange (NDRI; Philadelphia, PA) according to an Institutional Review Board (IRB) approved protocol in compliance with the Helsinki Declaration. Synovial tissue was digested in Dipase, collagenase, and DNAase before being seeded in 72 cm^2 flasks. Cells were grown in RPMI 1640 medium supplemented with 10% fetal bovine serum (FBS),

5000 U/ml penicillin, 5 mg/ml streptomycin, and 10 μg/ml gentamicin. Upon confluency (>85%) cells were passaged with brief trypsinization. All experiments were done using cells that were passed for additional 4 to 5 times to ensure enriched pure fibroblast population. For experimental purpose, we used RASFs between passages 5–10. All treatments were done in serum free media. All the experiments were performed on at least three or more cell lines established from different RA donors in this study.

Treatment of RASFs

RASFs were seeded in 6-well plates and grown to >85% confluency. RASFs were pretreated with 10 or 20 μM of JWH-015 for 10 min prior to the addition of IL-1β (10 ng/mL). The duration of stimulation was for 30 min for signaling studies and/or 24 h to evaluate the production of IL-6, IL-8, and cyclooxygenase (COX) enzymes. Conditioned media was subjected to IL-6, IL-8, and PGE_2 quantitation by ELISA, while whole cell extracts were used for the analysis of IL-1β signaling proteins like p-P38, p-JNK, p-ERK, and p-TAK-1Thr$^{184/187}$ using Western immunoblotting.

Small-Interfering RNA (siRNA)

siRNA for CB2 [Catalog SASI_Hs01_00041077, SASI_Hs01_00041084, Sigma] and GR [SASI_Hs01_00188611, SASI_Hs01_00188614] were purchased from Sigma MISSION predesigned siRNA and RASFs were transfected as previously described (12). RASFs were transfected with 120 pmoles of negative (SIC001), CB2, or GR siRNA with Lipofectamine 2000 (Thermo Fisher Scientific) in Opti-MEM media for 8 h in 6 well format. Media was replenished with complete RPMI supplemented with 10% FBS and antibiotics next day. Forty-eight hours post transfection, RASFs were serum starved overnight prior to IL-1β simulation with or without JWH-015 for additional 24 h.

Cell Fractionation

Cellular sub-fractionation to obtain nuclear and cytosolic fractions were performed as described previously (13). Briefly, RASFs were pretreated with 1 μM dexamethasone (Dex) 1 h or JWH-015 (20 μM) 10 min prior to IL-1β stimulation for 30 min. After preparation of cytoplasmic extract, nuclear pellet were subjected to 2–3 times sonication in RIPA buffer to obtain complete nuclear extract. Cytoplasmic and nuclear lysates were quantitated using Bio-Rad DC method followed by 25 μg of each treatment sample were subjected to Western immunoblotting. β-Tubulin was used for evaluating purity of cytosolic fraction and Lamin B was used for the nuclear fraction.

Western Immunoblotting

Whole cell extract was prepared using RIPA buffer (50 mM Tris pH 7.6, 150 mM CaCl, 1% Triton X-100, 1 mM EDTA, 1 mM DTT, 0.5% sodium deoxycholate, and 0.1% SDS) containing protease and phosphatase inhibitors (Roche Basel, Switzerland). Protein was measured using BioRad DC method (Bio-Rad, Hercules, CA). Equal amount of protein (25 μg) for each sample was loaded and separated on a 10% acrylamide gel and transferred onto PVDF membrane (EMD Millipore, Billerica, MA). Blots were then blocked in TBST containing 5% nonfat dry milk for 2 h prior to overnight incubation with respective primary antibody with dilution according to manufacturer. Protein bands were visualized using chemiluminescence and analyzed using Image Lab software (Bio Rad) for band intensity. Blots were probed with β-actin to ensure equal loading.

qRT-PCR

Treated RASFs were collected in 1mL of TRIzol Reagent (ThermoFisher Scientific, cat 15596026). RNA was extracted using the company provided protocol. 400 ng of RNA was used to make cDNA using Superscript II cDNA kit (ThermoFisher, cat 11904018). SYBR Green quantitative real-time PCR was used for analysis of CB2 (Sigma KiCqStart™ Primer H_CNR2_1) and GR (Qiagen QuantiTect primer GRQT00020608) with GAPDH (Qiagen QuantiTect primer QT00079247) as a control. Quantification of the relative expression was done using the ΔΔCt method.

Assay for IL-6 and IL-8, PGE_2, RANKL, and OPG Production

The conditioned media was collected from 24-h IL-1β stimulated samples with or without JWH-015, spun down at 10,000 rpm for 10 min at 4°C to remove particulate matter, and collected in fresh Eppendorf tubes. The collected supernatants were analyzed for human IL-6 and IL-8 levels using colorimetric sandwich ELISA kits (R&D Systems, Minneapolis, MN) as per manufacturer's instructions. PGE_2 was assayed using colorimetric ELISA kit from Cayman Chemical (Ann Arbor, MI Cat# 514010) according to manufacturer's instructions.

RANKL and OPG were purchased from Ray Biotech (Norcross, GA cat # ELM-TRANCE-1 and ELM-OPG-1). Minor modification was made to OPG assay where samples and standard were incubated overnight at 4°C with gentle shaking. The remaining steps were performed as per manufacturer's instructions.

Rat Adjuvant-Induced Arthritis (AIA)

All animal studies were approved by the ethics committee of the Washington State University and conformed to the NIH Guide for the Care the Use of Laboratory Animals (8th edition, 2011). Rat adjuvant arthritis studied was performed using similar parameters as described previously (14, 15). Briefly, ∼120g female Lewis rats were purchased from Envigo (East Millstone, NJ) and allowed to acclimate for 1 week prior to start in campus vivarium accredited by the American Association for Accreditation of Laboratory Animal Care. On day 0, rats were administered 300 μl of 5 mg/ml lyophilized *Mycobacterium butyricum* (Difco Laboratories, Detroit, MI, USA) in sterile mineral oil subcutaneously at the base of the tail. Clinical parameters measured included articular index (AI) and ankle circumferences (AC) using parameters referenced in Ahmed et al. (14) AI scores were recorded for each hind joint by a consistent observer blinded to the treatment regimen and then averaged for each animal. AI scores were based on a 0–4 scale where 0 = no swelling or erythema, 1 = slight swelling and/or erythema, 2 = low to moderate oedema, 3 = pronounced edema with

limited joint usage and 4 = excess oedema with joint rigidity. AC were also measured by the same blinded observer and the change in ankle circumference was presented as delta (Δ) ankle circumference. The Δ ankle circumferences of both the hind ankles from each animal were averaged and "n" is represented as the number of animals used in each of the experimental groups. Treatment of Animals with JWH-015.

JWH-015 was brought into suspension in phosphate buffered saline (PBS) with 3% DMSO. JWH-015 was administered daily via intraperitoneal injection (5 mg/kg) starting on day 9 after arthritis induction when the first signs of joint inflammation and swelling are usually noted and continued until day 17. On day 17, animals were sacrificed for biochemical, cytokine, and serum analysis.

Behavioral Assays

Von Frey testing was performed 60 min after JWH-015 administration. Rats were acclimatized to testing cases for 15 min prior to testing. The amount of force applied to elicit a response (paw withdrawal or vocalization) was measured in grams. Three measurements were taken per hind paw with 30 s intervals in-between measurements and the order of paw testing (left vs. right paw first) was counter-balanced in each test group. In most cases, AIA arthritis was asymmetric where one paw was highly inflamed compared to the other thus, baseline data was compared between naïve, AIA, and JWH-015 groups was transformed to a ratio of the rat's own baseline score at day 8 compared to day 17. Therefore, mechanical threshold = [mechanical threshold in more inflamed paw- other hind paw at day 17]/[mechanical threshold in more inflamed paw-other hind paw at day 8].

Imaging Studies: μ-CT Scanning

Ankles were fixed in formalin for preservation. One day prior to scan, ankles were placed in 1X PBS to mimic physiological conditions. Ankles were imaged using Quantum GX micro-CT Imaging System (Perkin Elmer Waltham, MA) using in-built "High Resolution Scan Mode." Images were acquired at 90 kV and the standard total acquisition time was 4 min producing a 144 mm voxel image.

Bone mineral analysis was performed by standardizing images to QRM-MicroCT-HA phantom (QRM Moehrendorf, Germany). Rat tarsus bone was oriented vertically for analysis.

Histological Analysis of Joint

For histological evaluation of the synovial joint, joints were decalcified with 10% EDTA for 14 days before being embedded with paraffin. Five μm slices were cut sagittally through the center line of the joint. Sections from naïve, AIA alone, and AIA + JWH-015 groups were stained with hematoxylin and eosin. Slides were photographed at 10× magnification using Leica DM2500 microscope and were then evaluated for the presence of infiltrates, angiogenesis, and bone destruction.

For an objective evaluation of synovitis and inflammation, slides were analyzed for the following parameters: polymorphonuclear inflammation, immune cell infiltration (lymphocytes, plasma cells, and macrophages), neovascularization, and fibrosis (**Supplementary Table 1**).

Molecular Dynamics Simulations

The binding pose and molecular interactions of JWH-015 with GR predicted by the docking simulations were further investigated by a 100 ns long molecular dynamics (MD) simulation of the docked complex. Prior to MD simulation, the crystal structure of the glucocorticoid receptor (PDB ID 4UDD) was prepared using MOE (16). Mutations introduced during protein crystallization were changed back to their respective wild type residues for the mutations, N517D, V571M, F602S, and C638D. The native sequence was preserved, all the amino acids were assigned their appropriate protonation states at pH 7.0, and miscellaneous ligands, water, and lipid molecules were removed. As the glucocorticoid receptor is primarily found in the cytosol of the cell, therefore, the receptor-ligand complex was simulated in a cubicle box of water with periodic boundary conditions (17). Charges and atom types of JWH-015 were assigned using the CGenFF server (18). The protein and water molecules were modeled using the CHARMM36 force field and TIP3P water model, respectively (19). The CHARMM-GUI input generator was used to setup all the simulated systems (20, 21). All MD simulations were run using the GPU version of NAMD 2.12 and trajectory analysis was done using visual molecular dynamics (VMD) software (22, 23). The system was neutralized (total charge equal to zero) by adding sufficient K^+ ions (5) to the solvated receptor-ligand complex. The particle mesh Ewald method was used to treat long range electrostatic interactions (24). The non-bonded interaction list was generated with a distance cutoff of 14 Å and updated heuristically and Lennard-Jones interactions were truncated at 12 Å. The simulation was run at a constant pressure (1 atm) and temperature of 310 K. The temperature was controlled by using Langevin temperature coupling with a friction coefficient of 1 ps^{-1} (25). The pressure was maintained using a Nose-Hoover Langevin-piston method with a piston period of 50 fs and a decay of 25 fs (26). Covalent bonds to hydrogen atoms were constrained by SHAKE algorithm (27). The 1 fs/step time step was used in equilibration runs and 2 fs/step was used in production runs.

Statistical Analysis

Statistical analysis was performed using GraphPad Prism Software. Data was analyzed using one-way ANOVA followed by Tukey's test for multiple comparisons test to determine which groups are significantly different from each other. **Figures 3A,B** were analyzed using two-way ANOVA followed by multiple comparisons test due to determine the effects of siRNA. All tests assumed normal distribution where $\alpha = 0.05$ was considered significant. *In vitro* experiments were done in at least three different RA cell lines derived from three different RA patients; and data from at least six different rats are presented for *in vivo* experiments. All data are presented at mean ± SEM where error bars represent SEM.

RESULTS

JWH-015 Is Anti-inflammatory in Human RASFs

To begin, we tested the effect of JWH-015 on common RA inflammatory markers (IL-6, IL-8, and COX-2). Before beginning

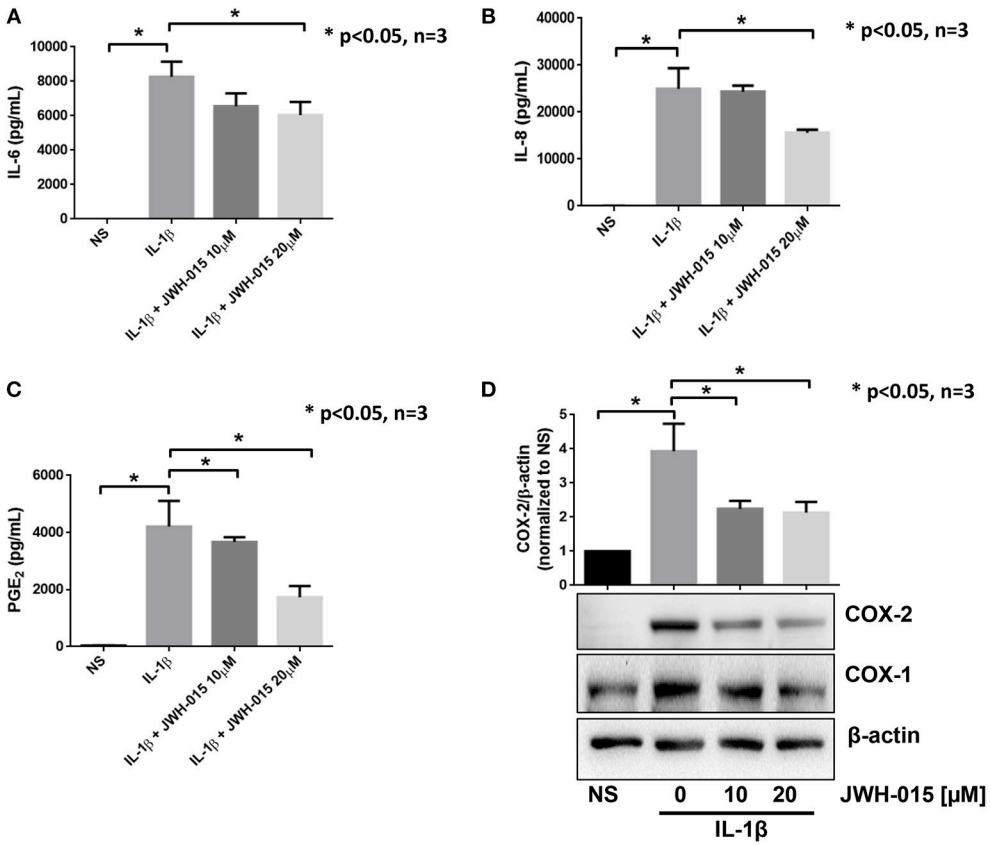

FIGURE 1 | JWH-015 is anti-inflammatory in human RASFs. Upon confluency, RASFs were serum starved overnight prior to being pre-treated with JWH-015 (10 and 20 μM) for 10 min prior to the addition of IL-1β (10 ng/mL) for 24 h. Conditioned media was assayed for IL-6 **(A)**, IL-8 **(B)**, and PGE_2 **(C)**, and **(D)** cell lysates were assayed for COX expression. JWH-015 at either dose did produce a response and was removed for clarity. Bars represent mean ± SEM of $^*p < 0.05$, one-way ANOVA $n = 3$ where 3 different cell lines derived from 3 different RA patients was used. NS, non-stimulated.

studies, we performed a viability assay like the one described previously (28) where we saw no toxicity at the highest tested dose (20 μM). Based on the viability assay and previous literature (29), we selected the 10 and 20 μM doses of JWH-015 for *in vitro* studies.

RASFs were grown to <80% confluency before being serum starved overnight. JWH-015 was added 10 min prior to the addition to IL-1β (10 ng/mL) for 24 h. Evaluation of the conditioned media using ELISA assay showed a ∼46% reduction of IL-6 and a ∼50% reduction of IL-8 (**Figures 1A,B**). COX-2 expression was reduced significantly by ∼40% correlating with a similar reduction of PGE_2 production (**Figures 1C,D**).

JWH-015 Inhibits IL-1β Induced Phosphorylation of TAK1

Because JWH-015 inhibited IL-1β-induced inflammation, we were interested in understanding the mechanism of action of JWH-015 in pretreated human RASFs. We examined the expression of key IL-1β proteins proximal to the IL-1 receptor (IRAK4/TRAF6/TAK1) to the downstream MAPKs (P38, JNK, ERK) in **Figure 2A**. Our Western blot results and densitometric analysis showed that JWH-015 inhibited the activation of p-$TAK1^{Thr184/187}$, a site critical for its kinase activation and important to IL-1β signaling (30, 31). The inhibition of p-TAK1 resulted in a dose-dependent reduction in p-JNK activation, with no marked effect on p-P38 or p-ERK pathways (**Figures 2B,C**). Densitometric analysis showed that p-JNKp46 isoform was significantly inhibited at the highest dose (**Figure 2D**).

JWH-015 Produces Anti-inflammatory Effects Independent of CB2

Recent studies suggest that JWH-015 does not have high enough specificity to solely activate CB2 signaling (32, 33). Therefore, we wanted to examine if the anti-inflammatory action of JWH-015 observed in RASFs was through CB2 activation. Using small interfering RNA (siRNA), we knocked down CB2 expression and performed a similar experiment as shown in **Figure 1** but with the addition of siRNA. CB2 knockdown was confirmed using Western immunoblotting and qRT-PCR (**Supplementary Figures 1A,C**) prior to data analysis. The knockdown of CB2 suppressed IL-1β-induced IL-6 and IL-8 production in human RASFs (**Figures 3A,B**). Interestingly, JWH-015 was still able to further inhibit IL-6 and IL-8

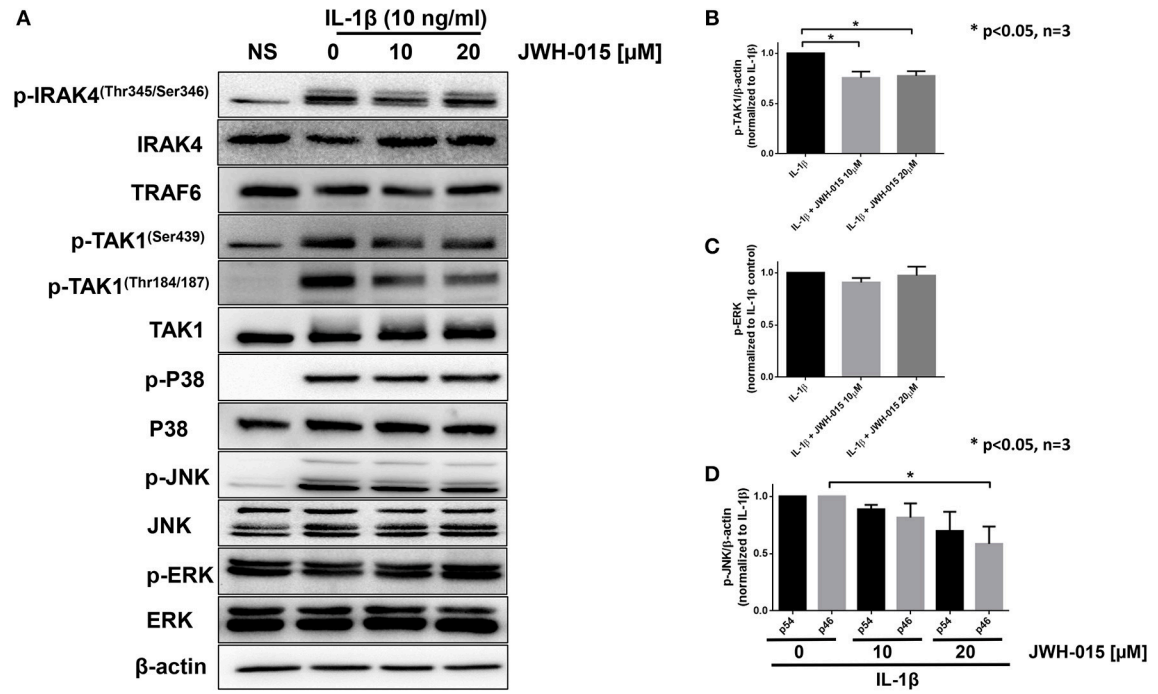

FIGURE 2 | JWH-015 inhibits TAK1 activation. For signaling studies, RASFs were again pre-treated with JWH-015 (10 and 20 μM) for 10 min prior to the addition of IL-1β (10 ng/mL) for 30 min. **(A)** Cell lysates were collected and assayed for IL-1 signaling proteins using Western immunoblotting. Densitometric analysis of **(B)** pTAK-1$^{Thr184/187}$, **(C)** p-ERK, and **(D)** p-JNK p54 and p46 is shown. JWH-015 alone at either dose did produce a response and was removed for clarity. *$p < 0.05$, one-way ANOVA $n = 3$ where 3 different cell lines derived from 3 different RA patients was used. NS, non-stimulated.

production even in the absence of CB2, suggesting JWH-015 may exploit non-canonical pathway independent of endocannabinoid receptors to elicit its anti-inflammatory effects (**Figures 3A,B**).

JWH-015 Binds to Glucocorticoid Receptor

Next, we performed *in silico* molecular docking simulations to determine which receptors JWH-015 may bind to. We looked at receptors that are either known to bind endocannabinoid ligands or have anti-inflammatory effects in RASFs. One receptor which stood out to us was the glucocorticoid receptor (GR) because glucocorticoids have been used to treat RA since the 1950's (34). JWH-015 was docked to GR (PDB ID 4UDD) using MOE software program by induced-fit method allowing protein sidechain flexibility (16). Interestingly, the docked pose of JWH-015 within the GR binding site was found to be very similar to the bound structure of well-known GR ligand dexamethasone co-crystalized with the GR (**Supplementary Figure 2A**). The structurally fit binding pose along with the energetically favorable docking score (-8.0686 kcal/mol) accounting for interactions suggest JWH-015 may interact with GR.

The binding pose and molecular interactions of JWH-015 with GR predicted by the docking simulations were further investigated by a 100 ns long molecular dynamics (MD) simulation of the docked complex. The trajectory analysis (using VMD and in-house *tcl* scripts) revealed some interesting rearrangement (dynamics) of the ligand within the binding site (22). To begin, we observed a transient water-mediated electrostatic interaction between the indole ring nitrogen and the sidechain carbonyl oxygen of N564 that lasted for the first 20 ns (**Figure 3C**). After 20 ns into the simulation, the indole ring of JWH-015 flipped 180° (**Figures 3C,D**) from its initial orientation and engaged in lasting aryl-aryl interaction with W600. The napthyl ring was very stable in its docked orientation and was constantly surrounded by both F623 and L566 throughout the simulation (red and purple lines in **Figure 3E**). There is a strong and stable electrostatic interaction observed between the carbonyl oxygen of the ligand and backbone –NH group of N564 in the binding site. The distance between these two functional groups fluctuated between 3.5 and 5 Å throughout the simulation time (blue line **Figure 3E**) indicating strong electrostatic interactions.

We performed a similar simulation of JWH-015 docked to the CB2 receptor to compare the binding interactions (**Supplementary Figures 2B,C**). The trajectory analysis of CB2-JWH-015 complex revealed several hydrophobic interactions between the ligand and the binding site residues (**Supplementary Figure 2B**). The napthyl and indole rings of the ligand were well surrounded by several aromatic rings of F91, H95, F94, and F106. However, we did not observe any specific electrostatic interactions between the carbonyl oxygen of the ligand and the binding site residues nor any changes in the docked binding pose throughout the simulation time. Because hydrophobic interactions are inherently weaker than hydrogen bonds, MD simulations suggest that JWH-015 has an equal or stronger binding to affinity to GR than to CB2 (**Supplementary Figure 2C**).

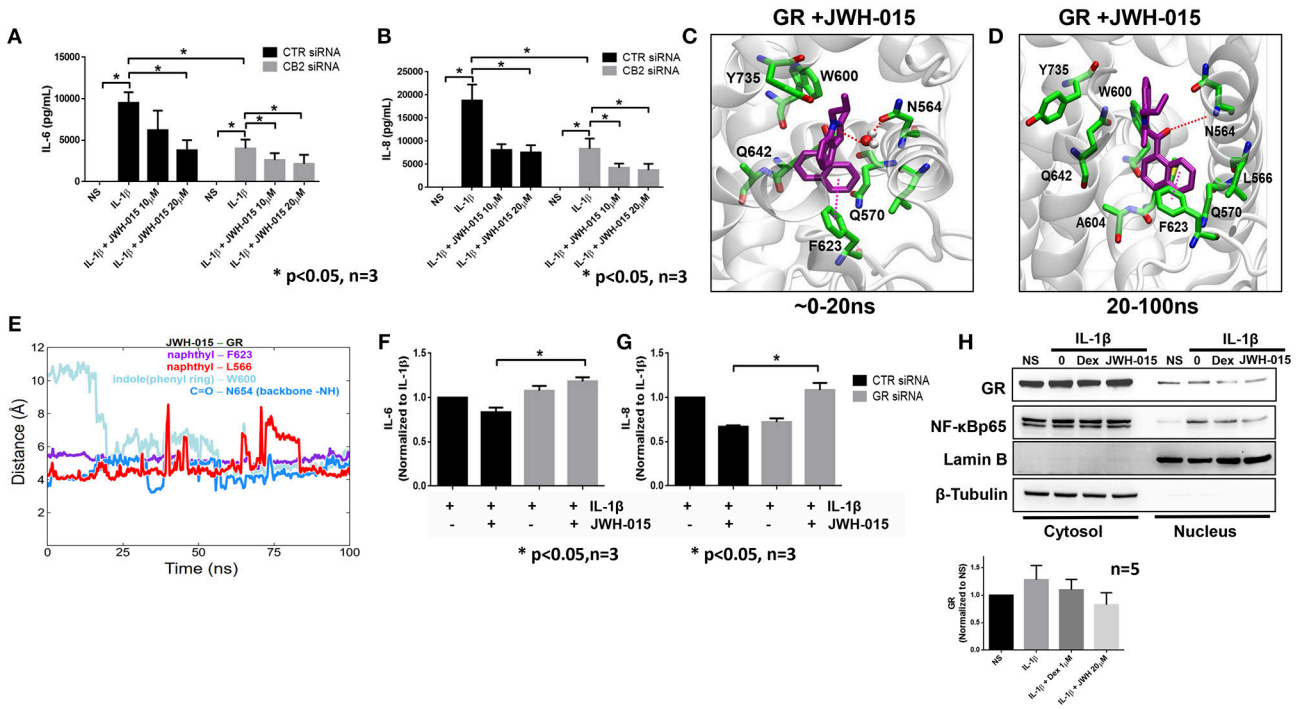

FIGURE 3 | JWH-015 may utilize glucocorticoid receptor for anti-inflammatory action. CB2 was knocked down using 120 pM of targeted siRNA using Lipofectamine 2000 for 8 h. Media was replaced 24 h after transfection then serum starved overnight 48 h later. Next morning cells were stimulated with IL-1β (10 ng/ml) and JWH-015 (10 and 20 μM) for 24 h. Conditioned media was assayed for **(A)** IL-6 and **(B)** IL-8. JWH-015 was docked to the glucocorticoid receptor using MOE software. **(C)** A transient water-mediated electrostatic interaction was observed between the ligand and the sidechain carbonyl oxygen of N564 in GR; **(D)** The indole ring of the ligand flipped 180 degrees and enabling a lasting electrostatic interaction between carbonyl oxygen of the ligand and backbone –NH group of N564; **(E)** distances between the indole and naphthyl rings of the ligand and aromatic rings of W600 and F623 and side chain CH3 group of L566 indicating stable hydrophobic aryl-aryl and aryl-alkyl interactions. GR was knocked down using siRNA for 48 h prior to the addition of IL-1β ± JWH-015 (20 μM) for 24 h. Conditioned media was assayed for **(F)** IL-6 and **(G)** IL-8 production. **(H)** RASFs were pre-treated with Dex (1 μM) for 1 h or JWH-015 (20 μM) for 10 min before IL-1β for 30 min. Cytosolic and nuclear fractions were made and assayed for GR translocation. Densitometric analysis of GR nuclear localization in the presence of JWH-015 (20 μM) and Dex (1 μM). *$p < 0.05$, two-way ANOVA $n = 3$ where 3 different cell lines derived from 3 different RA patients was used. NS, non-stimulated.

To confirm *in vitro* simulation findings, we knocked down the GR receptor using siRNA for 48 h prior to the addition of IL-1β and JWH-015 for 24 h. Again, GR knockdown was confirmed using Western and qRT-PCR (**Supplementary Figures 1B,D**). The absence of GR completely abrogated the ability of JWH-015 to reduce IL-1β-induced IL-6 and IL-8 production (**Figures 3F,G**). Finally, we compared JWH-015 with dexamethasone (Dex) at inhibiting nuclear localization of GR. Indeed, JWH-015 showed a modest effect in inhibiting GR and NF-κBp65 nuclear localization, which suggests another possible mechanism of JWH-015's anti-inflammatory properties (**Figure 3H**).

JWH-015 Is Anti-inflammatory in AIA Rat Model of Arthritis

To confirm our *in vitro* findings, we tested the efficacy of JWH-015 *in vivo* using a rat AIA model of inflammatory RA. Rats were administered a daily intraperitoneal dose of JWH-015 (5 mg/kg) followed by AI scores and ankle circumferences measured starting day 9 (at the onset of arthritis) until termination (day 17). One of the few parameters JWH-015 administration was able to significantly reduce were ankle circumference and AI scores by 10.5% and 22.2%, respectively, by day 17 (**Figures 4A,B**) suggesting that JWH-015 is anti-inflammatory.

Von frey measurements were taken every other day beginning on day 8 at onset of inflammation. The amount of force applied in grams to elicit response (paw withdrawal or vocalization) was normalized to day 8 measurements. Rats began to show antinociceptive effects beginning on day 15 however, the effect was the strongest at day 17 (**Figure 4E**, $p = 0.06$). Cachexia is a common side effect of the AIA rat model therefore a gain in body weight shows signs of improvement overall improvement (35). In addition to cachexia, AIA also have enlarged spleens therefore a slight reduction of spleen weight at termination would suggest immunomodulatory effects (36). Although not statistically significant, JWH-015 was able to rescue body weight loss and reduce spleen enlargement in AIA rats at termination indicating reduction in overall inflammatory burden by JWH-015 without immunosuppression in this model (**Figures 4C,D**).

JWH-015 Administration Prevents Bone Degradation in AIA Rats

To better understand the effects of JWH-015 on bone remodeling, we performed μCT-imaging on the ankles using a

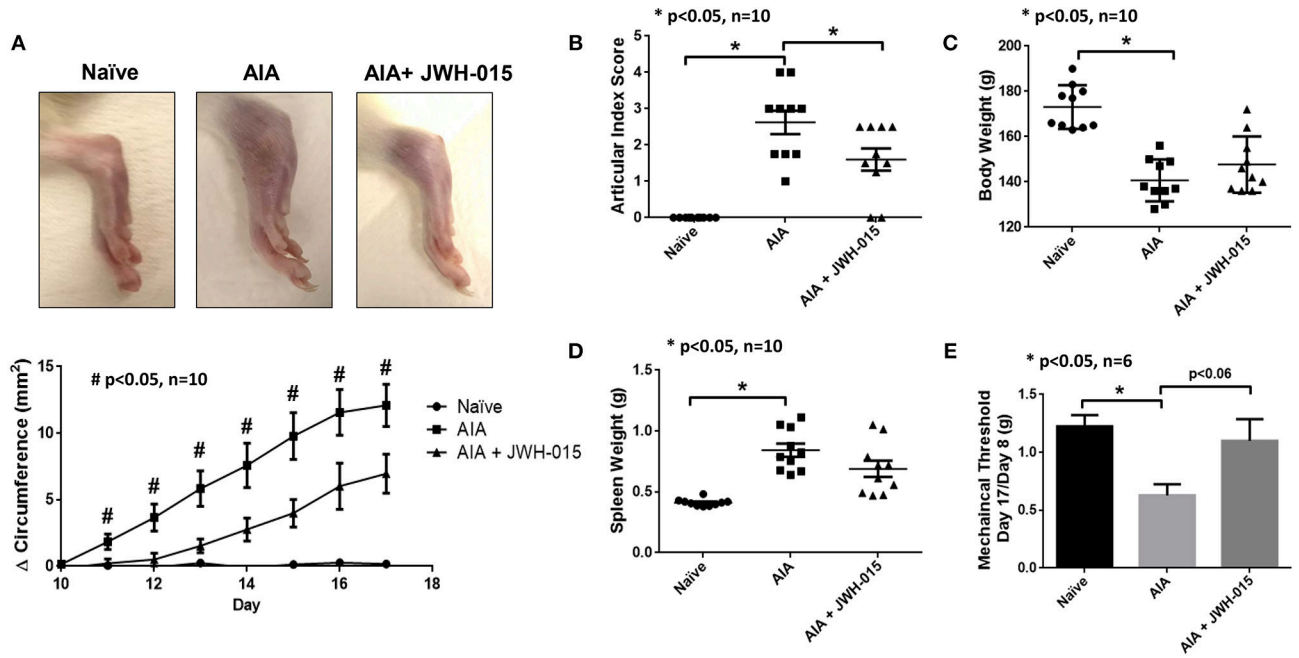

FIGURE 4 | JWH-015 is anti-inflammatory in AIA arthritic rats. JWH-015 was given (5 mg/kg, ip) from day 8–17. Articular index scores were averaged for each animal **(B)** and Δ ankle circumferences **(A)** (normalized to day 0) values were averaged for each animal before group comparisons and final values represented as the mean of "n" number of animals per group. Mean ± SEM is shown for ankle articular index scores (range 0–4) and ankle Δ circumferences (in millimeters) determined on indicated days after adjuvant injection. **(D)** The mean ± SEM increases in body weight and spleen weight **(E)** measured on the final day of the experimentation. **(C)** Mechanical alloydina was measured with Von Frey test where a ratio of the rat's own baseline score at day 8 compared to day 17 was taken before averaged. The mean ± SEM in grams is presented here. *$p < 0.05$ one-way ANOVA $n = 10$ rats per group; *$p < 0.05$ one-way ANOVA $n = 6$ rats per group for Von Frey test. #$p < 0.05$ one-way ANOVA where all comparisons (naïve vs. AIA vs. AIA + JWH-015) are statistically significant $n = 10$ rats per group.

"high resolution" scan mode. Interestingly, we noticed portions of the AIA ankles that were damaged with disease that were not as severely damaged as compared to rats given JWH-015 (**Figure 5A**). Histological analysis was done on the treated and untreated rat joints, in which AIA rats had clear signs of synovitis and considerable amounts of inflammatory cell infiltration and bone loss (**Figure 5D**). In comparison, JWH-015 animals had less inflammatory cell infiltration and cartilage erosion (**Figure 5A**; H&E). Histopathological analysis showed a significant reduction in the inflammation score which included a reduction in immune cell infiltrates (lymphocytes, plasma cells, and macrophages) **Figure 5D**. Because synovitis is associated with pain, this suggests why JWH-015 may have an analgesic effect.

Furthermore, bone mineral density analysis showed distinct changes between naïve and AIA rats where trabecular tissue increased while bone and cortex volume deceased with disease (**Figure 5B**). Among different parameters studied, JWH-015 tended to prevent the trabecular bone from increasing in volume as demonstrated by the statistically significant lower trabecular volume. Again, many of the JWH-015 rats had similar values for intra-trabecular volume to that of the naïve rats, suggesting bone protective effect.

To further confirm these μCT and histological observations, we looked at the serum levels of RANKL and OPG which are important in bone reformation (37). We observed a statistically significant increase serum levels of RANKL in AIA rats and interestingly JWH-015 treated rats had lowered levels of RANKL and concomitantly increased the serum levels of OPG (**Figure 5C**). This suggests that JWH-015 can simultaneously reduce inflammation and bone destruction in inflammatory arthritis.

DISCUSSION

The findings from the present study provide an evidence for the anti-inflammatory role of a CB2 agonist JWH-015 in regulating IL-1β activated inflammatory responses in human RASFs and a rat AIA model of human RA. More importantly, we have identified how JWH-015 does not utilize CB2 for its anti-inflammatory actions, rather we demonstrated that JWH-015 has the capability of interacting with the GR receptor. Interestingly, the site of GR that JWH-015 binds is also exploited by dexamethasone, which may explain the observed inhibitory action triggered by inflammatory pathways. Based on our results revealing how JWH-015 may suppress pain and inflammation by targeting GR receptor in human synovial fibroblasts and in experimental animals, these findings may have rapid clinical application where JWH-015 or structurally similar molecules could be used as an adjunct a non-opioid therapeutic option for the management of pain and inflammation in RA.

JWH-015 has been reported for numerous biological activities, including anti-obesity, pro-apoptotic in thymic atrophy, anti-

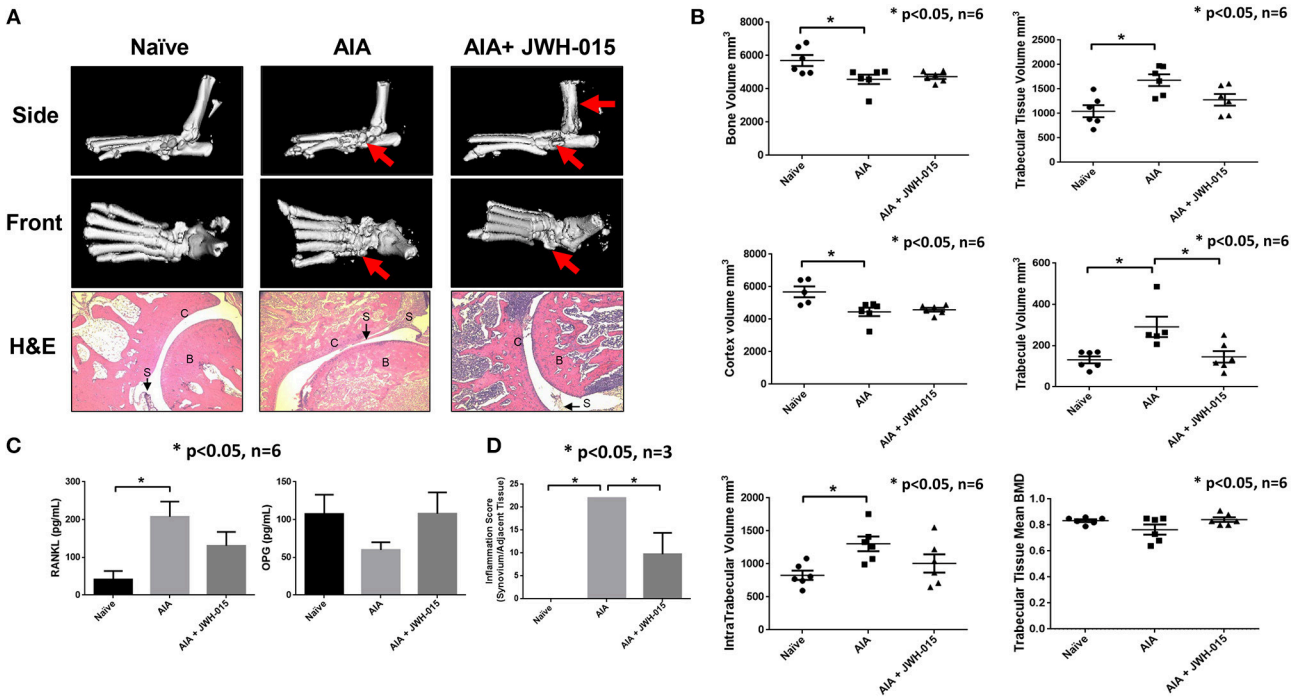

FIGURE 5 | Less bone degradation is observed in animals given JWH-015. **(A)** μCT-imaging was done on the ankles using a "high resolution" scan mode after termination. Red arrows point to areas of apparent bone damage. Joints were then decalcified and 5 μm slices were stained for H&E. "B" marks bone; "C" marks cartilage; and "S" marks synovium. **(B)** Bone mineral analysis was performed on the rat tarsus bone calibrated to a phantom standard. **(C)** Rat serum was assayed for OPG and RANKL using ELISA method. Bars represent mean ± SEM $^*p < 0.05$ $n = 6$ one-way ANOVA. **(D)** Histopathological analysis of H&E slides for synovial inflammation. Parameters and grading scale are described in detail in **Supplementary Tables 1**, **2**. Scores were averaged per group where bars represent mean ± SEM $^*p < 0.05$ $n = 3$ representative animals per group; one-way ANOVA.

cancer, anti-inflammatory, and antinociceptive (29, 32, 38–41). In our study, we observed JWH-015 has anti-inflammatory effects in human RASFs as well as in a rat AIA model of arthritis. In recognizing JWH-015 does not have the strongest specificity to CB2, we anticipated a possibility of JWH-015 utilizing another receptor to produce anti-inflammatory effects. Our results from *in silico* molecular docking of JWH-015 to several potential receptors identified GR as a potential target. These findings were confirmed *in vitro* using siRNA approach to confirm that JWH-015 potentially rely on GR to elicit its anti-inflammatory actions.

Previous studies in RA have been done with other CB2 agonists. Gui et al. used the CB2 agonist HU-308 which has a Ki value of 22.7 nM to CB2 (9); Richardson et al used HU-210 which has a Ki of 0.52 nM at CB2 (8); and a more recent study used WIN 55,212-2 which has a Ki of 3.3 nM to CB2 (42). JWH-015 has a Ki value of 13.8 nM to CB2 and has been looked at in other cells that are involved in RA. In macrophages, JWH-015 was used to show that CB2 is not a chemoattractant receptor in primary murine macrophages and JWH-015 can inhibit chemokine-induced monocyte migration to inflammatory sites (43, 44). However, the underlying mechanism of its action and its effect on RA pathogenesis remains elusive.

At the highest concentration tested (20 μM), JWH-015 was effective in inhibiting IL-6, IL-8, and COX-2 expression, which are prominent inflammatory products of IL-1β signaling in RASFs (14, 31, 45). Upon looking further at the IL-1β signaling, JWH-015 elicits anti-inflammatory effects by inhibiting activation of p-TAK1, which correlated with the inhibition of p-JNK, and p-ERK expression. Previous studies have shown a similar inhibition of p-ERK by HU-308 and HU-210 in RASFs, but without any detailed analysis (8, 9). Interestingly within JNK/SAPK, JWH-015 preferentially inhibited p-JNKp46 isoform, which has been shown by us to be critically involved in IL-1β signaling as it binds to the AP-1 binding site with higher affinity than other JNK isoforms (46).

Although JWH-015 is defined as a CB2 agonist, its selectivity to CB2 is low compared to other readily available agonists. In a recent study, Craft et al. showed JWH-015 to induce anti-nociceptive responses in CFA-induced inflammation in rats via both CB1 and CB2 activation (32). In the rat AIA model, we also observed some analgesic effects, which we hypothesize to be independent of CB2 receptor based on our *in vitro* findings. A recent study done by Soethoudt et al., characterized several CB2 agonists including JWH-015. Using a panel of 64 proteins associated with common side effects from CEREP. The authors reported JWH-015 has 7 off-target receptors. Within the panel, they reported that JWH-015 has 36% efficacy for GR (33). GR is of particular interest to our findings because glucocorticoids have been used as first-line of treatment for RA since 1955 (34). *In silico* molecular

docking of JWH-015 to GR not only produced a favorable binding score, but the docking pose of JWH-015 exhibited a striking resemblance to the bound poses of known GR ligand dexamethasone in the experimentally determined X-ray crystal structures. Molecular dynamic simulations reveals JWH-015 also forms additional hydrogen bonds with GR compared to CB2 where only hydrophobic interactions are observed.

Glucocorticoids mainly elicit their anti-inflammatory effects by interfering with pro-inflammatory transcription factors AP-1 or NF-κB from transcribing pro-inflammatory mediators, but other mechanisms of action for glucocorticoids are also described (34, 47). In our studies, JWH-015 inhibited GR translocation in a similar fashion to dexamethasone in RASFs. Although this result seems contradictory to GR's known mechanism of action, literature has shown that transrepression of GR is also important for its anti-inflammatory function where it can abrogate NF-κBp65 activation (48). Indeed, we observed JWH-015 was able to inhibit NF-κBp65 translocation to the nucleus. This suggests that JWH-015 mediated transrepression of GR into the nucleus may be responsible of JWH-015's anti-inflammatory action. In addition, the nuclear presence of GR can be misleading in that GR translocation does not necessarily produce anti-inflammatory effects. Pariante et al showed that IL-1α was able to enhance GR nuclear localization (49). As previously reported by our group, IL-1α has a similar function to IL-1β which suggests IL-1β can also enhance GR nuclear localization (13). Functional genomics studies are further warranted to validate GR response to extremal stimuli such as JWH-015. GR can also elicit its effects through non-genomic signaling which does not require translocation of GR into the nucleus. Non-genomic signaling has been reported to be important for the treatment of RA, but was not investigated in this study (50). Further studies are warranted to fully confirm that JWH-015 could mimic the functions of glucocorticoids without any adverse effects.

Among several limitations of long-term glucocorticoids use is progressive bone loss (47). Pharmacologically important, JWH-015 administration to AIA rats was able to ameliorate arthritis concomitant to preventing bone degradation. This could be strongly correlated with the significant reduction in serum RANKL and an increase in OPG in the treated rats around day 17 when arthritis peaks and inflammatory markers are highly expressed (36). While we observed histological and CT improvement in the limited window of JWH-015 treatment, extension of dose regimen and duration would have allowed us to validate if bone loss could be completely reverted to naïve levels in BMA analysis.

While the findings from this study are novel and clinically relevant, we acknowledge some limitations with our study. First, CB2 is also expressed in other cell types, including B cells, macrophages, and NK cells that have role in RA pathogenesis (3). Thus, characterizing the biological activity of JWH-015 in other cell types may help us understand the broader impact of JWH-015 or structurally similar molecules. Second, the study by Soethoudt et al., identified off target receptors that JWH-015 showed the binding affinity, including A3, 5-HT2A and 2B, and PPARγ.

In summary, JWH-015 exhibits anti-inflammatory action in human RASFs and in rat AIA model of RA. Further testing of JWH-015 in other models where its impact through GR could be validated may provide an opportunity to develop molecules on similar structure as an adjunct non-opioid analgesic and bone protective agents in inflammatory conditions such as RA.

ETHICS STATEMENT

De-identified human RA synovial tissues were obtained from Cooperative Human Tissue Network (CTHN; Columbus, OH) and National Disease Research Interchange (NDRI; Philadelphia, PA) according to an Institutional Review Board (IRB) approved protocol in compliance with the Helsinki Declaration. The WSU Office of Research Assurances has determined that the study satisfies the criteria for Exempt Research at 45 CFR 46.101(b)(4)(IRB # 17249). All animal studies were approved by the IACUC committee of the Washington State University and conformed to the NIH Guide for the Care the Use of Laboratory Animals. The Approved protocol number is: 004957-006.

AUTHOR CONTRIBUTIONS

SF, AS, SN, and SA conceived and designed experiments. SF, AS, IS, and CS performed the experiments. SF, AS, SN, TM, and SA analyzed the data. SF, SN, and SA wrote the manuscript.

FUNDING

This study was supported by NIH grant AR063104 (SA), the Rheumatology Research Foundation Medical and Graduate Student Preceptorship (SF), and the start-up funds from Washington State University (SA).

ACKNOWLEDGMENTS

The authors thank Dr. Rebecca M. Craft for aiding in the behavioral work in this study. The authors also thank Dr. David A. Fox for providing RASF cell lines. Finally, the authors thank the National Disease Research Interchange (NDRI), Philadelphia, PA and Co-operative Human Tissue Network (CHTN), Columbus, OH for providing additional synovial tissues for RASFs.

SUPPLEMENTARY MATERIAL

The Supplementary Material for this article can be found online at: https://www.frontiersin.org/articles/10.3389/fimmu.2019.01027/full#supplementary-material

REFERENCES

1. Matsuda LA, Lolait SJ, Brownstein MJ, Young AC, Bonner TI. Structure of a cannabinoid receptor and functional expression of the cloned cDNA. *Nature.* (1990) 346:561. doi: 10.1038/346561a0
2. Basu S, Dittel BN. Unraveling the complexities of cannabinoid receptor 2 (CB2) immune regulation in health and disease. *Immunol Res.* (2011) 51:26–38. doi: 10.1007/s12026-011-8210-5
3. Malfitano AM, Basu S, Maresz K, Bifulco M, Dittel BN. What we know and don't know about the cannabinoid receptor 2 (CB2). *Semin Immunol.* (2014) 26:369–79. doi: 10.1016/j.smim.2014.04.002
4. Huffman JW. Cannabimimetic indoles, pyrroles and indenes. *Curr Med Chem.* (1999) 6:705–20.
5. Huffman JW. The search for selective ligands for the CB2 receptor. *Curr Pharm Des.* (2000) 6:1323–37. doi: 10.2174/1381612003399347
6. Regeneron Pharmaceuticals I. *Survey Results Show Eighty Percent of Rheumatoid Arthritis Patients Report Life-Altering Pain Daily or Multiple Times a Week, Despite Treatment [Online]*. @PRNewswire. (2018). Available online at: https://www.prnewswire.com/news-releases.detail.html//content/prnewswire/us/en/news-releases.detail.html/survey-results-show-eighty-percent-of-rheumatoid-arthritis-patients-report-life-altering-pain-daily-or-multiple-times-a-week-despite-treatment-300449267.html.html (accessed April 2, 2019)
7. Lee YC, Cui J, Lu B, Frits ML, Iannaccone CK, Shadick NA, et al. Pain persists in DAS28 rheumatoid arthritis remission but not in ACR/EULAR remission: a longitudinal observational study. *Arthritis Res Ther.* (2011) 13:R83. doi: 10.1186/ar3353
8. Richardson D, Pearson RG, Kurian N, Latif ML, Garle MJ, Barrett DA, et al. Characterisation of the cannabinoid receptor system in synovial tissue and fluid in patients with osteoarthritis and rheumatoid arthritis. *Arthritis Res Ther.* (2008) 10:R43. doi: 10.1186/ar2401
9. Gui H, Liu X, Wang ZW, He DY, Su DF, Dai SM. Expression of cannabinoid receptor 2 and its inhibitory effects on synovial fibroblasts in rheumatoid arthritis. *Rheumatology (Oxford).* (2014) 53:802–9. doi: 10.1093/rheumatology/ket447
10. Burston JJ, Sagar DR, Shao P, Bai M, King E, Brailsford L, et al. Cannabinoid CB2 receptors regulate central sensitization and pain responses associated with osteoarthritis of the knee joint. *PLoS ONE.* (2013) 8:e80440. doi: 10.1371/journal.pone.0080440
11. Selvi E, Lorenzini S, Garcia-Gonzalez E, Maggio R, Lazzerini PE, Capecchi PL, et al. Inhibitory effect of synthetic cannabinoids on cytokine production in rheumatoid fibroblast-like synoviocytes. *Clin Exp Rheumatol.* (2008) 26:574–81.
12. Kim, E. Y., Sudini, K., Singh, A. K., Haque, M., Leaman, D., Khuder, S., et al. Ursolic acid facilitates apoptosis in rheumatoid arthritis synovial fibroblasts by inducing SP1-mediated Noxa expression and proteasomal degradation of Mcl-1. *FASEB J.* (2018) 32:fj201800425R. doi: 10.1096/fj.201800425R
13. Singh AK, Fechtner S, Chourasia M, Sicalo J, Ahmed S. Critical role of IL-1alpha in IL-1beta-induced inflammatory responses: cooperation with NF-kappaBp65 in transcriptional regulation. *FASEB J.* (2019) 33:2526–36. doi: 10.1096/fj.201801513R
14. Ahmed S, Marotte H, Kwan K, Ruth JH, Campbell PL, Rabquer BJ, et al. Epigallocatechin-3-gallate inhibits IL-6 synthesis and suppresses transsignaling by enhancing soluble gp130 production. *Proc Natl Acad Sci USA.* (2008) 105:14692–7. doi: 10.1073/pnas.0802675105
15. Marotte H, Ruth JH, Campbell PL, Koch AE, Ahmed S. Green tea extract inhibits chemokine production, but up-regulates chemokine receptor expression, in rheumatoid arthritis synovial fibroblasts and rat adjuvant-induced arthritis. *Rheumatology (Oxford).* (2010) 49:467–79. doi: 10.1093/rheumatology/kep397
16. MOE. *Molecular Operating Environment (MOE)*, 2013.08. C.C.G. ULC, ed. Montreal, QC: MOE (2019).
17. Oakley RH, Cidlowski JA. The biology of the glucocorticoid receptor: new signaling mechanisms in health and disease. *J Allergy Clin Immunol.* (2013) 132:1033–44. doi: 10.1016/j.jaci.2013.09.007
18. Vanommeslaeghe K, Hatcher E, Acharya C, Kundu S, Zhong S, Shim J, et al. CHARMM general force field: a force field for drug-like molecules compatible with the CHARMM all-atom additive biological force fields. *J Comput Chem.* (2010) 31:671–90. doi: 10.1002/jcc.21367
19. Huang J, MacKerell ADJr. CHARMM36 all-atom additive protein force field: validation based on comparison to NMR data. *J Comput Chem.* (2013) 34:2135–45. doi: 10.1002/jcc.23354
20. Jo S, Kim T, Iyer VG, Im W. CHARMM-GUI: a web-based graphical user interface for CHARMM. *J Comput Chem.* (2008) 29:1859–65. doi: 10.1002/jcc.20945
21. Lee J, Cheng X, Swails JM, Yeom MS, Eastman PK, Lemkul JA, et al. CHARMM-GUI input generator for NAMD, GROMACS, AMBER, OpenMM, and CHARMM/OpenMM simulations using the CHARMM36 additive force field. *J Chem Theory Comput.* (2016) 12:405–13. doi: 10.1021/acs.jctc.5b00935
22. Humphrey W, Dalke A, Schulten K. VMD: visual molecular dynamics. *J Mol Graph.* (1996) 14:33–38. plates: 27.
23. Phillips JC, Braun R, Wang W, Gumbart J, Tajkhorshid E, Villa E, et al. Scalable molecular dynamics with NAMD. *J Comput Chem.* (2005) 26:1781–802. doi: 10.1002/jcc.20289
24. Cheatham TEIII, Miller JL, Fox T, Darden TA, Kollman PA. Molecular dynamics simulations on solvated biomolecular systems: the particle mesh ewald method leads to stable trajectories of DNA, RNA, and proteins. *J Am Chem Soc.* (1995) 117:4193–4. doi: 10.1021/ja00119a045
25. Feller SE, Zhang YH, Pastor RW, Brooks BR. Constant-pressure molecular-dynamics simulation - the langevin piston method. *J Chem Phys.* (1995) 103:4613–21. doi: 10.1063/1.470648
26. Martyna GJ, Tobias DJ, Klein ML. Constant-pressure molecular-dynamics algorithms. *J Chem Phys.* (1994) 101:4177–89. doi: 10.1063/1.467468
27. Ryckaert J-P, Ciccotti G, Berendsen HJC. Numerical integration of the cartesian equations of motion of a system with constraints: molecular dynamics of n-alkanes. *J Comput Phys.* (1977) 23:327–41. doi: 10.1016/0021-9991(77)90098-5
28. Ahmed S, Pakozdi A, Koch AE. Regulation of interleukin-1beta-induced chemokine production and matrix metalloproteinase 2 activation by epigallocatechin-3-gallate in rheumatoid arthritis synovial fibroblasts. *Arthritis Rheum.* (2006) 54:2393–401. doi: 10.1002/art.22023
29. Lombard C, Nagarkatti M, Nagarkatti P. CB2 cannabinoid receptor agonist, JWH-015, triggers apoptosis in immune cells: potential role for CB2-selective ligands as immunosuppressive agents. *Clin Immunol.* (2007) 122:259–70. doi: 10.1016/j.clim.2006.11.002
30. Singh AK, Umar S, Riegsecker S, Chourasia M, Ahmed S. Regulation of TAK1 activation by epigallocatechin-3-gallate in RA synovial fibroblasts: Suppression of K63-linked autoubiquitination of TRAF6. *Arthr Rheumatol.* (2016) 68:347–58. doi: 10.1002/art.39447
31. Fechtner S, Singh A, Chourasia M, Ahmed S. Molecular insights into the differences in anti-inflammatory activities of green tea catechins on IL-1beta signaling in rheumatoid arthritis synovial fibroblasts. *Toxicol Appl Pharmacol.* (2017) 329:112–20. doi: 10.1016/j.taap.2017.05.016
32. Craft RM, Greene NZ, Wakley AA. Antinociceptive effects of JWH015 in female and male rats. *Behav Pharmacol.* (2017) 29(2 and 3-Spec Issue):280–9. doi: 10.1097/fbp.0000000000000337
33. Soethoudt M, Grether U, Fingerle J, Grim TW, Fezza F, de Petrocellis L, et al. Cannabinoid CB2 receptor ligand profiling reveals biased signalling and off-target activity. *Nat Commun.* (2017) 8:13958. doi: 10.1038/ncomms13958
34. Buttgereit F, Burmester G-R, Straub RH, Seibel MJ, Zhou H. Exogenous and endogenous glucocorticoids in rheumatic diseases. *Arthritis Rheum.* (2010) 63:1–9. doi: 10.1002/art.30070
35. Roubenoff R, Freeman LM, Smith DE, Abad LW, Dinarello CA, Kehayias JJ. Adjuvant arthritis as a model of inflammatory cachexia. *Arthritis Rheum.* (1997) 40:534–9.
36. Bendele A. Animal models of rheumatoid arthritis. *J Musculoskel Neuron Interact.* (2001) 1:377–85.
37. Boyce BF, Xing L. Biology of RANK, RANKL, and osteoprotegerin. *Arthritis Res Ther.* (2007) 9(Suppl. 1):S1. doi: 10.1186/ar2165
38. Verty AN, Stefanidis A, McAinch AJ, Hryciw DH, Oldfield B. Anti-obesity effect of the CB2 receptor agonist JWH-015 in diet-induced obese mice. *PLoS ONE.* (2015) 10:e0140592. doi: 10.1371/journal.pone.0140592
39. Ravi J, Elbaz M, Wani NA, Nasser MW, Ganju RK. Cannabinoid receptor-2 agonist inhibits macrophage induced EMT in non-small cell lung cancer

by downregulation of EGFR pathway. *Mol Carcinog.* (2016) 55:2063–76. doi: 10.1002/mc.22451

40. Bort A, Alvarado-Vazquez PA, Moracho-Vilrriales C, Virga KG, Gumina G, Romero-Sandoval A, et al. Effects of JWH015 in cytokine secretion in primary human keratinocytes and fibroblasts and its suitability for topical/transdermal delivery. *Mol Pain.* (2017) 13:1744806916688220. doi: 10.1177/1744806916688220
41. Elbaz M, Ahirwar D, Ravi J, Nasser MW, Ganju RK. Novel role of cannabinoid receptor 2 in inhibiting EGF/EGFR and IGF-I/IGF-IR pathways in breast cancer. *Oncotarget.* (2017) 8:29668–78. doi: 10.18632/oncotarget.9408
42. Lowin T, Pongratz G, Straub RH. The synthetic cannabinoid WIN55,212-2 mesylate decreases the production of inflammatory mediators in rheumatoid arthritis synovial fibroblasts by activating CB2, TRPV1, TRPA1 and yet unidentified receptor targets. *J Inflamm (Lond).* (2016) 13:15. doi: 10.1186/s12950-016-0114-7
43. Montecucco F, Burger F, Mach F, Steffens S. CB2 cannabinoid receptor agonist JWH-015 modulates human monocyte migration through defined intracellular signaling pathways. *Am J Physiol Heart Circ Physiol.* (2008) 294:H1145–55. doi: 10.1152/ajpheart.01328.2007
44. Taylor L, Christou I, Kapellos TS, Buchan A, Brodermann MH, Gianella-Borradori M, et al. Primary macrophage chemotaxis induced by cannabinoid receptor 2 agonists occurs independently of the CB2 receptor. *Sci Rep.* (2015) 5:10682. doi: 10.1038/srep10682
45. Ahmed S, Rahman A, Hasnain A, Lalonde M, Goldberg VM, Haqqi TM. Green tea polyphenol epigallocatechin-3-gallate inhibits the IL-1 beta-induced activity and expression of cyclooxygenase-2 and nitric oxide synthase-2 in human chondrocytes. *Free Radic Biol Med.* (2002) 33:1097–105. doi: 10.1016/S0891-5849(02)01004-3
46. Singh R, Ahmed S, Malemud CJ, Goldberg VM, Haqqi TM. Epigallocatechin-3-gallate selectively inhibits interleukin-1beta-induced activation of mitogen activated protein kinase subgroup c-Jun N-terminal kinase in human osteoarthritis chondrocytes. *J Orthop Res.* (2003) 21:102–9. doi: 10.1016/s0736-0266(02)00089-x
47. Rhen T, Cidlowski JA. Antiinflammatory action of glucocorticoids — new mechanisms for old drugs. *N Engl J Med.* (2005) 353:1711–23. doi: 10.1056/NEJMra050541
48. Ray A, Prefontaine KE. Physical association and functional antagonism between the p65 subunit of transcription factor NF-kappa B and the glucocorticoid receptor. *Proc Natl Acad Sci USA.* (1994) 91:752–6.
49. Pariante CM, Pearce BD, Pisell TL, Sanchez CI, Po C, Su C, et al. The proinflammatory cytokine, interleukin-1alpha, reduces glucocorticoid receptor translocation and function. *Endocrinology.* (1999) 140:4359–66. doi: 10.1210/endo.140.9.6986
50. Löwenberg M, Stahn C, Hommes DW, Buttgereit F. Novel insights into mechanisms of glucocorticoid action and the development of new glucocorticoid receptor ligands. *Steroids.* (2008) 73:1025–9. doi: 10.1016/j.steroids.2007.12.002

Conflict of Interest Statement: TM is employed by the ETHICON. All other authors declare no competing interests.

frontiers in Immunology

ORIGINAL RESEARCH
published: 06 June 2019
doi: 10.3389/fimmu.2019.01304

Kirenol Inhibits the Function and Inflammation of Fibroblast-like Synoviocytes in Rheumatoid Arthritis *in vitro* and *in vivo*

Jing Wu[1†], Qiang Li[1†], Li Jin[1], Yuan Qu[1], Bi-Bo Liang[1], Xiao-Tong Zhu[1], Hong-Yan Du[2], Li-Gang Jie[1] and Qing-Hong Yu[1*]*

[1] Rheumatology and Clinical Immunology, ZhuJiang Hospital, Southern Medical University, Guangzhou, China, [2] School of Laboratory Medicine and Biotechnology, Southern Medical University, Guangzhou, China

OPEN ACCESS

Edited by:
Hanshi Xu,
First Affiliated Hospital of Sun Yat-sen University, China

Reviewed by:
Wenfeng Tan,
Nanjing Medical University, China
Balik Dzhambazov,
Plovdiv University Paisii Hilendarski, Bulgaria

***Correspondence:**
Li-Gang Jie
jieligang@hotmail.com
Qing-Hong Yu
yuqinghong@smu.edu.cn

[†] These authors have contributed equally to this work

Specialty section:
This article was submitted to Autoimmune and Autoinflammatory Disorders, a section of the journal Frontiers in Immunology

Received: 04 March 2019
Accepted: 22 May 2019
Published: 06 June 2019

Citation:
Wu J, Li Q, Jin L, Qu Y, Liang B-B, Zhu X-T, Du H-Y, Jie L-G and Yu Q-H (2019) Kirenol Inhibits the Function and Inflammation of Fibroblast-like Synoviocytes in Rheumatoid Arthritis in vitro and in vivo. Front. Immunol. 10:1304. doi: 10.3389/fimmu.2019.01304

Kirenol is a diterpenoid extracted from the Chinese herbal medicine *Siegesbeckiae*. *Siegesbeckiae* has been used to treat Rheumatoid arthritis (RA) in China for several centuries. RA is characterized by the proliferation of synoviocytes in inflamed synovia, as well as by their expression of inflammatory cytokines. In the present study, we found that Kirenol inhibited the migration, invasion, and proinflammatory of IL-6 secretion of RA-associated synovial fibroblasts (FLS) at a concentration of 100–200 μg/ml *in vitro*. Proinflammatory cytokines production and synovium hyperplasia and cartilage erosion were also inhibited in a collagen-induced arthritis (CIA) mouse model upon Kirenol treatment. Together, our results thus confirm that Kirenol has potent therapeutic efficacy in RA owing to its ability to suppress negative FLS activities.

Keywords: kirenol, Rheumatoid arthritis, fibroblast-like synoviocytes, IL-6, migration, invasion

INTRODUCTION

RA is a chronic and refractory autoimmune joint disease characterized by the proliferation of synoviocytes in the inflamed synovia, and by the expression of inflammatory cytokines on these cells (1). Synovial fibroblasts (FLS) promote joint destruction via their attachment to the cartilage, and thus are key mediators of the pathogenesis of RA (2). Although there are many RA treatment options available, including traditional disease-modifying antirheumatic drugs (DMARDs) as well new and effective biologicals agents, these treatments ultimately induce remission in only 20–68% of patients (3). Moreover, there is still ample opportunity for the development of novel drugs capable of inhibiting synovial hyperplasia. Kirenol is a diterpenoid compound derived from *Herba Siegesbeckia* that has been traditionally used in China to treat RA for centuries. Kirenol has been suggested to exhibit primary anti-inflammatory and anti-rheumatic activities (4, 5). The active ingredient Kirenol in *Herba Siegesbeckia* extracts was shown to reduce the inflammatory pathology in collagen induced arthritis (CIA) model rats, and additional studies suggest that Kirenol is able to suppress the production of IL-1β and TNF-α in the serum of adjuvant arthritis model animals (5, 6). While multiple studies have thus demonstrated the anti-inflammatory properties of Kirenol, there is still very limited information available regarding the specific mechanisms and dynamics whereby Kirenol affects RA-associated FLS cells both *in vitro* and *in vivo*. The inflammatory milieu in the synovial compartment is regulated by a complex cytokine network. Many pro-inflammatory cytokines such as TNF-α, IL-1β, and IL-6, are thought to contribute to the pathological

development and progression of RA (7). Activated FLS cells secrete large quantities of IL-6 and IL-8 (8). Antibodies directed against TNF-α and IL-6 have shown efficacy for the treatment of RA, consistent with the fact that joint destruction is positively correlated with pro-inflammatory cytokine levels in the serum or synovial tissue. Multiple cytokines and matrix metalloproteinases (MMPs) are present in the synovium of RA patients, where they play important roles in the maintenance of inflammatory responses (9, 10). Certain proteins and cytokines, including IL-6, IL-8, TNF-α, IL-1β, and MMP-1, 2, 3, 9 have been identified as diagnostic indicators of RA and as possible therapeutic targets. As such, any effort to determine how Kirenol affects FLS cells necessitates an investigation of its effects on cytokine production.

The pathophysiology of RA involves chronic inflammation and pannus formation in the synovial membrane, which can lead to the destruction of articular cartilage and bone. As these pro-inflammatory cytokines and MMPs are specifically involved in the pathogenesis in RA and are highly expressed in the serum and synovial fluid of RA patients, we hypothesized that these factors may be downregulated by Kirenol. The aims of this study were therefore to evaluate whether Kirenol treatment leads to decreased production of these factors by RA-associated FLS cells, and to explore the underlying molecular mechanisms governing such regulatory activity.

MATERIALS AND METHODS

Human FLS Culture

Synovial tissue samples were obtained from the knees of five patients with active RA (as diagnosed according to the 2010 Rheumatoid arthritis classification criteria) during knee joint arthroscopic operations. The synovial tissue was cut into 1–2 mm^3 pieces and distributed evenly in a culture flask. After 4 h, this flask was inverted and the synovial tissue was cultured in DMEM containing 10% fetal calf serum, 100 U/ml penicillin, and 100 μg/ml streptomycin in a humid incubator containing 5% CO_2. Cell media was changed every 3–4 days. The FLS cells were grown in a monolayer, and cells between the third and sixth generations were used for all experiments.

Cell Viability Assays

Cell viability was detected using the CCK-8 kit (Dojindo, China) according to the provided instructions. Briefly, cultured RA-FLS cells were plated in 96-well plates at a density of 1×10^3 cells/well in DMEM containing 10% FBS. Cells were then incubated with Kirenol (50, 100, and 200 μg/ml; Herbpurity, China) for another 24 h. Human IL-17A (100 ng/ml, R&D, USA) and TNF-α (100 ng/ml, R&D, USA) were used as positive controls. After this incubation period, 10 μL of the CCK-8 solution was added to each well and cells were incubated for 4 h. The absorbance at 450 nm was then measured via a microplate reader.

Quantitative PCR

RA-FLS cells were seeded in 24-well plates at a density of 2×10^4 cells/well for 24 h, and were then treated with Kirenol at concentrations of 50, 100, or 200 μg/ml for 4 h, with positive controls employed as above. Total FLS RNA was then isolated at appropriates using the Trizol reagent (Invitrogen, USA) according to the manufacturer's protocols. Reverse transcription was conducted using a first-strand cDNA synthesis kit (TaKaRa, China). To assess IL-6, IL-8, MMP1, MMP2, MMP3, MMP9, NFκB P50, NFκB P65, MAPK, JNK, and JAK expression, real-time PCR was performed using a SYBR Premix ExTaq kit (TaKaRa, China). Resultant heatmap figures were prepared using the R software [package(heatmap)].

ELISAs

After being treated as described above, 2×10^4 RA-FLS cells were treated with Kirenol for 4 or 24 h. Supernatants were then collected to measure IL-6, IL-8, IL-1β, and TNF-α. For *in vivo* experiments, murine serum was similarly used for cytokine detection. ELISA kits used included those specific for IL-1β (R&D, USA), TNF-α (Thermo Fisher Scientific, USA), IL-6 (Thermo Fisher Scientific, USA), IL-8 (Thermo Fisher Scientific, USA). The optical density (OD) value for each sample was determined at 450 nm.

Western Blotting

RIPA lysis buffer (50 mM Tris-Cl pH 7.4, 150 mM NaCl, 1% Triton X-100, 1% sodium deoxycholate, 0.1% SDS), containing protease and phosphatase inhibitors as well as phenylmethanesulfonyl fluoride (PMSF), was used to lyse and collect protein from cell samples. Protein was then loaded onto 8% polyacrylamide Tris/glycine gels and separated at 80 V for 30 min, followed by 110 V for 1 h, and samples were then transferred to a nitrocellulose membrane at 100 V for 2 h. After blocking, the membranes were probed using the MAPK Family Antibody Sampler Kit (Cell Signaling Technology, USA), NF-κB Pathway Sampler Kit (Cell Signaling Technology, USA), or Phospho-Jak Family Antibody Sampler Kit (Cell Signaling Technology, USA). Phospho-antibodies were diluted to 1:100, while all others were diluted to 1:500. After chemiluminescence development (SignalFire™ ECL Reagent, Cell Signaling Technology, USA), gel images were scanned and analyzed using the Image J (v1.52) image processing software.

Murine synovial tissues were taken from around the hip joints, as described in our previously research method (11). For murine synovium samples, western blotting was performed as above, using IL-6, IL-8, and TNF-α antibodies purchased from Biomathematics and Statistics Scotland (China).

Measures of FLS Migration and Invasion

Wound Healing Assay

To demonstrate the effects of Kirenol on the migratory capacity of FLS, a wound healing assay was performed. 2×10^5/well RA-FLS were seeded in 24-well plates for 24 h, after which a 200 μl pipette tip was used to create a straight scratch wound in the monolayer. Cells were then incubated with Kirenol (50, 100, or 200 μg/ml) for an additional 48 h, with cell being imaged after 0, 4, 24, and 48 h. Image J (v1.52) was used to analyze the migratory wound healing dynamics.

Transwell Migration and Invasion Assays

To further explore the effects of Kirenol on cellular responses, chemotaxis assays were performed using transwell chambers with an 8.0 μm pore size (Corning, USA). Cells were incubated with Kirenol concentrations as described above for 24 h, and then a total of 2×10^5 FLS in serum-free DMEM were added to the upper chambers of these Transwell systems for 8 h. In addition, 600 μl of DMEM medium containing 10% FBS was added to the lower chamber of each well in a 24-well plate. In parallel, similar invasion assays were performed using an 8.0 μm PET membrane (Corning, USA). For this experiment, FLS were seeded at a density of 1×10^5/ml and were grown in DMEM for 12 h. Cells that failed to migrate were removed with a cotton swab, after which the membranes were fixed with 4% paraformaldehyde for 30 min and then stained with 0.1% crystal violet. Migration was quantified by counting the number of stained cells that had migrated to the lower side of the filter using an optical microscope. The average of the number of invading cells from the six random fields of view after normalization to control were used to determine rates of chemotaxis/invasion.

Murine Experiments

Arthritis Model Development

CIA was induced in 9-week-old male DBA/1 mice. Mice were purchased from HuFukang Biotechnology Co., China (license number: SCXK (Jing) 2014-0004). All experiments were performed in accordance with the guidelines of the local animal ethics committee. A total of 15 mice were divided into 3 groups, and received 0, 7.5, or 30 mg/kg Kirenol q.d. Mice were treated with Kirenol for 1 week before being immunized with 100 μg of bovine type II collagen and complete Freund's adjuvant (CFA; 1:1, Xinbosheng, China and Sigma, Japan) by injection at the tail base. A booster injection was administered on day 21, at which time a total of 100 μg collagen II was administered in Freund's incomplete adjuvant (Sigma, Japan). Assessment of arthritis in each limb of these arthritic model mice was then performed via visual scoring from 0 to 4. A maximal score for an individual animal was 16 (12). The weight of each mouse was also recorded once per week.

Histological Scoring

Joints were removed from CIA model mice and fixed in 10% formalin, after which they were decalcified in 10% EDTA, embedded in paraffin, and stained with hematoxylin and eosin (H&E) for light microscopy. Infiltration of inflammatory cells, transformation of the synovial lining, cartilage destruction, and pannus formation were independently scored in a blinded manner from 0 to 3 as in previous studies (13). Of the four limbs analyzed per animal, the maximum score for each category was used, with a maximum possible histological score of 12. Synovial inflammation and bone erosion scores were also performed as described previously, with a maximum possible score of 4 (14). Synovial inflammation was scored as follows: 0- no inflammation; 1- slight synovitis with some cell infiltration; 2- moderate synovitis with moderate cell infiltration; 3- extensive synovitis with a moderate number of infiltrating cells; 4- extensive and severe synovitis, with the presence of numerous inflammatory cells. Bone erosion was scored as follows: 0- no erosion; 1- small areas of resorption; 2- numerous areas of resorption; 3- extensive osteolysis; 4- extensive and severe osteolysis.

Immunohistochemistry

Joints sections were deparaffinized and washed with Tris-buffered saline (TBS) for 10 min and distilled water for 10 min, after which antigen retrieval was performed via heating samples in citrate buffer for 15 min. Samples were then incubated with primary antibodies against IL-6 (Servicebio, USA), IL-8 (Servicebio, USA), and TNF-α (Servicebio, USA), (1:50) at 4°C for 12 h, followed by incubation with a secondary antibody (goat anti rabbit, 1:50, servicebio, USA) at room temperature for 50 min. For antigen visualization, DAB solution was used for color development for 5 min, after which the Image J (v1.52) and IHC Toolbox.jar (USA) programs were used for image analysis.

Statistical Analysis

Data are presented as means ± standard deviation. Differences among groups were analyzed via the Kruskal-Wallis test (more than two groups) or Mann-Whitney *U*-test (two groups) using GraphPad Prism v5.0 (USA). Differences were considered to be statistically significant at $p < 0.05$.

RESULTS

Kirenol Inhibits RA-FLS Proliferation

To determine whether Kirenol affects the proliferation of FLS, cells were stimulated with Kirenol (50, 100, or 200 μg/ml) and control in medium containing DMEM. As shown in **Figure 1A**, Kirenol impaired the proliferation of FLS in a dose-dependent manner. Even when FLS were stimulated with inflammatory cytokines as a positive control (TNF-α 100 ng/ml and IL-17A 100 ng/ml), Kirenol was still able to mildly inhibit their proliferation (**Figures 1B,C**).

Kirenol Inhibits the Secretion of Cytokines by RA-FLS

As shown in **Figures 1D–F**, Kirenol inhibited the secretion of IL-6 by FLS with a dose-dependent manner even when cells were stimulated using TNF-α and IL-17A. However, Kirenol only significantly inhibited FLS IL-8 secretion after 30 min (**Figure 1G**), and no changes in IL-8 secretion were observed at any time in the TNF-α and IL-17A-stimulated groups. We were not able to detect significant levels of IL-1β or TNF-α in FLS supernatants at any time.

Kirenol Downregulates IL-6, IL-8, MMP-9, MAPK, P65, P50, and JAK Expression in RA-FLS

RT-PCR was performed to assess the expression of IL-6, IL-8, MMP-1, 2, 3, 9, NFκBP65, P50, MAPK, and JAK in FLS cells treated with Kirenol. We found that expression of IL-6 and IL-8 were down-regulated by Kirenol in the presence or absence of IL-17A and TNF-α stimulation (**Figure 2A**). Similarly, MMP-9, NFκB, MAPK, and JAK were down-regulated

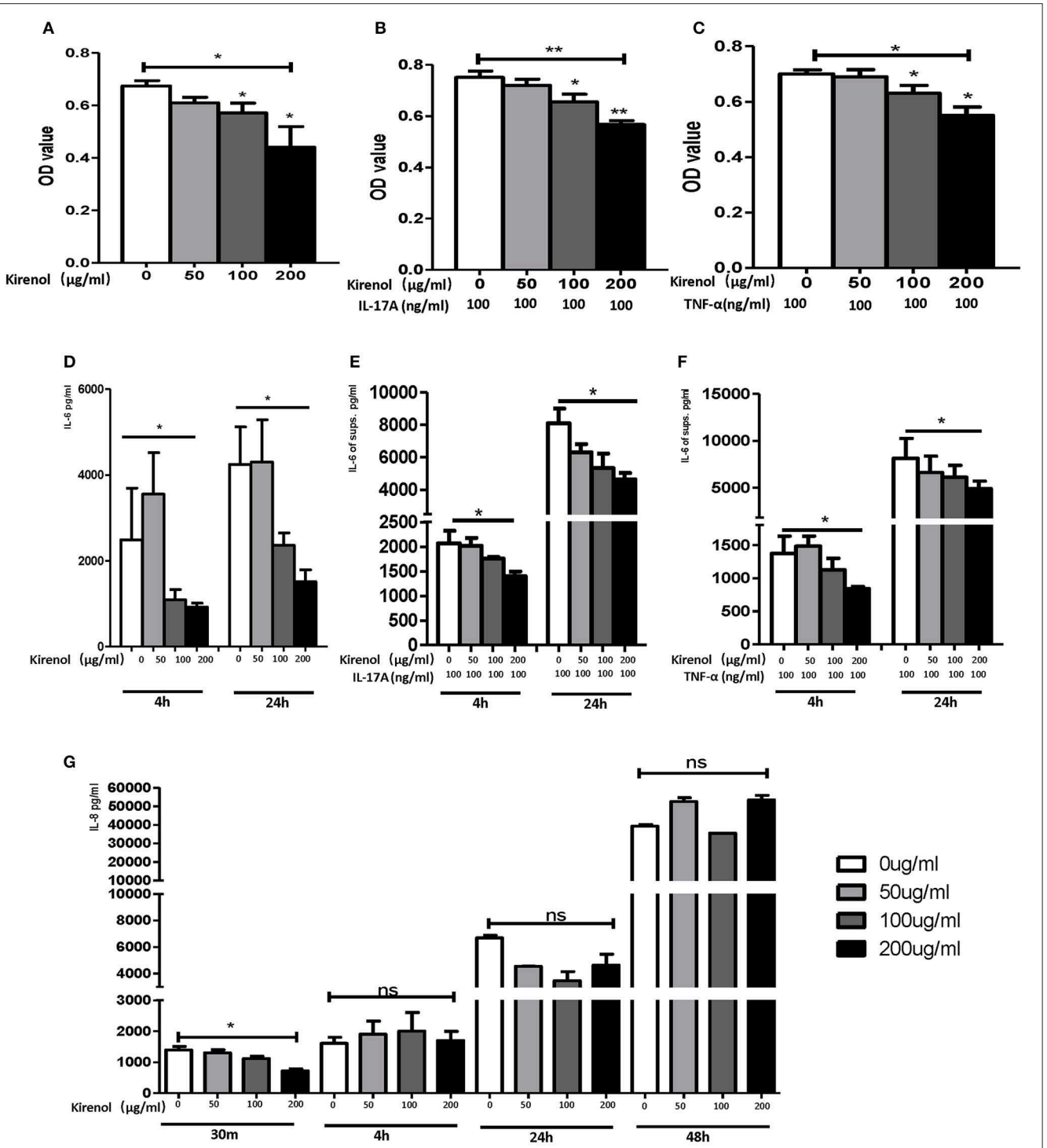

FIGURE 1 | (A) Kirenol inhibited FLS in a dose-dependent manner; **(B)** Kirenol inhibited the proliferation of FLS stimulated with IL-17A (100 ng/ml); **(C)** Kirenol inhibited the proliferation of FLS stimulated with TNF-α (100 ng/ml); **(D)** Kirenol inhibited the secretion of IL-6 by FLS in a dose-dependent manner after 4 and 24 h. **(E)** Kirenol inhibited the secretion of IL-6 by FLS stimulated with IL-17A in a dose-dependent after 4 and 24 h. **(F)** Kirenol inhibited the secretion of IL-6 by FLS stimulated with TNF-α in a dose-dependent after 4 and 24 h. **(G)** Kirenol inhibited the secretion of IL-8 by FLS in a dose-dependent manner after 30 min but not at other time points. $^{*}p < 0.05$, $^{**}p < 0.01$ as assessed by the Kruskal-Wallis test and the Mann-Whitney *U*-test.

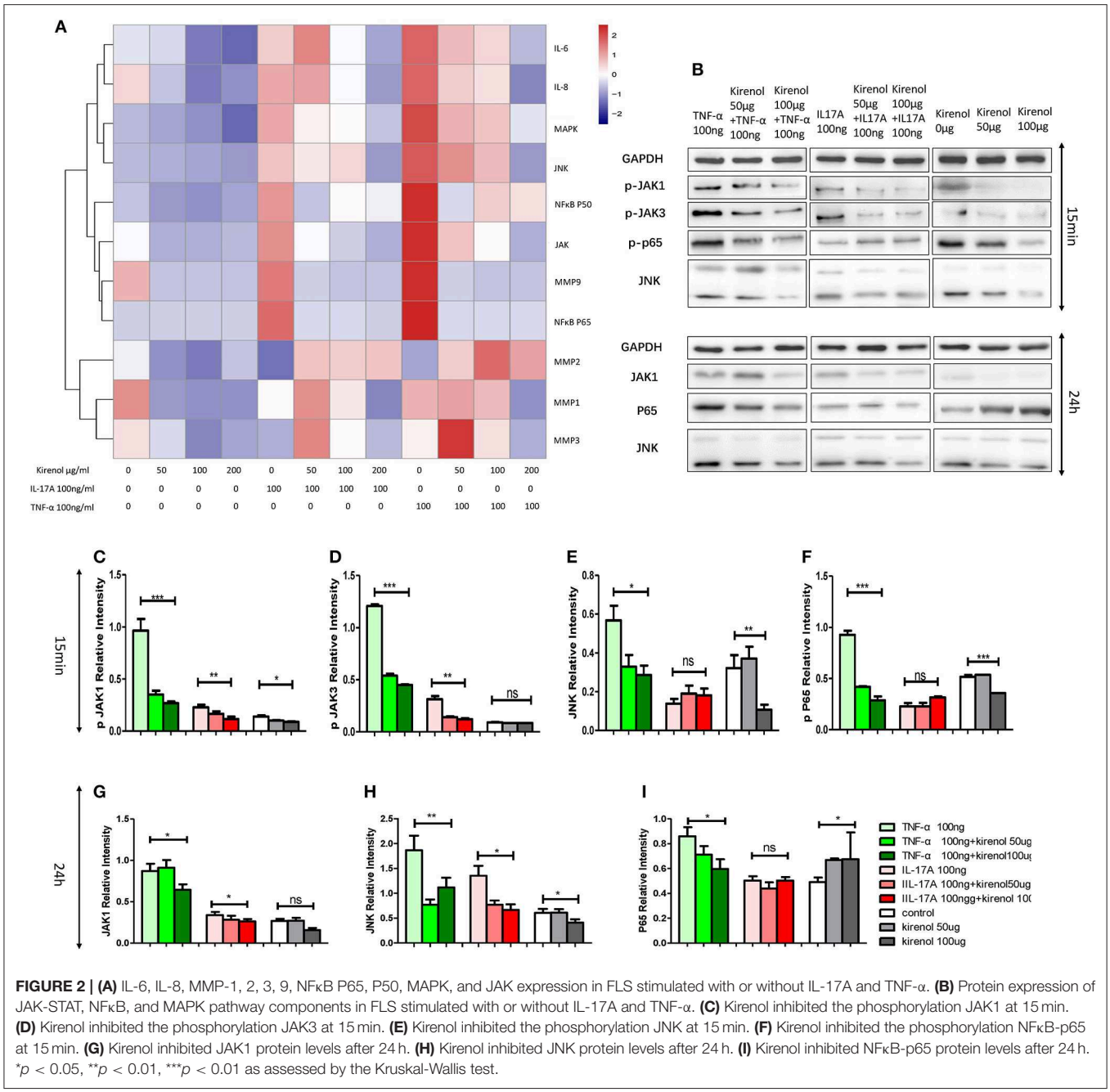

FIGURE 2 | (A) IL-6, IL-8, MMP-1, 2, 3, 9, NFκB P65, P50, MAPK, and JAK expression in FLS stimulated with or without IL-17A and TNF-α. **(B)** Protein expression of JAK-STAT, NFκB, and MAPK pathway components in FLS stimulated with or without IL-17A and TNF-α. **(C)** Kirenol inhibited the phosphorylation JAK1 at 15 min. **(D)** Kirenol inhibited the phosphorylation JAK3 at 15 min. **(E)** Kirenol inhibited the phosphorylation JNK at 15 min. **(F)** Kirenol inhibited the phosphorylation NFκB-p65 at 15 min. **(G)** Kirenol inhibited JAK1 protein levels after 24 h. **(H)** Kirenol inhibited JNK protein levels after 24 h. **(I)** Kirenol inhibited NFκB-p65 protein levels after 24 h. $^{*}p < 0.05$, $^{**}p < 0.01$, $^{***}p < 0.01$ as assessed by the Kruskal-Wallis test.

by Kirenol, particularly following TNF-α stimulation. Kirenol had no apparent effect on MMP-1, 2, or 3 expression.

Kirenol Down-Regulates JAK-STAT and NFκB but not MAPK Protein Levels in RA-FLS

To verify our RT-PCR results, Western blotting was next used to assess levels of key proteins in the MAPK, JAK-STAT, and NFκB pathways in these RA-FLS cells. We found that Kirenol affected the phosphorylation of JAK1 and JAK3 in the JAK-STAT pathways, as well as the phosphorylation of NFκB p65 in the first 15 min following TNF-α stimulation, after which no clear differences in protein phosphorylation were evident (**Figures 2B–I**).

Kirenol Alters the Migration and Invasion of FLS

We next assessed the effects of Kirenol on cellular migration and invasion, and found that it inhibited both activities even when cells were stimulated with IL-17 and TNF-α. In a wound healing assay, we found that the migratory ability of cells in the Kirenol-treated group was decreased compared with the control group (**Figures 3A–D**). Consistent with this, significantly fewer

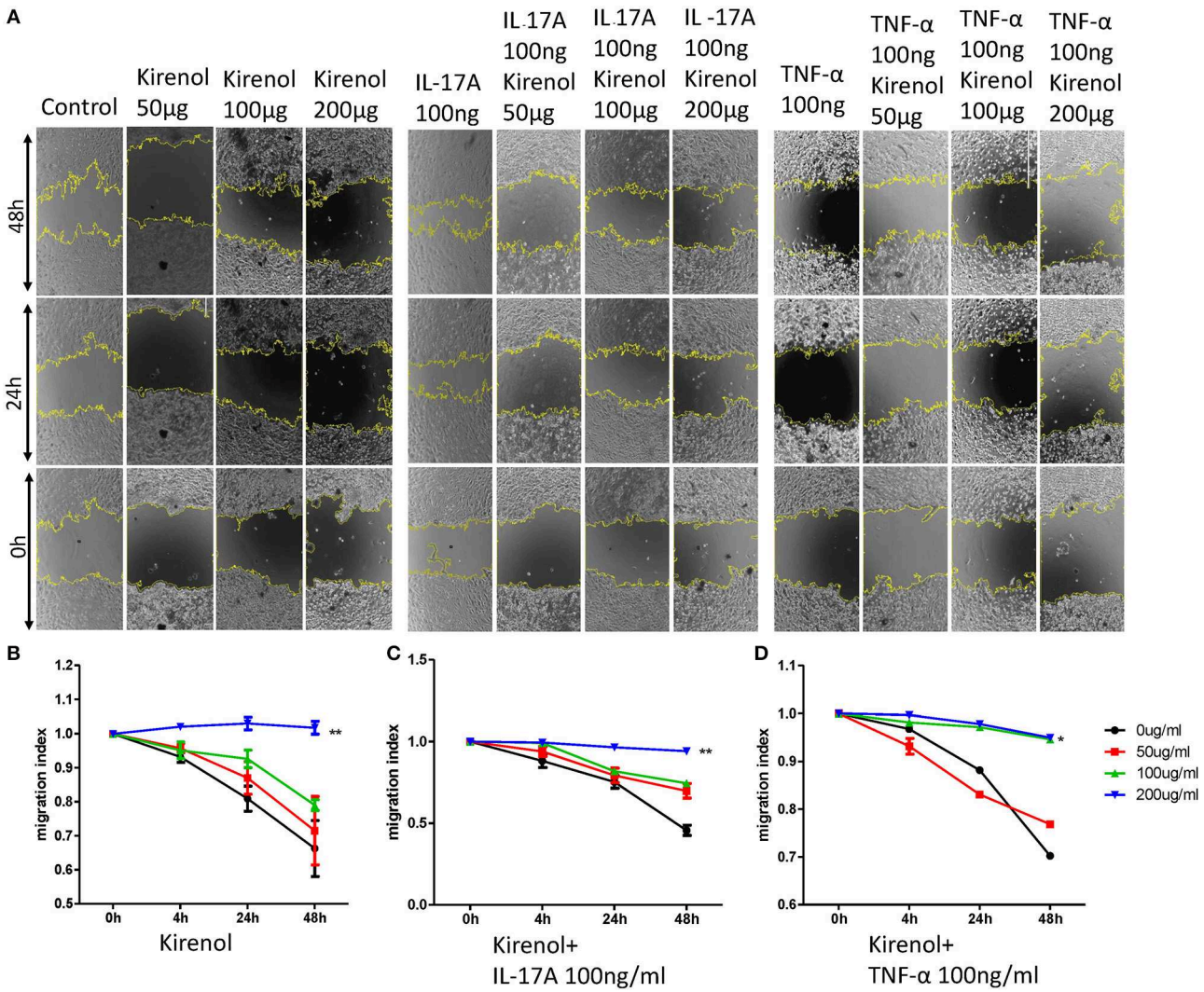

FIGURE 3 | (A) Wound healing assay images; **(B)** Kirenol inhibited the migration of FLS in a dose-dependent manner, with significant differences only at 200 μg/ml; **(C)** Kirenol inhibited the migration of FLS stimulated with IL-17A (100 ng/ml) in a dose-dependent manner, with significant differences only at 200 μg/ml; **(D)** Kirenol inhibited the migration of FLS stimulated with TNF-α (100 ng/ml) in a dose-dependent manner, with significant differences only at 200 μg/ml; $^{*}p < 0.05$, $^{**}p < 0.01$, as assessed by Mann- Whitney *U*-test.

migrated cells were detected upon Kirenol treatment for the invasion assay (**Figures 4A–H**).

Kirenol Alters Arthritic Progression *in vivo*

We next sought to extend our findings *in vivo*, in order to assess whether Kirenol was able to inhibit inflammation in a CIA mouse model of arthritis. We found that a low dose Kirenol (7.5 mg/kg) was able to delay the onset of arthritis, while a high dose (30 mg/kg) was able to reduce the incidence of arthritis (**Figures 5A,B**). Animals in the high dose group also exhibited reduced histological scores (**Figures 5D–G**), while body weight did not vary significantly at any tested dose (**Figure 5C**).

When murine serum was assessed via ELISA, we found that Kirenol was able to inhibit the production of TNF-α, IL-1β, IL-6, and IL-8 of in the serum (**Figures 6A–D**). Western blotting further confirmed that Kirenol was able to reduce levels of IL-6, IL-8, and TNF-α in the synovium, but only at the higher dose of 30 mg/kg (**Figure 6F**). Immunohistochemistry also confirmed that Kirenol can inhibit the levels of IL-6, IL-8, and TNF-α in the synovium, with differences only being significant at the 30 mg/kg dose (**Figures 6E,G**).

DISCUSSION

RA is characterized by the proliferation of synoviocytes in inflamed synovia, and by synoviocyte expression of inflammatory cytokines (15). FLS from RA patients exhibit extended hyperplasia, activation, and other aggressive behaviors such as abnormal migration and invasion (16, 17). As such, treatment strategies often focus on controlling the proliferation and

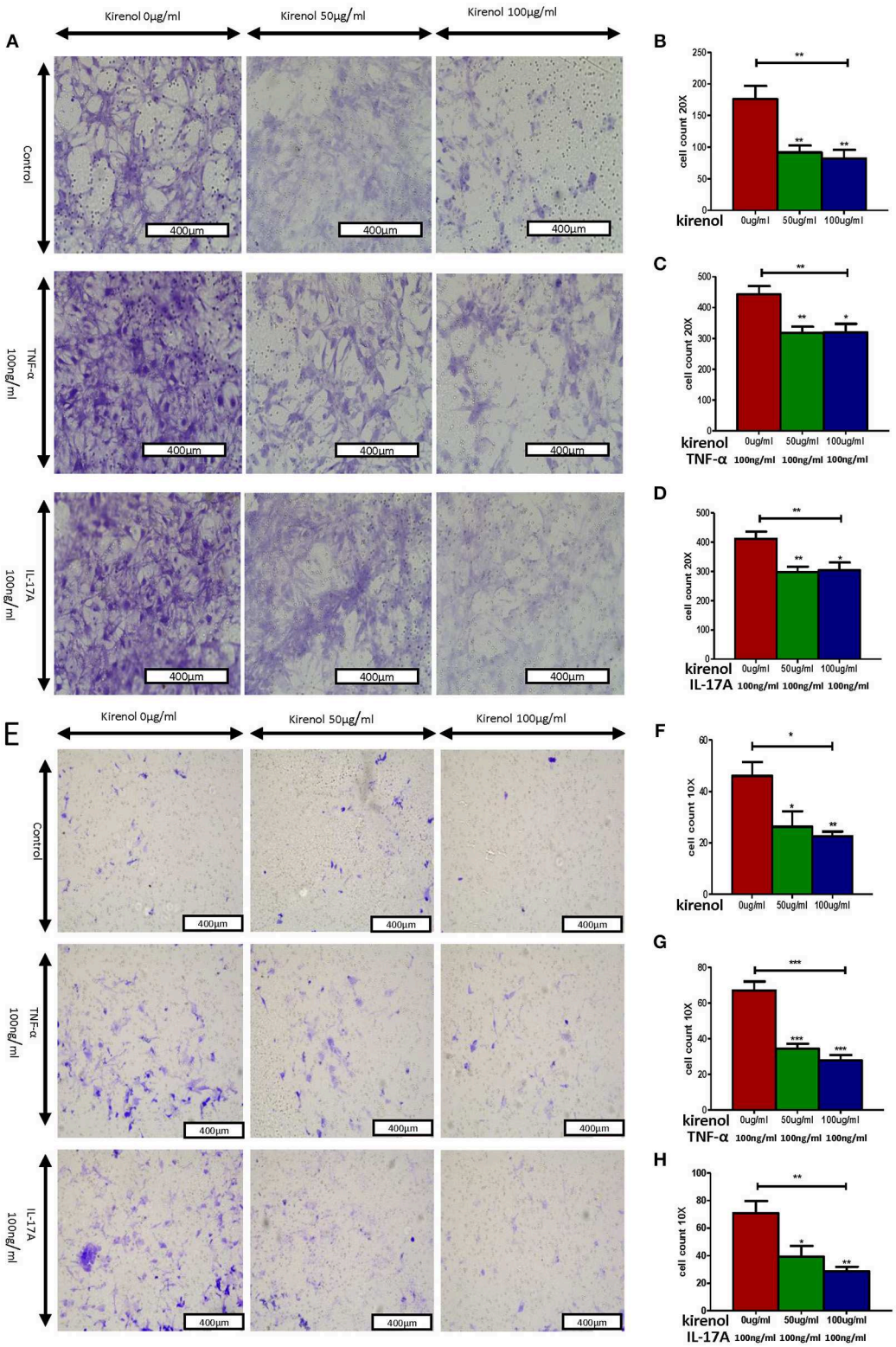

FIGURE 4 | (A) Migration assay images; **(B)** Kirenol inhibited the migration of FLS; **(C)** Kirenol inhibited the migration of FLS stimulated with TNF-α (100 ng/ml); **(D)** Kirenol inhibited the migration of FLS stimulated with IL-17A (100 ng/ml); **(E)** Invasion assay images; **(F)** Kirenol inhibited the invasion of FLS; **(G)** Kirenol inhibited the invasion of FLS stimulated with TNF-α (100 ng/ml); **(H)** Kirenol inhibited the invasion of FLS stimulated with IL-17A (100 ng/ml); $^{*}p < 0.05$, $^{**}p < 0.01$, $^{***}p < 0.01$ as assessed by the Kruskal-Wallis test and the Mann-Whitney *U*-test.

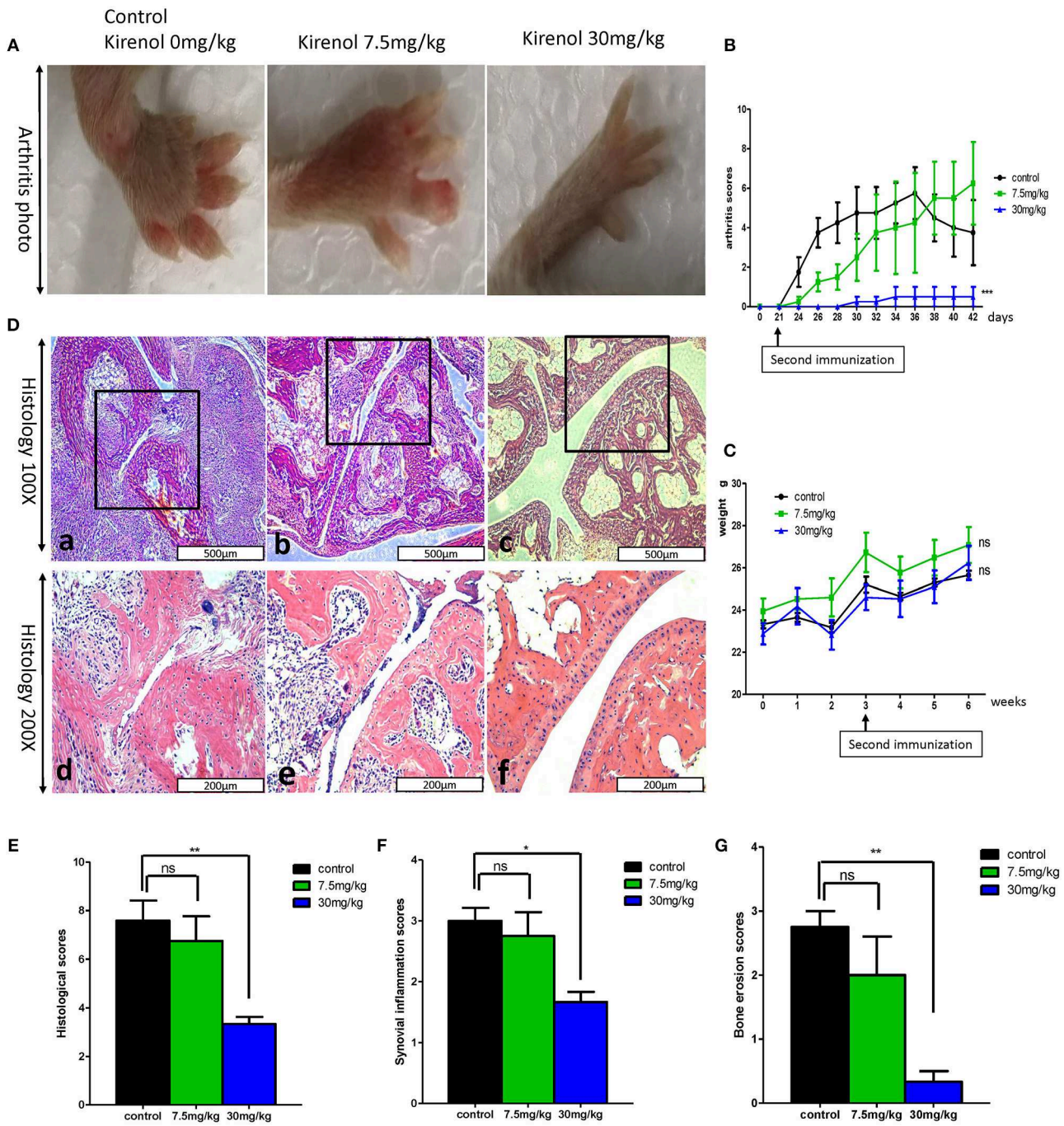

FIGURE 5 | (A) Murine arthritis model (control(0 mg/Kg.d), 7.5 mg/Kg.d, and 30 mg/Kg.d Kirenol groups); **(B)** Arthritis scores for these three groups, with a significant difference between the control vs. 30 mg/Kg.d group; **(C)** Body weight did not differ significantly between groups. **(D)** a and d: Immunohistochemistry in the control group showed severe synovial hyperplasia and bone and cartilage destruction; b and e: Immunohistochemistry in the 7.5 mg/Kg.d group showed synovial hyperplasia and bone and cartilage destruction; c and f: Immunohistochemistry in the 30 mg/Kg.d group showed no serious synovial hyperplasia or bone/cartilage destruction; **(E)** Histological scores in the three groups, with a significant difference between the control group vs. the 30 mg/Kg.d group; **(F)** Synovial inflammation scores for the three groups, with a significant difference between the control group vs. the 30 mg/Kg.d group; **(G)** Bone erosion scores of three groups, with a significant difference between the control group vs. the 30 mg/Kg.d group; $^{*}p < 0.05$, $^{**}p < 0.01$, $^{***}p < 0.01$ as assessed by the Kruskal-Wallis test.

inflammatory nature of these cells. Kirenol is a diterpenoid from Herba Siegesbeckia that has been used to treat RA for centuries. Kirenol has been suggested to exhibit anti-inflammatory and anti-rheumatic activities. Studies have found that Kirenol is effective in rat models of arthritis, but little is known about whether it can directly affect synovial cells. Therefore, in this

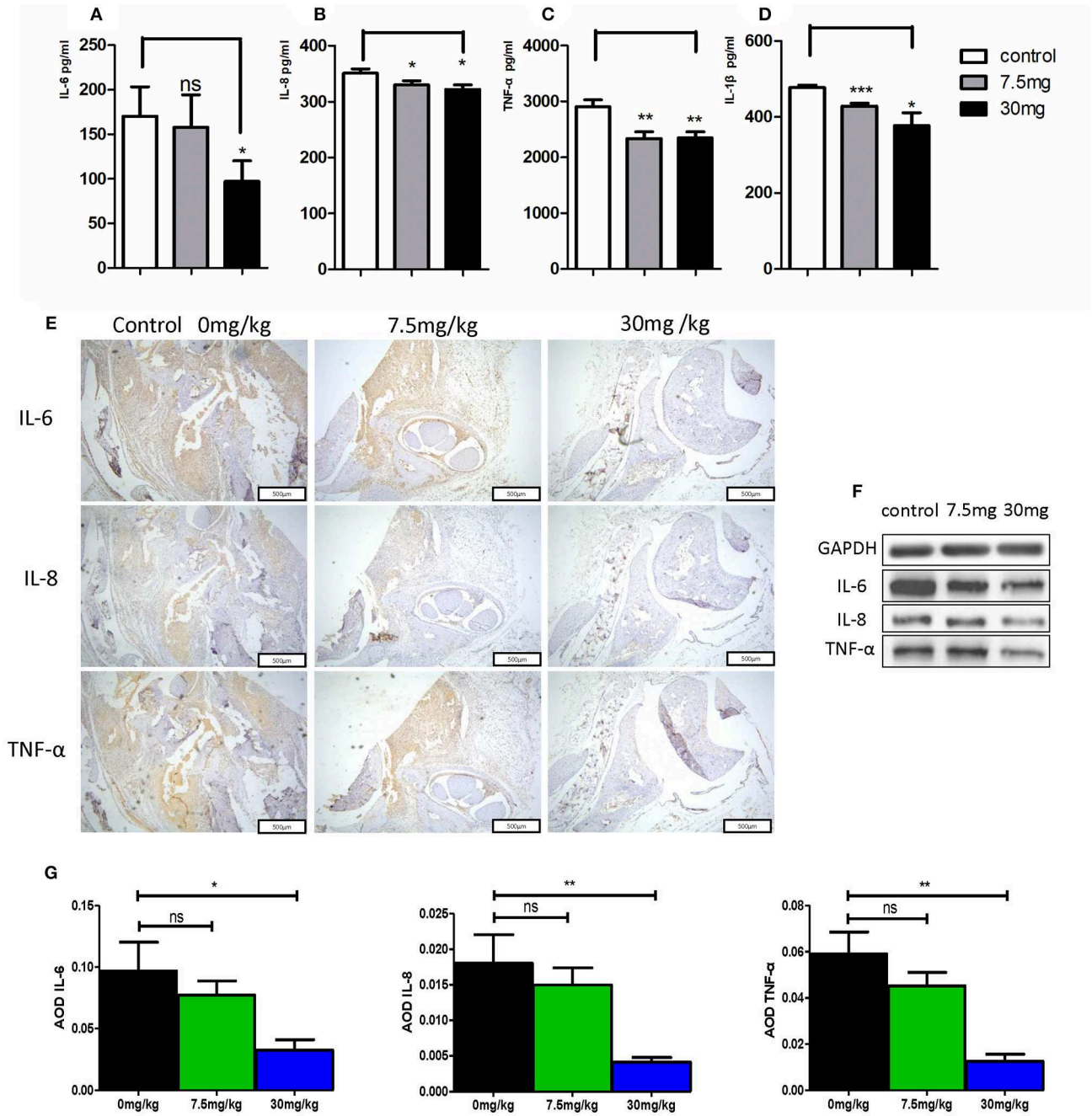

FIGURE 6 | (A) IL-6 concentrations in the three groups, with a significant difference between the control group vs. the 30 mg/Kg.d group; **(B)** IL-8 concentrations in the three groups, with a significant difference between the control group vs. the 7.5 mg/Kg.d and 30 mg/Kg.d groups; **(C)** TNF-α concentrations in the three groups, with a significant difference between the control group vs. the 7.5 mg/Kg.d and 30 mg/Kg.d groups; **(D)** IL-1β concentration in the three groups, with a significant difference between the control group vs. the 7.5 mg/Kg.d and 30 mg/Kg.d groups; **(E)** Immunohistochemistry results indicated that Kirenol can inhibit the level sof IL-6, IL-8, and TNF-α in the synovium. **(F)** Western blotting indicated that Kirenol can inhibit the levels of IL-6, IL-8, and TNF-α in the synovium. **(G)** IL-6, IL-8, and TNF-α levels differed significantly between the 30 mg/kg group and the other experimental groups. $^{*}p < 0.05$, $^{**}p < 0.01$, $^{***}p < 0.01$ as assessed by the Kruskal-Wallis test and the Mann-Whitney *U*-test.

study we designed a series of experiments to observe the effects of Kirenol on FLS both *in vitro* and *in vivo*.

In vitro, we found that Kirenol inhibited the proliferation and function of FLS in a dose-dependent manner. Interestingly, Kirenol exerted a more significant anti-proliferative and anti-inflammatory effect when these RA-FLS were first stimulated using TNF-α and IL-17. This confirms our previous findings indicating that Kirenol can dock the TNF-α (6). Furthermore, we found that only high-dose Kirenol (100–200 μg/ml) was able to affect FLS IL-6 secretion, even following TNF-α and

IL-17A stimulation. By RT-PCR we further found that Kirenol can inhibit the expression of IL-6 at the mRNA level, indicating that high-dose Kirenol can readily alter IL-6 production by FLS. We were only able to detect inhibited IL-8 production at 30 min after Kirenol treatment in FLS, and such inhibition was absent in cells first treated with cytokines, although at the mRNA level this inhibition was evident. Even so, as these results are inconsistent, it is unclear whether Kirenol can substantially alter IL-8 production *in vitro*, particularly not in the context of a strong cytokine stimulus. We were not able to detect TNF-α or IL-1β ain FLS supernatants. We further found that RT-PCR that MMP-9 can be inhibited by Kirenol *in vitro*, whereas MMP-1,2, and 3 were not. We did not assess MMP protein levels in this study, and as such this is an important area of future research. We suspect that these proteins may be regulated by Kirenol, given previous work showing that this compound can inhibit MMP-2, 3, 9, and 13 expression in Hs68 human dermal fibroblasts (18).

To evaluate how IL-6 secretion and FLS function were affected by Kirenol, we next assessed the MAPK, JAK-STAT, and NFκB pathways in FLS cells, revealing that at early time points this compound inhibited the activation of JAK-STAT and NFκB but not MAPK signaling. Many studies have shown that TNF-α and IL-17A signaling through the NFκB pathway regulate the function of FLS in RA (19–21). We found that Kirenol inhibits the function of FLS in response to TNF-α and IL-17A, and so we hypothesized that Kirenol plays a negative role in controlling the activation of the NFκB pathway by blocking TNF-α and IL-17A signaling. Western blotting results were consistent with this hypothesis. Other researchers have also found that TNF-α signaling through JAK-STAT pathways can affect FLS responses (22), suggesting that Kirenol can inhibit responses to TNF signaling via multiple pathways, with similar inhibitory activities also likely in response to IL-6.

Some studies have found that RA-FLS migrate and invade cartilage and bone, leading to vascularization and tissue damage during RA progression (23). We found that Kirenol also inhibited the migration and invasion of FLS in a dose-dependent manner, even in response to TNF-α and IL-17A stimulation, which is significant as both cytokines can strongly promote cellular migration and invasion (24–27). We therefore believe Kirenol has a clear inhibitory effect on the migration and invasion of synoviocytes.

According to previous reports, Kirenol reduces the expression of cytokines in synovial and synovial fluid in a CIA rat model (28, 29). Histological evaluation in this study similarly revealed that Kirenol treatment effectively reduced joint inflammation, cartilage damage, and bone erosion, confirming that it helped to protect CIA mice. Our results are similar to those of other studies (5, 30). Moreover, we also found that Kirenol only achieved a protective effect at a dose of 30 mg/kg in this CIA mice model, with the lower dose only delaying the occurrence of arthritis and ultimately not affecting the disease outcome. No clear cytotoxicity or death was observed at any tested dose, indicating these treatment doses are safe. We further found that Kirenol significantly reduced the levels of TNF-α, IL-1β, and IL-6 in murine serum, confirming that this compound exhibits a therapeutic effect in CIA model mice.

Our *in vitro* and *in vivo* experiments have thus demonstrated that Kirenol has an excellent ability to inhibit synoviocyte functionality, suggesting that Kirenol has potential as a possible anti-rheumatic drug. This study is, however, limited by the fact that inflammation was only examined in the serum, joints, and synovium. Future studies will need to focus more broadly on how Kirenol affects the immune system *in vivo*.

CONCLUSIONS

In this study, we found that Kirenol was able to strongly inhibit FLS proliferation, migration, and invasion, and to inhibit the release of pro-inflammatory IL-6 by FLS, even when these cells were activated with IL-17A and TNF-α. Kirenol is able to mediate this inhibitory activity in FLS via regulating various intracellular pathways. *In vivo* experiments further confirmed that Kirenol can inhibit bone erosion, synovial hyperplasia, and inflammation in the joints of arthritic mice in a dose dependent manner.

ETHICS STATEMENT

The study is approved by Ethics Committee of ZhuJiang Hospital of Southern Medical University. The research design and methodology of this study were consistent with the requirements of the 2013 Helsinki Declaration. All study participants provided written informed consent.

AUTHOR CONTRIBUTIONS

JW, QL, LJ, HD, L-GJ, YQ, B-BL, and XZ performed experiments. JW and QL conceived the study and analyzed the results. JW and QY supervised the study and prepared the manuscript. All authors read and approved the final manuscript.

FUNDING

This study was supported by the National Natural Science Foundation of China (Grant Nos. 81601397 and 81771727).

REFERENCES

1. Aletaha D, Smolen JS. Diagnosis and management of rheumatoid arthritis: a review. *JAMA*. (2018) 320:1360–72. doi: 10.1001/jama.2018.13103
2. Ospelt C. Synovial fibroblasts in 2017. *RMD Open*. (2017) 3:e000471. doi: 10.1136/rmdopen-2017-000471
3. Sokka T, Hetland ML, Makinen H, Kautiainen H, Horslev-Petersen K, Luukkainen RK, et al. Remission and rheumatoid arthritis: data on patients receiving usual care in twenty-four countries. *Arthritis Rheum*. (2008) 58:2642–51. doi: 10.1002/art.23794
4. Xiao J, Yang R, Yang L, Fan X, Liu W, Deng W. Kirenol attenuates experimental autoimmune encephalomyelitis by inhibiting differentiation of

Th1 and th17 cells and inducing apoptosis of effector T cells. *Sci Rep*. (2015) 5:9022. doi: 10.1038/srep09022
5. Lu Y, Xiao J, Wu ZW, Wang ZM, Hu J, Fu HZ, et al. Kirenol exerts a potent anti-arthritic effect in collagen-induced arthritis by modifying the T cells balance. *Phytomedicine*. (2012) 19:882–9. doi: 10.1016/j.phymed.2012.04.010
6. Wu J, Qu Y, Deng J, Liang W, Jiang Z, Lai R, et al. Molecular docking studies of Kirenol a traditional Chinese medicinal compound against rheumatoid arthritis cytokine drug targets (TNF-α, IL-1 and IL-6). *Biomed Res*. (2017) 28:1992–95.
7. Guo Q, Wang Y, Xu D, Nossent J, Pavlos NJ, Xu J. Rheumatoid arthritis: pathological mechanisms and modern pharmacologic therapies. *Bone Res*. (2018) 6:15. doi: 10.1038/s41413-018-0016-9
8. Wu J, Qu Y, Zhang YP, Deng JX, Yu QH. RHAMM induces progression of rheumatoid arthritis by enhancing the functions of fibroblast-like synoviocytes. *BMC Musculoskelet Disord*. (2018) 19:455. doi: 10.1186/s12891-018-2370-6
9. Szekanecz Z, Kim J, Koch AE. Chemokines and chemokine receptors in rheumatoid arthritis. *Semin Immunol*. (2003) 15:15–21. doi: 10.1016/S1044-5323(02)00124-0
10. Kuan WP, Tam LS, Wong CK, Ko FW, Li T, Zhu T, et al. CXCL 9 and CXCL 10 as Sensitive markers of disease activity in patients with rheumatoid arthritis. *J Rheumatol*. (2010) 37:257–64. doi: 10.3899/jrheum.090769
11. Zhao J, Ouyang Q, Hu Z, Huang Q, Wu J, Wang R, et al. A protocol for the culture and isolation of murine synovial fibroblasts. *Biomed Rep*. (2016) 5:171–75. doi: 10.3892/br.2016.708
12. Sekine C, Sugihara T, Miyake S, Hirai H, Yoshida M, Miyasaka N, et al. Successful treatment of animal models of rheumatoid arthritis with small-molecule cyclin-dependent kinase inhibitors. *J Immunol*. (2008) 180:1954–61. doi: 10.4049/jimmunol.180.3.1954
13. Schramm C, Kriegsmann J, Protschka M, Huber S, Hansen T, Schmitt E, et al. Susceptibility to collagen-induced arthritis is modulated by TGFbeta responsiveness of T cells. *Arthritis Res Ther*. (2004) 6:R114–9. doi: 10.1186/ar1039
14. Miranda JP, Camoes SP, Gaspar MM, Rodrigues JS, Carvalheiro M, Barcia RN, et al. The secretome derived from 3D-cultured umbilical cord tissue MSCs counteracts manifestations typifying rheumatoid arthritis. *Front Immunol*. (2019) 10:18. doi: 10.3389/fimmu.2019.00018
15. McInnes IB, Schett G. Pathogenetic insights from the treatment of rheumatoid arthritis. *Lancet*. (2017) 389:2328–37. doi: 10.1016/S0140-6736(17)31472-1
16. Bartok B, Firestein GS. Fibroblast-like synoviocytes: key effector cells in rheumatoid arthritis. *Immunol Rev*. (2010) 233:233–55. doi: 10.1111/j.0105-2896.2009.00859.x
17. Xu S, Xiao Y, Zeng S, Zou Y, Qiu Q, Huang M, et al. Piperlongumine inhibits the proliferation, migration and invasion of fibroblast-like synoviocytes from patients with rheumatoid arthritis. *Inflamm Res*. (2018) 67:233–43. doi: 10.1007/s00011-017-1112-9
18. Kim J, Kim MB, Yun JG, Hwang JK. Protective effects of standardized siegesbeckia glabrescens extract and its active compound kirenol against UVB-induced photoaging through inhibition of MAPK/NF-kappaB pathways. *J Microbiol Biotechnol*. (2017) 27:242–50. doi: 10.4014/jmb.1610.10050
19. Hwang SY, Kim JY, Kim KW, Park MK, Moon Y, Kim WU, et al. IL-17 induces production of IL-6 and IL-8 in rheumatoid arthritis synovial fibroblasts via NF-kappaB- and PI3-kinase/Akt-dependent pathways. *Arthritis Res Ther*. (2004) 6:R120–8. doi: 10.1186/ar1038
20. Makarov SS. NF-kappa B in rheumatoid arthritis: a pivotal regulator of inflammation, hyperplasia, and tissue destruction. *Arthritis Res*. (2001) 3:200–6. doi: 10.1186/ar300
21. Lee A, Qiao Y, Grigoriev G, Chen J, Park-Min KH, Park SH, et al. Tumor necrosis factor alpha induces sustained signaling and a prolonged and unremitting inflammatory response in rheumatoid arthritis synovial fibroblasts. *Arthritis Rheum*. (2013) 65:928–38. doi: 10.1002/art.37853
22. Malemud CJ. Negative regulators of JAK/STAT signaling in rheumatoid arthritis and osteoarthritis. *Int J Mol Sci*. (2017) 18:E484. doi: 10.3390/ijms18030484
23. Huber LC, Distler O, Tarner I, Gay RE, Gay S, Pap T. Synovial fibroblasts: key players in rheumatoid arthritis. *Rheumatology*. (2006) 45:669–75. doi: 10.1093/rheumatology/kel065
24. Li G, Zhang Y, Qian Y, Zhang H, Guo S, Sunagawa M, et al. Interleukin-17A promotes rheumatoid arthritis synoviocytes migration and invasion under hypoxia by increasing MMP2 and MMP9 expression through NF-kappaB/HIF-1alpha pathway. *Mol Immunol*. (2013) 53:227–36. doi: 10.1016/j.molimm.2012.08.018
25. Pickens SR, Volin MV, Mandelin AM II, Kolls JK, Pope RM, Shahrara S. IL-17 contributes to angiogenesis in rheumatoid arthritis. *J Immunol*. (2010) 184:3233–41. doi: 10.4049/jimmunol.0903271
26. Hot A, Miossec P. Effects of interleukin (IL)-17A and IL-17F in human rheumatoid arthritis synoviocytes. *Ann Rheum Dis*. (2011) 70:727–32. doi: 10.1136/ard.2010.143768
27. Zeng S, Wang K, Huang M, Qiu Q, Xiao Y, Shi M, et al. Halofuginone inhibits TNF-alpha-induced the migration and proliferation of fibroblast-like synoviocytes from rheumatoid arthritis patients. *Int Immunopharmacol*. (2017) 43:187–94. doi: 10.1016/j.intimp.2016.12.016
28. Huo L, Jiang Z, Lei M, Wang X, Guo X. Simultaneous quantification of Kirenol and ent-16beta,17-dihydroxy-kauran-19-oic acid from Herba *Siegesbeckiae* in rat plasma by liquid chromatography-tandem mass spectrometry and its application to pharmacokinetic studies. *J Chromatogr B Analyt Technol Biomed Life Sci*. (2013) 937:18–24. doi: 10.1016/j.jchromb.2013.08.019
29. Kim MB, Song Y, Kim C, Hwang JK. Kirenol inhibits adipogenesis through activation of the Wnt/beta-catenin signaling pathway in 3T3-L1 adipocytes. *Biochem Biophys Res Commun*. (2014) 445:433–8. doi: 10.1016/j.bbrc.2014.02.017
30. Lu Y, Xiao J, Wu Z, Wang Z, Fu H, Chen Y, et al. Effects of Kirenol on bovine type II collagen-induced rat lymphocytes *in vivo* and *in vitro*. *Nan Fang Yi Ke Da Xue Xue Bao*. (2012) 32:1–6.

Conflict of Interest Statement: The authors declare that the research was conducted in the absence of any commercial or financial relationships that could be construed as a potential conflict of interest.

frontiers in Immunology

ORIGINAL RESEARCH
published: 18 June 2019
doi: 10.3389/fimmu.2019.01384

The Rheumatoid Arthritis Risk Gene AIRE Is Induced by Cytokines in Fibroblast-Like Synoviocytes and Augments the Pro-inflammatory Response

Beatrice Bergström [1,2†], Christina Lundqvist [1†], Georgios K. Vasileiadis [1], Hans Carlsten [1,2], Olov Ekwall [1,3] and Anna-Karin H. Ekwall [1,2]*

[1] Department of Rheumatology and Inflammation Research, Institute of Medicine, The Sahlgrenska Academy, University of Gothenburg, Gothenburg, Sweden, [2] Centre for Bone and Arthritis Research, The Sahlgrenska Academy, University of Gothenburg, Gothenburg, Sweden, [3] Department of Pediatrics, Institute of Clinical Sciences, The Sahlgrenska Academy, University of Gothenburg, Gothenburg, Sweden

OPEN ACCESS

Edited by:
David Fox,
University of Michigan, United States

Reviewed by:
Erika H. Noss,
University of Washington, United States
Marko Radic,
University of Tennessee College of Medicine, United States

***Correspondence:**
Anna-Karin H. Ekwall
ak.ekwall@rheuma.gu.se

[†] These authors have contributed equally to this work

Specialty section:
This article was submitted to Autoimmune and Autoinflammatory Disorders, a section of the journal Frontiers in Immunology

Received: *07 March 2019*
Accepted: *31 May 2019*
Published: *18 June 2019*

Citation:
Bergström B, Lundqvist C, Vasileiadis GK, Carlsten H, Ekwall O and Ekwall A-KH (2019) The Rheumatoid Arthritis Risk Gene AIRE Is Induced by Cytokines in Fibroblast-Like Synoviocytes and Augments the Pro-inflammatory Response. Front. Immunol. 10:1384. doi: 10.3389/fimmu.2019.01384

The autoimmune regulator AIRE controls the negative selection of self-reactive T-cells as well as the induction of regulatory T-cells in the thymus by mastering the transcription and presentation of tissue restricted antigens (TRAs) in thymic cells. However, extrathymic AIRE expression of hitherto unknown clinical significance has also been reported. Genetic polymorphisms of *AIRE* have been associated with rheumatoid arthritis (RA), but no specific disease-mediating mechanism has been identified. Rheumatoid arthritis is characterized by a systemic immune activation and arthritis. Activated fibroblast-like synoviocytes (FLS) are key effector cells, mediating persistent inflammation, and destruction of joints. In this study, we identified AIRE as a cytokine-induced RA risk gene in RA FLS and explored its role in these pathogenic stroma cells. Using RNA interference and RNA sequencing we show that AIRE does not induce TRAs in FLS, but augments the pro-inflammatory response induced by tumor necrosis factor and interleukin-1β by promoting the transcription of a set of genes associated with systemic autoimmune disease and annotated as interferon-γ regulated genes. In particular, AIRE promoted the production and secretion of a set of chemokines, amongst them CXCL10, which have been associated with disease activity in RA. Finally, we demonstrate that AIRE is expressed in podoplanin positive FLS in the lining layer of synovial tissue from RA patients. These findings support a novel pro-inflammatory role of AIRE at peripheral inflammatory sites and provide a potential pathological mechanism for its association with RA.

Keywords: rheumatoid arthritis, fibroblast-like synoviocytes, inflammation, cytokines, AIRE, interferon response genes

INTRODUCTION

Rheumatoid arthritis (RA) is a systemic inflammatory autoimmune disease pre-dominantly affecting joints (1). If left untreated, the disease progresses to tissue destruction, functional disability, and comorbidities such as cardiovascular disease. RA most likely evolves over many years as a consequence of repeated environmental stress, causing inflammatory events, and immune

activation and eventually breakdown of tolerance, in genetically pre-disposed individuals (2). In the joints, the disease is characterized by persistent inflammation and formation of a hyperplastic invasive synovium. Key players in these processes are activated fibroblast-like synoviocytes (FLS), which possess tumor cell-like features such as increased cell proliferation and the ability to invade and destroy surrounding tissue (3). The pro-inflammatory cytokines tumor necrosis factor (TNF) and interleukin-1β (IL-1β) are typical activators of FLS, inducing production of e.g., pro-inflammatory molecules and matrix degrading enzymes (4, 5). In addition, in response to interferon-γ (IFN-γ) RA FLS up-regulate the expression of major histocompatibility complex (MHC) class II, which suggests a role in antigen presentation and direct interaction with immune cells (6). Once activated, RA FLS continue their aggressive tissue destructive behavior without the need of further stimulation from the immune system. This might contribute to the fact that only 20–40% of RA patients achieve sustained clinical remission by the currently available immunosuppressive anti-rheumatic therapies (7). It also demonstrates the urgent need for novel drugs targeting the RA FLS.

Today, more than 100 RA risk genes have been identified by analyses of single nucleotide polymorphisms in Genome Wide Association Studies (GWAS) (8, 9). Several GWA studies have demonstrated that polymorphisms (rs2075876, rs760426, rs878081) in the autoimmune regulator gene, *AIRE*, are associated with RA (10–12). Most studies on the mechanisms by which the RA-associated genetic variants influence disease have focused on immune cells. Interestingly, integrative analysis of multiple omics data including epigenetic marks from RA FLS and controls has identified AIRE as one of seven candidate genes for the pathogenic features of RA FLS (13). We have earlier demonstrated that *LBH*, another of these seven genes, regulates cell cycle progression in FLS (14, 15). The potential role of AIRE in FLS has not been investigated.

AIRE is a master regulator of the transcription of tissue restricted antigens (TRAs) in medullary thymic epithelial cells (mTEC) (16). The induced TRAs are subsequently presented on MHC class II for maturing thymocytes, and self-reactive thymocytes are either deleted or diverted into natural regulatory T cells (nTregs) as a central part of the T-cell tolerance induction in the thymus. The importance of this process is illustrated by the autoimmune polyendocrine syndrome type-1 in which mutations in *AIRE* result in multiple severe autoimmune manifestations (17). Interestingly, RA is not a feature of APS1 and only a few cases of arthritis has been described in APS1 patients. *AIRE* expression in mTEC is induced by RANKL and TNF, and tightly regulated by complex molecular mechanisms involving epigenetic modifications (18).

Apart from the well-established expression and function of *AIRE* in mTECs, *AIRE* expression in thymic B-cells and extra-thymic expression in lymph nodes and in keratinocytes has been described (19). Interestingly, as opposed to the tolerogenic role of AIRE in the thymus and lymph nodes, AIRE has been reported to interact with keratin 17 and induce the expression of pro-inflammatory genes, most notably *CXCL9*, *CXCL10*, and *CXCL11*, in keratinocytes in acute inflammation and tumorigenesis (20).

In this study, we investigated the transcriptome of TNF and IL-1β-activated RA FLS and identified AIRE as one of 24 differentially expressed RA risk genes in these cells. We demonstrate that AIRE is expressed in the RA synovium and augments the inflammatory response by promoting the expression of an interferon γ signature including the production of chemokines in FLS.

MATERIALS AND METHODS

Biological Samples

Human synovial tissue specimens were obtained from patients with RA or osteoarthritis (OA) during joint replacement surgery at Sahlgrenska University Hospital and Spenshult Hospital in Sweden. All RA patients fulfilled the American College of Rheumatology 1987 revised criteria for the disease (21). Human thymic tissue was obtained from children undergoing corrective cardiac surgery at Sahlgrenska University Hospital, Gothenburg, Sweden. The procedures were approved by the Ethics Committee of Gothenburg and all patients gave written informed consent. Homogenous cultures of primary FLS were established as described earlier (22) and used in passage 4–8.

Cell Culture and Stimulations

Primary FLS were cultured in Dulbecco's modified Eagle's medium (DMEM) GlutaMAX (Gibco, Carlsbad, CA, USA) supplemented with antibiotics (penicillin/streptomycin, gentamicin) and 10% heat-inactivated fetal bovine serum (FBS), in a humidified 5% CO_2 and 37°C atmosphere. Primary normal neonatal human dermal fibroblasts (HDFn) were obtained from ATCC (PCS-201-010). For stimulation experiments, cells were seeded into 6-well-plates (qPCR, flow cytometry, RNAseq) or 8-well-chamber slides (immunofluorescence) and incubated until confluence. The cells were serum-starved for 12 h in 1% FBS and then stimulated with the human recombinant proteins IL-1β (R&D Systems, Minneapolis, MN, USA), TNF (Invitrogen, Carlsbad, CA, USA), or RANKL (R&D Systems) for 12–24 h.

RNA Extraction and Gene Expression Analysis

Total RNA was isolated from cells using RNeasy Micro Kit (Qiagen) according to the manufacturer's instructions and quantified with a NanoDrop 100 spectrophotometer (Thermo Scientific). Complementary DNA (cDNA) was synthesized from isolated RNA using TaqMan reverse transcription agents (Applied Biosystems, Carlsbad, CA, USA). qPCR was performed on a ViiA 7 Real-Time PCR System, using TaqMan reagents, and pre-designed primer-probe sets (**Table S1**) from Applied Biosystems. Ct values were normalized to glyceraldehyde 3-phosphate dehydrogenase (GAPDH) expression and fold change in mRNA expression was calculated using the ΔΔct-method ($2^{\Delta\Delta Ct}$).

Immunofluorescence and Confocal Microscopy

Paraformaldehyde fixed paraffin-embedded tissue sections were rehydrated and subjected to antigen retrieval in a pressure chamber (2100 Retriever, Aptum Biologics Ltd., Southampton, UK). Unspecific binding was blocked using serum-free protein block (DAKO, Glostrup, Denmark) supplemented with 5% normal donkey serum (D9663, Sigma-Aldrich, Saint Louis, Mo, USA). Incubation with goat anti-human AIRE antibody and/or mouse anti-human podoplanin for 60 min in RT followed by secondary Alexa Fluor labeled antibodies (**Table S2**). Thresholds of positive signal in the confocal microscopy were set using normal goat serum (S-1000, Vector Laboratories, Burlingame, CA, USA) or normal rabbit serum (DAKO, Glostrup, Denmark) followed by the secondary antibody.

Flow Cytometry and ImageStream X

Cells were fixed with Foxp3 transcription factor fixation/permeabilization kit (00-5521-00, eBioscience) and blocked using Beriglobin (CSL Behring L, PA, USA). The cells were stained in 100 μL with antibodies and dilutions as shown in **Table S2**. For biotinylated antibodies, samples were stained with Streptavidin-Alexa Fluor 647 (S32357, Life Technologies). Before acquisition on a FACSVerse (BD Biosciences, San Jose, CA, USA) nuclear stain Hoechst 33342 (H3570, Life Technologies) was added to a concentration of 0.5 μg/ml. Data were analyzed using FlowJo software (TreeStar Inc., Ashland, OR, USA). For single cell imaging, cells were acquired and analyzed on an ImageStream X Mark II imaging flow cytometer (Amnis, Seattle, WA, USA). CXCL10 levels in undiluted cell culture supernatants were assessed using LEGENDplex reagents (BioLegend, San Diego, CA, USA) according to the manufacturer's instructions.

Gene Silencing

Small interfering RNA (siRNA) targeting human AIRE (#L-010993-00) and non-targeting (NT) control (#D-001810-10, Thermo Scientific Dharmacon, Lafayette, CO, USA) were transfected into primary FLS using Amaxa Nucleofector Technology and HDF Nucleofector solution (Lonza, Basel, Switzerland). The cells were plated in 6-well plates and incubated for 2 days prior to serum starvation and stimulation. One NT sample of each line was unstimulated ("no AIRE") and the other NT control and the AIRE silenced sample were stimulated with IL-1β+TNF for 24 h generating "high AIRE" and "low AIRE" samples. Samples were collected in RLT buffer and RNA isolated as described in Methods. The efficiency of gene silencing was assessed by qPCR and RNAseq.

RNA Sequencing and Bioinformatics Analysis

RNA sequencing was performed using the Nextseq500 plattform, 2 × 75 read length and Nextseq500 Kit High Output V2 reagents. The library was prepared using TruSeq stranded Total RNA Sample preparation kit with Zero Gold according to the preparation guide (15031048 Rev. E). A quality assessment was performed on the data using FastQC (https://www.bioinformatics.babraham.ac.uk/projects/fastqc/). The fastq files were filtered with prinseq (version 0.20.3). The quality filtered fastq files were mapped toward the human reference genome (hg19, UCSC assembly, February 2009) with STAR (version 2.5.2b). The alignment was sorted and indexed with SAM tools (version 1.3.1). Htseq (version 0.5.3p3) was used for calculation of the gene counts. Differentially expressed genes were identified with DEseq2 using Benjamini-Hochberg *p*-value adjustment (23). The identified genes were grouped into TRAs. The annotation of TRA was downloaded from BioGPS using the dataset GSE1133 (GeneAtlas U133A, gcrma). A pathway analysis was performed on the differentially expressed genes with IPA (Ingenuity® Systems, http://www.ingenuity.com/). The Gene Set Enrichment Analysis (GSEA) was performed as follows; all genes from the comparison STIM NTC vs. STIM AIRE KD were ranked based on fold change. The gene sets of Hallmark Inflammatory Response and Hallmark Interferon Gamma Response in gene matrix transposed file formats (gmt) were downloaded from molecular signature database [(24) http://www.broad.mit.edu/gsea/]. The gene set analysis itself was run as GSEA pre-ranked for 1,000 permutations.

Statistical Analysis

Statistical analysis of gene expression was performed on Δct values. Gaussian distribution was confirmed by Shapiro-Wilk's normality test followed by paired or unpaired two-tailed *t*-test as indicated. Graphs display mean with SEM and dots represent individual values. One-way ANOVA with Dunnett's multiple comparisons test was used for multiple tests to the unstimulated control. $P \leq 0.05$ was considered to be significant. Differentially expressed genes were considered significant if adjusted $p \leq 0.05$. Bioinformatics analysis of RNA seq data as stated above.

RESULTS

Pro-inflammatory Cytokines Modify Expression of RA Risk Genes in RA FLS

Interleukin-1β and TNF are abundant cytokines in the RA joint and known inducers of an "activated" RA FLS phenotype. In the search for novel important pathways in RA, we investigated the transcriptome of *cytokine-activated* compared to untreated control RA FLS using RNA sequencing. The combined IL-1β (2 g/ml) + TNF (5 ng/ml) stimulation induced a highly significant transcription of genes known to shape the aggressive phenotype of RA FLS. In total, more than 3,400 genes were significantly differentially expressed (adj. $p < 0.05$) by stimulation compared with unstimulated RA FLS (Top 30 in **Figure 1A**), illustrating the impact of these cytokines on the cells. In particular, a strong induction was seen on cytokines, chemokines, matrix degrading enzymes, and pro-migratory molecules with adjusted *p*-values in the range 10^{-8} to 10^{-62}, $n = 3$ (**Figure 1B**). The FLS also changed morphology, displaying a dendritic phenotype different from the unstimulated polygonal spread shape (not shown). Interestingly, we found differential expression (adj. $p < 0.05$) of 24 of the 105 known RA risk genes (9) in the TNF + IL-1β stimulated RA FLS compared to unstimulated (**Figure 1C**, **Table S3**). Most of them (17 genes) were up-regulated ≥2 fold (**Figure 1D**) and the

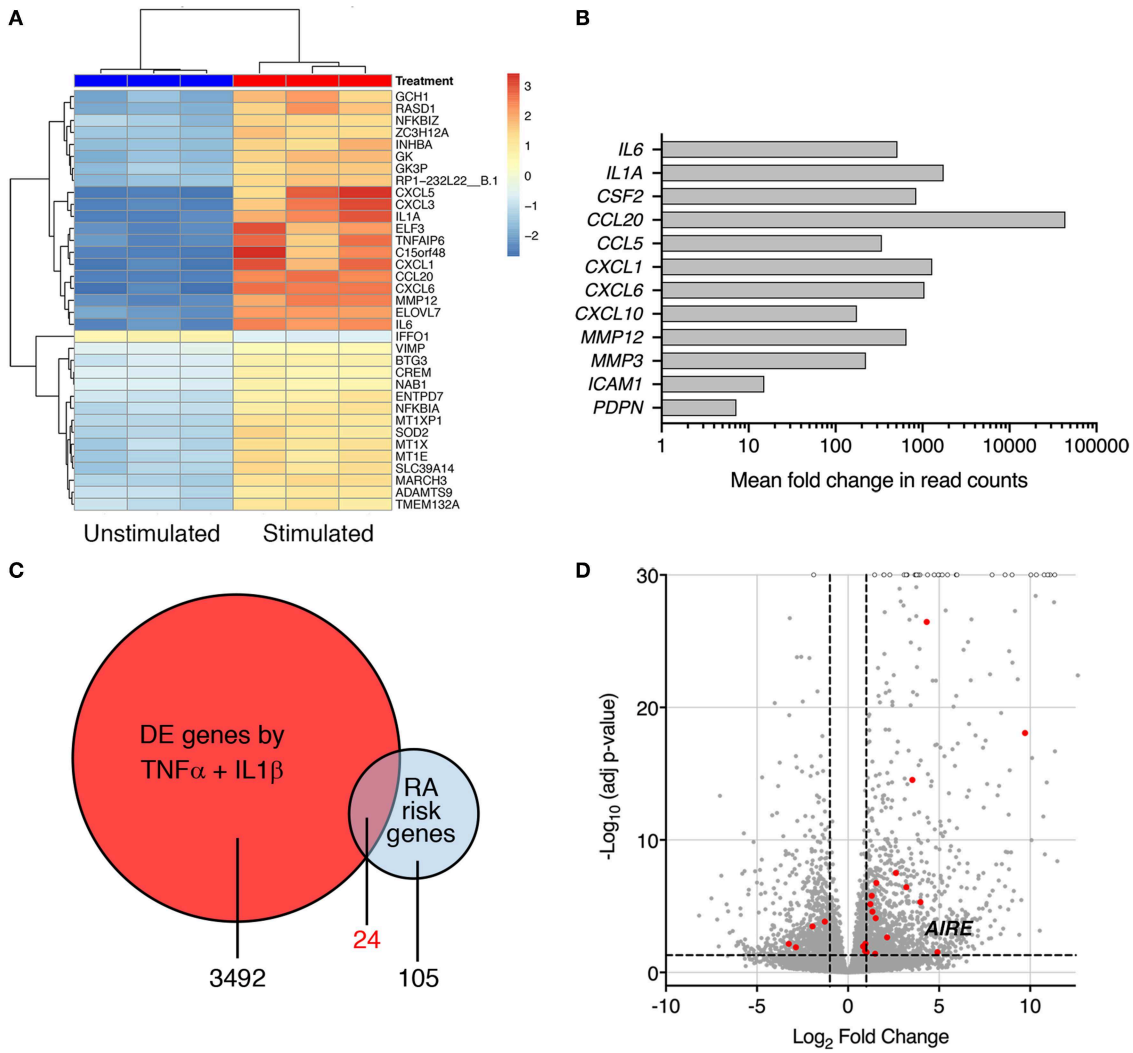

FIGURE 1 | Pro-inflammatory cytokines modify expression of RA risk genes in RA FLS. **(A)** A heatmap with hierarchical clustering of the top 35 significantly (Adj $P < 0.05$) differently expressed genes by RNA seq in IL-1β (2 ng/ml) + TNF (5 ng/ml) stimulated vs. unstimulated RA FLS from three different patients. **(B)** Increased expression of genes characterizing the "activated" aggressive RA FLS phenotype: pro-inflammatory cytokines (IL-6, IL-1A, GM-CSF), chemokines (CCL20, CCL5, CXCL1, CXCL6, and CXCL10), matrix degrading enzymes (MMP12 and 3) and adhesion molecules (ICAM-1, podoplanin) in IL-1β + TNF stimulated vs. unstimulated RA FLS by RNAseq (Log2 fold change in normalized read counts, $n = 3$). **(C)** Venn diagram of the RA-associated risk genes by GWAS and TNF + IL-1β induced DE genes by RNAseq. **(D)** Volcano plot (each dot representing one gene plotted based on log2 fold change and –log10 of adj *p*-value by DEseq2) of the TNF + IL-1β induced DE genes with the DE RA risk genes, including *AIRE*, highlighted in RED. Dashed lines at adjusted $p = 0.05$ and at fold change = ±2.

autoimmune regulator, *AIRE*, was one of them (fold change = 30.1, Adj $p = 0.030$).

Cytokine-Induced *AIRE* Expression Is Higher in RA Compared to Control FLS

To confirm this finding, we investigated AIRE expression in primary human FLS using qPCR. We did not detect any *AIRE* mRNA expression in unstimulated FLS from RA or control OA patients (**Figure 2A**). However, *AIRE* mRNA was strikingly induced, up to 191 ± 79 fold, by IL-1β in RA FLS ($p = 0.001$, $n = 4$) and 42 ± 4 fold ($p = 0.0006$, $n = 3$) in OA FLS (**Figure 2A**) after 24 h. The *AIRE* induction was significantly higher in RA than OA FLS ($p = 0.035$). Isolated RNA from human thymic epithelial cells was used as positive control and the *AIRE* mRNA expression in mTEC was 24-fold higher than average expression in RA FLS stimulated with IL-1β (data not shown). IL-1β 0.1–1 ng/ml was the most efficient dose within the bioactive range in FLS and the interindividual variations were greater in RA compared with OA FLS (**Figure 2B**). Furthermore, we found that *AIRE* was also induced 10 ± 5 fold ($p = 0.022$) by TNF compared to unstimulated in OA FLS and the largest effect was seen using IL-1β + TNF (66 ± 33 fold, $p = 0.018$) (**Figure 2C**). RANKL, the main inducer of AIRE expression in the thymus, did not induce *AIRE* mRNA in FLS (**Figure 2C**).

In the thymus, AIRE induces expression of hundreds of TRA in mTEC cells for tolerance purposes. However,

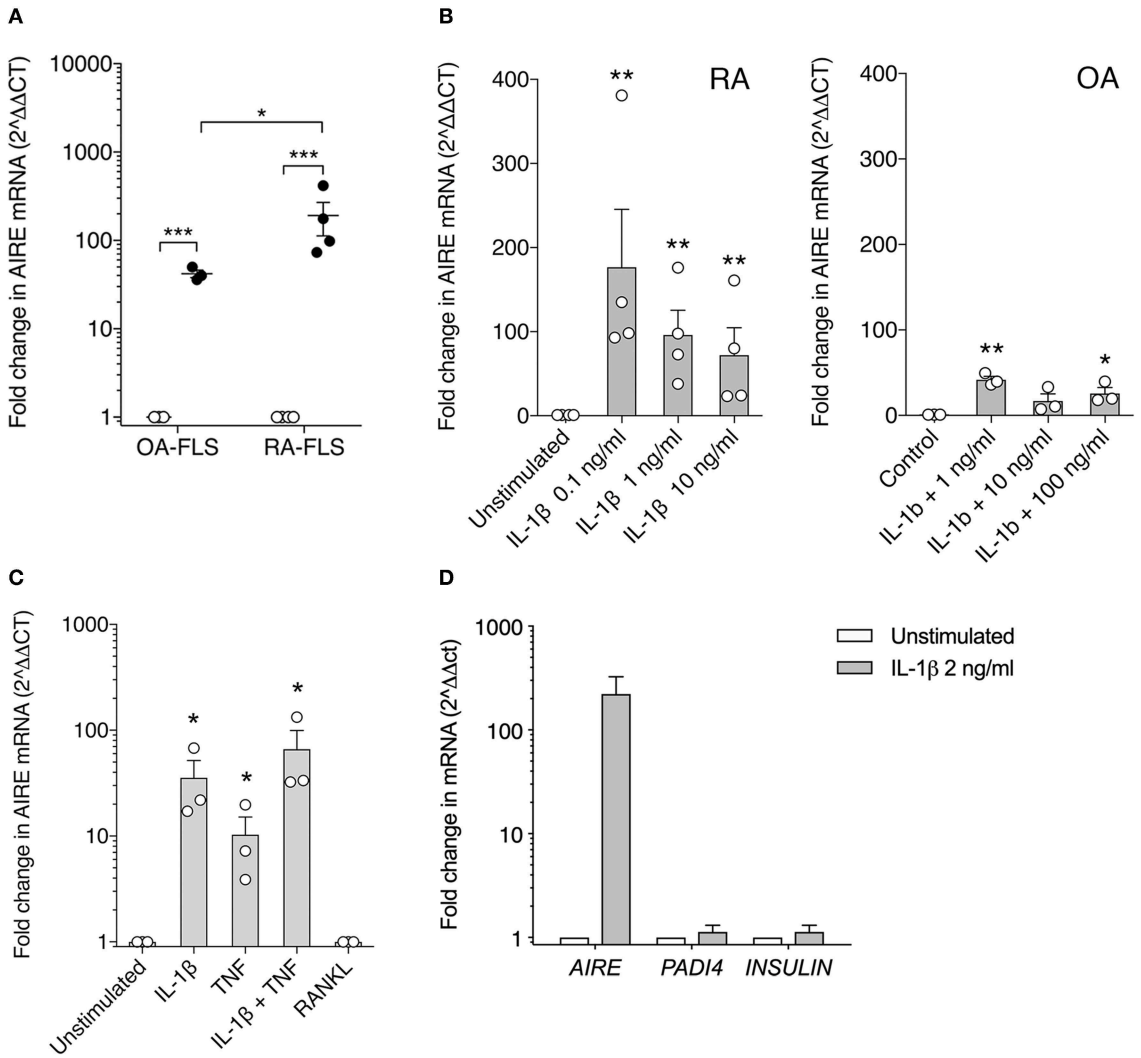

FIGURE 2 | AIRE mRNA expression is induced in FLS by pro-inflammatory cytokines. **(A)** AIRE mRNA expression is significantly increased by IL-1β 1 ng/ml (filled circles) compared to unstimulated (open circles) in both OA (42 ± 4 fold, $n = 3$, $p = 0.0006$) and RA FLS (191 ± 79 fold, $n = 4$, $p = 0.001$). Statistics with paired two-tailed *t*-test. The IL-1β -induced AIRE expression was significantly higher in RA compared to OA FLS ($p = 0.038$, unpaired two-tailed *t*-test). **(B)** Dose response of IL-1β stimulation on AIRE mRNA expression in RA FLS ($n = 4$, $p = 0.0001$) and OA FLS ($n = 3$, $p < 0.0001$) One-way ANOVA and Dunnett's test. **(C)** Effects of the FLS activating cytokines IL-1β (2 ng/ml) and TNF (5 ng/ml) and combined compared to unstimulated in OA-FLS ($n = 3$). One-way ANOVA and Dunnett's. RANKL (5 ng/ml) did not induce AIRE mRNA in FLS. **(D)** The tissue specific antigens; PADI4 and INSULIN mRNA are not induced in IL-1 β stimulated AIRE expressing FLS by qPCR (Fold change in stim vs. unstim, $n = 3$ FLS). *$p \leq 0.05$, **$p \leq 0.01$ and **$p \leq 0.001$.

no induction of the known AIRE-regulated genes, *INS* (insulin), and *PADI4* (peptidyl arginine deiminase type 4), were detected in the IL-1β stimulated AIRE expressing FLS (**Figure 2D**).

Nuclear AIRE Expression Is Present in TNF + IL-1β Stimulated RA FLS

Next, we investigated if AIRE is expressed also on the protein level in cytokine stimulated primary human FLS. A speckled nuclear, but also perinuclear, AIRE protein expression was detected using confocal immunofluorescence in a small fraction of IL-1β + TNF stimulated, but not in unstimulated RA FLS cultured in monolayer (**Figure 3A**). To further investigate the subcellular localization of AIRE in FLS we performed ImageStreamX flow cytometry on stimulated FLS and found that AIRE localized to the nuclei with the same speckled pattern as seen on tissue sections of RA synovium and thymus (**Figure 3B**). Using flow cytometry, the mean AIRE expression from two different experiments was increased by 68% ($n = 3$ per experiment) by IL-1β + TNF stimulation (**Figure 3C**). In this experimental setting, there was slightly lower fluorescence intensity in the isotype control compared to unstimulated control (possibly due to antibody/fluorochrome properties).

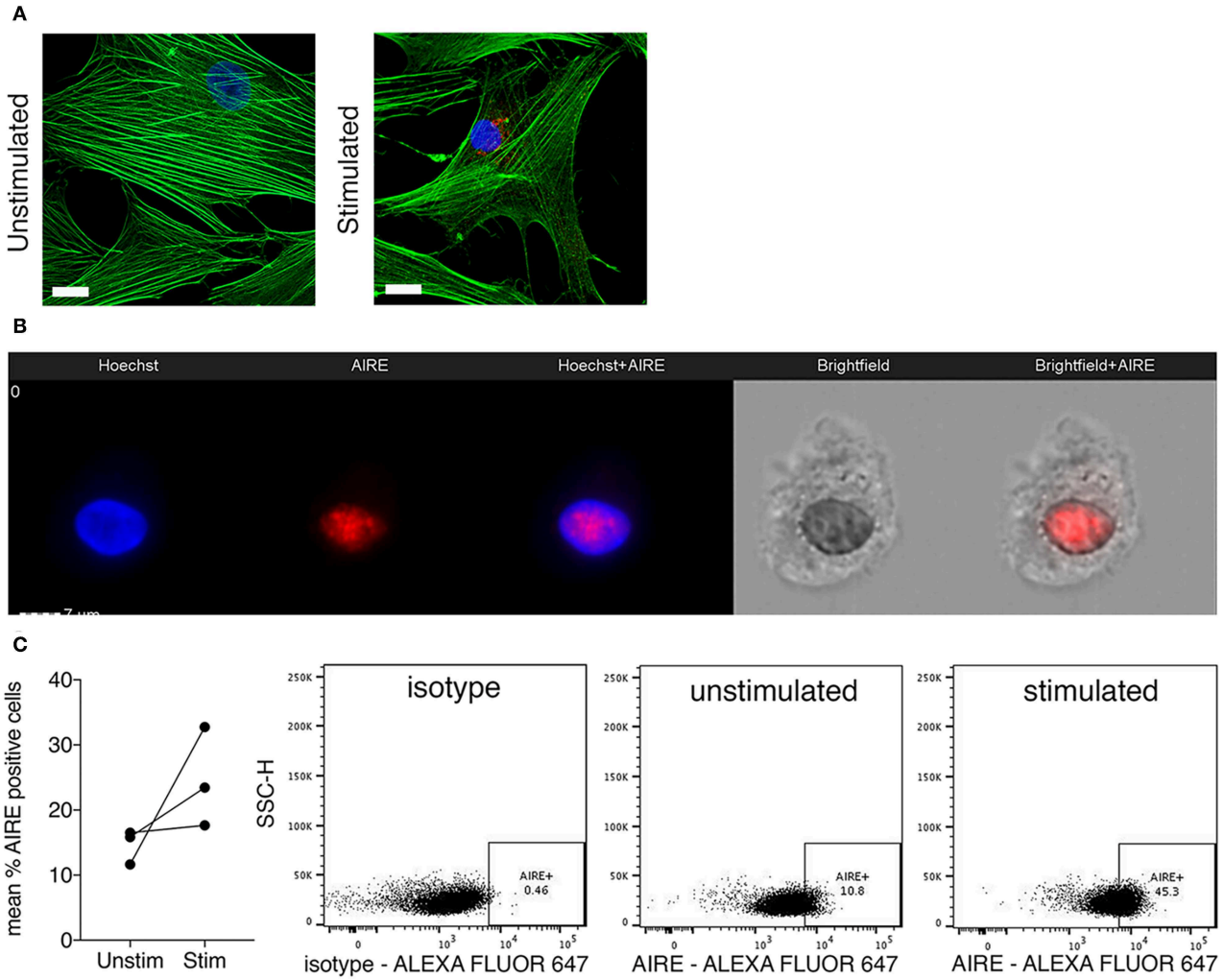

FIGURE 3 | Nuclear AIRE expression is present in cytokine stimulated RA FLS. **(A)** Representative immunofluorescence image of AIRE expression (red) in IL-1β +TNF stimulated but not in unstimulated RA FLS. Actin in green, nuclei in blue. Bar 5 μm. **(B)** Representative images of nuclear AIRE expression (red) in one IL-1β +TNF stimulated RA FLS using ImageStreamX flow cytometry. Nuclei in blue (Hoeschst). Merged Hoeschst + AIRE in the mid panel. Brightfield images to the right. **(C)** The mean AIRE protein expression (% positive cells) in unstimulated vs. IL-1β+TNF stimulated RA FLS ($n = 3$, two experiments) by flow cytometry. Representative dotplots of isotype, unstimulated, and IL-1 β +TNF stimulated samples.

AIRE Does Not Enrich for TRA Expression in Cytokine Activated RA FLS

While we have extensive knowledge of the functional consequences of AIRE expression in mTECs, the role of AIRE in other cell types is largely unknown. To explore the functional role of AIRE in FLS, we performed *AIRE* gene silencing using primary RA FLS cultures from four patients. The transfected cells were stimulated with 5 ng/ml TNF + 2 ng/ml IL-1β or kept in medium with 1% FBS for 24 h; generating samples of (1) no AIRE (unstimulated), (2) high AIRE (stimulated, non-target control siRNA), and (3) low AIRE expression (stimulated, *AIRE* siRNA); followed by RNA sequencing. The mean silencing efficiency was 71% as quantified by qPCR (3 samples had ≥84% knock-down) and the mean induction of *AIRE* in the stimulated samples was 20-fold (by normalized read counts) compared with unstimulated. However, the induction of AIRE was 12.5-fold different between the lowest and the highest expression illustrating the biologic variation in the patient samples (**Figure 4A**, see also **Figure 2B**, RA). Subsequent bioinformatic analysis identified in total 217 differentially expressed (DE) genes in stimulated "high AIRE" compared to stimulated "low AIRE" samples (adjusted $p < 0.05$) of which 171 genes were increased (up to 159-fold) and 46 decreased (down to 0.001). A heat map with the top 30 DE genes to the mean (adjusted $p < 0.05$) is shown in **Figure 4B**.

Based on the described function of AIRE in mTEC we first investigated if the induced genes were enriched for TRAs based on expression data from the BioGPS-database (www.biogps.org) and by defining TRAs as genes with an expression restricted to up to five tissues (25). However, of the 191 annotated (with

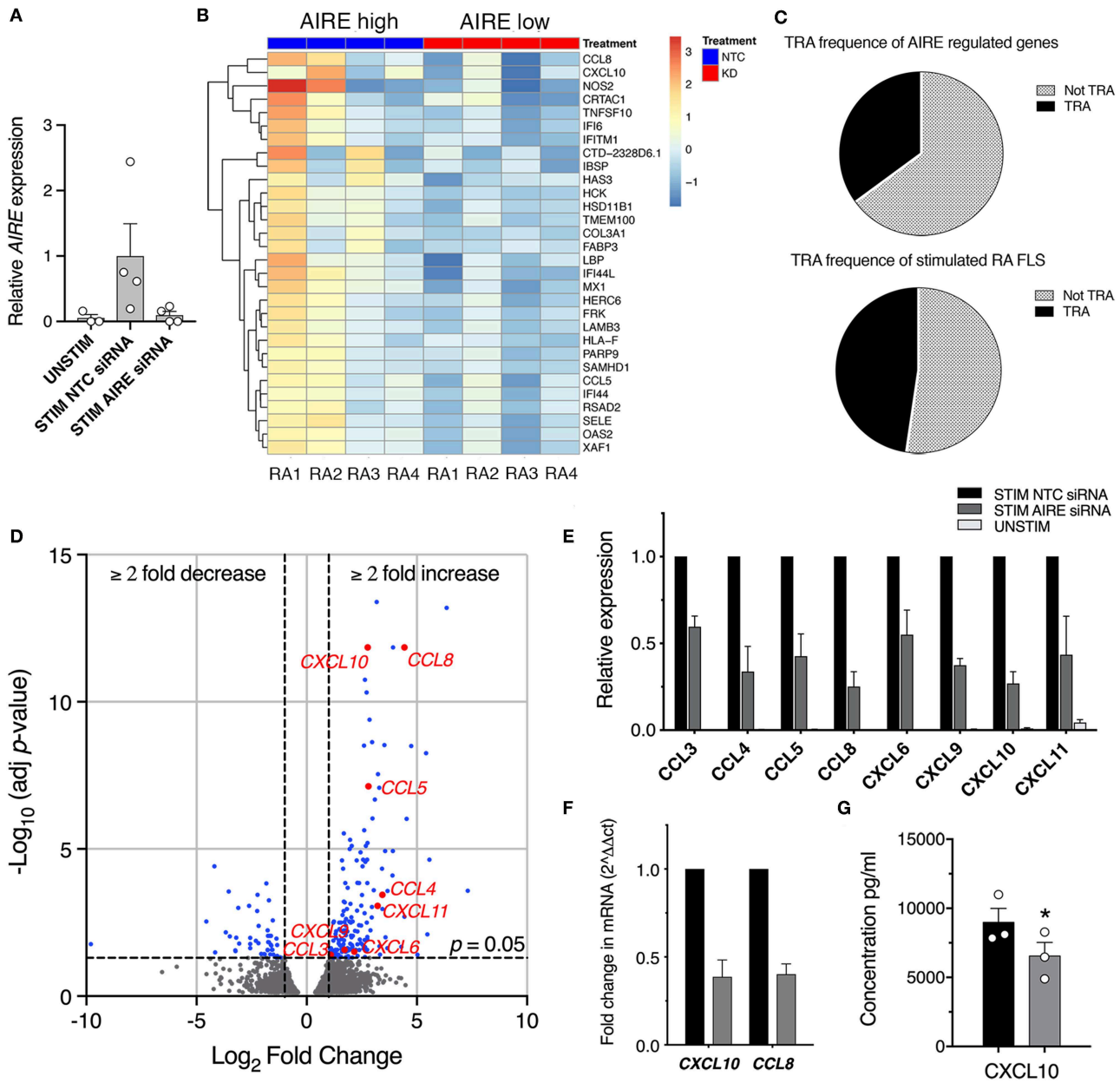

FIGURE 4 | AIRE regulates transcription of pro-inflammatory genes in activated RA FLS. **(A)** Relative *AIRE* expression in unstimulated, stimulated NTC, and AIRE silenced (KD) samples by normalized counts by size factor ($n = 4$ different RA FLS lines), **(B)** Heat map with hierarchical clustering of the top 30 of in total 217 significantly (Adj $P < 0.05$) DE genes by RNA seq in AIRE high vs. low samples. **(C)** Frequency of TRA (black) and not TRA (gray pattern) in stimulated RA FLS based on available data on tissue expression in the BioGPS database. Upper graph represents the 191 annotated AIRE regulated genes. Lower graph, the mean of three random sets of 191 annotated genes in the RNAseq dataset. **(D)** Volcano plot showing the 217 DE by in AIRE high compared to AIRE low samples (BLUE dots) and chemokines highlighted in RED. Dashed lines at adjusted $p = 0.05$ and at fold change $= \pm 2$. **(E)** Relative expression of chemokine genes in AIRE high vs. AIRE low samples normalized counts by size factor and **(F)** Relative expression of CXCL10 and CCL8 by qPCR in AIRE high vs. AIRE low samples ($n = 3$ transfected RA FLS lines). **(G)** Concentration of CXCL10 in the supernatant of TNF + IL-1β-stimulated transfected AIRE high (NTC) compared to AIRE low (AIRE siRNA) RA FLS ($p = 0.026$, $n = 3$ different RA FLS lines) by bead-based flow cytometric immunoassay. Statistics with paired two-tailed *t*-test. $^*p \leq 0.05$.

available tissue expression data) AIRE regulated genes, there was no enrichment of TRAs (35%) compared to non-AIRE regulated genes (48% TRA; mean of three random set of 191 genes in the data set using R statistics software) (**Figure 4C**, **Table S4**). As mentioned earlier, a functional up-regulation of MHC class II on RA FLS has been demonstrated *in vitro* in response to interferon γ. In addition, MHC class II expression on FLS has been demonstrated in synovial biopsies from RA joints (26).

However, we did not find any significant increase of the MHC class II trans-activator gene (CIITA) or the HLA genes encoding MHC class II proteins in the "High AIRE" samples (data not shown), further indicating that AIRE might have another role in FLS than inducing and presenting TRAs for tolerance induction purposes as in mTECs.

AIRE Augments Expression of Pro-inflammatory Genes in Activated FLS

Interestingly, the expression of eight chemokines (*CXCL10, CCL8, CCL5, CCL4, CXCL11, CXCL9, CXCL6,* and *CCL3*) were significantly higher in the High compared to Low AIRE samples (**Figure 4D**), indicating that AIRE might be regulating parts of the pro-inflammatory response induced by TNF and IL-1β. In particular, the monocyte chemoattractant protein 2 (MCP-2 or *CCL8*) was increased 21.6-fold ($p = 1.4 \cdot 10^{-12}$) and interferon γ-induced protein 10 (IP-10 or *CXCL10*) 6.8-fold ($p = 1.4 \cdot 10^{-12}$) (**Figure 4E**). Unstimulated FLS did not express any significant levels of these eight chemokines (**Figure 4E**). A reduced mRNA expression of *CXCL10* and *CCL8* in AIRE-silenced samples was confirmed by qPCR in RA FLS (**Figure 4F**).

In order to validate this, we measured the concentration of CXCL10 in the supernatants of transfected AIRE High and AIRE Low RA FLS using bead-based flow cytometric immunoassay. CXCL10 was significantly lower in AIRE silenced compared to AIRE high samples (6,548 ± 978.5 vs. 8,980 ± 1,008 pg/ml, $p = 0.026$, $n = 3$ RA FLS lines) (**Figure 4G**).

AIRE Masters Expression of an Interferon-γ Signature in Activated FLS

In addition to CXCL10 and CCL5, we found that several other genes associated with inflammation of skin (active lesions) in psoriasis (27, 28) were among the top DE genes by AIRE in RA FLS; *NOS2* (iNOS), *MX1, OAS2, IFI44, MX2*, and *OAS1*. And indeed, an unbiased Ingenuity Pathway Analysis (IPA) on the High vs. Low AIRE samples using adjusted $p < 0.05$ and differential expression $\geq \pm 1.0$ $\log_2$ fold change as cut off levels, identified "Antimicrobial response" and "Inflammatory response" ($p = 9.5 \cdot 10^{-25}$) as well as "Dermatological Diseases and Conditions" and "Organism Injury and Abnormalities" ($p = 6.6 \cdot 10^{-23}$) as the most significant pathways (**Figure 5A**) with antiviral response and psoriasis as top diseases. "Antimicrobial Response" was the most significant network with a score of 46 (**Table 1** and **Figure 5B**).

A list of predicted upstream regulators of target molecules in the dataset from the IPA prompted us to investigate if the AIRE induced genes were involved in interferon signaling. Using the Interferome v2.01 bioinformatics database of interferon responsive genes (www.interferome.org) we concluded that 96% of the annotated AIRE regulated genes were classified as interferon response genes (IRGs) with a pre-dominance (95.5%) of IFNγ (type II) IRGs (**Figure 5C**). Interestingly, IL-1β + TNF stimulation of RA FLS did not induce IFNγ mRNA (RNA seq data set) or secretion of IFNγ to the supernatant of the cell cultures (assessed by ELISA, data not shown) suggesting that AIRE induces the interferon signature independent of IFNγ.

TABLE 1 | Pathway analysis using Ingenuity Pathway Analysis of differentially expressed genes (Adjusted $p < 0.05$ and differential expression $\geq \pm 1.0$ $\log^2$ fold change) in "High AIRE" vs. "Low AIRE" samples identified the following top significant network.

Number	Molecules in Network	Score	Focus molecules	Top functions
1	Akt, CXCL10, DDX58, DHX58, EIF2AK2, IFI27, IFI35, IFI44, IFI44L, IFI6, IFIH1, IFIT1, IFIT3, IFITM1, IFN Beta, IRS2, ISG15, IFN gamma, IFN alpha, JAK, LBP, LEPR, MX1, MX2, OAS1, OAS2, OAS3, PARP9, PLSCR1, PRKAR2B, RSAD2, SAMHD1, TCR, USP18	46	28	Antimicrobial response, Inflammatory response

Relative expressions of the DE IRGs are displayed in **Figure 5D**. To test the hypothesis that AIRE promotes the expression of a pro-inflammatory IFNγ signature we performed GSEA of the gene set Hallmark Interferon Gamma Response on the AIRE High vs. AIRE Low data set which demonstrated an enrichment score (ES) of 0.550 ($p < 0.001$) and a negative ES of 2.126. *MX2* had the highest rank (5.567) and *STAT2* the highest running ES (**Figure 5E**). Running analysis of the Hallmark Inflammatory response gene set gave an ES of 0.411 ($p < 0.001$) and NES of 1.562 (**Figure 5F**). In both gene sets, the anti-inflammatory Interleukin-10 receptor α gene (*IL10RA*) had the lowest rank (-4.157) further supporting a pro-inflammatory role of AIRE.

AIRE Is Expressed in Activated FLS of the Synovial Lining Layer in RA

In RA, the number of FLS in the synovial lining layer increases and activated RA FLS play a key role in the formation of the pannus tissue. We performed immunofluorescence staining of synovial tissue samples from RA patients ($n = 5$), and found that AIRE expressing cells were present in the lining layer of the RA synovium (**Figure 6A**). The pro-invasive glycoprotein podoplanin is up-regulated on lining layer FLS in RA and by TNF and IL-1β *in vitro* (22). Double staining with AIRE and podoplanin demonstrated intense podoplanin staining in areas with AIRE positive cells including double positive cells (**Figure 6B**) indicating that AIRE is expressed in areas of FLS activation. We did not find AIRE expression in control tissue from patients with OA ($n = 4$) (**Figure 6C**). We confirmed AIRE reactivity of the antibodies on human thymic sections where a similar speckled staining pattern of mTEC nuclei was evident (**Figure 6D**).

DISCUSSION

More than 100 RA-associated risk genes have been identified, but for the majority of those, the mechanisms for disease susceptibility are unknown. It has been reported that genetic variations of *AIRE* pre-dispose for RA, and multiple omics

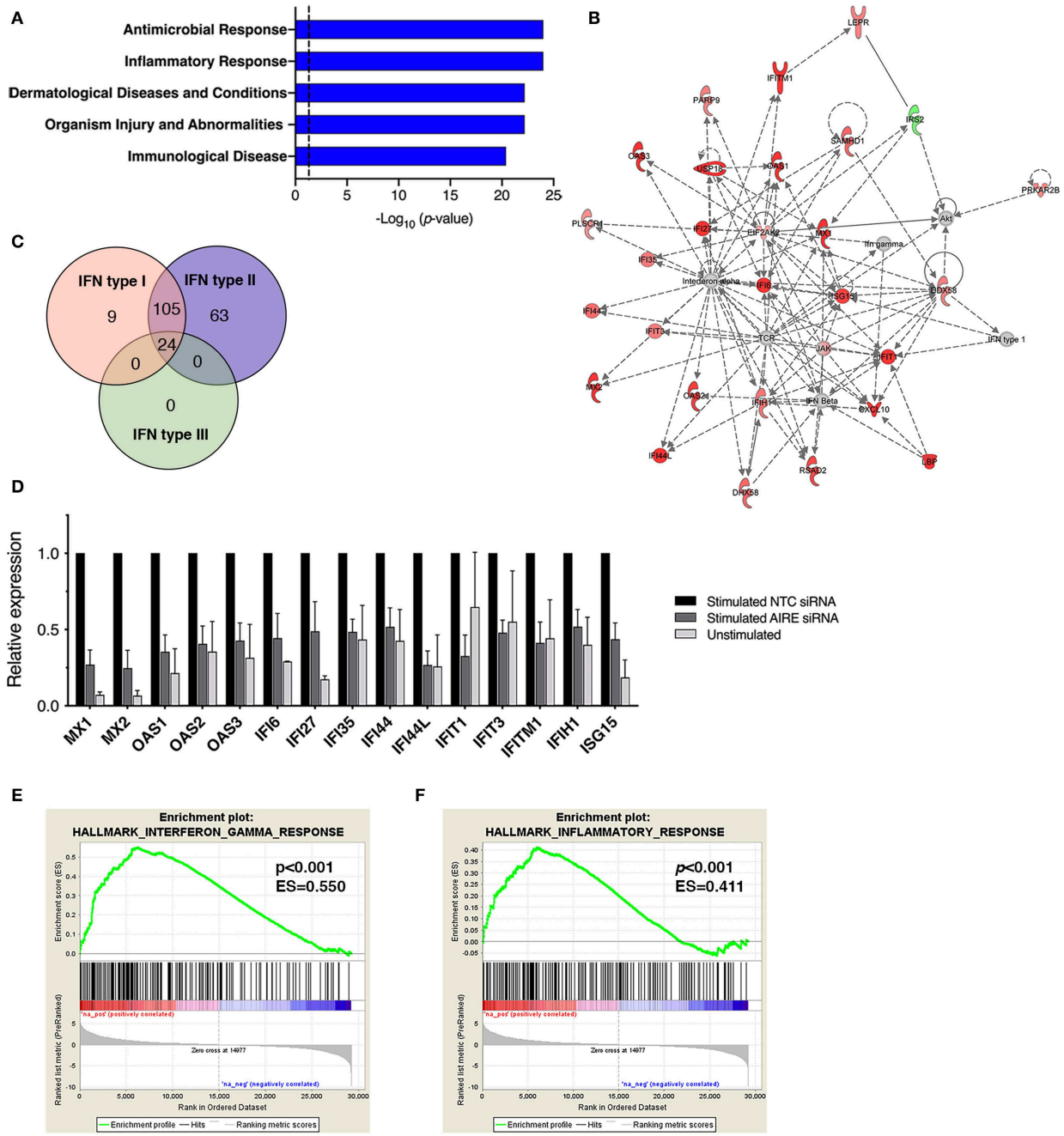

FIGURE 5 | AIRE masters expression of an interferon-γ signature in activated FLS. **(A)** The top five canonical pathways of an unbiased Ingenuity Pathway Analysis (IPA) of the DE AIRE high compared to AIRE low data set ($n = 4$ different RA FLS lines) using adjusted $p < 0.05$ and differential expression $\geq \pm 1.0$ log2 fold change as cut off levels. **(B)** The most significant network: "Antimicrobial response" with differentially expressed genes in AIRE high vs. AIRE low samples by IPA. Increased expression in RED and reduced expression in GREEN symbols. **(C)** Classification of the 201 (93%) AIRE regulated genes annotated as interferon regulated genes (IRG) by the INTERFEROME v2.01 database, showing a pre-dominance (96%) of IFN-γ (type II) regulated genes. **(D)** Relative expression (based on normalized counts by size factor) of AIRE-dependent IRGs in unstimulated (no AIRE) and stimulated AIRE low samples compared to AIRE high samples in the RNA seq data. **(E)** Gene set enrichment analysis (GSEA) of the *Hallmark Interferon Gamma Response* gene set in the DE AIRE high compared to AIRE low data set showing an enrichment score (ES) of 0.550 ($p < 0.001$) for AIRE-dependent genes in this gene set and an ES of 0.411 ($p < 0.001$) of the *Hallmark Inflammatory Response gene* set in **(F)**.

analysis (13) have pointed to a role for this autoimmune regulator in FLS. Our study demonstrates that as many as 24 RA risk genes, including *AIRE*, are differentially expressed in RA FLS stimulated by TNF and IL-1β. In particular, AIRE is not expressed in unstimulated FLS but induced upon activation by these pro-inflammatory cytokines.

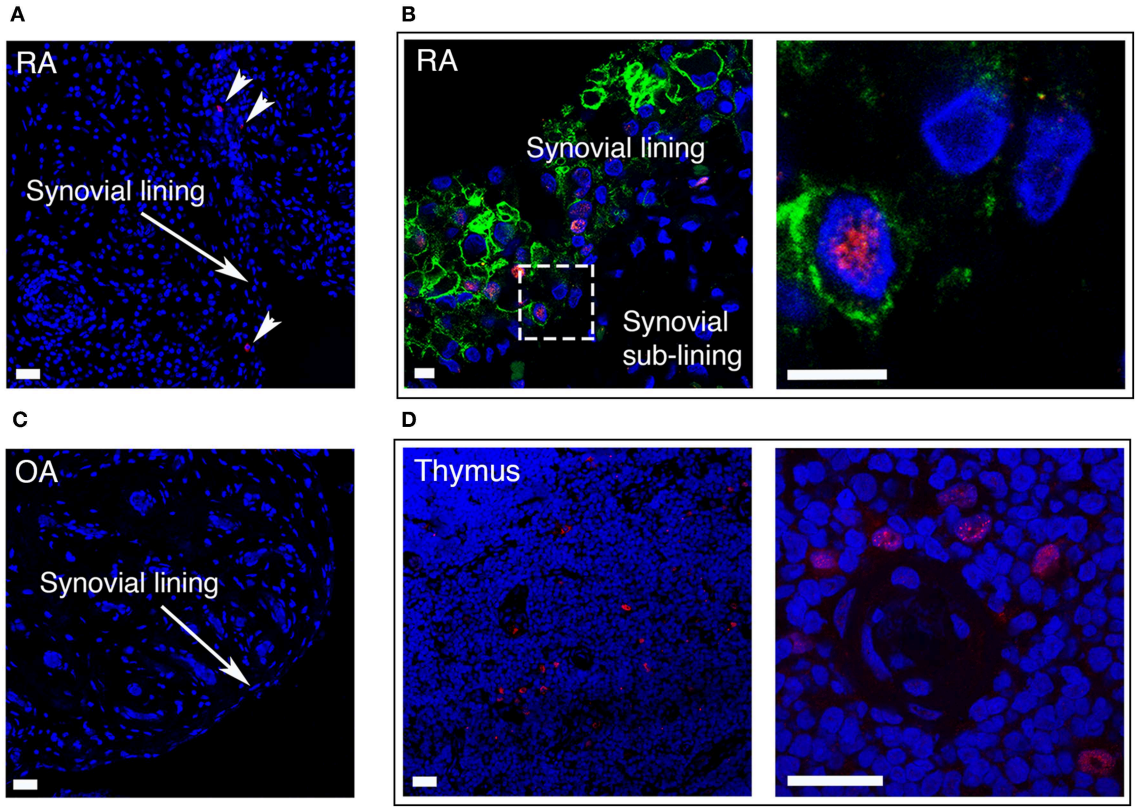

FIGURE 6 | AIRE is expressed in the synovial lining layer in RA. **(A)** RA synovium stained with S.C. anti-AIRE antibody (RED). Arrow heads show positive cells in the synovial lining layer. Bar 20 μm. **(B)** RA synovium double stained with antibodies toward the surface marker podoplanin (GREEN) of "activated" lining layer FLS and AIRE (RED, Abcam ab). Note the increased thickness of the lining layer in RA compared to OA in **Figure 1C**. Encircled area enlarged in the panel to the right showing an AIRE expressing activated FLS. Bar 5 μm. **(C)** OA synovium stained negative with S.C. anti-AIRE antibody. Bar 20 μm. **(D)** Positive control staining of human thymus tissue stained with S.C. anti-AIRE antibody (RED). Overview of the thymic medulla in the left panel and an area surrounding an Hassall's corpuscle with AIRE positive mTECs enlarged in the right panel. Bar 20 μm. Nuclei with Hoeschst (BLUE).

Interestingly, AIRE was also induced by TNF + IL-1β in OA FLS and in dermal fibroblast *in vitro,* but to a significantly lower level and with less variability than in RA FLS. It has been shown that RA FLS are primed to enhanced pathogenic responses by repeated or persistent cytokine stimulation *in vitro* (29). This together with genetic and epigenetic factors might explain the enhanced expression of AIRE in RA, which alone or in concert with other factors of the RA joint may have pathogenic impact on disease development and activity.

Based on the knowledge that MHC class II is upregulated on FLS in the RA joint we initially hypothesized that AIRE induces transcription of joint specific antigens in FLS. However, there was no enrichment of TRA genes and no induction of MHC class II genes in the AIRE high samples. Instead we found that AIRE mediates expression of IRGs in activated RA FLS, in particular a set of genes which have been associated with psoriasis skin lesions. This suggests a common inflammatory response in skin and the joint. Our data is supported by recent findings regarding keratin 17- and AIRE-dependent amplification of inflammatory and immune responses, in particular CXCL9, CXCL10, and CXCL11 expression, in skin undergoing acute inflammation or tumorigenesis (20). Furthermore, gene expression profiling of peripheral blood cells from healthy controls and RA patients in a Dutch study (30) revealed a significant up-regulation of IFN responsive genes in a subgroup of RA patients and six of these genes (*IFIT1, OAS2, MX1, IFI44L, OAS1,* and *MX2*) were also found in our dataset of top 65 AIRE regulated genes in FLS. In addition, response to anti-TNF treatment with infliximab in RA was associated with reduced expression of an IFN response gene set including *OAS1, MX2,* and *OAS2* (31) supporting a role for AIRE in the disease.

Within the interferon signature, there was a striking induction of chemokine genes also by AIRE in FLS, indicating that this master regulator promotes the recruitment of immune cells to the joint in arthritis. In particular, we found a strong AIRE-dependent induction and secretion of CXCL10 by TNF + IL-1β in RA FLS. CXCL10/IP10 is a chemoattractant for monocytes/macrophages, T lymphocytes, and dendritic cells and typically produced by fibroblasts and endothelial cells in response to INF-γ. A part from chemotaxis, CXCL10 have been reported to promote cancer invasion (32) and to increase invasive properties of RA FLS *in vitro* in a CXCR3-dependent autocrine fashion (33). The expression of CXCL10 is increased in synovial fluid and tissue in RA compared to controls (34) and serum levels of this

chemokine correlate with disease activity (35, 36), highlighting its role in disease pathogenesis.

Our finding that AIRE induces a limited number of pro-inflammatory IRGs in FLS, as opposed to the large number of TRAs induced in mTECs, is intriguing. In thymic cells, it is believed that AIRE binds to the chromatin at multiple transcription start sites, guided by epigenetic marks and Sirt1, followed by recruitment of specific enzymes and transcription factors (17). The epigenetic landscape, and hence the accessibility of promotors, most likely differ in FLS, in particular in an inflammatory context, compared to mTECs. For example, IL-1β has been demonstrated to induce alterations in DNA methylation patterns in FLS (37) and might not only lead to AIRE expression, but also affect which set of genes AIRE induces. It is also possible that another set of transcription factors (interferon regulating factors?) are available or active for AIRE to interact with in activated FLS compared to in thymic cells.

Podoplanin is a pro-invasive glycoprotein with in large unknown function which is expressed on lymphatic endothelia and other specialized tissues but also up-regulated on tumor cells and on fibroblasts in reactive tissues such as synovitis in RA (22). We found synovial AIRE expression pre-dominantly in areas of high podoplanin expression. Likewise, AIRE and podoplanin were both induced in RA FLS *in vitro* by TNF + IL-1β in our RNA seq data set. This finding strengthens the link of AIRE to a subpopulation of activated aggressive FLS.

In conclusion, we demonstrate that the autoimmune regulator AIRE is expressed in activated FLS in the RA joint and induced *in vitro* by pro-inflammatory cytokines. Furthermore, we found that AIRE augments expression of an IFN-γ signature in RA FLS including a set of chemokine genes which have been associated with disease activity and with response to treatment in RA. Our findings support a novel extrathymic pro-inflammatory role of AIRE of importance for inflammatory conditions. Although further studies are required to fully understand the importance for AIRE in arthritis, our data supports a role for AIRE in peripheral effector cells in RA.

DATA AVAILABILITY

The raw data supporting theconclusions of this manuscript will be made available by the authors upon request.

ETHICS STATEMENT

This study was carried out in accordance with the recommendations of the Regional Ethical Review Board in Gothenburg with written informed consent from all subjects. All subjects gave written informed consent in accordance with the Declaration of Helsinki.

AUTHOR CONTRIBUTIONS

A-KE, BB, and GV recruited the patients and established the biobank. A-KE, OE, BB, GV, and CL designed the experiments and analyzed the data. BB, CL, GV, and A-KE conduced the experiments and acquired the data. A-KE directed the research and drafted the manuscript. OE, BB, CL, GV, and HC participated in writing the manuscript.

FUNDING

This work was supported by grant from the Swedish Research Council [grant number 2018-02752], the Swedish Society of Medicine [grant number SLS-596391], the Swedish Rheumatism Foundation [grant number R-569341; R-663971], The Rune and Ulla Amlöv Foundation [grant number 2016-092], the King Gustav V:s 80 years Foundation [grant number FAI-2014-0086 and FAI-2017-0406], the Gothenburg Region Foundation for Rheumatology Research [grant number GSFR-20160413], the Sahlgrenska Academy and Sahlgrenska Hospital [grant number ALFGBG-771712, ALFGBG-775731, and C4I-2018-01-10], the IngaBritt and Arne Lundberg Research Foundation, and the Professor Nanna Svartz Foundation [grant number 2016-00147, 2018-00251].

ACKNOWLEDGMENTS

We gratefully acknowledge Dr. Thomas Eisler and Dr. Christian Anderberg for participating in the recruitment of patients to the synovial tissue biobank. We would like to thank the Genomics and Bioinformatics Core Facility platforms, Sahlgrenska Academy, University of Gothenburg for excellent work.

SUPPLEMENTARY MATERIAL

The Supplementary Material for this article can be found online at: https://www.frontiersin.org/articles/10.3389/fimmu.2019.01384/full#supplementary-material

Table S1 | TaqMan Gene expression assays used for qPCR.

Table S2 | Antibodies and dilutions.

Table S3 | RA susceptibility genes in activated RA FLS.

Table S4 | Random gene sets in the TRA analysis.

REFERENCES

1. Catrina AI, Svensson CI, Malmstrom V, Schett G, Klareskog L. Mechanisms leading from systemic autoimmunity to joint-specific disease in rheumatoid arthritis. *Nat Rev Rheumatol.* (2017) 13:79–86. doi: 10.1038/nrrheum.2016.200
2. Firestein GS, McInnes IB. Immunopathogenesis of rheumatoid arthritis. *Immunity.* (2017) 46:183–96. doi: 10.1016/j.immuni.2017.02.006
3. Bartok B, Firestein GS. Fibroblast-like synoviocytes: key effector cells in rheumatoid arthritis. *Immunol Rev.* (2010) 233:233–55. doi: 10.1111/j.0105-2896.2009.00859.x
4. Croft AP, Naylor AJ, Marshall JL, Hardie DL, Zimmermann B, Turner J, et al. Rheumatoid synovial fibroblasts differentiate into distinct subsets in the presence of cytokines and cartilage. *Arthritis Res Ther.* (2016) 18:270. doi: 10.1186/s13075-016-1156-1

5. Bottini N, Firestein GS. Duality of fibroblast-like synoviocytes in RA: passive responders and imprinted aggressors. *Nat Rev Rheumatol*. (2013) 9:24–33. doi: 10.1038/nrrheum.2012.190
6. Tran CN, Davis MJ, Tesmer LA, Endres JL, Motyl CD, Smuda C, et al. Presentation of arthritogenic peptide to antigen-specific T cells by fibroblast-like synoviocytes. *Arthritis Rheum*. (2007) 56:1497–506. doi: 10.1002/art.22573
7. Nagy G, van Vollenhoven RF. Sustained biologic-free and drug-free remission in rheumatoid arthritis, where are we now? *Arthritis Res Ther*. (2015) 17:181. doi: 10.1186/s13075-015-0707-1
8. Okada Y, Wu D, Trynka G, Raj T, Terao C, Ikari K, et al. Genetics of rheumatoid arthritis contributes to biology and drug discovery. *Nature*. (2014) 506:376–81. doi: 10.1038/nature12873
9. Yarwood A, Huizinga TW, Worthington J. The genetics of rheumatoid arthritis: risk and protection in different stages of the evolution of RA. *Rheumatology*. (2016) 55:199–209. doi: 10.1093/rheumatology/keu323
10. Terao C, Yamada R, Ohmura K, Takahashi M, Kawaguchi T, Kochi Y, et al. The human AIRE gene at chromosome 21q22 is a genetic determinant for the predisposition to rheumatoid arthritis in Japanese population. *Hum Mol Genet*. (2011) 20:2680–5. doi: 10.1093/hmg/ddr161
11. Feng ZJ, Zhang SL, Wen HF, Liang Y. Association of rs2075876 polymorphism of AIRE gene with rheumatoid arthritis risk. *Hum Immunol*. (2015) 76:281–5. doi: 10.1016/j.humimm.2015.01.026
12. Garcia-Lozano JR., Torres-Agrela B, Montes-Cano MA, Ortiz-Fernandez L, Conde-Jaldon M, Teruel M, et al. Association of the AIRE gene with susceptibility to rheumatoid arthritis in a European population: a case control study. *Arthritis Res Ther*. (2013) 15:R11. doi: 10.1186/ar4141
13. Whitaker JW, Boyle DL, Bartok B, Ball ST, Gay S, Wang W, et al. Integrative omics analysis of rheumatoid arthritis identifies non-obvious therapeutic targets. *PLoS ONE*. (2015) 10:e0124254. doi: 10.1371/journal.pone.0124254
14. Ekwall AK, Whitaker JW, Hammaker D, Bugbee WD, Wang W, Firestein GS. The rheumatoid arthritis risk gene LBH regulates growth in fibroblast-like synoviocytes. *Arthritis Rheumatol*. (2015) 67:1193–202. doi: 10.1002/art.39060
15. Hammaker D, Whitaker JW, Maeshima K, Boyle DL, Ekwall AH, Wang W, et al. LBH gene transcription regulation by the interplay of an enhancer risk allele and DNA methylation in rheumatoid arthritis. *Arthritis Rheumatol*. (2016) 68:2637–45. doi: 10.1002/art.39746
16. Meredith M, Zemmour D, Mathis D, Benoist C. Aire controls gene expression in the thymic epithelium with ordered stochasticity. *Nat Immunol*. (2015) 16:942–9. doi: 10.1038/ni.3247
17. Abramson J, Husebye ES. Autoimmune regulator and self-tolerance–molecular and clinical aspects. *Immunol Rev*. (2016) 271:127–40. doi: 10.1111/imr.12419
18. Abramson J, Anderson G. Thymic epithelial cells. *Ann Rev Immunol*. (2017) 35:85–118. doi: 10.1146/annurev-immunol-051116-052320
19. Anderson MS, Su MA. AIRE expands: new roles in immune tolerance and beyond. *Nat Rev Immunol*. (2016) 16:247–58. doi: 10.1038/nri.2016.9
20. Hobbs RP, DePianto DJ, Jacob JT, Han MC, Chung BM, Batazzi AS, et al. Keratin-dependent regulation of Aire and gene expression in skin tumor keratinocytes. *Nat Genet*. (2015) 47:933–8. doi: 10.1038/ng.3355
21. Arnett FC, Edworthy SM, Bloch DA, McShane DJ, Fries JF, Cooper NS, et al., The American Rheumatism Association 1987 revised criteria for the classification of rheumatoid arthritis. *Arthritis Rheum*. (1988) 31:315–24. doi: 10.1002/art.1780310302
22. Ekwall AK, Eisler T, Anderberg C, Jin C, Karlsson N, Brisslert M, Bokarewa MI. The tumour-associated glycoprotein podoplanin is expressed in fibroblast-like synoviocytes of the hyperplastic synovial lining layer in rheumatoid arthritis. *Arthritis Res Ther*. (2011) 13:R40. doi: 10.1186/ar3274
23. Love MI, Huber W, Anders S. Moderated estimation of fold change and dispersion for RNA-seq data with DESeq2. *Genome Biol*. (2014) 15:550. doi: 10.1186/s13059-014-0550-8
24. Subramanian A, Tamayo P, Mootha VK, Mukherjee S, Ebert BL, Gillette MA, et al. Gene set enrichment analysis: a knowledge-based approach for interpreting genome-wide expression profiles. *Proc Natl Acad Sci USA*. (2005) 102:15545–50. doi: 10.1073/pnas.0506580102
25. Derbinski J, Gabler J, Brors B, Tierling S, Jonnakuty S, Hergenhahn M, et al. Promiscuous gene expression in thymic epithelial cells is regulated at multiple levels. *J Exp Med*. (2005) 202:33–45. doi: 10.1084/jem.20050471
26. Firestein GS, Paine MM, Littman BH. Gene expression (collagenase, tissue inhibitor of metalloproteinases, complement, and HLA-DR) in rheumatoid arthritis and osteoarthritis synovium. Quantitative analysis and effect of intraarticular corticosteroids. *Arthritis Rheum*. (1991) 34:1094–105. doi: 10.1002/art.1780340905
27. Yao Y, Richman L, Morehouse C, de los Reyes M, Higgs BW, Boutrin A, et al. Type I interferon: potential therapeutic target for psoriasis? *PLoS ONE*. (2008) :e2737. doi: 10.1371/journal.pone.0002737
28. Murphy MJ. *Molecular Diagnostics in Dermatology and Dermatopathology*. New York: Humana Press (2011).
29. Crowley T, O'Neil JD, Adams H, Thomas AM, Filer A, Buckley CD, et al. Priming in response to pro-inflammatory cytokines is a feature of adult synovial but not dermal fibroblasts. *Arthritis Res Ther*. (2017) 19:35. doi: 10.1186/s13075-017-1248-6
30. van der Pouw Kraan TC, Wijbrandts CA, van Baarsen LG, Voskuyl AE, Rustenburg F, Baggen JM, et al. Rheumatoid arthritis subtypes identified by genomic profiling of peripheral blood cells: assignment of a type I interferon signature in a subpopulation of patients. *Ann Rheum Dis*. (2007) 66:1008–14. doi: 10.1136/ard.2006.063412
31. van Baarsen LG, Wijbrandts CA, Rustenburg F, Cantaert T, van der Pouw Kraan TC, Baeten DL, et al. Regulation of IFN response gene activity during infliximab treatment in rheumatoid arthritis is associated with clinical response to treatment. *Arthritis Res Ther*. (2010) 12:R11. doi: 10.1186/ar2912
32. Zipin-Roitman A, Meshel T, Sagi-Assif O, Shalmon B, Avivi C, Pfeffer RM, et al. CXCL10 promotes invasion-related properties in human colorectal carcinoma cells. *Cancer Res*. (2007) 67:3396–405. doi: 10.1158/0008-5472.CAN-06-3087
33. Laragione T, Brenner M, Sherry B, Gulko PS. CXCL10 and its receptor CXCR3 regulate synovial fibroblast invasion in rheumatoid arthritis. *Arthritis Rheum*. (2011) 63:3274–83. doi: 10.1002/art.30573
34. Ueno A, Yamamura M, Iwahashi M, Okamoto A, Aita T, Ogawa N, Makino H. The production of CXCR3-agonistic chemokines by synovial fibroblasts from patients with rheumatoid arthritis. *Rheumatol Int*. (2005) 25:361–7. doi: 10.1007/s00296-004-0449-x
35. Kuan WP, Tam LS, Wong CK, Ko FW, Li T, Zhu T, et al. CXCL 9 and CXCL 10 as sensitive markers of disease activity in patients with rheumatoid arthritis. *J Rheumatol*. (2010) 37:257–64. doi: 10.3899/jrheum.090769
36. Pandya JM, Lundell AC, Andersson K, Nordstrom I, Theander E, Rudin A. Blood chemokine profile in untreated early rheumatoid arthritis: CXCL10 as a disease activity marker. *Arthritis Res Ther*. (2017) 19:20. doi: 10.1186/s13075-017-1224-1
37. Nakano K, Boyle DL, Firestein GS. Regulation of DNA methylation in rheumatoid arthritis synoviocytes. *J Immunol*. (2013) 190:1297–303. doi: 10.4049/jimmunol.1202572

Conflict of Interest Statement: The authors declare that the research was conducted in the absence of any commercial or financial relationships that could be construed as a potential conflict of interest.

frontiers in Immunology

ORIGINAL RESEARCH
published: 23 July 2019
doi: 10.3389/fimmu.2019.01620

A Novel Phytochemical, DIM, Inhibits Proliferation, Migration, Invasion and TNF-α Induced Inflammatory Cytokine Production of Synovial Fibroblasts From Rheumatoid Arthritis Patients by Targeting MAPK and AKT/mTOR Signal Pathway

Hongyan Du[1], Xi Zhang[1], Yongchang Zeng[1], Xiaoming Huang[1], Hao Chen[1], Suihai Wang[1], Jing Wu[2], Qiang Li[2], Wei Zhu[3], Hongwei Li[1], Tiancai Liu[1], Qinghong Yu[2], Yingsong Wu[1] and Ligang Jie[2]**

[1] School of Laboratory Medicine and Biotechnology, Southern Medical University, Guangzhou, China, [2] Department of Rheumatology and Clinical Immunology, Zhujiang Hospital, Southern Medical University, Guangzhou, China, [3] Department of Toxicology, Guangzhou Center for Disease Control and Prevention, Guangzhou, China

In rheumatoid arthritis(RA) pathogenesis, activated RA fibroblast-like synoviocytes (RA-FLSs) exhibit similar proliferative features as tumor cells and subsequent erosion to cartilage will eventually lead to joint destruction. Therefore, it is imperative to search for compounds, which can effectively inhibit the abnormal activation of RA-FLSs, and retard RA progression.3′3-Diindolylmethane (DIM), the major product of the acid-catalyzed oligomerization of indole-3-carbinol from cruciferous vegetables, has been reported to be functionally relevant to inhibition of migration, invasion and carcinogenesis in some solid tumors. In this study, we explored the anti-proliferation, anti-metastasis and anti-inflammation effects of DIM on RA-FLSs as well as the underlying molecular mechanisms. To do this, primary RA-FLSs were isolated from RA patients and an animal model. Cell proliferation, migration and invasion were measured using CCK-8, scratch, and Transwell assays, respectively. The effects of DIM on Matrix metalloproteinases (MMPs) and some inflammatory factors mRNA and key molecules such as some inflammatory factors and those involved in aberrantly-activated signaling pathway in response to tumor necrosis factor α(TNF-α), a typical characteristic mediator in RA-FLS, were quantitatively measured by real-time PCR and western blotting. Moreover, the effect of DIM on adjuvant induced arthritis(AIA) models was evaluated with C57BL/6 mice *in vivo*. The results showed that DIM inhibited proliferation, migration and invasion of RA-FLS *in vitro*. Meanwhile, DIM dramatically suppressed TNF-α–induced increases in the mRNA levels of *MMP-2*, *MMP-3*, *MMP-8,* and *MMP-9*; as well as the proinflammatory factors *IL-6, IL-8,* and *IL-1β*. Mechanistic studies revealed that DIM is able to suppress phosphorylated activation not only of p38, JNK in MAPK pathway but of AKT, mTOR and downstream molecules in the AKT/mTOR pathway. Moreover, DIM

OPEN ACCESS

Edited by:
Hanshi Xu,
First Affiliated Hospital of Sun Yat-sen University, China

Reviewed by:
Laura Mandik-Nayak,
Lankenau Institute for Medical Research, United States
Yunfeng Zhao,
Louisiana State University Health Sciences Center Shreveport, United States

***Correspondence:**
Yingsong Wu
wg@smu.edu.cn
Ligang Jie
jieligang@hotmail.com

Specialty section:
This article was submitted to Autoimmune and Autoinflammatory Disorders, a section of the journal Frontiers in Immunology

Received: *12 March 2019*
Accepted: *28 June 2019*
Published: *23 July 2019*

Citation:
Du H, Zhang X, Zeng Y, Huang X, Chen H, Wang S, Wu J, Li Q, Zhu W, Li H, Liu T, Yu Q, Wu Y and Jie L (2019) A Novel Phytochemical, DIM, Inhibits Proliferation, Migration, Invasion and TNF-α Induced Inflammatory Cytokine Production of Synovial Fibroblasts From Rheumatoid Arthritis Patients by Targeting MAPK and AKT/mTOR Signal Pathway. Front. Immunol. 10:1620. doi: 10.3389/fimmu.2019.01620

treatment decreased expression levels of proinflammatory cytokines in the serum and alleviated arthritis severity in the knee joints of AIA mice. Taken together, our findings demonstrate that DIM could inhibit proliferation, migration and invasion of RA-FLSs and reduce proinflammatory factors induced by TNF-α *in vitro* by blocking MAPK and AKT/mTOR pathway and prevent inflammation and knee joint destruction *in vivo*, which suggests that DIM might have therapeutic potential for RA.

Keywords: 3′3-Diindolylmethane(DIM), suppress, rheumatoid arthritis fibroblast-like synoviocytes (RA-FLSs), adjuvant-induced arthritis (AIA), MAPK, AKT/mTOR

INTRODUCTION

Rheumatoid arthritis (RA) is one of the prevalent systemic, inflammatory, and autoimmune diseases characterized by persistent synovitis in limb joints and resulted in bone erosion, even malformation and disability. According to reports, the disability rate from RA patients is up to 60% within 5–10 years and to 90% within 30 years. The 5-years survival rate of patients with external articular phenotype is only 50% (1). Because of the complicated immune mechanism, the RA etiology is still unclear. However, it is well-known that the terminal target of RA is synovium which characterized by Synovial hyperplasia, synovium pannus invasion and finally destroying the bone and cartilage. In RA pathogenesis activated RA-FLSs exhibit similar aggressive characteristic as tumor cells, which is the main trigger for abnormal hyperplasia and joint destruction (2, 3). Therefore, it is of great scientific significance to find pathways and targets to inhibit the proliferation and invasion of RA-FLS.

Many natural compounds from fruits and vegetables have been reported pharmaceutically effective against tumors and some inflammatory diseases (4, 5). Indolyl-3-carbinol (I3C) is a bioactive glucobrassicin with indole group originally found in cruciferous vegetables (**Figure 1Aa**). Because of its high instability, I3C is usually converted to more than 15 oligomeric and dimer bioactive compounds under acid conditions *in vivo*. Especially, 3′3-Diindolylmethane (DIM), a indole derivative (**Figure 1Ab**), is the unique dimer form converted from I3C and exert main function for I3C *in vivo* (6–8). Recently more and more concerns have been put on DIM due to its anti-proliferation, anti-cancer activity and anti-inflammatory effects in various cancers including oral, prostate, breast, colorectal, pancreatic, liver, and gastric cancer (9–13). Moreover, some researchers even give recommendations for DIM intake contributing to a greater understanding of exposure estimates (14).

Recurrent and chronic inflammation is involved in the development of a variety of human cancer and autoimmune diseases. Inflammation promotes the proliferation and inhibits apoptosis of related cells. It also encourages angiogenesis and production of proinflammatory cytokines in RA (1, 15). Considering that RA is a typical chronic inflammatory autoimmune disease and DIM can exert anti-inflammatory and chemopreventive effects, we muse boldly that DIM would be a potential natural product contributing for RA treatment. However, the effects of DIM on RA is still not clear. Therefore, in this study, we not only investigated the effects of DIM in treating RA in terms of proliferation, migration, invasion and producing proinflammatory cytokines but explored the underlying molecular mechanisms. Furthermore, we tried to test the effects of DIM on controlling inflammatory progress in adjuvant-induced arthritis (AIA) models.

MATERIALS AND METHODS

Isolation and Culture of Cells

Six synovial tissues were obtained from active RA patients who were undergoing synovectomy with arthroscopy. The RA patients included 2 men and 4 women(average age 52.8 ± 14.3 years; range 24–61 years, whose detailed information were shown in **Table S1**. All selected RA patients fulfilled the American College of Rheumatology revised criteria of the diagnosis of RA (16) and were informed consent. This study complied with the rules enacted by the Medical Ethics Committee of the Zhujiang Hospital, Southern Medical University and was performed according to the recommendations of the Declaration of Helsinki. The harvested synovial tissue were cut into small parts and incubated with collagenase I for 1–3 h at 37°C to isolate synoviocytes (RA-FLSs) according to previous published research (17–19). RA-FLSs were cultured in DMEM/F12 supplemented with 10% fetal bovine serum (FBS), 100 U/mL penicillin, and 100 mg/L streptomycin at 37°C and 5% CO_2. Until ∼95% confluency, cells were subsequently digested using 0.25% trypsin, collected, re-suspended, and planted for proliferation. RA-FLSs obtained from passage three to six were used for the following experiments. All cell culture reagents were from Gibco® (Thermo Fisher Scientific, MA, USA).

Cell Viability Assay

The Cell Counting Kit (CCK-8) assay (KeyGEN BioTECH) was utilized to determine the cell viability according to the manufacture's instruction. RA-FLSs were planted into a 96-well plate with a density of 2.0×10^3/well and cultured in 100 μL DMEM medium with 10% (v/v) FBS. Twelve hours later cells were treated with DIM(C17H14N2, ≥98% HPLC, CAS:1968-05-4, Sigma-Aldrich) at various concentration. DIM was dissolved in dimethyl sulfoxide (DMSO) and the solution was diluted to the final concentration in DMEM supplemented with 10% FBS. Cells in the control group were treated with vehicle (DMSO in DMEM supplemented with 10% FBS). After 24 and 48 h

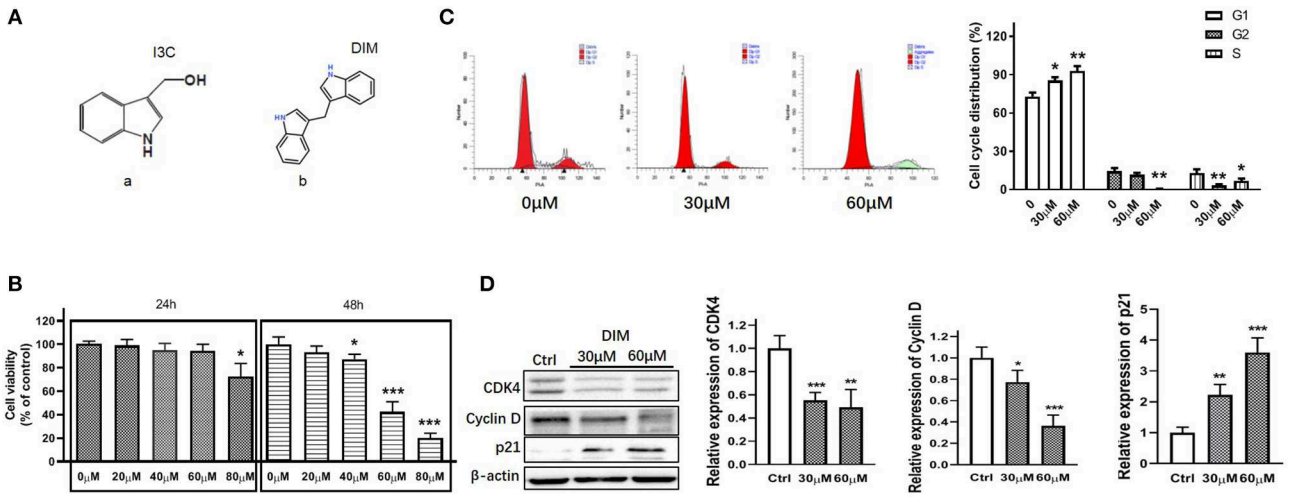

FIGURE 1 | DIM suppresses the viability of RA-FLSs and arrests the cell cycle in G1 phase. **(A)** Molecular structure of (a) indole-3-carbinol (I3C) and (b) 3,3′-diindolylmethane (DIM). **(B)** The cell viability of RA-FLSs treated with DIM at various concentrations (0,20,40,60,80 μM) for 24 h and 48 h. **(C)** The cell cycle of RA-FLSs treated with DIM at various concentrations (0,30,60 μM) for 24 h. **(D)** Expression levels of CDK4, Cyclin D and p21 in RA-FLSs after treated with DIM (0,30,60 μM) for 24 h measured by Western blot(left panel). Representative images of immune blot and densitometric quantification of CDK4, Cyclin D and p21 expression(right panel). Data are represented as the mean ± SD ($n = 3$). $^{*}P < 0.05$, $^{**}P < 0.01$, $^{***}P < 0.001$ vs. 0 μM (Ctrl).

pretreated with DIM, the RA-FLSs incubated with 10 μL CCK-8 at 37°C for 2 h. The absorbance was measured at 450 nm with a microplate reader.

Cell Cycle Analysis

The Cell Cycle Detection Kit (KeyGEN BioTECH) was utilized to determine the cell cycle according to the manufacture's instruction. Before treating RA-FLSs were serum starved for 24 h, then incubated with DIM in various concentrations for 24 h. Cells were harvested and fixed at 4°C with 70% cold ethanol overnight. Next, fixed cells were subsequently washed with PBS again and incubated with 100 μL RNase A at 37°C for 30 min. To stain the cells nuclei propidium iodide was added into suspension and incubated with cells at room temperature in a dark place for 30 min. Finally, stained cells were detected with BD FACSCalibur™ Flow Cytometer(BD Bioscience, USA) as described previously (18).

Cell Migration and Invasion

The Boyden chamber method was used to RA-FLSs migration assay in 24-well plate with 6.5 mm diameter inserts containing 8 μm pores (Costar, New York, NY, USA). Briefly, RA-FLSs were pretreated with 1% (v/v) dimethyl sulfoxide (DMSO) and DIM respectively for 24 h. Then, cells were trypsinized and re-suspended with serum-free DMEM medium at a final concentration of 2×10^4 /mL. Two hundred microliter cell suspension was put into the upper chamber of the Transwell insert. 500 μL DMED with 10% FBS as chemoattractant was placed in the lower wells. The plate was incubated at 37°C under 5% CO_2 for 6–12 h. The non-migrating cells remaining on the upper surface of the chamber were removed using a cotton swab. The cells adhering beneath the chamber, which went through the filter, were fixed with methanol for 15 min and stained with 0.1% crystal violet for 15 min. The filter was removed carefully with a knife and fixed on a glass slide with resin. The cells was quantified by counting the stained cells that migrated to the lower side of the filter using an optical microscope. The stained cells were counted as the mean number of cells per 6 random fields for each assay.

For the *in vitro* invasion assay, similar experiment was performed using inserts coated with Matrigel basement membrane matrix (BD Biosciences, Oxford, UK). Finally, the stained cells were counted as the mean number of cells per 6 random fields for each assay. All of the experiments were replicated 3 times.

Wound Healing Assay

The first day RA-FLSs were planted into a 12-well culture plate and grown to confluence up to more than 90%. Next day the culture media were replaced with fresh DMEM within various concentration DIM individually. The plate was then scratched with a sterile plastic pipette tip and washed with PBS twice to remove deciduous cells. There was a single wound was created in the center of the cell monolayer. After 48 h the wound areas were respectively photographed using microscope (Olympus IX51, Japan) equipped with a digital camera, and three assays of wound area were made at randomly fields. The extent of wound closure was presented as the percentage by which the original scratch area had decreased at each measured time point. The data are presented as the mean ± SD of three independent experiments.

RNA Isolation and Real-Time PCR Analysis

To measure the effect of DIM on RA-FLSs some cytokines and MMPs expression were detected by real-time PCR analysis as described previously (20). Cells were seeded in 12-well plates at a density of 5×10^4/well for overnight and treated with TNF-α (10 ng/mL) or/and DIM(25 and 50 μM) for 24 h. Total RNA was

isolated using Trizol reagent (Invitrogen, San Diego, CA, USA) and cDNAs were reversely transcripted using the Prime Script RT Reagent kit (Takara Biotechnology, Dalian, China) according to the manufacturer's protocol. Quantification of expressions of human cytokines and MMPs mRNAs was determined using SYBR Premix Ex TaqTM kit (Takara Biotechnology, Dalian, China) on an ABI-7500 Thermal Cycler (Applied Biosystems Inc., Foster City, CA, USA) according to the manufacturer's instructions. All experiments were performed in triplicate and replicated 3 times and negative (ddH_2O containing no template) controls were included. The primers for real-time PCR were listed in **Table S2**. To quantify the relative expression of each gene, Ct values were normalized to the endogenous β-actin ($\Delta Ct = Ct_{target} - Ct_{\beta\text{-actin}}$) and compared with a calibrator using the $\Delta\Delta Ct$ method ($\Delta\Delta Ct = \Delta Ct_{sample} - \Delta Ct_{control}$).

Western Blot Assay

The levels of protein expression were detected by western blot analysis as described previously (18). RA-FLSs were treated with 40 and 80 μM DIM for 24 h. Briefly, total cellular protein was extracted using RIPA lysis buffer and phosphatase inhibitors(Beyotime Biotechnolgoy, Nantong, China) on ice. After aspirated and thawed repeatly the lysates were separated by centrifugation at 12,000 rpm for 20 min at 4°C. The supernatants were transferred and the debris were discarded. The concentration in supernatants were detected with Pierce® BCA Protein Assay Kit(Thermo Scientific, USA). Equal amounts of protein lysate were separated by 10% SDS-PAGE and then transferred to PVDF membranes. The membranes were blocked with 5% non-fat dry milk at room temperature for 1–2 h and incubated overnight at 4°C with primary antibodies. Subsequently membranes were incubated for 1 h at room temperature with secondary antibodies. Endogenous β-actin or GAPDH were used as an internal standard for normalization. The protein bands were exposed with Clarity™ Western ECL Substrate kit (Bio-Rad Laboratories, Shanghai, China) and measured by ChemiDoc® XRS+ System (Bio-Rad Laboratories, Shanghai, China). The band density was quantified by Image J software. Primary antibodies included p38 MAPK, JNK, p44/42 MAPK (Erk1/2),FAK, AKT, mTOR, p70S6K, 4E-BP1, and their corresponding phosphorylation antibody, Phospho-p38 MAPK(Thr180/Tyr182), Phospho-JNK (Thr183/Tyr185), Phospho-p44/42 MAPK (Erk1/2) (Thr202/Tyr204), phospo-FAK (Tyr397), Phospho-Akt (Ser473), Phospho-p70 S6 Kinase (Thr389), and Phospho-4E-BP1 (Ser65), which were all purchased from Cell Signaling Technology, USA. Anti-β-actin and GAPDH antibodies were purchased from bioworld technology Inc.

Measurements of Cytokines Level by ELISA

Cytokines level were measured by human enzyme-linked immunosorbent assay (ELISA) kits (Jiangsu Meimian Industrial Co., Ltd, Jiangsu, China) according to the manufacturer's instructions. For IL-6 releasing from RA-FLSs, cells were seeded into 6-well plates at a density of 5×10^5/well overnight. Following treated with TNF-α (10 ng/mL) or/and DIM(25 and 50 μM) for 48 h the supernatant was collected from culture, then centrifuged (2,000 g for 10 min) and analyzed for the secretion of IL-6 using Microplate spectrophotometer(Biorad, USA) at 450 nm as described previously (20). Other Cytokines assays were performed just like IL-6 protocol. All experiments were performed in triplicate and replicated 3 times.

Animals

Male C57BL/6 mice aged 10–12weeks were purchased from Experimental Animal Center of the Southern Medical University. Mice were fed in well ventilated cages with free access to commercial diet and tap water. The room housed mice was fixed temperature (22 ± 2) °C and humidity (50 ± 20%) under standard laboratory conditions of 12 h/12 h light/dark cycles. All the experimental procedures abided by the guidelines of ethical regulations for institutional animal care and use in the Southern Medical University and approved by The Southern Medical University Ethics Committee for Animal Laboratory Research.

Animal Treatments

Eighteen male C57BL/6 mice (about 20 g/body weigh) were randomly divided into three groups of six, which were the normal group, the AIA model group and AIA model treated with DIM group. The induction procedures of AIA mice were refer to previously described (21–24) and adjusted in some points. The detail procedures as follows: same volume of 5% bovine serum albumin (BSA, Sigma, USA) dissolved in PBS and Freund's complete adjuvant (Sigma-Aldrich, USA) supplemented with 1.0 mg/ml heat-killed Mycobacterium tuberculosis(strain H37Ra, ATCC25177) were mixed and emulsified. On day 0, except for the normal group, mice were immunized by subcutaneously injecting 100 μL emulgator into the each side of forelimb respectively. On day 14, mice were immunized by injecting 10 μL emulgator emulsified with 5%BSA and Freund's incomplete adjuvant (Sigma-Aldrich, USA) into each sides of knee articular cavity. From day 2 to day 31 after immunizing, mice were administered with oral gavage of 100 μL DIM (10 mg/kg) suspended in 1% sodium carboxylmethyl cellulose(viscocity:600–1,000 mpa.s, USP, Shanghai Macklin Biochemical Co., Ltd.) once a day consecutively. Normal and AIA model groups were given an equal volume of 1% sodium carboxylmethyl cellulose suspension i.g. simultaneously. The mice were then monitored every day by examiners who were blinded to the experimental design. Body weight and the mediolateral knee joint diameter were measured with an electronic scale and an vernier caliper as general physical signs every 5 day (24, 25).

Measurement of Serum Pro-inflammatory Cytokines Concentration

On day 40 and 80 after immunization, about 0.5 mL each blood samples were collected from the eyeballs of mice and allowed to clot for 1 h at room temperature. Serum was separated by centrifuging at 2,000 g for 10 min and stored at −80°C for analysis. The levels of inflammatory cytokines in serum *in vivo* were respectively detected with Mice IL-6, IL-17, TNF-α, IL-8, and IL-1β ELISA Kits (Jiangsu Meimian Industrial Co., Ltd,

Jiangsu, China) according to the manufacturer's instructions, and absorbance was measured at 450 nm (26, 27).

Spleen and Liver Indices Assays

On day 80 after immunization following blood collection, the mice anesthetized with CO_2 were sacrificed by cervical dislocation. The spleen and liver were removed and weighed. The spleen and liver indices were expressed as the ratio of spleen and liver wet weight to mice body weight (g/g), respectively. That is, organ index=organ wet weight (g)/animal body weight (g) × 100% (27, 28).

Histopathological Examination of Joints

The two hind limbs with knee articular of each mice were immediately cut off after removing spleen and liver. After removing the muscle tissue the joint parts were fixed in Roles-Bio® Universal Tissue Fixative (Roles-Bio, Guangzhou Routh Biotechnology Co., Ltd.) for 2 days, then decalcified with Roles-Bio® Quick Decalcifying Solution (Roles-Bio, Guangzhou Routh Biotechnology Co., Ltd.) for 1-2 day at room temperature. After decalcification, the tissues were dehydrated, processed, and then embedded in paraffin. Serial paraffin sections (5 μm) were stained with hematoxylin and eosin (H&E) (27) and synovitis and joint destruction were graded in a blinded manner. A histologic scoring system was used, where 1=mild, 2=moderate, and 3=severe (24).

Statistical Analysis

Results of multiple experiments were presented as the mean ± standard deviation (SD). Data analysis was performed using GraphPad 6.0 Software (GraphPad, San Diego, CA, USA). The statistical comparisons (*P*-values) between two groups were calculated using Student's *t*-test and *P*-values between more than three groups were calculated using one-way and/or two-way analysis of variance (ANOVA). *P*-values <0.05 were considered statistically significant. Number of replicates and/or total number of animals were shown in figure legends or within the figures.

RESULTS

DIM Suppresses the Viability of RA-FLSs and Arrests the Cell Cycle in G1 Phase

To explore the effect of DIM on the viability of FLSs, we measured the effect of DIM with serial concentrations(0, 20, 40, 60, and 80 μM) on the viability of RA-FLSs. DIM almost did not affect cell viability except for concentrations of 80 μM after 24 h treatment, while higher concentrations DIM(40, 60, and 80 μM) showed a dose-dependent decrease in cell viability after 48 h treatment (**Figure 1B**). Similarly, cell cycle analysis also indicated that DIM resulted in a significant increase in proportion of cells in the G1 phase and a significant decrease in the S and G2/M phase (**Figure 1C**), which suggested DIM could arrest the cell cycle in G1 phase. Next, how DIM affected cell cycle regulators was explored. As shown in **Figure 1D**, the G1/S CDKs (CDK4) and the G1/S cyclin (cyclin D1) were all downregulated. On the contrary, p21, a cyclin-depend kinase inhibitor, was upregulated in RA-FLSs treated with DIM. Collectively, these results suggest that DIM could suppress the proliferation of RA-FLSs and arrest the cell cycle in G1 phase through regulating cell-cycle proteins.

DIM Suppresses the Migration and Invasion of RA-FLSs

To evaluate the effect of DIM on migration and invasion *in vitro*, the migration and invasion of RA-FLSs were evaluated using the transwell Boyden chamber and wound closure assays. 25 and 50 μM DIM treatment markedly decreased both migratory and invasion capacity of RA-FLSs comparing with control as shown in **Figures 2A,B**. This result was further confirmed by wound healing assay. Although 20 μM DIM did not influence the ability of RA-FLSs migrating from one end of wound to the other, higher concentration DIM (40 and 80 μM) did reduce the wound healing ability significantly as shown in **Figure 2C**. All of which indicated DIM could suppress the migration and invasion of RA-FLSs *in vitro*.

DIM Suppresses the Pro-inflammatory Cytokines and MMPs Expression

The pro-inflammatory cytokines and matrix metalloproteinases(MMPs) play important roles on proliferation, migration and invasion of RA-FLSs and even erosion of cartilago articularis (15). TNF-α is a key pro-inflammatory cytokine contributing to RA-FLSs surviving and developing arthritis. In our results shown in **Figure 3A**, TNF-α promoted the viability of RA-FLSs and although 25 μM DIM did not decrease the cell viability induced by TNF-α(10 ng/mL), 50 μM DIM did. To determine the role of DIM on main pro-inflammatory cytokines expression, the mRNA levels of *IL-6, IL-8, IL-1β, IL-17*, *Receptor Activator of Nuclear Factor-κ B Ligand (RANKL)* and special *Osteoprotegerin(OPG)* stimulating by TNF-α in RA-FLSs were measured with quantitative PCR after treated with 25 and 50 μM DIM for 24 h. As shown in **Figure 3B**, except for *OPG* the mRNA expression of *IL-6, IL-8, IL-1β,* and *RANKL* in RA-FLSs up-regulated more or less after induced by TNF-α(10 ng/mL), but DIM(25 and 50 μM) inhibited *IL-6, IL-8,* and *IL-1β* mRNA expression levels increase caused by TNF-α(10 ng/mL) and had no significant effect to *RANKL*. Neither TNF-α nor DIM treatment obviously altered *IL-17* mRNA expression. Distinguishingly, 50 μM DIM promoted the mRNA expression of *OPG* comparing to control and TNF-α treatment groups. As shown in **Figure 3C**, the mRNA expression of *MMP-2, MMP-3, MMP-8,* and *MMP-9* were very less and almost undetectable after DIM(25 and 50 μM) treatment, which indicated DIM profoundly inhibited increase in mRNA expression of *MMP-2, MMP-3, MMP-8,* and *MMP-9* induced by TNF-α in RA-FLSs.

Furthermore, Except for mRNA level the effect of DIM on some pro-inflammatory cytokines release induced by TNF-α was also explored. After treating with 25 and 50 μM DIM for 48 h, cells culture supernatant were collected and ELISA assays for IL-6, IL-8, IL-1β, and IL-17 were performed. The data in **Figure 3D** indicated TNF-α(10 ng/mL) significantly up-regulated the IL-6 and IL-1β release from RA-FLSs especially IL-6, but DIM treatment could inhibit their increase in culture supernatant (**Figures 3Da,b**). Interestingly, TNF-α(10 ng/mL) stimulation

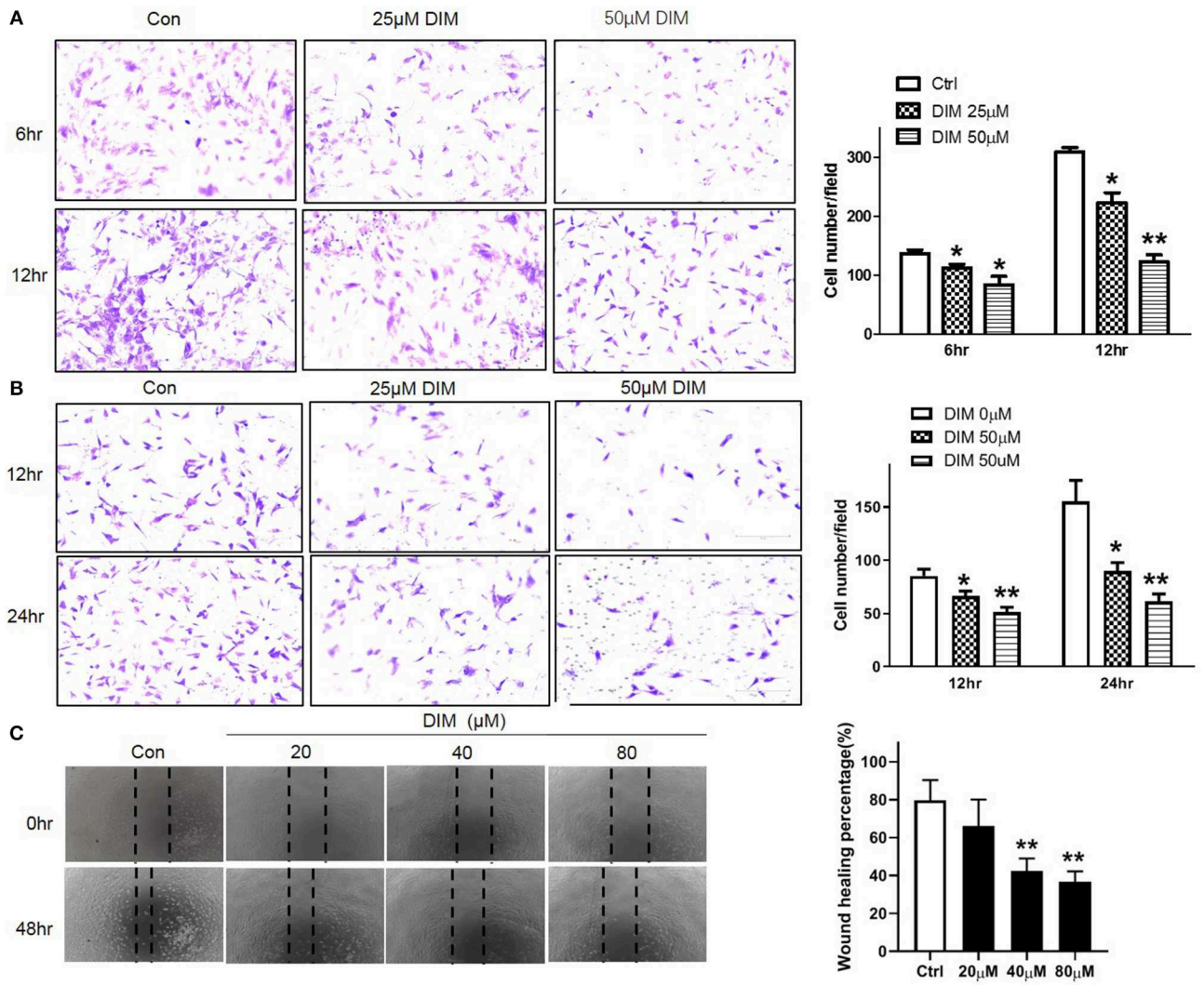

FIGURE 2 | DIM Suppresses the migration and invasion of RA-FLSs. **(A)** The effect of DIM (0, 25, 50 μM) on migration was detected with transwell Boyden chamber after 6 and 12 h. The images are representative of migration or invasion through the membrane after staining. Original magnification 200 × (left panel). Cell numbers/field are presented as the mean ± SD of six independent fields (right panel). **(B)** The effect of DIM (0, 25, 50 μM) on invasion was detected with transwell Boyden chamber coated with a Matrigel basement membrane matrix after 12 and 24 h. The images are representative of migration or invasion through the membrane after staining. Original magnification 200 × (left panel). Cell numbers/field are presented as the mean ± SD of six independent fields (right panel). **(C)** The effect of DIM (0, 20, 40, 80 μM) on wound healing was detected with cell scratching assay. After 48 h the wound area was photographed using microscope. Original magnification 100 × (left panel). The extent of wound closure was presented as the percentage by which the original scratch width had decreased at each measured time point (right panel). The values are the mean ± SEM from at least 3 independent experiments. $^{*}P < 0.05$, $^{**}P < 0.01$ vs. 0 μM (Ctrl).

did not cause profound increase in IL-8 releasing, 50 μM DIM indeed down-regulated IL-8 expression (**Figure 3Dc**). IL-17 was undetectable in this ELISA-based assay. Collectively, these results suggest that DIM may contribute to reduce producing and releasing some pro-inflammatory cytokines and MMPs in RA-FLSs.

DIM Suppresses the Activation of MAPK and Akt/mTOR Pathways Induced by TNF-α in RA-FLSs

Mitogen Activated Protein Kinases (MAPK), including ERK, JNK, and P38MAP kinase (P38), play the major role in stress-induced cellular responses such as cell proliferation, survival, apoptosis and invasion and are intracellular effector molecules that are embedded in a highly active signaling cascade in RA-FLSs (29). Since DIM could suppress viability and proliferation of RA-FLSs, we presume that MAPK pathway was affected by DIM in RA-FLSs. Therefore, the effect of DIM on MAPKwas investigated. The cells were treated with 10 ng/mL TNF-α in the presence or absence of 40 and 80 μM DIM for 24 h, western blot analysis was conducted to assess the expression and phosphorylated levels of p38MAPK, JNK, ERK. According to results in **Figure 4A** the DIM could obviously decrease the phosphorylation level of p38MAPK, JNK induced by TNF-α,

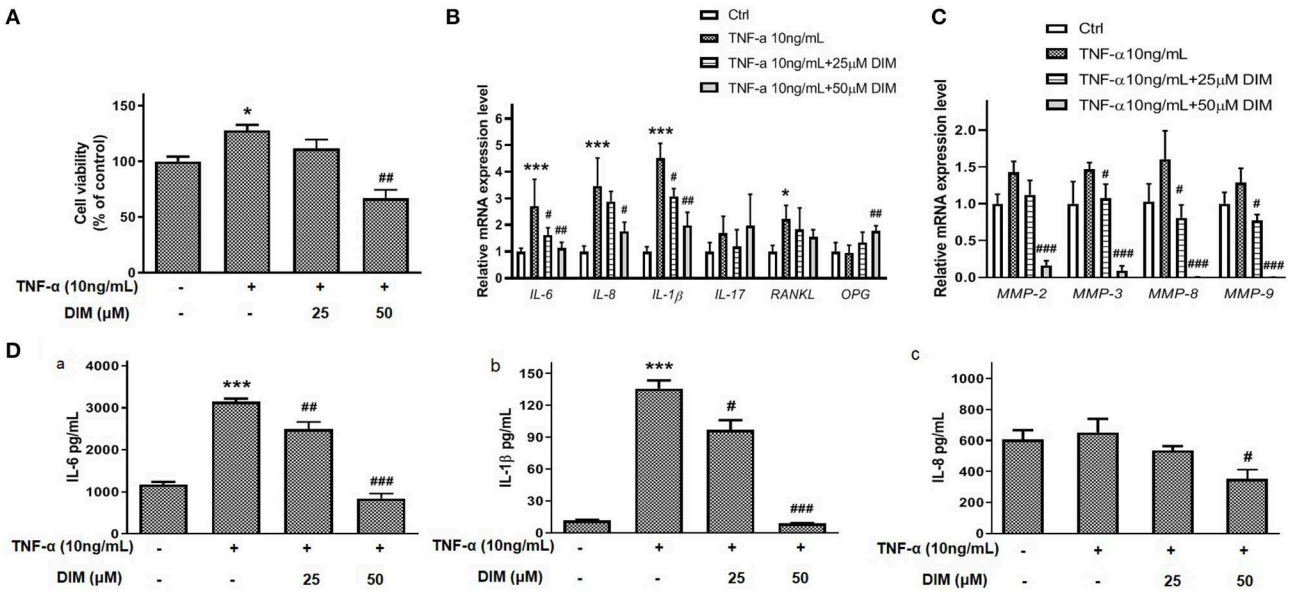

FIGURE 3 | The effect of DIM on producing pro-inflammatory cytokines and MMPs of RA-FLSs. **(A)** The effect of DIM (25 and 50 μM) on cell viability induced by TNF-α(10 ng/mL). **(B)** The effect of 25 and 50 μM DIM on relative mRNA expression of *IL-6, IL-8, IL-1β, IL-17, RANKL,* and *OPG* induced by TNF-α (10 ng/mL) to β-actin in RA-FLSs. **(C)** The effect of DIM (25and 50 μM) on relative mRNA expression of *MMP-2, MMP-3, MMP-8*, and *MMP-9* induced by TNF-α (10 ng/mL) to β-actin in RA-FLSs. **(D)** The effect of DIM (25 and 50 μM) on IL-6, IL-8, and IL-1β releasing in culture supernatant induced by TNF-α(10 ng/mL) in RA-FLSs. (a) The effect of DIM (25 and 50 μM) on IL-6 releasing induced by TNF-α (10 ng/mL) determined by ELISA. (b) The effect of DIM (25 and 50 μM) on IL-1β releasing induced by TNF-α (10 ng/mL) determined by ELISA. (c) The effect of DIM (25 and 50 μM) on IL-8 releasing induced by TNF-α (10 ng/mL) determined by ELISA. The values are the mean ± SEM from at least 3 independent experiments. $^{*}P < 0.05$, $^{***}P < 0.001$ vs. Ctrl(0 μM DIM and 0 ng/mL TNF-α). $^{\#}P < 0.05$, $^{\#\#}P < 0.01$, $^{\#\#\#}P < 0.001$ vs. group treated by TNF-α(10 ng/mL).

however, had no effect on ERK phosphorylated activation. Therefore, detailed investigations of components of MAPK have shown that DIM strongly reduced p38MAPK, JNK activity, which may be responsible for controlling abnormal hyperplasia caused with RA-FLSs. There are some evidences from studies activation of the FAK family signaling cascade in RA lining cells contributed to cell adhesion and migration into the diseased synovial tissue (30). Therefore, how DIM regulated FAK signaling was studied. As shown in **Figure 4A**, the levels of non-phospho FAK were not changed in all groups after stimulating with TNF-α but that of phospho-FAK was decreased in RA-FLSs treated with DIM.

In addition, AKT/mTOR pathway in promoting aggressive immune-cells and synoviocytes proliferation and survival plays an important role in progress of RA (31). To clear the effect of DIM on the Akt/mTOR pathway in RA-FLSs, the phosphorylation level of Akt, mTOR and downsteam p70S6K and 4E-BP1 were determined. Although the Akt phosphorylated activation was not obviously increased after treated with TNF-α, DIM indeed decreased the phosphorylation of Akt and mTOR (**Figure 4B**). Moreover, DIM also respectively, down-regulated and up-regulated the phosphorylated level of downstream p70S6K and 4E-BP1 stimulating with TNF-α (**Figure 4B**), which suggested DIM suppressed the Akt/mTOR pathway for cell growth and proliferation. Altogether, DIM affected the biological behaviors of RA-FLSs via suppressing intracellular phosphorylated activation of MAPK and Akt/mTOR pathway.

DIM Ameliorates Arthritis Severity in Mice With AIA

The Effect of DIM on the Weight and Knee Joint Diameter of the Mice

The effect of DIM on mean change in body weight of mice after immunization (from day 0 to day 55) monitored every 5 days. During the experiment the mice from three groups were eating and drinking normally. As shown in **Figure 5A**, on the day 20 after immunization the body weight of mice with AIA obviously occurred decrease comparing to normal group. However, the treatment of the mice with DIM (10 mg/kg) via gavage had significant difference comparing with AIA group at day 30 after immunization.

Synchronously, the effect of DIM on arthritis development by measurement of the knee joint diameter was followed every 5 days. The mean diameter of knee joints from AIA group mice increased rapidly from the 15th day after immunization because of obvious swelling and at the 25th day the mean diameter was up to peak value. After that the mean diameter gradually declined. However, the mice from DIM treatment group decreased the mean diameter of knee joints comparing with mice form AIA group from the 20th day (**Figure 5B**).

The Effects of DIM on Spleen and Liver Indices in AIA Mice

To evaluate the DIM effect on immune organs the spleen and liver indices in mice were calculated as shown in

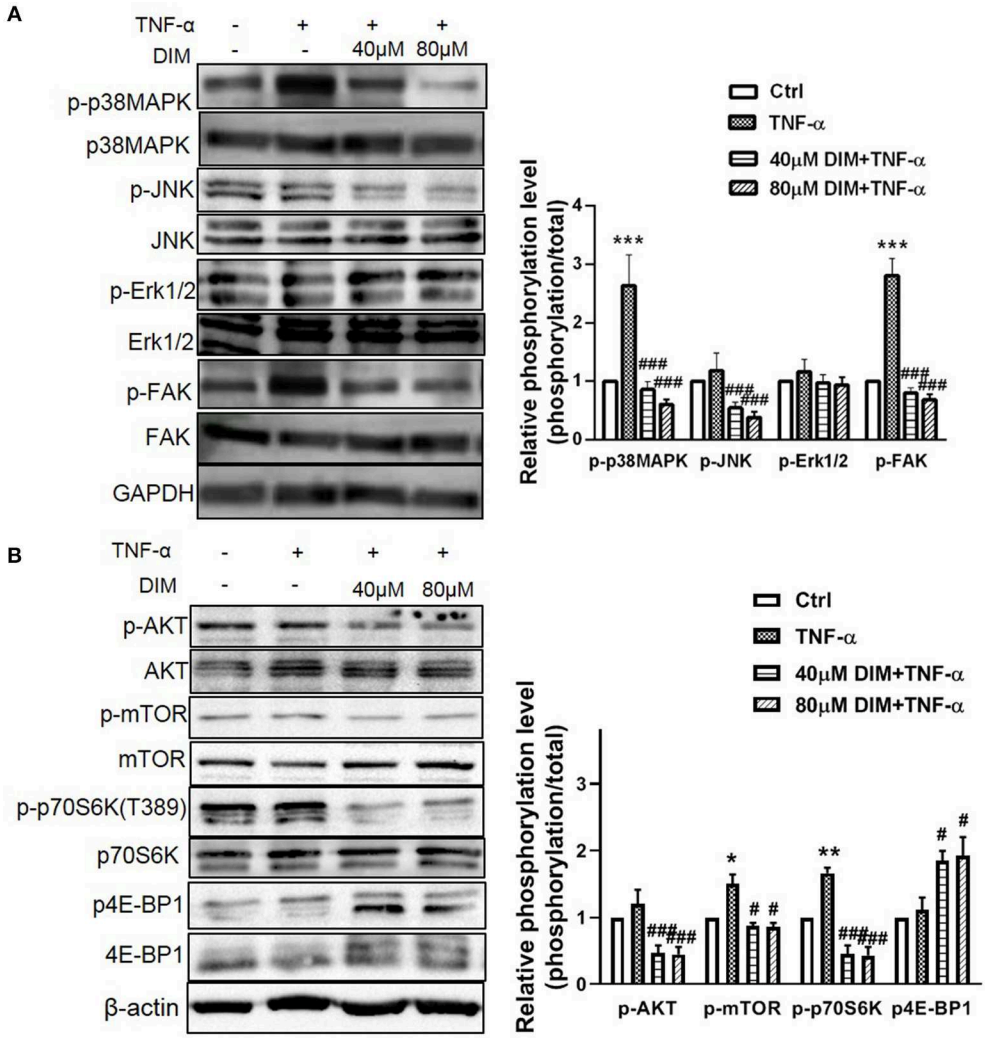

FIGURE 4 | The effect of DIM on the intracellular phosphorylated activation of MAPK and Akt/mTOR pathway induced by TNF-α in RA-FLSs. **(A)** RA-FLSs were treated with TNF-α(10 ng/mL) or/and DIM (40 and 80 μM) for 24 h, western blot analysis was conducted to assess the expression and phosphorylation level of p38MAPK, JNK, ERK, and FAK. Representative images of immune blot (left panel) and densitometric quantification phosphorylation/total of p38MAPK, JNK, ERK, and FAK expression(right panel). **(B)** RA-FLSs were treated with TNF-α(10 ng/mL) or/and DIM (40 and 80 μM) for 24 h, western blot analysis was conducted to assess the expression and phosphorylation level of AKT, mTOR, p70S6K and 4E-BP1. Representative images of immune blot (left panel) and densitometric quantification phosphorylation/total of AKT, mTOR, p70S6K and 4E-BP1 expression(right panel). Densitometry analysis from three independent experiments was used to quantitate the protein expression. $^{*}P < 0.05$, $^{**}P < 0.01$, $^{***}P < 0.001$ vs. Ctrl (0 μM DIM), $^{\#}P < 0.05$, $^{\#\#}P < 0.01$, $^{\#\#\#}P < 0.001$ vs. group treated by TNF-α(10 ng/mL).

Figure 5C. Compared with the normal group, the spleen and liver indices of AIA model group mice significantly increased. However, compared with the AIA model group, DIM (10 mg/kg) significantly reduced spleen and liver indices in AIA mice.

The Effect of DIM on Pro-inflammatory Cytokines Expression in AIA

To explore how the DIM affecting the proinflammatory cytokines in AIA, the IL-6, IL-17, TNF-α, IL-8, and IL-1β expressions in serum of AIA mice with and without DIM treatment after immunization on day 40 and 80 were detected by ELISA. The results were shown in **Figure 5D**. Firstly, IL-6 expression in mice from AIA model group were obviously increased comparing to ones from normal control group. Moreover, the IL-6 expression was inhibited in mice treated with DIM comparing to AIA model group both on day 40 and 80 after immunization. Next, the similar trends were observed in IL-17 IL-8 and IL-1β expressions in three groups. Although no difference in IL-8 was witnessed between normal mice and AIA mice group on day 40, there was difference occurred on day 80. The last, The data indicated that despite DIM had no notable effect on TNF-α expression on day 40, it did significantly decrease the TNF-α expression in AIA mice on day 80. Altogether, DIM (10mg/kg) could inhibit expression of the proinflammatory cytokines, IL-6, IL-17, TNF-α, IL-8, and IL-1β, in serum of AIA mice.

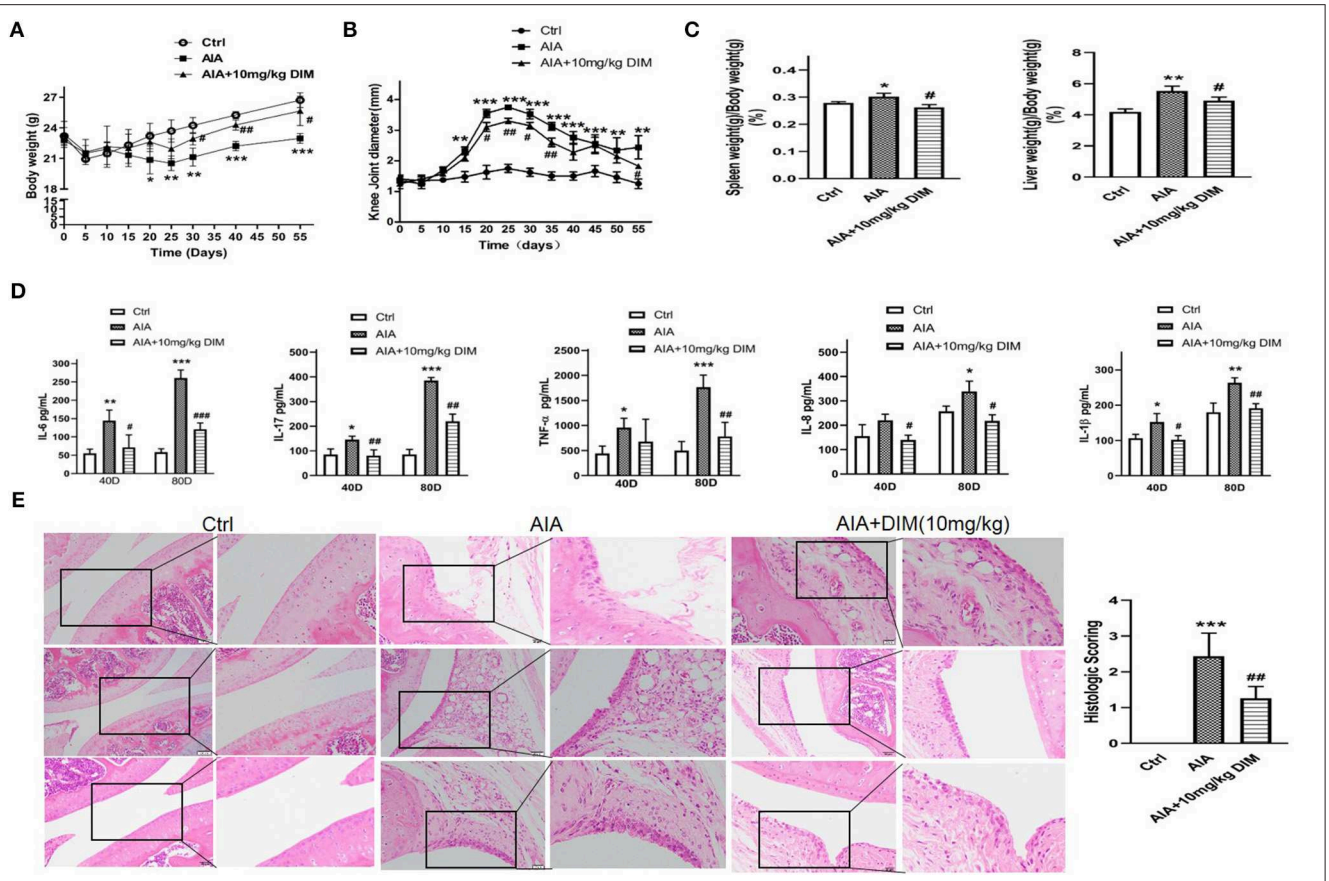

FIGURE 5 | DIM ameliorates arthritis severity in mice with AIA. **(A)** The effect of DIM on mean change in body weight of mice after immunization (from day 0 to day 55) monitored every 5 days. **(B)** The effect of DIM on mean change in knee joint diameter after immunization (from day 0 to day 55) monitored every 5 days. **(C)** The effect of DIM on the spleen and liver index of mice with AIA and control. Data shown as spleen or liver weight (g)/body weight (g) ×100%. **(D)** The effect of DIM on IL-6, IL-17, TNF-α, IL-8, and IL-1β expression in serum of mice with AIA and control after immunization on day 40 and 80. **(E)** The effect of DIM on the pathohistological features of knee joints in mice with AIA. Photomicrographs for knee joint sections stained with H&E (left panel, original magnification 400×). The scores for inflammatory severity (right panel). All the data were expressed as means ± S.D. $n = 6$, $^{*}P < 0.05$, $^{**}P < 0.01$, $^{***}P < 0.001$ vs. Ctrl (normal mice group), $^{\#}P < 0.05$, $^{\#\#}P < 0.01$, $^{\#\#\#}P < 0.001$ vs. AIA model group.

The Effect of DIM on the Pathohistological Features on Knee Joints and Arthritis Severity in AIA Mice

The mice knee joints were removed after euthanization on day 80 for histological examination of tissue sections, and then pathohistological sections were stained with H&E. As shown in **Figure 5E**, the knee joint from normal control group appeared clear and complete histological architecture under the microscope, whereas the knee joints from AIA mice showed abnormal histological architecture covering synovial hyperplasia, infiltration of massive inflammatory cells, together with angiogenesis (increased microvessel density) and degradation of epithelial cell. The mice from DIM (10 mg/kg i.g.) group were preserved almost normal histological architecture of the knee joints with mild synovial hyperplasia, less inflammatory cells infiltration and less erosion of synovial tissues. Meanwhile, the pathohistological score was remarkably decreased in DIM group compared with model group. All the data suggested that DIM did ameliorate arthritis severity in mice with AIA and had a potential anti-arthritic efficacy.

DISCUSSION

RA is a chronic autoimmune disease characterized by a hyperplastic, aggressive and invasive phenotype and involved in the formation of pannus angiogenesis, cartilage degradation, and bone erosion (32). Currently used anti-RA drugs have been found to have many side effects because they have high toxic reaction *in vivo*. It is urgent to find some natural products with less toxicity to inhibit inflammatory reaction and provide a quality of life to the patients suffering from RA.

Many fruits and vegetables contain natural bioactive components that could affect multiple signaling pathways. This feature gives these natural products pharmaceutical potential in treating some diseases where the related signaling pathways go wrong (4, 5). DIM, an indole derivative, is a bioactive compound found in cruciferous vegetables and converted from I3C in an aqueous and gastric-acidic environment (6). I3C initially drew many attentions due to its anti-cancer function. But it later was found that DIM, the converted version of I3C in body

with longer half-life, was the functional ingredient exerting anti-cancer effects (7, 8). During uncovering the mechanism of DIM, anti-inflammatory effect surfaced (9). Inflammation promotes cellular proliferation, angiogenesis, inhibits apoptosis, and induces DNA damage, increasing the risk of developing disease related inflammation. DIM exhibited a significant anti-inflammatory activity was associated with reduction of pro-inflammatory cytokines (11, 33).

Due to its anti-inflammatory activity, we creatively tried to apply DIM in treating RA. According to our experiments, the DIM could in a dose-dependent manner suppress the proliferation, migration and invasion of RA-FLSs had been identified, which coincided with reports from variety of cancers research (9, 11, 34, 35). In the molecular level, DIM can arrest G1-phase cell cycle by reducing CDK4, and Cyclin D1 and elevating p21, a CDK (cyclin-dependent kinase) inhibitor.This finding is in line with previously reported mechanisms of DIM in gastric cancer and esophageal squamous carcinoma (36, 37). All of these suggest DIM suppresses cell proliferation and arrests cell cycle at G1 phase via affecting related cell cycle proteins expression. Meanwhile, some researchers found DIM could induce apoptosis of some cancer cells through both the intrinsic and extrinsic pathway by activating Caspase 8 (9, 38).

However, we did not find DIM could induce apoptosis of RA-FLSs (**Figure S1**). We speculated that it may be due to differences in cell types or/and individual differences.

RA-FLSs usually secret various proinflammatory cytokines and chemokines, especially IL-6, IL-8, IL-1β, TNF-α, and IL-17 to recruit and activate more immune cells to the inflammatory microenvironment, and thereby are responsible for cartilage damage and joint destruction (39, 40). TNF-α is one of the major mediators involved in RA. It had also been confirmed stimulation of 10 ng/mL TNF-α resulted in the activation of RA-FLSs and increased production of inflammatory cytokines (17, 41). In our study, we got the similar results with 10 ng/mL TNF-α. Whereas, DIM inhibited the increase both cell viability and mRNA expression and release of IL-6, IL-8, and IL-1β. Therefore, we consider DIM play the anti-inflammatory role via inhibiting pro-inflammatory cytokines at least in part. No change has been observed in *IL-17* mRNA expression upon TNF-α stimulation and DIM treatment in our RA-FLSs system. We thought it might have something to do with individual patient differences. In addition, DIM also increased the *OPG* mRNA expression in RA-FLSs, which suggested DIM was related to protection from bone damage. Nevertheless, uncovering more mechanisms has to do further work. From ELISA results we noticed although the tendency of IL-1β increase induced by TNF-α was superficially suppressed with DIM. The amount is so low that it is beyond the detection capacity of ELISA, which could account for the failure to detect IL-1β in culture supernatant.In inflammatory diseases, the degradation of synovial collagen in RA maybe related to the expression of MMPs in fibroblasts in synovial joints (42). More than fifteen synovial MMPs are reportedly expressed in RA patients, mainly including collagenase, gelatinase, and matrix metalloproteinase (43). DIM inhibited the mRNA expression of collagenase *MMP-8*, gelatinase *MMP-2* and *MMP-9*, and matrix metalloproteinase *MMP-3*. Although we could not detect these MMPs in protein level, probably due to the undetectably low amount, it indeed implied that suppression of MMPs could be the core of DIM inhibiting migration and invasion of RA-FLSs.

In addition, as for migration and invasion, FAK (focal adhesion kinase), a non-receptor tyrosine kinase, promotes cell motility, survival, and proliferation through kinase-dependent and -independent mechanisms (44). There is research on DIM treating liver cancer cells indicated DIM inhibits the migration, invasion, and metastasis of HCC cells via inhibiting phosphorylation of focal adhesion kinase (FAK, tyr397) with decreased expression of MMP-2 and MMP-9 (12), which is basically consistent with our data.

It has been confirmed DIM influences the proliferation, migration, and invasion of cancer cells through multiple signaling pathways. But what's happened in RA-FLSs caused by DIM need to be uncovered. Mitogen-activated protein kinases(MAPK) is a family of serine/threonine protein kinases widely conserved among eukaryotes and involved in many cellular key programs (45). Moreover, MAPK pathway takes part in the activation of RA-FLSs (15). We found DIM blocked the phosphorylated activation of p38 and JNK stimulated by TNF-α, but not the ERK in RA-FLSs, suggesting that the p38 and JNK pathway might mediate the action of DIM in RA-FLSs. Indeed, p38 and JNK are expressed and activated in synovial tissue from patients with RA. They not only regulates RA-FLSs growth, apoptosis and differentiation but also are critical for synovial inflammation and joint destruction in inflammatory arthritis (15, 41). There were other reports that DIM inhibited cell growth by downregulation of Akt/FoxM1 signaling pathway in gastric cancer (46), by inactivation of β-catenin/c-Myc in colorectal cancer (47). These results suggest that DIM might possess a cell type-specific function in modulating cell growth. Moreover, JNK pathway and its downstream proteins are also involved in cell migration. Additionally, FAK, a movement-associated signal pathway, finally converge at JNK, and JNK activation predicted the development of bone erosion in RA (48).

Akt is also contributed to the growth of cells via phosphorylating the downstream mTOR complex 1 (mTORC1), a translator of mRNAs to protein by means of p70S6K-S6 and 4E-BP1-eIF4E pathways (49). The mammalian target of rapamycin (mTOR) signaling pathway plays an important role in regulating a variety of cellular functions at the interface of cell metabolism, growth, and differentiation. mTOR signaling pathway is involved in the regulation of RA-FLSs invasion and might be a new target for RA therapy (50). Many investigations had demonstrated that mTOR was activated in the rheumatoid synovium especially induced by TNF-α (51). It was worth mentioning that DIM blocked the activation of AKT/mTOR and downstream p70S6K-S6 and 4E-BP1 caused by TNF-α was verified in our data, which was first direct evidence on DIM affecting AKT/mTOR pathway. This provides proofs for the anti-arthritic properties of DIM and corroborates its potential use for the treatment of RA.

In addition to the cell signaling pathway on DIM affecting there are some researches on the effect of DIM on microRNA in some cancer cells (52). MiRNA21 and miR-150-5P had been identified as target of DIM in cancer cells, which indicated that DIM could be used in target-based therapy and also as a lead for further development of potent small molecule miRNA

antagonist (27, 53). Considering miRNAs play important roles in development and progression of RA, and then there are a lot of work need to discover key microRNA influenced by DIM in RA.

As a typical animal model of RA, AIA has been used in many studies to survey the pathogenesis of arthritis and to find potential therapeutic targets (25, 54). The decrease in arthritis looks like small shown in **Figure 5B** but the reduction in inflammatory cytokines in the DIM-treated mice is significant. We speculate that swelling of the joints is only part of the appearance of arthritis and does not indicate the severity of the overall inflammation. Moreover, the swelling of the joints is local inflammatory character and the inflammatory cytokines detected from serum are related with inflammatory of whole body. Additionally, during the peak of inflammatory response we measured the inflammatory cytokines at 28th day, but there was no significant difference between AIA model group and AIA model treated with DIM group. There was report that DIM could alleviate oxazolone-induced colitis through Th2 and Th17 suppression and Treg induction (55). Therefore, we speculate that the mechanism of DIM is not like a non-steroidal anti-inflammatory drugs, which paly direct and quick anti-inflammatory role *in vivo*. It is worth to make further study to uncover the mechanism of DIM from another angle. Moreover, it is usual that there is a lag between swelling of the joints and the inflammatory cytokines up-regulation and down-regulation, which is similar with clinical manifestations of some inflammation. Our results from the mice with AIA that DIM not only decreased the swell of knee joint caused with arthritis and down-regulated the proinflammatory factors, but improved pathohistological features, which further support our initial suppose *in vivo* that DIM may have potential to control synovial joint destruction in RA. In conclusion, our study provides a novel insight into the specific role of DIM on TNF-dependent arthritogenesis, offering *ex vivo* and *in vivo* evidence on DIM functions in regulating the proliferation, migration and invasion of RA-FLSs by inhibiting the MAPK and AKT/mTOR pathway and ameliorating arthritis severity and pathological outcome in an AIA model. Therefore, DIM may harbor a huge therapeutic and pharmaceutical potential in treating RA. Furthermore, DIM, in combination with other compounds inducing RA-FLSs apoptosis, may give a better therapeutic effect as well as improve the quality life of RA patients.

DATA AVAILABILITY

The raw data supporting the conclusions of this manuscript will be made available by the authors, without undue reservation, to any qualified researcher.

ETHICS STATEMENT

This study complied with the rules enacted by the Medical Ethics Committee of the Zhujiang Hospital, Southern Medical University and was performed according to the recommendations of the Declaration of Helsinki. All the animal experimental procedures abided by the guidelines of ethical regulations for institutional animal care and use in the Southern Medical University and approved by The Southern Medical University Ethics Committee for Animal Laboratory Research.

AUTHOR CONTRIBUTIONS

HD, WZ, YW, and LJ designed the research. HD, XZ, YZ, XH, JW, and QL performed the experiments. HC and SW contributed analysis and animal model construction. HD, HL and LJ analyzed the experimental data. HD, YW, and LJ wrote and revised the manuscript. All authors read and approved the final manuscript.

ACKNOWLEDGMENTS

This work was supported by grants from the National Natural Science Foundation of China (81601397, 81771727, 81102688, 81401920), Natural Science Foundation of Guangdong Province (2016A030313624), Guangzhou Science and Technology Plan Project: Major Project of Collaborative Innovation of Industry, University and Research (201604046010), Program from Guangdong Innovation and Entrepreneurship training for college students (201812121108) and Scientific Enlightenment Project from Southern Medical Universtiy. Moreover, we want to thank Ningchao Du, Wei Wang, Lijun Dong, Yang Li, Lvlan Ye, Dingfei Liu, Qiong Li and Yuting Chen for their help during the experiments.

SUPPLEMENTARY MATERIAL

The Supplementary Material for this article can be found online at: https://www.frontiersin.org/articles/10.3389/fimmu.2019.01620/full#supplementary-material

Figure S1 | The effect of DIM on apoptosis of RA-FLSs. There is almost no cell apoptosis occurred after treated with 0,30,60,90 μM DIM, which indicated that DIM could not induce RA-FLSs apoptosis.

Table S1 | The information of RA patients whose tissue samples were used in our research.

Table S2 | The primers of human cytokines and MMPs for mRNA expression assay.

REFERENCES

1. Smolen JS, Aletaha D, McInnes IB. Rheumatoid arthritis. *Lancet*. (2016) 388:2023–38. doi: 10.1016/S0140-6736(16)30173-8
2. Huber LC, Distler O, Tarner I, Gay RE, Gay S, Pap T. Synovial fibroblasts: key players in rheumatoid arthritis. *Rheumatology*. (2006) 45:669–75. doi: 10.1093/rheumatology/kel065
3. Liu Y, Pan YF, Xue YQ, Fang LK, Guo XH, Guo X, et al. uPAR promotes tumor-like biologic behaviors of fibroblast-like synoviocytes through PI3K/Akt signaling pathway in patients with rheumatoid arthritis. *Cell Mol Immunol*. (2018) 15:171–81. doi: 10.1038/cmi.2016.60
4. Alam J, Jantan I, Bukhari S. Rheumatoid arthritis: recent advances on its etiology, role of cytokines and pharmacotherapy. *Biomed Pharmacother*. (2017) 92:615–33. doi: 10.1016/j.biopha.2017.05.055

5. Dudics S, Langan D, Meka RR, Venkatesha SH, Berman BM, Che CT, et al. Natural products for the treatment of autoimmune arthritis: their mechanisms of action, targeted delivery, and interplay with the host microbiome. *Int J Mol Sci*. (2018) 19:E2508. doi: 10.3390/ijms19092508
6. Patel AR, Spencer SD, Chougule MB, Safe S, Singh M. Pharmacokinetic evaluation and *in vitro-in vivo* correlation (IVIVC) of novel methylene-substituted 3,3′ diindolylmethane (DIM). *Eur J Pharm Sci*. (2012) 46:8–16. doi: 10.1016/j.ejps.2012.01.012
7. Noroozi MK, Mahmoodi M, Jafarzadeh A, Darekordi A, Hajizadeh MR, Hassanshahi G. Molecular targets, anti-cancer properties and potency of synthetic indole-3-carbinol derivatives. *Mini Rev Med Chem*. (2019) 19:540–54. doi: 10.2174/1389557518666181116120145
8. Popolo A, Pinto A, Daglia M, Nabavi SF, Farooqi AA, Rastrelli L. Two likely targets for the anti-cancer effect of indole derivatives from cruciferous vegetables: PI3K/Akt/mTOR signalling pathway and the aryl hydrocarbon receptor. *Semin Cancer Biol*. (2017) 46:132–7. doi: 10.1016/j.semcancer.2017.06.002
9. Kim SM. Cellular and molecular mechanisms of 3,3′-diindolylmethane in gastrointestinal cancer. *Int J Mol Sci*. (2016) 17:E1155. doi: 10.3390/ijms17071155
10. Chang X, Tou JC, Hong C, Kim HA, Riby JE, Firestone GL, et al. 3,3′-Diindolylmethane inhibits angiogenesis and the growth of transplantable human breast carcinoma in athymic mice. *Carcinogenesis*. (2005) 26:771–8. doi: 10.1093/carcin/bgi018
11. Zhang WW, Feng Z, Narod SA. Multiple therapeutic and preventive effects of 3,3′-diindolylmethane on cancers including prostate cancer and high grade prostatic intraepithelial neoplasia. *J Biomed Res*. (2014) 28:339–48. doi: 10.7555/JBR.28.20140008
12. Li WX, Chen LP, Sun MY, Li JT, Liu HZ, Zhu W. 3′3-Diindolylmethane inhibits migration, invasion and metastasis of hepatocellular carcinoma by suppressing FAK signaling. *Oncotarget*. (2015) 6:23776–92. doi: 10.18632/oncotarget.4196
13. Shin JA, Shim JH, Choi ES, Leem DH, Kwon KH, Lee SO, et al. Chemopreventive effects of synthetic C-substituted diindolylmethanes originating from cruciferous vegetables in human oral cancer cells. *Eur J Cancer Prev*. (2011) 20:417–25. doi: 10.1097/CEJ.0b013e32834473c3
14. Thomson CA, Ho E, Strom MB. Chemopreventive properties of 3,3′-diindolylmethane in breast cancer: evidence from experimental and human studies. *Nutr Rev*. (2016) 74:432–43. doi: 10.1093/nutrit/nuw010
15. Bustamante MF, Garcia-Carbonell R, Whisenant KD, Guma M. Fibroblast-like synoviocyte metabolism in the pathogenesis of rheumatoid arthritis. *Arthritis Res Ther*. (2017) 19:110. doi: 10.1186/s13075-017-1303-3
16. Arnett FC, Edworthy SM, Bloch DA, McShane DJ, Fries JF, Cooper NS, et al. The American Rheumatism Association 1987 revised criteria for the classification of rheumatoid arthritis. *Arthritis Rheum*. (1988) 31:315–24. doi: 10.1002/art.1780310302
17. Shi M, Wang J, Xiao Y, Wang C, Qiu Q, Lao M, et al. Glycogen metabolism and rheumatoid arthritis: the role of glycogen synthase 1 in regulation of synovial inflammation via blocking AMP-Activated Protein Kinase Activation. *Front Immunol*. (2018) 9:1714. doi: 10.3389/fimmu.2018.01714
18. Jie L, Du H, Huang Q, Wei S, Huang R, Sun W. Tanshinone IIA induces apoptosis in fibroblast-like synoviocytes in rheumatoid arthritis via blockade of the cell cycle in the G2/M phase and a mitochondrial pathway. *Biol Pharm Bull*. (2014) 37:1366–72. doi: 10.1248/bpb.b14-00301
19. Liu F, Feng XX, Zhu SL, Huang HY, Chen YD, Pan YF, et al. Sonic hedgehog signaling pathway mediates proliferation and migration of fibroblast-like synoviocytes in rheumatoid arthritis via MAPK/ERK signaling pathway. *Front Immunol*. (2018) 9:2847. doi: 10.3389/fimmu.2018.02847
20. Jie LG, Huang RY, Sun WF, Wei S, Chu YL, Huang QC, et al. Role of cysteinerich angiogenic inducer 61 in fibroblastlike synovial cell proliferation and invasion in rheumatoid arthritis. *Mol Med Rep*. (2015) 11:917–23. doi: 10.3892/mmr.2014.2770
21. Markides H, Kehoe O, Morris RH, El HA. Whole body tracking of superparamagnetic iron oxide nanoparticle-labelled cells–a rheumatoid arthritis mouse model. *Stem Cell Res Ther*. (2013) 4:126. doi: 10.1186/scrt337
22. Atkinson SM, Nansen A. Pharmacological value of murine delayed-type hypersensitivity arthritis: a robust mouse model of rheumatoid arthritis in C57BL/6 Mice. *Basic Clin Pharmacol Toxicol*. (2017) 120:108–14. doi: 10.1111/bcpt.12657
23. Sardar S, Andersson A. Old and new therapeutics for rheumatoid arthritis: *in vivo* models and drug development. *Immunopharmacol Immunotoxicol*. (2016) 38:2–13. doi: 10.3109/08923973.2015.1125917
24. Grotsch B, Bozec A, Schett G. *In vivo* models of rheumatoid arthritis. *Methods Mol Biol*. (2019) 1914:269–80. doi: 10.1007/978-1-4939-8997-3_14
25. Frey O, Huckel M, Gajda M, Petrow PK, Brauer R. Induction of chronic destructive arthritis in SCID mice by arthritogenic fibroblast-like synoviocytes derived from mice with antigen-induced arthritis. *Arthritis Res Ther*. (2018) 20:261. doi: 10.1186/s13075-018-1720-y
26. Pan T, Cheng TF, Jia YR, Li P, Li F. Anti-rheumatoid arthritis effects of traditional Chinese herb couple in adjuvant-induced arthritis in rats. *J Ethnopharmacol*. (2017) 205:1–7. doi: 10.1016/j.jep.2017.04.020
27. Gou KJ, Zeng R, Ren XD, Dou QL, Yang QB, Dong Y, et al. Anti-rheumatoid arthritis effects in adjuvant-induced arthritis in rats and molecular docking studies of Polygonum orientale L. extracts. *Immunol Lett*. (2018) 201:59–69. doi: 10.1016/j.imlet.2018.11.009
28. Hu F, Hepburn HR, Li Y, Chen M, Radloff SE, Daya S. Effects of ethanol and water extracts of propolis (bee glue) on acute inflammatory animal models. *J Ethnopharmacol*. (2005) 100:276–83. doi: 10.1016/j.jep.2005.02.044
29. Muller-Ladner U, Ospelt C, Gay S, Distler O, Pap T. Cells of the synovium in rheumatoid arthritis. Synovial fibroblasts. *Arthritis Res Ther*. (2007) 9:223. doi: 10.1186/ar2337
30. Stanford SM, Svensson MN, Sacchetti C, Pilo CA, Wu DJ, Kiosses WB, et al. Receptor protein tyrosine phosphatase alpha-mediated enhancement of rheumatoid synovial fibroblast signaling and promotion of arthritis in mice. *Arthritis Rheumatol*. (2016) 68:359–69. doi: 10.1002/art.39442
31. Malemud CJ. Intracellular Signaling Pathways in Rheumatoid Arthritis. *J Clin Cell Immunol*. (2013) 4:160. doi: 10.4172/2155-9899.1000160
32. McInnes IB, Schett G. Pathogenetic insights from the treatment of rheumatoid arthritis. *Lancet*. (2017) 389:2328–37. doi: 10.1016/S0140-6736(17)31472-1
33. Kim YH, Kwon HS, Kim DH, Shin EK, Kang YH, Park JH, et al. 3,3′-diindolylmethane attenuates colonic inflammation and tumorigenesis in mice. *Inflamm Bowel Dis*. (2009) 15:1164–73. doi: 10.1002/ibd.20917
34. Zou M, Xu C, Li H, Zhang X, Fan W. 3,3′-Diindolylmethane suppresses ovarian cancer cell viability and metastasis and enhances chemotherapy sensitivity via STAT3 and Akt signaling *in vitro* and *in vivo*. *Arch Biochem Biophys*. (2018). doi: 10.1016/j.abb.2018.07.002. [Epub ahead of print].
35. Lanza-Jacoby S, Cheng G. 3,3′-Diindolylmethane enhances apoptosis in docetaxel-treated breast cancer cells by generation of reactive oxygen species. *Pharm Biol*. (2018) 56:407–14. doi: 10.1080/13880209.2018.1495747
36. Kim SJ, Lee JS, Kim SM. 3,3′-Diindolylmethane suppresses growth of human esophageal squamous cancer cells by G1 cell cycle arrest. *Oncol Rep*. (2012) 27:1669–73. doi: 10.3892/or.2012.1662
37. Li XJ, Park ES, Park MH, Kim SM. 3,3′-Diindolylmethane suppresses the growth of gastric cancer cells via activation of the Hippo signaling pathway. *Oncol Rep*. (2013) 30:2419–26. doi: 10.3892/or.2013.2717
38. Kim EJ, Park SY, Shin HK, Kwon DY, Surh YJ, Park JH. Activation of caspase-8 contributes to 3,3′-Diindolylmethane-induced apoptosis in colon cancer cells. *J Nutr*. (2007) 137:31–6. doi: 10.1093/jn/137.1.31
39. Bottini N, Firestein GS. Duality of fibroblast-like synoviocytes in RA: passive responders and imprinted aggressors. *Nat Rev Rheumatol*. (2013) 9:24–33. doi: 10.1038/nrrheum.2012.190
40. Bartok B, Firestein GS. Fibroblast-like synoviocytes: key effector cells in rheumatoid arthritis. *Immunol Rev*. (2010) 233:233–55. doi: 10.1111/j.0105-2896.2009.00859.x
41. Yang Y, Ye Y, Qiu Q, Xiao Y, Huang M, Shi M, et al. Triptolide inhibits the migration and invasion of rheumatoid fibroblast-like synoviocytes by blocking the activation of the JNK MAPK pathway. *Int Immunopharmacol*. (2016) 41:8–16. doi: 10.1016/j.intimp.2016.10.005
42. Agere SA, Akhtar N, Watson JM, Ahmed S. RANTES/CCL5 induces collagen degradation by activating MMP-1 and MMP-13 expression in human rheumatoid arthritis synovial fibroblasts. *Front Immunol*. (2017) 8:1341. doi: 10.3389/fimmu.2017.01341
43. Konttinen YT, Ainola M, Valleala H, Ma J, Ida H, Mandelin J, et al. Analysis of 16 different matrix metalloproteinases (MMP-1 to MMP-20) in the synovial

membrane: different profiles in trauma and rheumatoid arthritis. *Ann Rheum Dis*. (1999) 58:691–7. doi: 10.1136/ard.58.11.691
44. Sulzmaier FJ, Jean C, Schlaepfer DD. FAK in cancer: mechanistic findings and clinical applications. *Nat Rev Cancer*. (2014) 14:598–610. doi: 10.1038/nrc3792
45. Tong B, Wan B, Wei Z, Wang T, Zhao P, Dou Y, et al. Role of cathepsin B in regulating migration and invasion of fibroblast-like synoviocytes into inflamed tissue from patients with rheumatoid arthritis. *Clin Exp Immunol*. (2014) 177:586–97. doi: 10.1111/cei.12357
46. Jin H, Park MH, Kim SM. 3,3′-Diindolylmethane potentiates paclitaxel-induced antitumor effects on gastric cancer cells through the Akt/FOXM1 signaling cascade. *Oncol Rep*. (2015) 33:2031–6. doi: 10.3892/or.2015.3758
47. Leem SH, Li XJ, Park MH, Park BH, Kim SM. Genome-wide transcriptome analysis reveals inactivation of Wnt/beta-catenin by 3,3′-diindolylmethane inhibiting proliferation of colon cancer cells. *Int J Oncol*. (2015) 47:918–26. doi: 10.3892/ijo.2015.3089
48. de Launay D, van de Sande MG, de Hair MJ, Grabiec AM, van de Sande GP, Lehmann KA, et al. Selective involvement of ERK and JNK mitogen-activated protein kinases in early rheumatoid arthritis (1987 ACR criteria compared to 2010 ACR/EULAR criteria): a prospective study aimed at identification of diagnostic and prognostic biomarkers as well as therapeutic targets. *Ann Rheum Dis*. (2012) 71:415–23. doi: 10.1136/ard.2010.143529
49. Wendel HG, De Stanchina E, Fridman JS, Malina A, Ray S, Kogan S, et al. Survival signalling by Akt and eIF4E in oncogenesis and cancer therapy. *Nature*. (2004) 428:332–7. doi: 10.1038/nature02369
50. Laragione T, Gulko PS. mTOR regulates the invasive properties of synovial fibroblasts in rheumatoid arthritis. *Mol Med*. (2010) 16:352–8. doi: 10.2119/molmed.2010.00049
51. Karonitsch T, Kandasamy RK, Kartnig F, Herdy B, Dalwigk K, Niederreiter B, et al. mTOR senses environmental cues to shape the fibroblast-like synoviocyte response to inflammation. *Cell Rep*. (2018) 23:2157–67. doi: 10.1016/j.celrep.2018.04.044
52. Biersack B. Non-coding RNA/microRNA-modulatory dietary factors and natural products for improved cancer therapy and prevention: Alkaloids, organosulfur compounds, aliphatic carboxylic acids and water-soluble vitamins. *Noncoding RNA Res*. (2016) 1:51–63. doi: 10.1016/j.ncrna.2016.09.001
53. Junaid M, Dash R, Islam N, Chowdhury J, Alam MJ, Nath SD, et al. Molecular simulation studies of 3,3′-Diindolylmethane as a potent MicroRNA-21 antagonist. *J Pharm Bioallied Sci*. (2017) 9:259–265. doi: 10.4103/jpbs.JPBS_266_16
54. Yu J, Feng Y, Wang Y, An R. Aryl hydrocarbon receptor enhances the expression of miR-150-5p to suppress in prostate cancer progression by regulating MAP3K12. *Arch Biochem Biophys*. (2018) 654:47–54. doi: 10.1016/j.abb.2018.07.010
55. Huang Z, Jiang Y, Yang Y, Shao J, Sun X, Chen J, et al. 3,3′-Diindolylmethane alleviates oxazolone-induced colitis through Th2/Th17 suppression and Treg induction. *Mol Immunol*. (2013) 53:335–44. doi: 10.1016/j.molimm.2012.09.007

Conflict of Interest Statement: The authors declare that the research was conducted in the absence of any commercial or financial relationships that could be construed as a potential conflict of interest.

frontiers in Immunology

MINI REVIEW
published: 02 August 2019
doi: 10.3389/fimmu.2019.01743

Fibroblast-Like Synoviocytes Glucose Metabolism as a Therapeutic Target in Rheumatoid Arthritis

Patricia Gnieslaw de Oliveira[1], *Mirian Farinon*[1], *Elsa Sanchez-Lopez*[2], *Shigeki Miyamoto*[2] *and Monica Guma*[1]*

[1] Department of Medicine, School of Medicine, University of California, San Diego, La Jolla, CA, United States,
[2] Pharmacology, School of Medicine, University of California, San Diego, La Jolla, CA, United States

Metabolomic studies show that rheumatoid arthritis (RA) is associated with metabolic disruption that may be therapeutically targetable. Among them, glucose metabolism and glycolytic intermediaries seem to have an important role in fibroblast-like synoviocytes (FLS) phenotype and might contribute to early stage disease pathogenesis. RA FLS are transformed from quiescent to aggressive and metabolically active cells and several works have shown that glucose metabolism is increased in activated FLS. Glycolytic inhibitors reduce not only FLS aggressive phenotype *in vitro* but also decrease bone and cartilage damage in several murine models of arthritis. Essential glycolytic enzymes, including hexokinase 2 (HK2) and 6-phosphofructo-2-kinase/fructose-2,6-biphosphatase (PFKFB) enzymes, have important roles in FLS behavior. Of interest, HK2 is an inducible enzyme present only in the inflamed rheumatic tissues compared to osteoarthritis synovium. It is a contributor to glucose metabolism that could be selectively targeted without compromising systemic homeostasis as a novel approach for combination therapy independent of systemic immunosuppression. More information about metabolic targets that do not compromise global glucose metabolism in normal cells is needed.

Keywords: rheumatoid arthritis, fibroblast-like synoviocytes, hexokinase-2, glucose metabolism, glycolytic inhibitors

OPEN ACCESS

Edited by:
Hanshi Xu,
First Affiliated Hospital of Sun Yat-sen University, China

Reviewed by:
Aleksander M. Grabiec,
Jagiellonian University, Poland
David S. Gyori,
Semmelweis University, Hungary

***Correspondence:**
Monica Guma
mguma@ucsd.edu

Specialty section:
This article was submitted to Autoimmune and Autoinflammatory Disorders, a section of the journal Frontiers in Immunology

Received: *15 May 2019*
Accepted: *10 July 2019*
Published: *02 August 2019*

Citation:
de Oliveira PG, Farinon M, Sanchez-Lopez E, Miyamoto S and Guma M (2019) Fibroblast-Like Synoviocytes Glucose Metabolism as a Therapeutic Target in Rheumatoid Arthritis. Front. Immunol. 10:1743. doi: 10.3389/fimmu.2019.01743

Rheumatoid arthritis (RA) pathogenesis includes synovial hyperplasia or *pannus*, which consists of accumulation of macrophages and fibroblast like synoviocytes (FLS) (1–4), resulting in enhanced invasiveness and destruction of adjacent cartilage and bone (3, 5). FLS are the major component of rheumatoid *pannus* and have a key role in its formation (4). In healthy individuals, these cells ensure the structural integrity of a normally organized synovial lining (6) and secretes hyaluronic acid and lubricin, two important constituents of synovial fluid that are responsible for lubricating the joint (7, 8). However, after acquiring an aggressive phenotype, FLS have reduced contact inhibition, resistance to apoptosis, increased migration, and increased ability to invade periarticular tissues including bone and cartilage (4, 9). These activated cells produce several mediators that induce angiogenesis, cell growth, and recruitment and activation of immune cells (4). In addition to contributing to the inflammatory environment, FLS also produce matrix metalloproteases (MMPs) that degrade the extracellular matrix and contributes to cartilage destruction (10).

Recently, an increasing number of studies have shown that FLS activation and the subsequent joint damage are associated with an altered metabolism which may be therapeutically targetable. The metabolism of all four major classes of macromolecules (carbohydrates, proteins, lipids, and nucleic acids) will change after cell activation. Carbohydrate metabolism is a fundamental biochemical process that ensures a constant supply of energy to living cells. The most important carbohydrate is glucose, which is first transported into the cell through glucose transporter 1 (GLUT1), then broken down via glycolysis by sequential metabolic enzymes [including hexokinase (HK), aldolase, phosphoglycerate kinase (PGK1), and pyruvate kinase] to generate pyruvate, and afterwards will either enter into the tricarboxylic acid (TCA) cycle and oxidative phosphorylation to generate ATP, or will be converted to lactate via lactate dehydrogenase (LDH).

Activation of FLS by hypoxia, platelet-derived growth factor (PDGF), tumor necrosis factor (TNF), and other inflammatory mediators increases glucose metabolism and transforms the FLS from quiescent to aggressive and metabolically active cells. Specifically, prior work—ours and others—has shown that glucose metabolism is increased in activated FLS, and glycolytic inhibition reduces not only FLS aggressive phenotype *in vitro* but also decreases bone and cartilage damage in several murine models of arthritis [(11–13); **Table 1**]. These works have suggested potential metabolic targets to reprogram metabolic disruptions and complement current therapies (11–13). In this brief review, we will summarize what is known about glucose metabolism in FLS and about potential metabolic therapies for RA that could modulate the aggressive behavior of FLS.

GLUCOSE METABOLISM ACTIVATION IN THE RA FLS

Glucose metabolism seems to be especially enhanced in joints with arthritis and involved in RA pathology. The high consumption of glucose by the RA joints can be visualized by PET imaging with 18F-FDG, a probe that detects glycolytic tissues (25). Synovial FLS and macrophages were shown to contribute to FDG-PET accumulation in the RA synovial tissue (26). The synovial tissue of RA patients also presents an enhanced level of lactate compared to non-inflamed synovial tissue (27). The local lower glucose levels and higher ratio of lactate to glucose in the RA synovial tissue suggest an increase in anaerobic cellular metabolism of resident cells, triggered by the inflammation and the hypoxic environment commonly detected in the RA joints (28, 29). This dysregulation is further suggested by the increase of lactate and glucose in the serum of RA patients (30). Moreover, glucose levels are lower in the synovial fluid of RA patients in comparison to non-inflamed synovial fluid (31). This is also supported by metabolic studies using mass spectrometry, which show differential metabolite profile in RA FLS and osteoarthritis (OA) FLS (32). Glycolysis, pentose phosphate pathway (PPP), and amino acid metabolism were different in RA FLS compared to OA FLS (32). In addition, FLS increased its intracellular levels of glucose after TNF stimulation (33).

Shift from oxidative phosphorylation to glycolytic ATP production is a common feature of activated and reactive cells like fibroblasts and macrophages. Micro environmental factors in the RA joint seem to potentiate this metabolic adaptation of FLS and macrophages. The synovial tissue is enriched in hypoxia-inducible factor 1 alpha (HIF1α), a transcription factor induced in hypoxic environments that contributes to RA pathogenesis at multiple steps (29), including supporting enhanced glycolytic activity. Among the HIF1α-transcriptionally regulated glucose metabolism related genes, GLUT1, HK2, and LDH are upregulated in RA FLS (14, 19, 34–36). The effect of HIF1α on glycolysis contributes to FLS survival (37), myeloid recruitment by FLS, angiogenesis (38), and FLS migration and invasion (29). In addition, it promotes the expression in RA FLS of inflammatory mediators that perpetuates interactions with other synovial cells including T and B cells (39, 40).

Other signaling pathways critical for FLS expression of adhesion molecules, pro-inflammatory cytokines, and MMPs, as well as for apoptosis inhibition, and for FLS migration and invasion are mitogen-activated protein kinases (MAPK), nuclear factor kappa B (NF-κB), and phosphoinositide-3-kinase (PI3K)/AKT (41–50). These pathways are activated by both hypoxia and inflammation. They also regulate glucose metabolism through several mechanisms including the upregulation of GLUT1 (51). These pathways are also involved in the phosphorylation of rate-limiting glycolytic enzymes, including 6-phosphofructo-2-kinase/fructose-2,6-bisphosphatases (PFKFB) and HKs (52, 53). JAK/STAT signaling, which also plays a role in FLS activation (54–56), was also shown to mediate glucose uptake and HK2 expression (57). Therefore, the phenotypic changes from FLS at rest to an activated and invasive state are coupled with metabolic alterations like increased GLUT1 and HK2 expression and lactate production (14, 17).

Likewise, the inhibition of glycolysis decreases the aggressive behavior of these cells by decreasing cytokine production, proliferation, migration, and invasion (14, 17). Three targetable glycolytic enzymes were recently shown to be involved in FLS aggressive phenotype. One is the bifunctional PFKFB3 enzyme, which converts fructose-6-phosphate to fructose-2,6-bisP (F2,6BP). F2,6BP is an allosteric activator of 6-phosphofructokinase-1 (PFK-1) and stimulates glycolysis overriding the inhibitory effect of ATP on PFK-1 (58). It was identified as a regulator of insulin/IGF-1 signaling pathway. Suppression of PFKFB3 was found to decrease insulin-stimulated glucose uptake, GLUT4 translocation, Akt signaling, and glycolytic flux (59). In FLS, PFKFB3 inhibition reduced glucose uptake which resulted in decreased lactate production (17, 18). The inhibition of the glycolytic flux by small molecule inhibitors of PFKFB3 significantly reduced FLS migration and invasion, and the production of inflammatory mediators (17). Of interest, FPFK15, a PFKFB3 inhibitor, not only suppressed glucose uptake and lactate secretion but also NF-κB and MAPK activation in RA FLS (18). The second enzyme is the rate-limiting enzyme HK2. Overexpression of HK2 in FLS provides a migratory and invasive advantage that is abolished when HK2 is ablated (19, 20). The last enzyme is phosphoglycerate kinase (PGK)1. Anti-PGK1

TABLE 1 | Glycolytic intermediate metabolites and their effect on RA FLS and animal models of arthritis.

Intermediate	Enzyme	Trigger response	References
Glucose		Glucose deprivation decreased IL-6, MMP-1 and MPP-3 production and the rate of proliferation and migration of FLS. In the SKG mouse model of arthritis, the glucose analog 2-DG decreased clinical score and thickness	(14, 15)
Fructose 1,6-bisphosphate	FBP1	Treatment with fructose 1,6-biphosphate reduced MPO activity, IL-6 and TNF-α joint levels, nociception, and neutrophil migration to the joint of mice with ZIA and AIA	(16)
Fructose 2,6-bisphosphate	PFKFB3	Inhibition of fructose 2,6-bisphosphate production decreased IL-6 secretion and proliferation, migration and invasion of FLS	(17, 18)
Glucose-6-phosphate	HK2	HK2 ablation decreased FLS invasive phenotype and also attenuated the severity of bone and cartilage damage in a mouse model of inflammatory arthritis	(19–21)
1,3-bisphosphoglycerate/ 3-phosphoglycerate	PGK1	Silencing of PGK1 decreased the secretion of IL-1β and IFN-γ as well as proliferation of FLS	
Pyruvate		Use of BrPa (a halogenated analog of pyruvate that inhibits glycolysis) decreased histologic score and levels of arthritis in K/BxN mouse models of arthritis	(14, 15, 20, 22)
Lactate	LDH/MCT	Increased levels of lactate induced FLS invasiveness	(17)
Succinate	SDH	Succinate induced fibrosis and angiogenesis and SDH inhibition attenuated the severity of rat CIA	(23, 24)

FLS, fibroblast-like synoviocyte; FBP1, fructose 1,6-biphosphatase; 2-DG, 2-deoxy-D-glucose; MPO, myeloperoxidase; ZIA, zymosan-induced arthritis; AIA, antigen-induced arthritis; PGK1, phosphoglycerate kinase 1; BrPa, bromopyruvate; MCT, monocarboxylate transporters.

siRNA treatment of RA FLS not only decreased cell proliferation and cell migration, but also interleukin (IL)-1β and interferon (IFN)-γ secretion (21).

Since metabolic pathways are highly interconnected, other metabolic pathways described in activated FLS might also affect global glucose metabolism. Glutamine metabolism is increased in FLS, with glutaminase 1 (GLS1) playing a role in regulating the proliferation of these cells. FLS proliferation is reduced under glutamine-deprived conditions, or after GLS1 silencing or inhibition (60). Choline metabolism is also highly activated in FLS. Inhibition of choline kinase (ChoKα) suppressed the RA FLS aggressive phenotype by increasing apoptosis and decreasing cell migration (61). Glycogen synthase 1 (GYS1)-mediated glycogen accumulation was shown to block AMPK activation and to contribute to FLS phenotype as well (62). Finally, RA FLS also overexpresses the neutral amino acid transporter LAT1, and has an increased uptake of leucine after IL-17 stimulation, which potentiate FLS migratory capacity that was eliminated by blocking LAT1 (63). Other amino acids including tryptophan might also play a role in FLS phenotype (64).

FLS GLUCOSE METABOLISM AND CHRONIC ACTIVATION IN RA

Although researchers have suggested a role for metabolic alterations in RA pathology, we are far from understanding which changes are normal responses to cell activation and are transient metabolic responses to acute inflammation, and which are the result of damage and chronic activation that could play a role in driving the pathology of RA. These chronic metabolic changes in FLS can have not only profound effects on the biology of other cells through intermediate metabolites but also can create a new epigenetic landscape that results in a stable FLS activation that is maintained even without continuous stimulation (**Figure 1A**).

Some pro-inflammatory mediators increase several TCA cycle intermediates, and emerging evidence show that these intermediates classically associated with metabolic functions also possess signaling functions as inflammatory mediators and drive chronic activation. For instance, metabolic profiling has revealed itaconic acid as a potential marker of RA, and TNF increased its concentration in the K4IM human fibroblast cell line (65). Importantly, the increased levels in itaconic acid can be attenuated by treatment with infliximab, a biologic drug targeting TNF (65). Succinate is another TCA cycle intermediate that is abundant in RA synovial fluids. Synovial succinate correlates with enhanced release of IL-1β by macrophages in a mechanism that involves the overexpression of succinate receptor Sucnr1/GPR91 (66). In addition, Sucnr1/GPR91 functions as a chemotactic signal for recruitment of dendritic cells into lymph nodes which leads to Th17 cells expansion in a murine model of inflammatory arthritis (67). In FLS, succinate has a myofibroblast effect on FLS (23). A recent paper also evaluated Sucnr1/GPR91 in FLS and concluded that both intra- and extracellular succinate play a role in synovial angiogenesis. Intracellular succinate induced angiogenesis through HIF1α induction, while extracellular succinate increased vascular endothelial growth factor (VEGF) through GPR91 receptor (24).

Pyruvate is another metabolite generated during glycolysis and is converted to acetyl-CoA to fuel the TCA cycle. Acetyl-CoA is an important cofactor that catalyzes the transfer of an acetyl group. Histone acetyltransferases (HATs) are enzymes that use this co-factor and regulate histone acetylation and

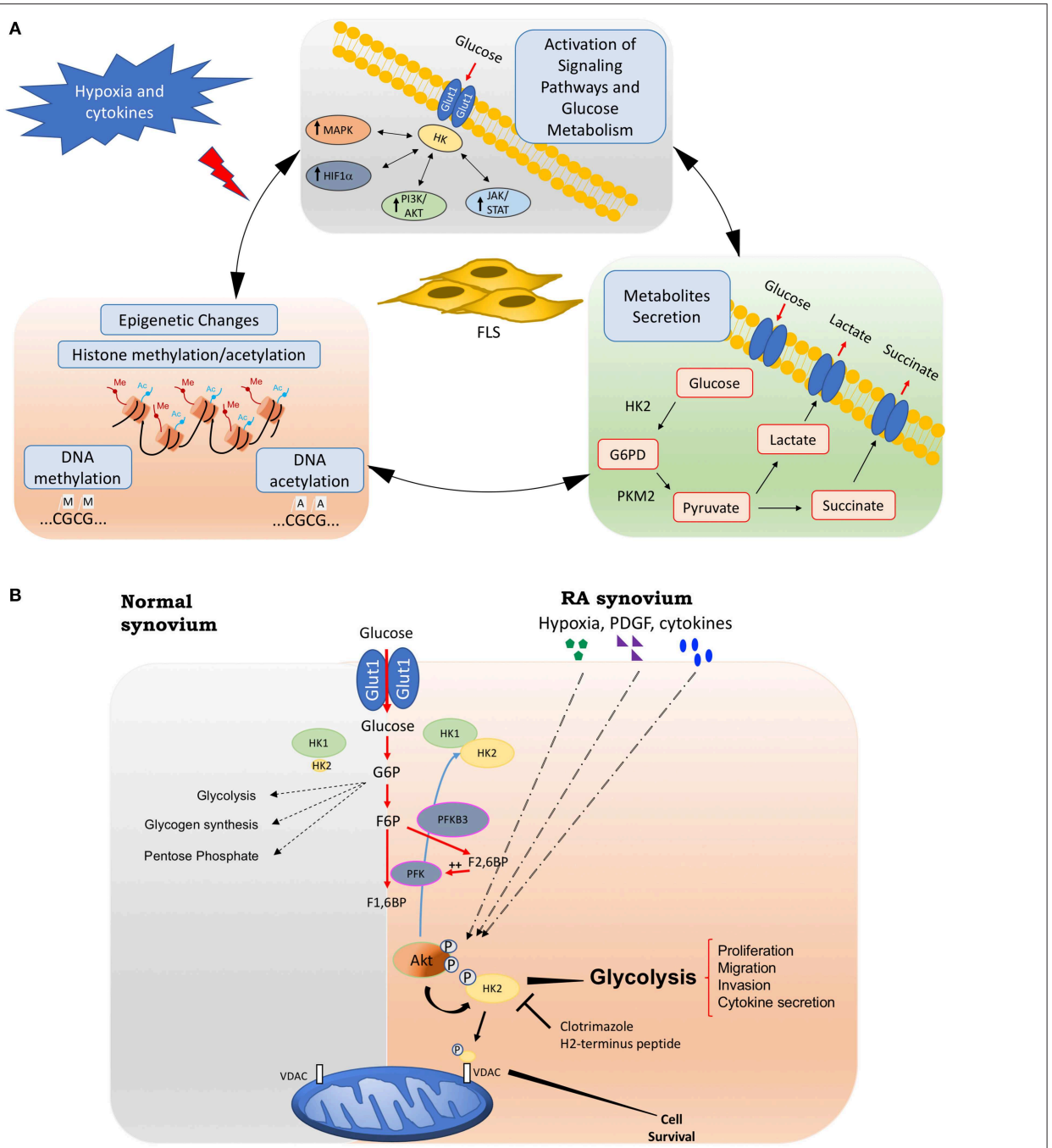

FIGURE 1 | Fibroblasts-like synoviocytes (FLS) glucose metabolism and chronic activation in RA. **(A)** Chronic glucose metabolic changes induced by hypoxia and inflammatory mediators in FLS will activate many signaling pathways, including HIF, MAPK, PI3K/Akt, and JAK/STAT pathways, which also increases the expression of key glucose metabolism related genes such as GLUT1, HK2, or LDH. Intermediate glucose metabolites including pyruvate, lactate, succinate, a-ketoglutarate, fumarate, and acetyl-coenzyme will create a chronic and sustained FLS activation, either by being secreted extracellularly and triggering profound effects on the biology of other cells, or by inducing a new epigenetic landscape that results in a stable FLS activation that is maintained even without continuous stimulation. **(B)** Hypoxia, growth factors, and cytokines in arthritis synovium stimulate Akt phosphorylation, which will up-regulate HK2 expression and HK2 phosphorylation. The phosphorylation of HK2 by Akt is accompanied by an increased binding of the enzyme to mitochondrial outer membrane voltage-dependent anion channel (VDAC). Binding to VDAC enhances the affinity of hexokinases. Therefore, HK2 mitochondrial binding might promote glucose metabolism and FLS invasive phenotype. Mitochondrial HK2 might also inhibit apoptosis. Thus, mitochondrial association of HK2 might promote resistance to growth, invasion, and apoptosis of RA FLS, which contribute to joint destruction in RA. Selective HK2 mitochondrial dissociation might be an attractive potential selective target for arthritis therapy and safer than global glycolysis inhibition. HK2, hexokinase 2; G6PD, glucose 6 phosphate dehydrogenase; PKM2, pyruvate kinase muscle isozyme M2; PFK, phosphofructokinase; PFKB3, 6-phosphofructo-2-kinase/fructose-2,6-biphosphatase 3; G6P, glucose-6-phosphate; F6P, fructose-6-phosphate; F1,6BP, Fructose 1,6-bisphosphate; F2,6FB, Fructose 2,6-bisphosphate; VDAC: voltage-dependent anion channel.

therefore link metabolism and epigenetics in cells (68, 69). Other metabolites elevated after glucose metabolism activation such as fumarate, succinate, and lactate also modify chromatin and nucleic acid-modifying enzymes activity by competitively inhibiting substrate utilization (68). The relationship between metabolic intermediates and chromatin-modifying enzymes implies that metabolic changes could directly affect gene expression by modulating chromatin-modifying enzymes and triggering epigenetic dysfunction (68, 69). Of interest, several reports have shown that epigenetic alterations, such as histone modification, might contribute to RA pathogenesis (70). In fact, a comprehensive epigenomic characterization of RA FLS has recently been described (71), suggesting that synovial fibroblasts stimulation results in a stable activation that is maintained even without continuous stimulation through epigenetic changes. Further FLS studies are needed to better understand the epigenetic modifications affecting metabolic gene expression and glucose metabolism that can drive chronic RA FLS activation and may help to identify novel metabolic targets.

GLUCOSE METABOLISM TARGETS IN RA FLS

The concept of metabolic reprogramming to improve immunotherapy and to complement current therapies is being slowly translated into the autoimmune disease field (11, 72–74). In fact, glycolytic inhibitors not only reduce FLS aggressive phenotype *in vitro* but also decrease bone and cartilage damage in several murine models of arthritis. More specifically, ablation of glycolytic genes or treatment with 3-bromopyruvate, which antagonizes HK2, significantly reduced the severity of several murine arthritis models (14, 15, 19, 20, 22). Although HK2 specific inhibitors are not available, HK2 can be inhibited by the use of 2-deoxyglucose (2-DG), which is a derivative of glucose that can be phosphorylated by HK2 but not mobilized through succeeding steps of glycolysis. Murine studies have shown that 2-DG reduces cell proliferation and the severity of a spontaneous model of RA arthritis (15). HK2 ablation has also attenuated the severity of bone and cartilage damage in a murine model of inflammatory arthritis (19). Interestingly, the administration of fructose 1,6-bisphosphate (FBP), a glycolytic intermediate, decreased arthritis scores in two different animal models. Mechanistic studies showed that this metabolic intermediate activated the anti-inflammatory adenosinergic pathway instead of enhancing FLS glycolysis (16). Treatment with a saponin that inhibits succinate dehydrogenase (SDH) activity ameliorated the clinical symptoms of the arthritis as well as histopathologic features of synovial hyperplasia, infiltration of inflammatory cells, and fibrosis (23). In addition, treatment with dimethylmalonate, another inhibitor of SDH, decreased succinate content in the synovial tissue of rats with collagen-induced arthritis (CIA) in addition to amelioration of the disease (24). Finally, inhibition of the enzyme ChoKα (61) and GLS1 (62) also ameliorated the severity of experimental autoimmune arthritis.

Yet, although all these works have demonstrated a role of glucose metabolism in RA, inhibiting global glucose metabolism is not desirable. In addition, inhibition of some of the above pathways can have other detrimental effects. For instance, a recent report demonstrated a key anti-inflammatory function of HIF1α by driving the expression of IL-10 in B cells (75). PFKFB3 activity is also defective in CD4 T cells in RA patients which results in energy deprivation that prone cells to undergo apoptosis (76). Thus, there is a need of finding specific metabolic targets that are induced in activated FLS.

Out of all the glycolytic enzymes described to play a role in RA pathogenesis, HK2 could function as a selective metabolic target (**Figure 1B**). HKs catalyze the phosphorylation of glucose to glucose-6-phosphate (G6P) that facilitates glucose entry into cells. G6P initiates several metabolic pathways that need glucose, including glycolysis, the hexosamine pathway, glycogen synthesis, and the PPP (77). HK2 also plays important roles in angiogenesis (78). HKs has four different isoforms: HK1 is the ubiquitous isoform in all adult issues. However, HK2 is an inducible isoform that is only highly expressed in skeletal and cardiac muscles, and adipose tissue (77). HK2 is also highly upregulated in tumor cells and HK2 inhibition synergies with anti-tumor treatment and improves response to therapy (79). In addition to its canonical metabolic roles in tumor or cardiac tissues, HK2 translocates to the nucleus or mitochondria and triggers an autophagic and anti-apoptotic responses through its interaction with the voltage-dependent anion channel (VDAC) (80, 81). Of interest, HK2 plays a small role in inflammation driven by T cells, so HK2 inhibition should have limited immunosuppressive effects (82). Importantly, we and others have shown that the synovial expression of HK2 is elevated only in RA compared to OA samples (19, 20). Given HK2 selective overexpression in inflamed RA synovium, its small role in T cells, and its expression in a very limited number of adult tissues, HK2 is an attractive selective target for arthritis therapy that is safer than global glucose metabolism inhibition (19). In addition to its expression profile, its diverse effects at various cellular compartments could offer another level of specificity since targeting a specific intracellular compartment of HK2 (i.e., cytosol, nucleus, or mitochondria) would also provide a selective means to block deleterious effects of this enzyme in RA without affecting glucose metabolism in normal cells. Therefore, HK2 could be selectively targeted offering a safer and novel additional approach for combination therapy in RA joint disease independent of systemic immunosuppression.

Of interest, rheumatologists already have antimetabolites in the current RA armamentarium, such as methotrexate and leflunomide. Although they were thought to inhibit the proliferation of synovial and immune cells, methotrexate and other disease-modifying antirheumatic drugs (DMARDs) also have effect on glucose metabolism. For instance, methotrexate treatment significantly reduced HK2 expression and glucose/fructose carriers (SLC2A5, a member of the solute carrier family 2) in human FLS, suggesting that FLS glycolytic activity can be modulated by methotrexate (83). Anti-TNF treatment decreases the synovial expression of GLUT1 and of the glycolytic enzymes pyruvate kinase muscle isozyme M2 (PKM2)

and glyceraldehyde 3-phosphate dehydrogenase (GAPDH) in patients that responded to TNF inhibition compared to non-responders (17). Anti-IL-6 receptor therapy inhibited oxidative stress and improved endothelial function in RA leucocytes, although whether or not this therapy also has a metabolic effect on the synovial tissue is not known yet (84). Finally, inhibition of JAK/STAT3 signaling with tofacinib, a drug approved for severe RA and active psoriasis, induces oxidative phosphorylation and maximal respiratory capacity of FLS while shutting down key glycolytic enzymes including HK2 and LDH. This effect correlated with the reduction of inflammatory mediators and FLS activation (85).

CONCLUSION

Growing evidence suggests that the study of activated metabolism not only of immune cells but also of stroma cells including FLS can provide critical pathways for therapeutic intervention. Pre-clinical studies in mouse models of inflammatory arthritis strongly suggest that agents that interfere with certain steps of glycolysis can be therapeutic in RA and have identified potential targetable glycolytic enzymes such as HK2, and glycolytic intermediate metabolites (**Table 1**). In addition, therapeutic effects of DMARDs could be due, at least partially, to the inhibition of glucose metabolism, highlighting the pathogenic role of this metabolic pathway. As global inhibition of glucose metabolism is not desirable, more information about inducible glycolytic genes, the specific distribution of these targets, their effect in different cellular compartments, and their additional non-metabolic functions, may help us to identify new targets that do not compromise global glucose metabolism in normal cells.

AUTHOR CONTRIBUTIONS

All authors listed have made a substantial, direct and intellectual contribution to the work, and approved it for publication.

FUNDING

MG was supported by the National Institutes of Health under Award Numbers R01AR073324 and by Rheumatology Research Foundation.

REFERENCES

1. Smolen JS, Aletaha D, McInnes IB. Rheumatoid arthritis. *Lancet*. (2016) 388:2023–38. doi: 10.1016/S0140-6736(16)30173-8
2. Wegner N, Lundberg K, Kinloch A, Fisher B, Malmström V, Feldmann M, et al. Autoimmunity to specific citrullinated proteins gives the first clues to the etiology of rheumatoid arthritis. *Immunol Rev*. (2010) 233:34–54. doi: 10.1111/j.0105-2896.2009.00850.x
3. McInnes IB, Schett G. The pathogenesis of rheumatoid arthritis. *N Engl J Med*. (2011) 365:2205–19. doi: 10.1056/NEJMra1004965
4. Bottini N, Firestein G. Duality of fibroblast-like synoviocytes in RA: passive responders and imprinted aggressors. *Nat Rev Rheumatol*. (2013) 9:10. doi: 10.1038/nrrheum.2012.190
5. Smolen JS, Aletaha D, Barton A, Burmester GR, Emery P, Firestein GS, et al. Rheumatoid arthritis. *Nat Rev Dis Primers*. (2018) 4:18001. doi: 10.1038/nrdp.2018.1
6. Kiener HP, Watts GF, Cui Y, Wright J, Thornhill TS, Sköld M, et al. Synovial fibroblasts self-direct multicellular lining architecture and synthetic function in three-dimensional organ culture. *Arthritis Rheum*. (2010) 62:742–52. doi: 10.1002/art.27285
7. Filer A. The fibroblast as a therapeutic target in rheumatoid arthritis. *Curr Opin Pharmacol*. (2013) 13:413–9. doi: 10.1016/j.coph.2013.02.006
8. Bartok B, Firestein GS. Fibroblast-like synoviocytes: key effector cells in rheumatoid arthritis. *Immunol Rev*. (2010) 233:233–55. doi: 10.1111/j.0105-2896.2009.00859.x
9. Turner JD, Filer A. The role of the synovial fibroblast in rheumatoid arthritis pathogenesis. *Curr Opin Rheumatol*. (2015) 27:175–82. doi: 10.1097/BOR.0000000000000148
10. Tolboom TC, van der Helm-Van Mil AH, Nelissen RG, Breedveld FC, Toes RE, Huizinga TW. Invasiveness of fibroblast-like synoviocytes is an individual patient characteristic associated with the rate of joint destruction in patients with rheumatoid arthritis. *Arthritis Rheum*. (2005) 52:1999–2002. doi: 10.1002/art.21118
11. Guma M, Tiziani S, Firestein GS. Metabolomics in rheumatic diseases: desperately seeking biomarkers. *Nat Rev Rheumatol*. (2016) 12:269–81. doi: 10.1038/nrrheum.2016.1
12. Falconer J, Murphy AN, Young S, Clark AR, Tiziani S, Guma M, et al. Synovial cell metabolism and chronic inflammation in rheumatoid arthritis. *Arthritis Rheumatol*. (2018) 70:984–99. doi: 10.1002/art.40504
13. Fearon U, Canavan M, Biniecka M, Veale DJ. Hypoxia, mitochondrial dysfunction and synovial invasiveness in rheumatoid arthritis. *Nat Rev Rheumatol*. (2016) 12:385–97. doi: 10.1038/nrrheum.2016.69
14. Garcia-Carbonell R, Divakaruni AS, Lodi A, Vicente-Suarez I, Saha A, Cheroutre H, et al. Critical role of glucose metabolism in rheumatoid arthritis fibroblast-like synoviocytes. *Arthritis Rheumatol*. (2016) 68:1614–26. doi: 10.1002/art.39608
15. Abboud G, Choi SC, Kanda N, Zeumer-Spataro L, Roopenian DC, Morel L. Inhibition of glycolysis reduces disease severity in an autoimmune model of rheumatoid arthritis. *Front Immunol*. (2018) 9:1973. doi: 10.3389/fimmu.2018.01973
16. Veras FP, Peres RS, Saraiva AL, Pinto LG, Louzada-Junior P, Cunha TM, et al. Fructose 1,6-bisphosphate, a high-energy intermediate of glycolysis, attenuates experimental arthritis by activating anti-inflammatory adenosinergic pathway. *Sci Rep*. (2015) 5:15171. doi: 10.1038/srep15171
17. Biniecka M, Canavan M, McGarry T, Gao W, McCormick J, Cregan S, et al. Dysregulated bioenergetics: a key regulator of joint inflammation. *Ann Rheum Dis*. (2016) 75:2192–200. doi: 10.1136/annrheumdis-2015-208476
18. Zou Y, Zeng S, Huang M, Qiu Q, Xiao Y, Shi M, et al. Inhibition of 6-phosphofructo-2-kinase suppresses fibroblast-like synoviocytes-mediated synovial inflammation and joint destruction in rheumatoid arthritis. *Br J Pharmacol*. (2017) 174:893–908. doi: 10.1111/bph.13762
19. Bustamante MF, Oliveira PG, Garcia-Carbonell R, Croft AP, Smith JM, Serrano RL, et al. Hexokinase 2 as a novel selective metabolic target for rheumatoid arthritis. *Ann Rheum Dis*. (2018) 77:1636–43. doi: 10.1136/annrheumdis-2018-213103
20. Song G, Lu Q, Fan H, Zhang X, Ge L, Tian R, et al. Inhibition of hexokinases holds potential as treatment strategy for rheumatoid arthritis. *Arthritis Res Ther*. (2019) 21:87. doi: 10.1186/s13075-019-1865-3
21. Zhao Y, Yan X, Li X, Zheng Y, Li S, Chang X. PGK1, a glucose metabolism enzyme, may play an important role in rheumatoid arthritis. *Inflamm Res*. (2016) 65:815–25. doi: 10.1007/s00011-016-0965-7
22. Okano T, Saegusa J, Nishimura K, Takahashi S, Sendo S, Ueda Y, et al. 3-bromopyruvate ameliorate autoimmune arthritis by modulating Th17/Treg cell differentiation and suppressing dendritic cell activation. *Sci Rep*. (2017) 7:42412. doi: 10.1038/srep42412
23. Li Y, Zheng JY, Liu JQ, Yang J, Liu Y, Wang C, et al. Succinate/NLRP3 inflammasome induces synovial fibroblast activation: therapeutical effects

of clematichinenoside AR on arthritis. *Front Immunol*. (2016) 7:532. doi: 10.3389/fimmu.2016.00532
24. Li Y, Liu Y, Wang C, Xia WR, Zheng JY, Yang J, et al. Succinate induces synovial angiogenesis in rheumatoid arthritis through metabolic remodeling and HIF-1alpha/VEGF axis. *Free Radic Biol Med*. (2018) 126:1–14. doi: 10.1016/j.freeradbiomed.2018.07.009
25. Lee SJ, Jeong JH, Lee CH, Ahn BC, Eun JS, Kim NR, et al. Development and validation of an (18) F-FDG PET/CT-based tool for the evaluation of joint counts and disease activity in patients with rheumatoid arthritis. *Arthritis Rheumatol*. (2019) 2019:40860. doi: 10.1002/art.40860
26. Matsui T, Nakata N, Nagai S, Nakatani A, Takahashi M, Momose T, et al. Inflammatory cytokines and hypoxia contribute to 18F-FDG uptake by cells involved in pannus formation in rheumatoid arthritis. *J Nucl Med*. (2009) 50:920–6. doi: 10.2967/jnumed.108.060103
27. Volchenkov R, Dung Cao M, Elgstoen KB, Goll GL, Eikvar K, Bjorneboe O, et al. Metabolic profiling of synovial tissue shows altered glucose and choline metabolism in rheumatoid arthritis samples. *Scand J Rheumatol*. (2017) 46:160–1. doi: 10.3109/03009742.2016.1164242
28. Quinonez-Flores CM, Gonzalez-Chavez SA, Pacheco-Tena C. Hypoxia and its implications in rheumatoid arthritis. *J Biomed Sci*. (2016) 23:62. doi: 10.1186/s12929-016-0281-0
29. Hua S, Dias TH. Hypoxia-inducible factor (HIF) as a target for novel therapies in rheumatoid arthritis. *Front Pharmacol*. (2016) 7:184. doi: 10.3389/fphar.2016.00184
30. Young SP, Kapoor SR, Viant MR, Byrne JJ, Filer A, Buckley CD, et al. The impact of inflammation on metabolomic profiles in patients with arthritis. *Arthritis Rheum*. (2013) 65:2015–23. doi: 10.1002/art.38021
31. Anderson JR, Chokesuwattanaskul S, Phelan MM, Welting TJM, Lian LY, Peffers MJ, et al. (1)H NMR metabolomics identifies underlying inflammatory pathology in osteoarthritis and rheumatoid arthritis synovial joints. *J Proteome Res*. (2018) 17:3780–90. doi: 10.1021/acs.jproteome.8b00455
32. Ahn JK, Kim S, Hwang J, Kim J, Kim KH, Cha HS. GC/TOF-MS-based metabolomic profiling in cultured fibroblast-like synoviocytes from rheumatoid arthritis. *Joint Bone Spine*. (2016) 83:707–13. doi: 10.1016/j.jbspin.2015.11.009
33. Ahn JK, Kim S, Hwang J, Kim J, Lee YS, Koh EM, et al. Metabolomic elucidation of the effects of curcumin on fibroblast-like synoviocytes in rheumatoid arthritis. *PLoS ONE*. (2015) 10:e0145539. doi: 10.1371/journal.pone.0145539
34. Hurter K, Spreng D, Rytz U, Schawalder P, Ott-Knusel F, Schmokel H. Measurements of C-reactive protein in serum and lactate dehydrogenase in serum and synovial fluid of patients with osteoarthritis. *Vet J*. (2005) 169:281–5. doi: 10.1016/j.tvjl.2004.01.027
35. Wright AJ, Husson ZMA, Hu DE, Callejo G, Brindle KM, Smith ESJ. Increased hyperpolarized [1-(13) C] lactate production in a model of joint inflammation is not accompanied by tissue acidosis as assessed using hyperpolarized (13) C-labelled bicarbonate. *NMR Biomed*. (2018) 31:e3892. doi: 10.1002/nbm.3892
36. Bustamante MF, Garcia-Carbonell R, Whisenant KD, Guma M. Fibroblast-like synoviocyte metabolism in the pathogenesis of rheumatoid arthritis. *Arthritis Res Ther*. (2017) 19:110. doi: 10.1186/s13075-017-1303-3
37. Del Rey MJ, Valin A, Usategui A, Garcia-Herrero CM, Sanchez-Arago M, Cuezva JM, et al. Hif-1alpha knockdown reduces glycolytic metabolism and induces cell death of human synovial fibroblasts under normoxic conditions. *Sci Rep*. (2017) 7:3644. doi: 10.1038/s41598-017-03921-4
38. del Rey MJ, Izquierdo E, Caja S, Usategui A, Santiago B, Galindo M, et al. Human inflammatory synovial fibroblasts induce enhanced myeloid cell recruitment and angiogenesis through a hypoxia-inducible transcription factor 1alpha/vascular endothelial growth factor-mediated pathway in immunodeficient mice. *Arthritis Rheum*. (2009) 60:2926–34. doi: 10.1002/art.24844
39. Hu F, Liu H, Xu L, Li Y, Liu X, Shi L, et al. Hypoxia-inducible factor-1alpha perpetuates synovial fibroblast interactions with T cells and B cells in rheumatoid arthritis. *Eur J Immunol*. (2016) 46:742–51. doi: 10.1002/eji.201545784
40. Hu F, Mu R, Zhu J, Shi L, Li Y, Liu X, et al. Hypoxia and hypoxia-inducible factor-1alpha provoke toll-like receptor signalling-induced inflammation in rheumatoid arthritis. *Ann Rheum Dis*. (2014) 73:928–36. doi: 10.1136/annrheumdis-2012-202444
41. Vincenti MP, Coon CI, Brinckerhoff CE. Nuclear factor kappaB/p50 activates an element in the distal matrix metalloproteinase 1 promoter in interleukin-1beta-stimulated synovial fibroblasts. *Arthritis Rheum*. (1998) 41:1987–94.
42. Miagkov AV, Kovalenko DV, Brown CE, Didsbury JR, Cogswell JP, Stimpson SA, et al. NF-kappaB activation provides the potential link between inflammation and hyperplasia in the arthritic joint. *Proc Natl Acad Sci U S A*. (1998) 95:13859–64.
43. Han Z, Boyle DL, Chang L, Bennett B, Karin M, Yang L, et al. c-Jun N-terminal kinase is required for metalloproteinase expression and joint destruction in inflammatory arthritis. *J Clin Invest*. (2001) 108:73–81. doi: 10.1172/JCI12466
44. Han Z, Chang L, Yamanishi Y, Karin M, Firestein GS. Joint damage and inflammation in c-Jun N-terminal kinase 2 knockout mice with passive murine collagen-induced arthritis. *Arthritis Rheum*. (2002) 46:818–23. doi: 10.1002/art.10104
45. Pillinger MH, Rosenthal PB, Tolani SN, Apsel B, Dinsell V, Greenberg J, et al. Cyclooxygenase-2-derived E prostaglandins down-regulate matrix metalloproteinase-1 expression in fibroblast-like synoviocytes via inhibition of extracellular signal-regulated kinase activation. *J Immunol*. (2003) 171:6080–9. doi: 10.4049/jimmunol.171.11.6080
46. Bradley K, Scatizzi JC, Fiore S, Shamiyeh E, Koch AE, Firestein GS, et al. Retinoblastoma suppression of matrix metalloproteinase 1, but not interleukin-6, through a p38-dependent pathway in rheumatoid arthritis synovial fibroblasts. *Arthritis Rheum*. (2004) 50:78–87. doi: 10.1002/art.11482
47. Hwang SY, Kim JY, Kim KW, Park MK, Moon Y, Kim WU, et al. IL-17 induces production of IL-6 and IL-8 in rheumatoid arthritis synovial fibroblasts via NF-kappaB- and PI3-kinase/Akt-dependent pathways. *Arthritis Res Ther*. (2004) 6:R120–8. doi: 10.1186/ar1038
48. Bartok B, Boyle DL, Liu Y, Ren P, Ball ST, Bugbee WD, et al. PI3 kinase delta is a key regulator of synoviocyte function in rheumatoid arthritis. *Am J Pathol*. (2012) 180:1906–16. doi: 10.1016/j.ajpath.2012.01.030
49. Li GQ, Zhang Y, Liu D, Qian YY, Zhang H, Guo SY, et al. PI3 kinase/Akt/HIF-1alpha pathway is associated with hypoxia-induced epithelial-mesenchymal transition in fibroblast-like synoviocytes of rheumatoid arthritis. *Mol Cell Biochem*. (2013) 372:221–31. doi: 10.1007/s11010-012-1463-z
50. Duvel K, Yecies JL, Menon S, Raman P, Lipovsky AI, Souza AL, et al. Activation of a metabolic gene regulatory network downstream of mTOR complex 1. *Mol Cell*. (2010) 39:171–83. doi: 10.1016/j.molcel.2010.06.022
51. Barthel A, Okino ST, Liao J, Nakatani K, Li J, Whitlock JP Jr, et al. Regulation of GLUT1 gene transcription by the serine/threonine kinase Akt1. *J Biol Chem*. (1999) 274:20281–6.
52. Miyamoto S, Murphy AN, Brown JH. Akt mediates mitochondrial protection in cardiomyocytes through phosphorylation of mitochondrial hexokinase-II. *Cell Death Differ*. (2008) 15:521–9. doi: 10.1038/sj.cdd.4402285
53. Deprez J, Vertommen D, Alessi DR, Hue L, Rider MH. Phosphorylation and activation of heart 6-phosphofructo-2-kinase by protein kinase B and other protein kinases of the insulin signaling cascades. *J Biol Chem*. (1997) 272:17269–75.
54. Gao W, McCormick J, Connolly M, Balogh E, Veale DJ, Fearon U. Hypoxia and STAT3 signalling interactions regulate pro-inflammatory pathways in rheumatoid arthritis. *Ann Rheum Dis*. (2015) 74:1275–83. doi: 10.1136/annrheumdis-2013-204105
55. Migita K, Komori A, Torigoshi T, Maeda Y, Izumi Y, Jiuchi Y, et al. CP690,550 inhibits oncostatin M-induced JAK/STAT signaling pathway in rheumatoid synoviocytes. *Arthritis Res Ther*. (2011) 13:R72. doi: 10.1186/ar3333
56. Rosengren S, Corr M, Firestein GS, Boyle DL. The JAK inhibitor CP-690,550 (tofacitinib) inhibits TNF-induced chemokine expression in fibroblast-like synoviocytes: autocrine role of type I interferon. *Ann Rheum Dis*. (2012) 71:440–7. doi: 10.1136/ard.2011.150284
57. Heiss EH, Schachner D, Donati M, Grojer CS, Dirsch VM. Increased aerobic glycolysis is important for the motility of activated VSMC and inhibited by indirubin-3'-monoxime. *Vascular Pharmacol*. (2016) 83:47–56. doi: 10.1016/j.vph.2016.05.002
58. Clem BF, O'Neal J, Tapolsky G, Clem AL, Imbert-Fernandez Y, Kerr DA II, et al. Targeting 6-phosphofructo-2-kinase (PFKFB3) as a therapeutic strategy against cancer. *Mol Cancer Ther*. (2013) 12:1461–70. doi: 10.1158/1535-7163.MCT-13-0097
59. Trefely S, Khoo PS, Krycer JR, Chaudhuri R, Fazakerley DJ, Parker BL, et al. Kinome screen identifies PFKFB3 and glucose metabolism as important

regulators of the insulin/insulin-like growth factor (IGF)-1 signaling pathway. *J Biol Chem*. (2015) 290:25834–46. doi: 10.1074/jbc.M115.658815
60. Takahashi S, Saegusa J, Sendo S, Okano T, Akashi K, Irino Y, et al. Glutaminase 1 plays a key role in the cell growth of fibroblast-like synoviocytes in rheumatoid arthritis. *Arthritis Res Ther*. (2017) 19:76. doi: 10.1186/s13075-017-1283-3
61. Guma M, Sanchez-Lopez E, Lodi A, Garcia-Carbonell R, Tiziani S, Karin M, et al. Choline kinase inhibition in rheumatoid arthritis. *Ann Rheum Dis*. (2015) 74:1399–407. doi: 10.1136/annrheumdis-2014-205696
62. Shi M, Wang J, Xiao Y, Wang C, Qiu Q, Lao M, et al. Glycogen metabolism and rheumatoid arthritis: the role of glycogen synthase 1 in regulation of synovial inflammation via blocking AMP-activated protein kinase activation. *Front Immunol*. (2018) 9:1714. doi: 10.3389/fimmu.2018.01714
63. Yu Z, Lin W, Rui Z, Jihong P. Fibroblast-like synoviocyte migration is enhanced by IL-17-mediated overexpression of L-type amino acid transporter 1 (LAT1) via the mTOR/4E-BP1 pathway. *Amino Acids*. (2018) 50:331–40. doi: 10.1007/s00726-017-2520-4
64. Szanto S, Koreny T, Mikecz K, Glant TT, Szekanecz Z, Varga J. Inhibition of indoleamine 2,3-dioxygenase-mediated tryptophan catabolism accelerates collagen-induced arthritis in mice. *Arthritis Res Ther*. (2007) 9:R50. doi: 10.1186/ar2205
65. Michopoulos F, Karagianni N, Whalley NM, Firth MA, Nikolaou C, Wilson ID, et al. Targeted metabolic profiling of the Tg197 mouse model reveals itaconic acid as a marker of rheumatoid arthritis. *J Proteome Res*. (2016) 15:4579–90. doi: 10.1021/acs.jproteome.6b00654
66. Littlewood-Evans A, Sarret S, Apfel V, Loesle P, Dawson J, Zhang J, et al. GPR91 senses extracellular succinate released from inflammatory macrophages and exacerbates rheumatoid arthritis. *J Exp Med*. (2016) 213:1655–62. doi: 10.1084/jem.20160061
67. Saraiva AL, Veras FP, Peres RS, Talbot J, de Lima KA, Luiz JP, et al. Succinate receptor deficiency attenuates arthritis by reducing dendritic cell traffic and expansion of Th17 cells in the lymph nodes. *FASEB J*. (2018) 2018:fj201800285. doi: 10.1096/fj.201800285
68. Reid MA, Dai Z, Locasale JW. The impact of cellular metabolism on chromatin dynamics and epigenetics. *Nat Cell Biol*. (2017) 19:1298–306. doi: 10.1038/ncb3629
69. Etchegaray JP, Mostoslavsky R. Interplay between metabolism and epigenetics: a nuclear adaptation to environmental changes. *Mol Cell*. (2016) 62:695–711. doi: 10.1016/j.molcel.2016.05.029
70. Doody KM, Bottini N, Firestein GS. Epigenetic alterations in rheumatoid arthritis fibroblast-like synoviocytes. *Epigenomics*. (2017) 9:479–92. doi: 10.2217/epi-2016-0151
71. Ai R, Laragione T, Hammaker D, Boyle DL, Wildberg A, Maeshima K, et al. Comprehensive epigenetic landscape of rheumatoid arthritis fibroblast-like synoviocytes. *Nat Commun*. (2018) 9:1921. doi: 10.1038/s41467-018-04310-9
72. McGarry T, Fearon U. Cell metabolism as a potentially targetable pathway in RA. *Nat Rev Rheumatol*. (2019) 15:70–2. doi: 10.1038/s41584-018-0148-8
73. Rhoads JP, Major AS, Rathmell JC. Fine tuning of immunometabolism for the treatment of rheumatic diseases. *Nat Rev Rheumatol*. (2017) 13:313–20. doi: 10.1038/nrrheum.2017.54
74. Weyand CM, Goronzy JJ. Immunometabolism in early and late stages of rheumatoid arthritis. *Nat Rev Rheumatol*. (2017) 13:291–301. doi: 10.1038/nrrheum.2017.49
75. Meng X, Grotsch B, Luo Y, Knaup KX, Wiesener MS, Chen XX, et al. Hypoxia-inducible factor-1alpha is a critical transcription factor for IL-10-producing B cells in autoimmune disease. *Nat Commun*. (2018) 9:251. doi: 10.1038/s41467-017-02683-x
76. Yang Z, Fujii H, Mohan SV, Goronzy JJ, Weyand CM. Phosphofructokinase deficiency impairs ATP generation, autophagy, and redox balance in rheumatoid arthritis T cells. *J Exp Med*. (2013) 210:2119–34. doi: 10.1084/jem.20130252
77. Wilson JE. Isozymes of mammalian hexokinase: structure, subcellular localization and metabolic function. *J Exp Biol*. (2003) 206(Pt 12):2049–57. doi: 10.1242/jeb.00241
78. Yu P, Wilhelm K, Dubrac A, Tung JK, Alves TC, Fang JS, et al. FGF-dependent metabolic control of vascular development. *Nature*. (2017) 545:224–8. doi: 10.1038/nature22322
79. Jones AT, Narov K, Yang J, Sampson JR, Shen MH. Efficacy of dual inhibition of glycolysis and glutaminolysis for therapy of renal lesions in Tsc2(+/-) mice. *Neoplasia*. (2019) 21:230–8. doi: 10.1016/j.neo.2018.12.003
80. Chang CH, Curtis JD, Maggi LB Jr, Faubert B, Villarino AV, O'Sullivan D, et al. Posttranscriptional control of T cell effector function by aerobic glycolysis. *Cell*. (2013) 153:1239–51. doi: 10.1016/j.cell.2013.05.016
81. Yu X, Li S. Non-metabolic functions of glycolytic enzymes in tumorigenesis. *Oncogene*. (2016) 36:2629–36. doi: 10.1038/onc.2016.410
82. Mehta MM, Weinberg SE, Steinert EM, Chhiba K, Martinez CA, Gao P, et al. Hexokinase 2 is dispensable for T cell-dependent immunity. *Cancer Metab*. (2018) 6:10. doi: 10.1186/s40170-018-0184-5
83. Shervington L, Darekar A, Shaikh M, Mathews R, Shervington A. Identifying reliable diagnostic/predictive biomarkers for rheumatoid arthritis. *Biomark Insights*. (2018) 13:1177271918801005. doi: 10.1177/1177271918801005
84. Ruiz-Limon P, Ortega R, Arias de la Rosa I, Abalos-Aguilera MDC, Perez-Sanchez C, Jimenez-Gomez Y, et al. Tocilizumab improves the proatherothrombotic profile of rheumatoid arthritis patients modulating endothelial dysfunction, NETosis, and inflammation. *Transl Res*. (2017) 183:87–103. doi: 10.1016/j.trsl.2016.12.003
85. McGarry T, Orr C, Wade S, Biniecka M, Wade S, Gallagher L, et al. JAK/STAT blockade alters synovial bioenergetics, mitochondrial function, and proinflammatory mediators in rheumatoid arthritis. *Arthritis Rheumatol*. (2018) 70:1959–70. doi: 10.1002/art.40569

Conflict of Interest Statement: The authors declare that the research was conducted in the absence of any commercial or financial relationships that could be construed as a potential conflict of interest.

frontiers in Immunology

ORIGINAL RESEARCH
published: 18 September 2019
doi: 10.3389/fimmu.2019.02218

Long Non-coding RNA HIX003209 Promotes Inflammation by Sponging miR-6089 via TLR4/NF-κB Signaling Pathway in Rheumatoid Arthritis

Shushan Yan[1,2†], Pingping Wang[3†], Jinghua Wang[1,4†], Jinghan Yang[1,4†], Hongying Lu[5], Chengwen Jin[5], Min Cheng[6] and Donghua Xu[1,4*]*

[1] Clinical Medicine College, Weifang Medical University, Weifang, China, [2] Department of Gastrointestinal and Anal Diseases Surgery, The Affiliated Hospital of Weifang Medical University, Weifang, China, [3] Department of Gynecology and Obstetrics, Weifang Hospital of Maternal and Child Health, Weifang, China, [4] Department of Rheumatology, The Affiliated Hospital of Weifang Medical University, Weifang, China, [5] Functional Laboratory, Clinical Medicine College of Weifang Medical University, Weifang, China, [6] Department of Physiology, Weifang Medical University, Weifang, China

OPEN ACCESS

Edited by:
Hanshi Xu,
First Affiliated Hospital of Sun Yat-sen University, China

Reviewed by:
Yun Feng Pan,
Third Affiliated Hospital of Sun Yat-sen University, China
Runsheng Chen,
Institute of Biophysics (CAS), China

***Correspondence:**
Donghua Xu
flower322@163.com
Min Cheng
mincheng@wfmc.edu.cn

†*Co-first authors*

Specialty section:
This article was submitted to Autoimmune and Autoinflammatory Disorders, a section of the journal Frontiers in Immunology

Received: *16 May 2019*
Accepted: *02 September 2019*
Published: *18 September 2019*

Citation:
Yan S, Wang P, Wang J, Yang J, Lu H, Jin C, Cheng M and Xu D (2019) Long Non-coding RNA HIX003209 Promotes Inflammation by Sponging miR-6089 via TLR4/NF-κB Signaling Pathway in Rheumatoid Arthritis. Front. Immunol. 10:2218. doi: 10.3389/fimmu.2019.02218

Accumulating studies have suggested that long non-coding RNAs (lncRNAs) have drawn more and more attention in rheumatoid arthritis (RA), which can function as competitive endogenous RNAs (ceRNAs) in inflammation and immune disorders. Previously, we have found that lncRNA HIX003209 is differentially expressed in RA. However, the precise mechanism of lncRNA HIX003209 in RA is still vague. We aim to elucidate the role and its targeted microRNA of lncRNA HIX003209 in RA as ceRNA. Significantly increased expression of lncRNA HIX003209 was observed in the peripheral blood mononuclear cells (PBMCs) from RA cases. It was positively associated with TLR2 and TLR4 in RA. Besides, peptidoglycan (PGN) and lipopolysaccharide (LPS) could enhance the expression of lncRNA HIX003209, which reversely promoted the proliferation and activation of macrophages through IκBα/NF-κB signaling pathway. Moreover, HIX003209 was involved in TLR4-mediated inflammation via targeting miR-6089 in macrophages. LncRNA HIX003209 functions as a ceRNA and exaggerates inflammation by sponging miR-6089 through TLR4/NF-κB pathway in macrophages, which offers promising therapeutic strategies for RA.

Keywords: long non-coding RNA, competitive endogenous RNA, miRNA, inflammation, toll-like receptor, NF-κB

INTRODUCTION

Rheumatoid arthritis (RA) is a systemic autoimmune disease, the etiology of which remains largely unknown (1, 2). RA Patients usually have decreased quality of life due to progressive disability and systemic complications (3, 4). It has been well-documented that genetics and environmental factors, such as smoking, are associated with the development of RA (4). Apart from autoimmune, uncontrolled and systemic inflammation lead to joint damage, disability, decreased life quality, and increased risk of cardiovascular comorbidities among RA patients. Accordingly, it is essential to explore molecular mechanisms involved in inflammation in order to explore novel potential therapeutic strategy for RA.

Accumulating studies have suggested that non-coding RNAs, particularly long non-coding RNAs (lncRNAs), have been revealed in inflammation, cancer and autoimmune (5, 6). LncRNAs

can crosstalk with immune cells and mediate immunological and inflammatory response through nuclear factor-κB (NF-κB) signaling pathway (7–10). Recent studies have implicated a number of dysregulated lncRNAs contribute to the inflammatory response in RA (8, 11). Certain differentially expressed lncRNAs in RA have been demonstrated to affect the disease activity (12). Increasing evidence has revealed lncRNAs may regulate microRNAs (miRNAs) via functioning as competitive endogenous RNAs (ceRNAs), and thus participate in autoimmune diseases, including RA (13, 14). It is well-known that miRNAs can cause gene silencing by binding to mRNAs, while lncRNAs are capable of promoting the expression of targeted mRNAs by sponging miRNAs through the response element. Therefore, the lncRNA-miRNA-mRNA network possesses great significance in various biological processes. However, little has been known about the altering effect of lncRNA-miRNA-mRNA network in RA up till now. Previously, we have identified a novel lncRNA HIX003209 up-regulated in RA patients by microarray analysis (15). Nevertheless, the precise role and mechanisms of lncRNA HIX003209 in RA pathogenesis remain unclear, particularly regarding its role as a ceRNA in regulating inflammation and autoimmunity. The object of the study is to explore the role and molecular mechanisms of lncRNA HIX003209 in RA.

MATERIALS AND METHODS

Participants

RA patients (76) and age and sex-matched controls (60) were recruited from the hospital at the same period. Controls came to the same hospital for health examination. There was no difference for the status of ethnicity, smoking, alcohol consumption, and citizens of origin between the two groups. **Table 1** showed detailed information about the characteristics of all participants. Written informed consent was obtained from all participants before blood samples preparation. The study was permitted by the ethical committees in the Affiliated Hospital of Weifang Medical University.

Cell Culture and Transfection

THP-1 cells were cultured in RPMI 1640 (Invitrogen, USA) adding 10% fetal bovine serum (Gibco, USA) in company with penicillin/streptomycin (Invitrogen, USA). Firstly, THP-1 Cells were induced to be macrophages-like cells (pTHP-1) by 100 nM phorbol-12-myristate-13 acetate (PMA, Sigma, USA). Cells were activated by PMA for 48 h. After being cultured in fetal bovine serum-free serum for another 24 h, pTHP-1 cells were transfected by lentivirus particles in accompany with polybrene reagent. Peripheral blood mononuclear cells (PBMCs) of all participants were purified by Ficoll-Paque gradient centrifugation. $CD14^+$ mononuclear macrophages were separated by use of the CD14 microbeads (Miltenyi Biotec, San Diego, CA) according to the instructions.

TABLE 1 | Characteristics of patients and controls.

	RA	Controls
Age (mean ± SD)	57.9 ± 20.1	55.3 ± 19.8
Sex (women/man)	50/26	40/20
Smoking (years)	28.9 ± 10.1	27.0 ± 11.3
Alcohol (years)	19.8 ± 8.5	15.2 ± 6.9
CRP (mg/L)	41.2 ± 15.9	5.0 ± 5.1
ESR (mm/h)	58.4 ± 17.6	13.1 ± 9.0
RF (IU/ml)	161.5 ± 45.4	14.6 ±6.3

Real-Time Polymerase Chain Reaction (PCR)

Based on the instructions of Trizol reagent (Invitrogen, CA, USA), RNAs were isolated from human PBMCs, primary macrophages, or cell lines. A total of 0.5 μg RNAs were used as model for the synthesis of cDNAs. We used the Takara SYBR Green Mastermix kit (Tianjin, China) for PCR with a total of 5 ng cDNAs as template. The relative expression of TLR2, IL-6, TLR4, TNF-α, and IL-8 mRNAs was normalized to GAPDH. Genes primers were as follows: TNF-α: (F): 5′∼3′ GTCAACCTCCTCTCTGCCAT, (R): 5′∼3′ CCAAAG TAGACCTGCCCAGA; HIX003209, (F): 5′∼3′ ACTGCTCGC CAGAACACTAC, (R): 5′∼3′ GGTGAGGTTGATCGGGGTTT; IL-6, (F): 5′∼3′ AGTCCTGATCCAGTTCCTGC, (R): 5′∼3′ CTA CATTTGCCGAAGAGCCC; IL-8: (F): 5′∼3′, CGGAAGGAA CCATCTCACTG, (R): 5′∼3′ TTGGGGTGGAAAGGTTTGGA; TLR2: (F): 5′∼3′, CTATGAATCAAGGCGGCCAC, (R): 5′∼3′, AAAGATCCTGAGCTGCCCTT; TLR4: (F): 5′∼3′ CCAGCC TCCTCAGAAACAGA, (R): 5′∼3′ TCCCTCCAGCAGTGA AGAAG; GAPDH: (F): 5′∼3′ CTGACTTCAACAGCGACACC, (R): 5′∼3′ GTGGTCCAGGGGTCTTACTC.

Enzyme-Linked Immunosorbent Assay (ELISA)

We performed ELISA to detect c-responsive protein (CRP) and rheumatic factor (RF) in serum and cytokines (TNF-α, IL-6, IL-1β, and IL-17) in the culture supernatant of cells, based on protocols of the ELISA kit (R&D Systems, USA; Yanhui Biological Reagent Co., China). We detected the erythrocyte sedimentation rate (ESR) according to the Westergren method.

Western Blot

Proteins in pTHP-1 cells were purified by use of RIPA buffer (Beyotime, Shanghai, China). And the protease and phosphates inhibitors (Beyotime, Shanghai, China) were also used for protein isolation. A total of 30 μg proteins plus loading buffer were separated by gel electrophoresis. Specific monoclonal antibodies of TLR2, TLR4 (Santa Cruz Biotechnology, CA, USA), p-IκBα, p-NF-κB, and NF-κB (CST, USA) were adopted to capture proteins. The expression of specific proteins was normalized to β-actin (CST, USA) with three replicates.

Cell Proliferation Assay

In this study, we used cell counting kit-8 (CCK-8) to detect cell proliferation at 24, 48, and 72 h by reagent kits (Sigma, USA). Cells were treated by the use of CCK-8 reagent solution, and

then used for subsequent absorption determination. EdU was also performed to estimate the cell proliferation as previously reported (16).

Fluorescence *in situ* Hybridization (FISH) Assay

After crawling, pTHP-1 cells were fixed with 4% paraformaldehyde for 10 min and then incubated with protease-K at 37°C for another 10 min. After washing with PBS, cells were gradient dehydrated with ethanol of different concentrations. Fluorescent labeled HIX003209 probe was used for hybridization. DAPI solution (Beyotime Biotechnology, Shanghai, China) was applied to nucleus staining.

Immunofluorescence

The nuclear translocation of p-NF-κB in cells was determined by confocal laser scanning microscope after incubating with p-NF-κB monoclonal antibody (CST, USA). Nucleus was stained with DAPI solution (Beyotime Biotechnology, Shanghai, China).

RNA Binding Protein Immunoprecipitation (RIP) Assay

RIP assay was carried out according to the protocol of Magna RIP RNA-Binding Protein Immunoprecipitation Kit (Millipore, Bedford, MA, USA). Cell lysate was incubated with RIP immunoprecipitation buffer containing magnetic beads, which could conjugate with TLR2, TLR4 (Abcam, Cambridge, USA), NF-κB (CST, USA), and IgG control antibody (Abcam, Cambridge, USA). HIX003209 RNA level in immunoprecipitates was determined by real-time PCR.

Statistical Analysis

We applied the *T*-test or one-way ANOVA to estimate the data. A two-sided $P < 0.05$ was significant. In this study, SPSS (16.0v) and Graphpad (5.0v) softwares were used for statistical analysis.

RESULTS

Increased Expression of lncRNA HIX003209 in RA

We have found increased expression of lncRNA HIX003209 in serum from RA patients in a previous study (15).

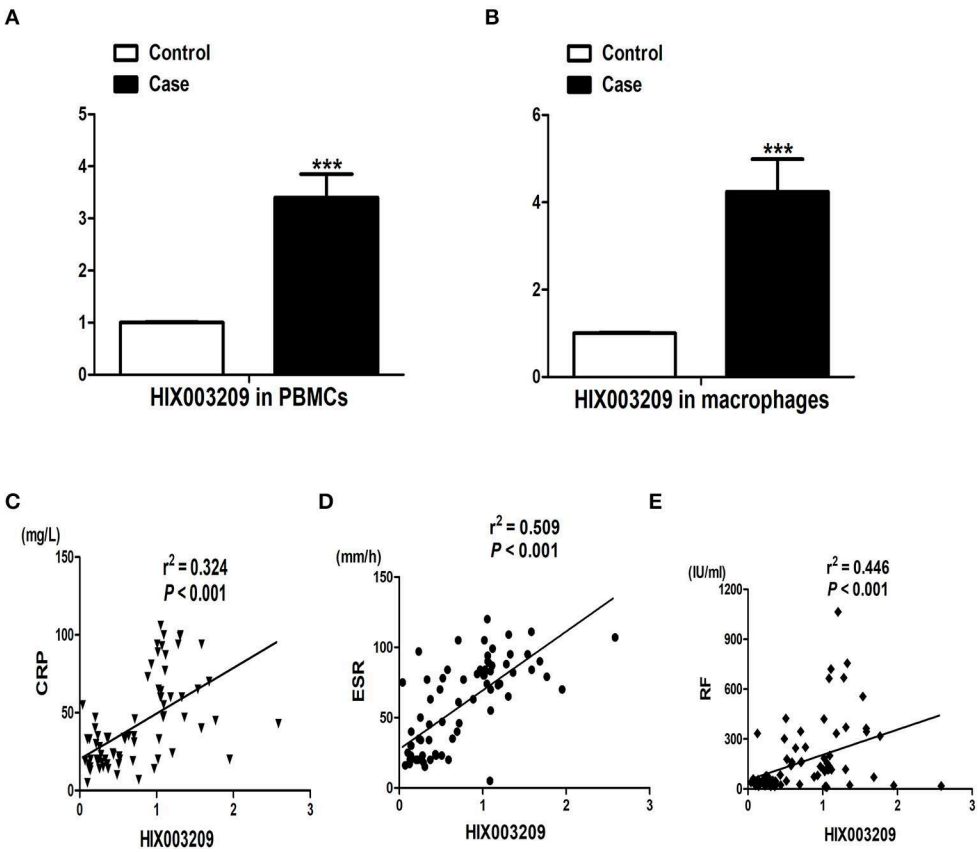

FIGURE 1 | Expression of lncRNA HIX003209 and its association with disease activity in RA. **(A)** LncRNA HIX003209 expression in PBMCs samples from patients with RA in contrast to controls (patients/controls: 76/60; ***$P < 0.001$). **(B)** LncRNA HIX003209 expression in primary CD14$^+$ mononuclear macrophages from RA patients and controls (patients/controls: 36/30; ***$P < 0.001$). **(C)** Positive association of lncRNA HIX003209 with CRP in RA (76 RA patients). **(D)** Positive association of lncRNA HIX003209 with ESR in RA (76 RA patients). **(E)** Positive association of lncRNA HIX003209 with RF in RA (76 RA patients).

Similarly, elevated expression of lncRNA HIX003209 was observed in PBMCs and primary $CD14^+$ macrophages from patients with RA (**Figures 1A,B**). Besides, positive association between the expression of lncRNA HIX003209 in PBMCs and CRP, ESR, and RF was identified in RA patients, respectively (**Figures 1C–E**). Taken together, lncRNA HIX003209 was up-regulated in RA and positively related to the disease activity.

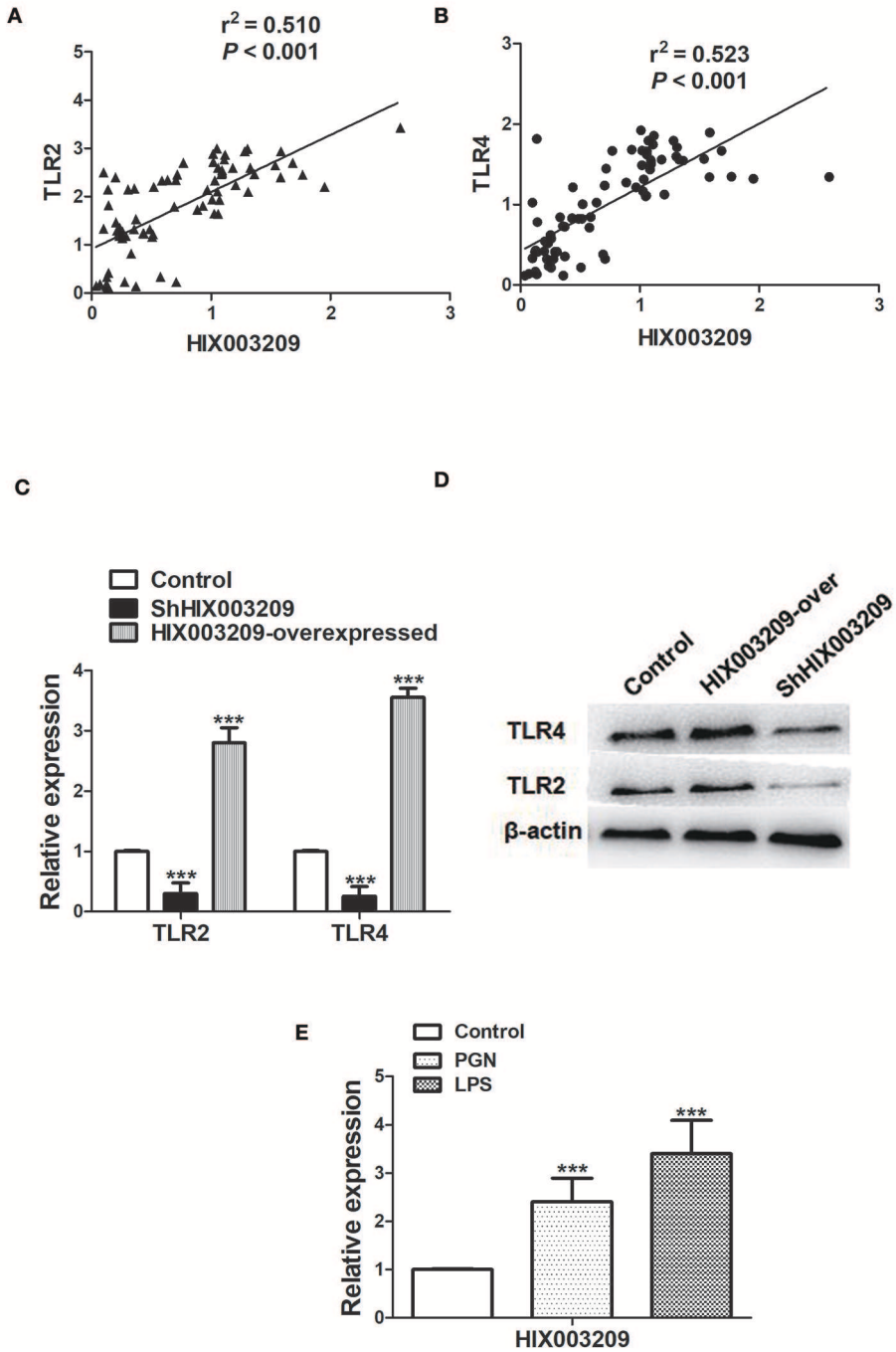

FIGURE 2 | Association of lncRNA HIX003209 with TLR2 and TLR4 in RA. **(A)** Expression of lncRNA HIX003209 was positively associated with TLR2 in PBMCs of RA patients (76 cases). **(B)** Expression of lncRNA HIX003209 was positively associated with TLR4 in PBMCs of RA patients (76 cases). **(C)** Decreased TLR2 and TLR4 mRNAs in HIX003209 knockdown (shHIX003209) pTHP-1 cells while increased TLR2 and TLR4 mRNAs in HIX003209-overexpressed pTHP-1 cells (***$P <$ 0.001; $n = 3$). **(D)** Decreased TLR2 and TLR4 proteins in shHIX003209 pTHP-1 cells while increased TLR2 and TLR4 proteins in HIX003209-overexpressed pTHP-1 cells. **(E)** Increased expression of HIX003209 in pTHP-1 cells when stimulated by PGN and LPS (***$P < 0.001$; $n = 3$) (Representative pictures of three independent experiments).

Association Between lncRNA HIX003209 and TLR2 and TLR4

As shown in **Figures 2A,B**, the expression of lncRNA HIX003209 was positively correlated with TLR2 and TLR4 in RA. To further elucidate their relationship, the expression of lncRNA HIX003209 was knocked down with lentivirus shHIX003209 in pTHP-1 cells. The mRNA level of TLR2 and TLR4 was significantly reduced in HIX003209 knockdown macrophages compared with the control group (**Figure 2C**). Similarly, decreased expression of TLR2 and TLR4 proteins was also confirmed in HIX003209 knockdown pTHP-1 cells (**Figure 2D**) (Details were shown in **Supplementary Material**). However, over-expression of lncRNA HIX003209 promoted the expression of TLR2 and TLR4 in pTHP-1 cells (**Figures 2C,D**). Peptidoglycan (PGN) and lipopolysaccharide (LPS) were ligands for TLR2 and TLR4, respectively. When pTHP-1 macrophages were stimulated by PGN or LPS for 12 h, the expression of lncRNA HIX003209 was obviously enhanced as evidenced by real-time PCR (**Figure 2E**). Accordingly, TLR ligands (PGN and LPS) promoted the expression of lncRNA HIX003209 in pTHP-1 cells. Taken together, inflammatory stimuli enhanced the expression of lncRNA HIX003209 and thus further exaggerate the inflammatory response in macrophages.

LncRNA HIX003209 Promoted Cell Proliferation and Activation Through IκBα/NF-κB Pathway

As assayed by cell proliferation assays (CCK-8 and EdU), over-expression of lncRNA HIX003209 could promote cell proliferation (**Figures 3A–C**). Increased levels of TNF-α, IL-6 and IL-1β mRNAs were found in PGN- and LPS-stimulated pTHP-1 macrophages (**Figures 4A,B**). Besides, the generation of TNF-α, IL-6, and IL-1β mRNAs was significantly promoted in lncRNA HIX003209-overexpressed macrophages stimulated by PGN and LPS (**Figures 4A,B**). Similarly, proteins of TNF-α, IL-6, and IL-1β were obviously increased in the cultural supernatant of PGN- and LPS-stimulated lncRNA HIX003209-overexpressed macrophages (**Figures 4C,D**). Nevertheless, obviously reduced

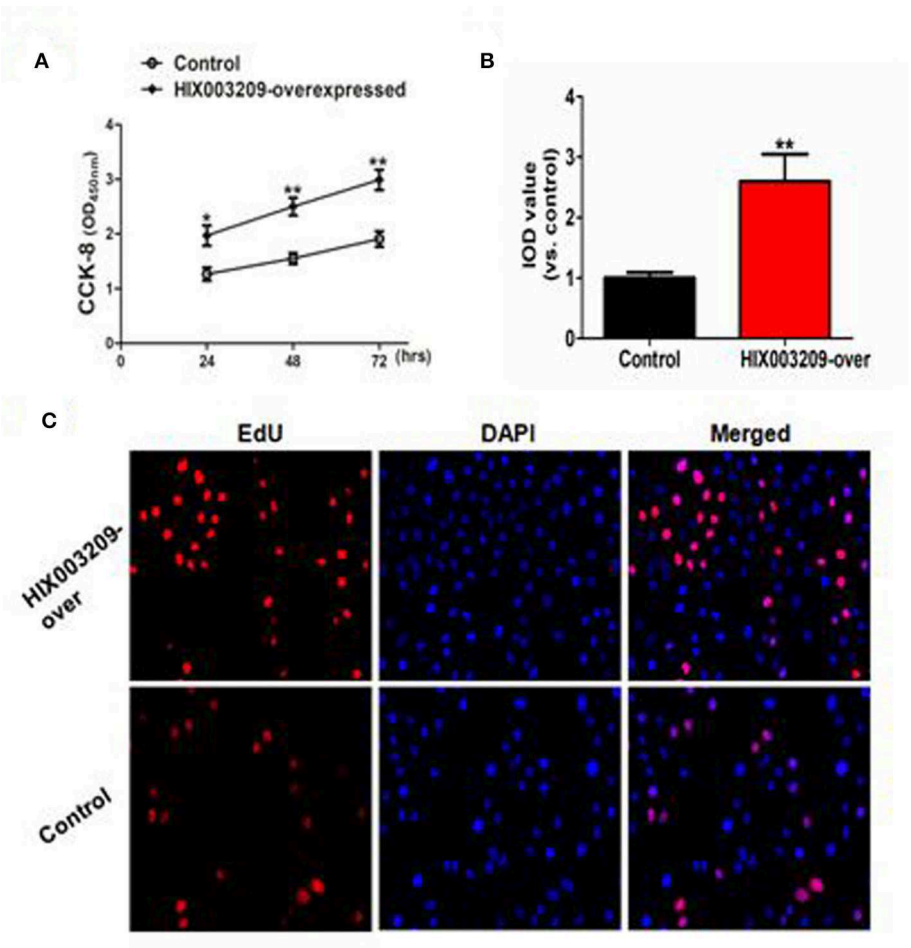

FIGURE 3 | LncRNA HIX003209 promoted the proliferation of macrophages. **(A)** As demonstrated by CCK-8, the cell proliferation was enhanced in HIX003209-overexpressed cells (*$P < 0.05$; **$P < 0.01$; $n = 3$). **(B)** The integrated optical density (IOD) estimating pTHP-1 macrophages proliferation (**$P < 0.01$; $n = 3$). **(C)** As demonstrated by EdU the cell proliferation was significantly promoted when HIX003209 was over-expressed in cells (Representative pictures of three independent tests).

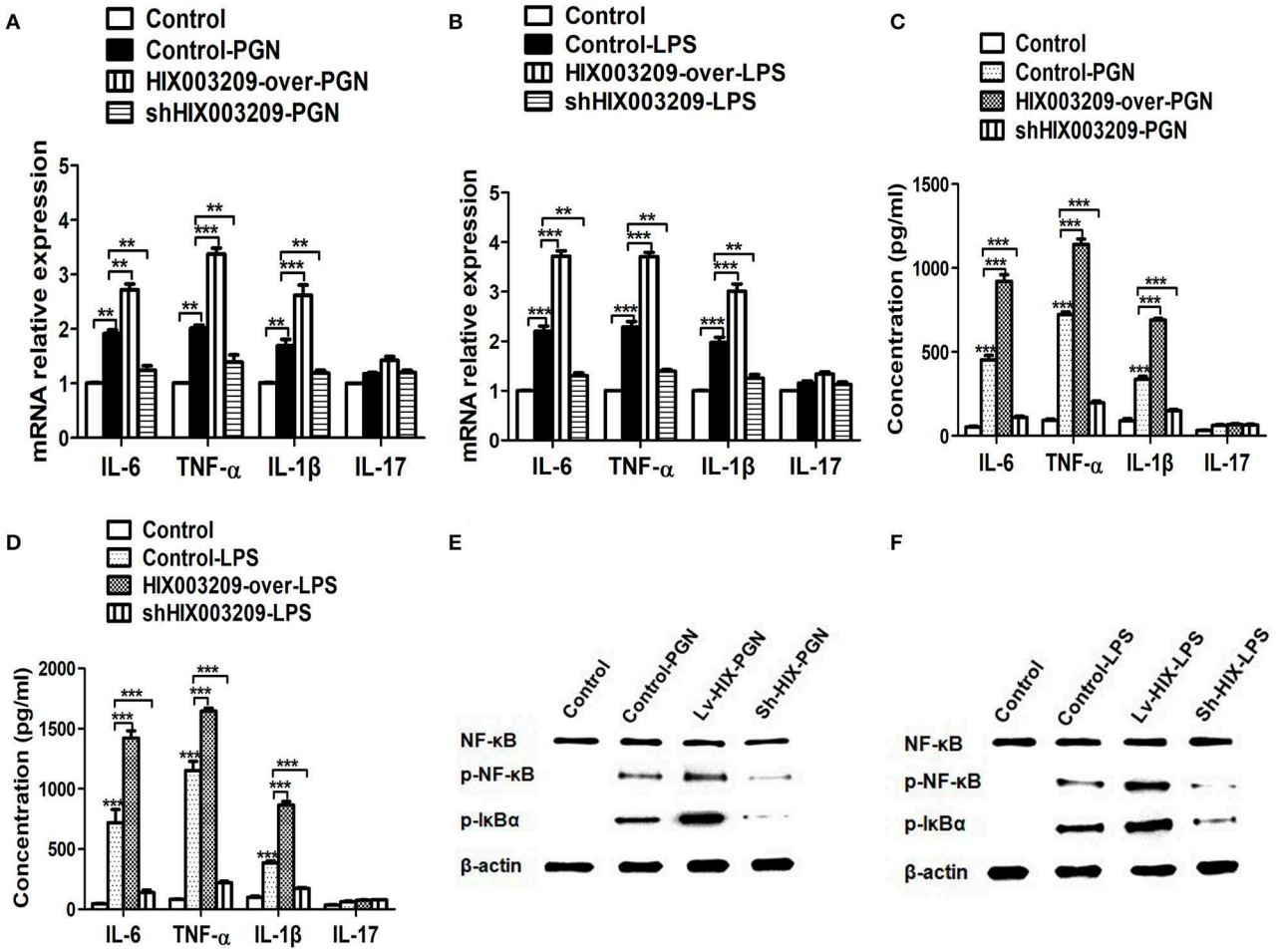

FIGURE 4 | LncRNA HIX003209 enhanced the activation of macrophages through IκBα/NF-κB signaling pathway. **(A)** Expression of cytokines (IL-6, TNF-α, IL-1β, and IL-17) mRNAs was increased in HIX003209-overexpressed cells but decreased in shHIX003209 pTHP-1 cells despite the stimulation of PGN (**$P < 0.01$; ***$P < 0.001$; $n = 3$). **(B)** Expression of cytokines mRNAs was increased in HIX003209-overexpressed cells but decreased in shHIX003209 pTHP-1 cells although stimulated by LPS (**$P < 0.01$; ***$P < 0.001$; $n = 3$). **(C)** The production of cytokines in the supernatant of pTHP-1 cells stimulated by PGN was promoted when HIX003209 was over-expressed, but it was inhibited when HIX003209 was knocked down in cells (***$P < 0.001$; $n = 3$). **(D)** The generation of cytokines in the supernatant of pTHP-1 cells stimulated by LPS was enhanced when HIX003209 was over-expressed, but it was restrained when HIX003209 was knocked down in cells (***$P < 0.001$; $n = 3$). **(E,F)** Western blot analysis showed increased phosphorylation and activation of IκBα/NF-κB in macrophages with HIX003209 overexpression ($n = 3$, representative pictures).

levels of inflammatory cytokines (TNF-α, IL-6, and IL-1β) were observed in lncRNA HIX003209 knockdown pTHP-1 cells in spite of the stimulation of PGN and LPS (**Figures 4A–D**). There was no statistical difference for IL-17 between groups (**Figures 4A–D**). Moreover, lncRNA HIX003209 promoted the production of inflammatory cytokines in macrophages depending on the activation of IκBα/NF-κB signaling pathway (**Figures 4E,F**, **5A**). Taken together, lncRNA HIX003209 could enhance the proliferation and activation of macrophages through TLR/NF-κB pathway. Given this, we hypothesized whether HIX003209 could bind directly to these proteins to display its regulatory role in macrophages. Unfortunately, we found that lncRNA HIX003209 could not directly bind to TLR2, TLR4, and NF-κB, suggesting RNA binding protein immunoprecipitation (**Figures 5B–D**).

MiR-6089 Was a Target of lncRNA HIX003209

In our previously study, miR-6089 was found to play an important role in RA pathogenesis by targeting TLR4 (16). In this study, we had found a positive association between lncRNA HIX003209 and TLR4 with regard to their expression in RA (**Figure 2B**), and the modifying effect of LPS/TLR4-mediated inflammation in macrophages. As a result, we hypothesized that lncRNA HIX003209 might affect inflammatory response by regulating miR-6089/TLR4. Interestingly, it was demonstrated that lncRNA HIX003209 was negatively related to miR-6089 regarding the expression in PBMCs samples of RA cases (**Figure 6A**). LncRNA HIX003209 was primarily expressed in the cytoplasm of pTHP-1 cells (**Figures 6B,C**). The expression of miR-6089

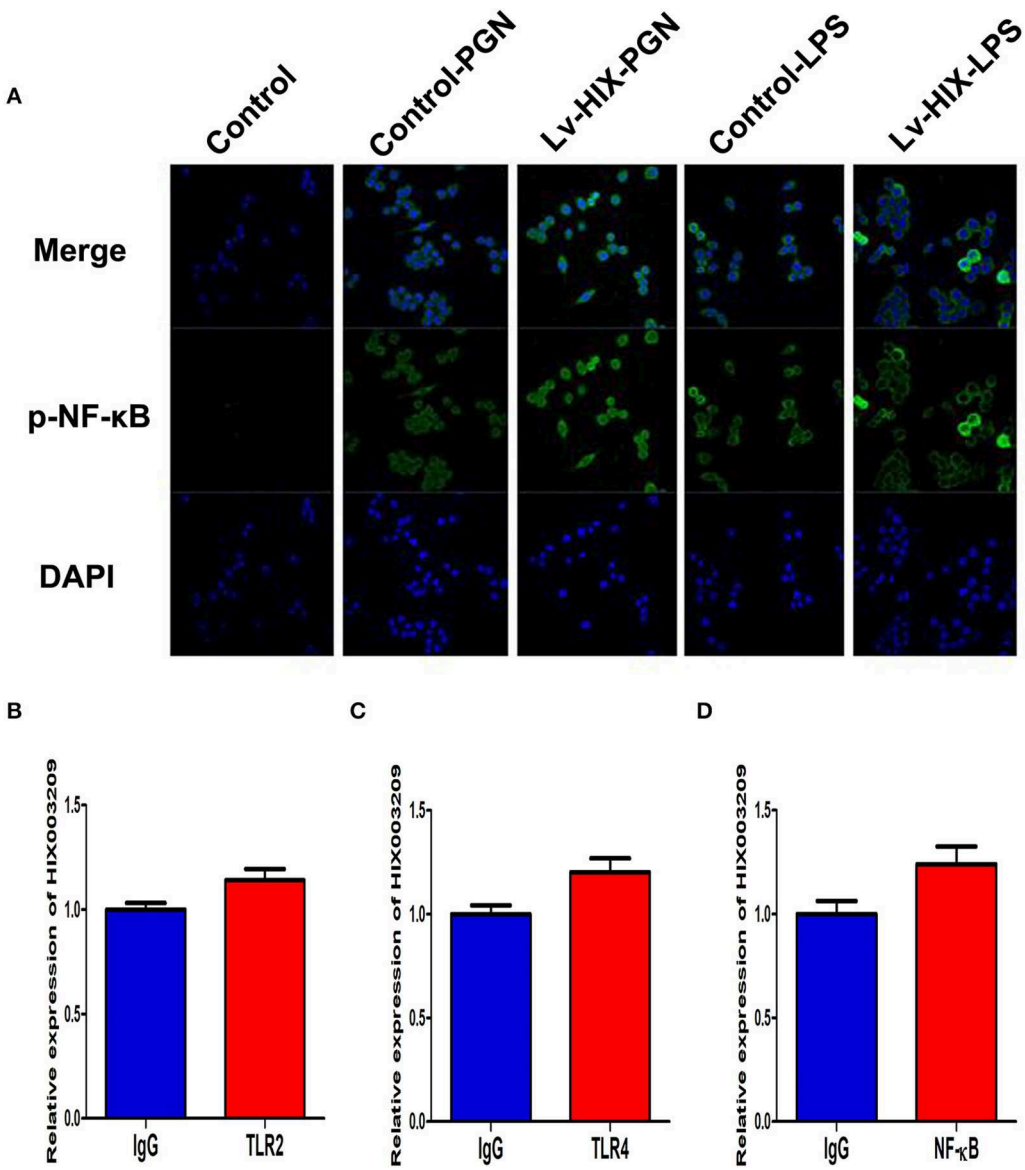

FIGURE 5 | LncRNA HIX003209 activated NF-κB signaling but not directly bound to TLR2, TLR4, and NF-κB in macrophages. **(A)** Immunofluorescence demonstrated increased activation and nuclear translocation of p-NF-κB in macrophages with HIX003209 upregulation (representative figures of three repeated tests). **(B)** RIP showed expression level of HIX003209 in immunoprecipitates as fold enrichment of TLR2 relative to IgG determined by real-time PCR ($n = 3$). **(C)** Expression of HIX003209 in immunoprecipitates as fold enrichment of TLR4 relative to IgG ($n = 3$). **(D)** HIX003209 expression in immunoprecipitates from macrophages extracts as fold enrichment of NF-κB relative to IgG ($n = 3$).

was significantly decreased when HIX003209 was over-expressed in macrophages (**Figure 6D**). Accordingly, lncRNA HIX003209 might function as a ceRNA by sponging miR-6089 in pTHP-1 macrophages. There were six complementary pairing bases between HIX003209 and miR-6089 (**Figure 6E**). Furthermore, the luciferase reporter assay showed that HIX003209 could specifically recognize miR-6089 (**Figure 6F**). Taken together, miR-6089 was a direct target of lncRNA HIX003209. LncRNA HIX003209 could sponge miR-6089 as a ceRNA.

LncRNA HIX003209 Influenced the Downstream Signaling of miR-6089/TLR4 in Macrophages Via NF-κB

The regulatory mechanism of HIX003209 in RA pathogenesis is not yet clear. Here, lncRNA HIX003209 was shown to promote the expression of TLR4 by functioning as a ceRNA and sponging miR-6089, while mimics of miR-6089 could inhibit the expression of TLR4, although HIX003209 was over-expressed in cells (**Figures 7A,B**) (Details were shown in **Supplementary Material**). Besides, lncRNA HIX003209

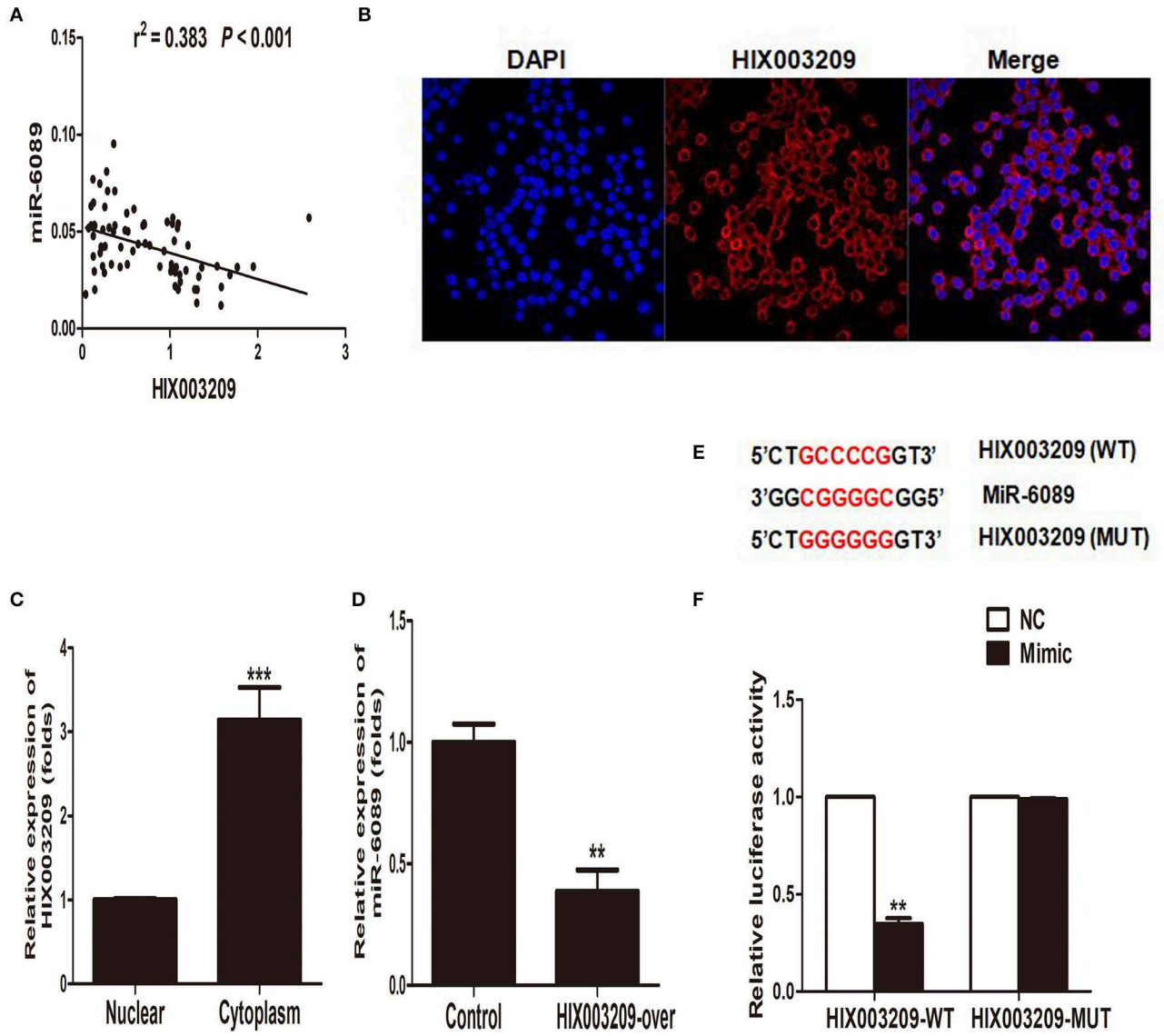

FIGURE 6 | MiR-6089 was a targeted gene of lncRNA HIX003209. **(A)** The expression of LncRNA HIX003209 was negatively associated with miR-6089 in PBMCs from RA (76 cases). **(B)** FISH assay showed lncRNA HIX003209 was primarily expressed in cytoplasm of macrophages (one representative figure from three repeated tests). **(C)** Real-time PCR detected the expression of lncRNA HIX003209 in macrophages (***$P < 0.001$; $n = 3$). **(D)** HIX003209 inhibited the expression of miR-6089 in macrophages (**$P < 0.01$; $n = 3$). **(E)** Complementary pairing bases of HIX003209 and miR-6089 (WT, wild type; MUT, mutant). **(F)** Luciferase reporter assay demonstrated HIX003209 could targetedly regulate miR-6089 (**$P < 0.01$; $n = 3$).

enhanced the activation of NF-κB with a high level of phosphorylation and increased nuclear translocation in macrophages (**Figures 7B,C**). However, mimics of miR-6089 could restrain phosphorylation and nuclear translocation of NF-κB in macrophages. Taken together, lncRNA HIX003209 acted as a ceRNA and regulated miR-6089/TLR4 through NF-κB signaling in macrophages.

DISCUSSION

The current study firstly provides evidence that lncRNA HIX003209 is involved in the pathogenesis of RA by enhancing macrophage-mediated inflammatory response via TLR2/TLR4. LncRNA HIX003209 enhances macrophages proliferation and activation through IκBα/NF-κB signaling pathway. Most importantly, lncRNA HIX003209 can function as a ceRNA by effectively binding to miR-6089, which restores the expression of TLR4 and the activation of downstream signaling molecule NF-κB in macrophages. The lncRNA HIX003209-miR6089-TLR4 network offers promising therapeutic strategy for RA patients.

LncRNAs have more than 200 nucleotides in length, which possess capacities of regulating a variety of coding genes (17). It has been well-established that lncRNAs play important roles in the regulation of autoimmunity and inflammatory response

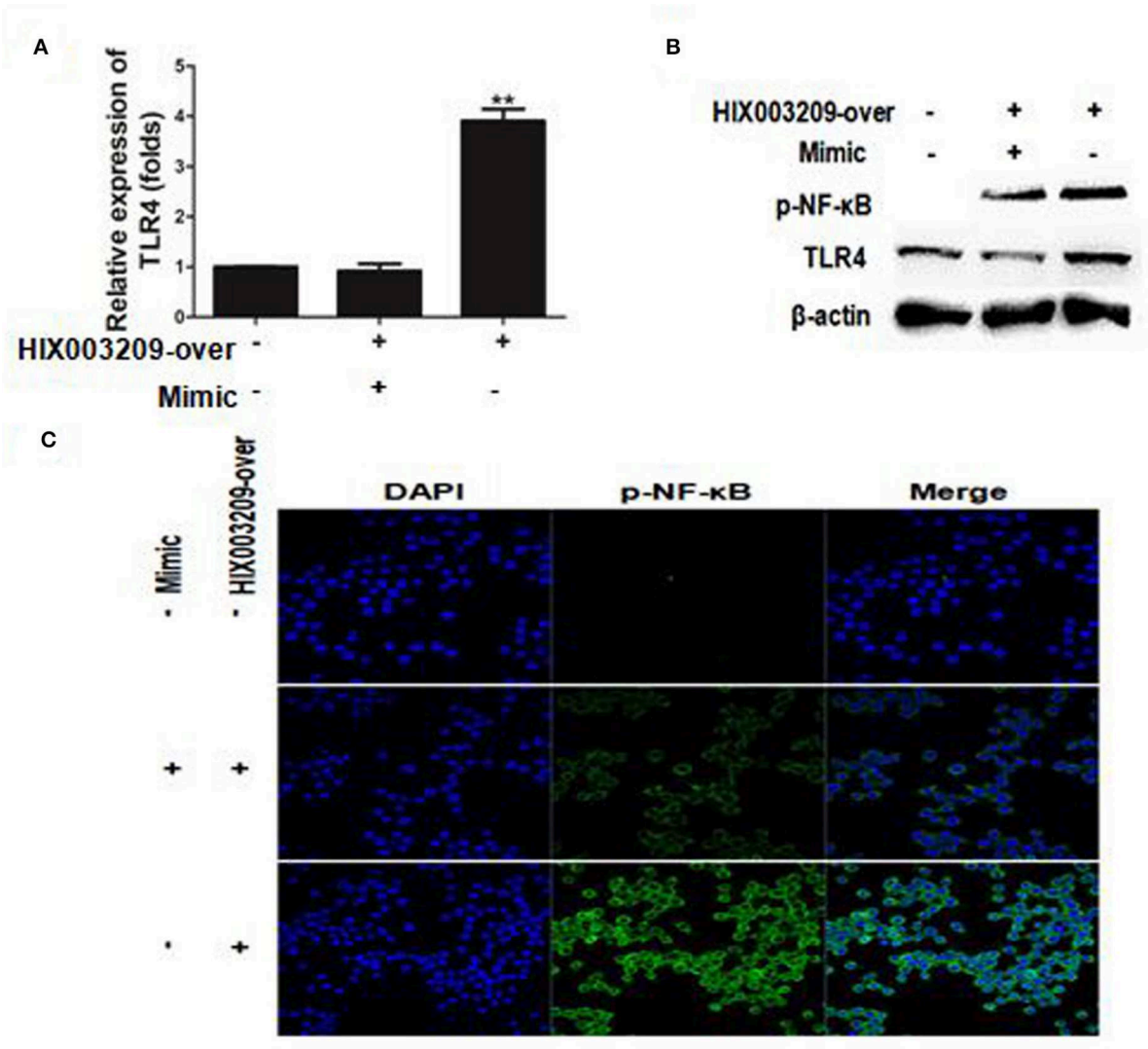

FIGURE 7 | LncRNA HIX003209 functioned as a ceRNA by sponging miR-6089 through TLR4/NF-κB signaling in macrophages. **(A)** LncRNA HIX003209 promoted the expression of TLR4 by sponging miR-6089 in macrophages (**$P < 0.01$; $n = 3$). **(B)** LncRNA HIX003209 enhanced the expression of TLR4 and the phosphorylation of NF-κB by sponging with miR-6089 ($n = 3$, representative pictures). **(C)** LncRNA HIX003209 boosted the nuclear translocation of p-NF-κB in macrophages by sponging with miR-6089 ($n = 3$, representative pictures).

(18–20). Dysregulation of lncRNAs in lymphocytes is established to be involved in the immunopathogenesis of rheumatoid diseases, including systematic lupus erythematosus (SLE) and RA (13, 19, 21). Apart from directly binding to proteins, some lncRNAs can indirectly regulate mRNAs by sponging miRNAs. During the past few years, lncRNA-miRNA-mRNA ceRNA theory has been demonstrated in the development of multiple diseases, such as malignancies, cardiovascular diseases and autoimmune diseases (21–24). LncRNAs are capable of acting as miRNA decoys to restore the expression of targeted genes via competitive regulatory interactions between lncRNAs, miRNAs, and mRNAs. Aberrant expression of any non-coding RNAs in this network would contribute to the occurrence and progression of certain diseases. A recent study by Jiang and the colleagues has revealed functional lncRNAs in RA based on the ceRNA theory (13). There are a few lncRNAs that have been demonstrated to affect the proliferation, invasion, and migration of fibroblast-like synoviocytes in RA by suppressing miRNAs via ceRNA network, such as GAPLINC (21) and ZFAS1 (25). Nevertheless, the molecular mechanisms of well-established lncRNAs as miRNAs sponge in RA still need to be further elucidated, which will facilitate the identification of valuable and effective targets for RA diagnosis and treatment based on the lncRNA-miRNA-mRNA ceRNA network. Our study firstly provides evidence that lncRNA HIX003209 is dysregulated in macrophages, and promotes the proliferation and inflammatory cytokines (TNF-α, IL-6, and IL-1β) generation of macrophages through

IκBα/NF-κB pathway. LncRNA HIX003209 cannot directly bind to TLR2, TLR4, and the downstream protein NF-κB, but it can sponge miR-6089 and further promotes the expression of TLR4/NF-κB in macrophages through ceRNA mechanism. Knockdown of lncRNA HIX003209 can alleviate inflammation in macrophages. Accordingly, the newly identified lncRNA HIX003209-miR6089-TLR4 ceRNA network will provide new insight into understanding the pathogenesis of RA. Novel targets for RA treatment require further investigation in future studies based on this ceRNA network.

Toll-like receptors (TLRs) and TLRs-mediated signaling transduction are closely associated with inflammation, tumors and autoimmune regulations (26, 27). TLRs and its downstream signaling pathways, such as MAPK, Wnt, and NF-κB pathways, have been elucidated in synovial inflammation and bone remodeling of RA (28–30). Previously, we have found that TLR4-mediated innate immune and inflammatory response play a vital role in RA, primarily depending on NF-κB signaling activation (16, 31, 32). TLR2-mediated immune and inflammatory response also play important roles in RA (33, 34). Taken together, TLRs confer significant effects on the pathogenesis of RA. It has been well-documented that many non-coding RNAs can targetedly regulate specific TLRs, and thus contribute to the development of RA, including lncRNAs (15, 16, 30). Many studies have implicated the critical role of lncRNAs in regulating autoimmune and inflammation by targeting TLRs, such as TLR2, TLR4, and TLR3 (35–37). Most interestingly, more and more published studies have suggested that some established lncRNAs can regulate TLR signaling transduction and the relevant immune function in cancer, autoimmune and inflammatory disorders by acting as ceRNAs, such as networks of lncRNA SNHG1-miR-140-TLR4, lncRNA X-miR-154-5p-TLR5, and lncRNA Gm6135-miR-203-3p-TLR4 (38–41). However, no available data can support the interaction between lncRNA and miRNA in regulating TLR signaling pathway in RA up to date. In this study, we have found lncRNA HIX003209 contributes to RA by regulating TLR2- and TLR4-mediated inflammation in macrophages. Most importantly, lncRNA HIX003209 is capable of restoring the expression of TLR4 and activation of NF-κB by sponging miR-6089 in macrophages. As a result, HIX003209 can function as a ceRNA and regulate TLR4/NF-κB signaling pathway via targeting miR-6089 in RA. However, future studies are warranted to identify more promising targets in the network of HIX003209-miR-6089-TLR4, particularly in the downstream of TLR4 signaling.

Inflammatory cells and inflammatory mediators play crucial roles in soft tissue injuries and bone lesions in RA, such as IL-6, TNF-α, and IL-1β. Increased inflammatory cytokines result in infiltration of macrophages and progressive destruction of articular cartilage, and ultimately bone (42, 43). Accordingly, it is useful for treatment by blocking inflammation-associated molecules and pathways involved in RA. Certain inhibitors of inflammatory cytokines have been applied into clinical treatments of RA, such as IL-6R monoclonal antibody and TNF-α inhibitors. Researchers have attempted to explore novel strategies for RA treatment by inhibiting NF-κB signaling pathway, a key pathway regulating inflammation (44, 45). In the present study, we have elucidated that lncRNA HIX003209 promotes PGN- and LPS-induced inflammatory response via TLR2 and TLR4 signaling pathway in macrophages. Knockdown of lncRNA HIX003209 helps to alleviate inflammation in macrophages. As a result, shHIX003209 may be a useful reagent for the treatment of RA. However, more research is warranted to explore a useful strategy for RA targeted treatment by blocking any node in the HIX003209-miR-6089-TLR4 network, particularly experiments *in vivo*.

To summarize, the study firstly demonstrates the altering effect of lncRNA HIX003209 in RA by regulating macrophages-mediated inflammation. The HIX003209-miR-6089-TLR4 network provides novel therapeutic targets for RA patients in future.

DATA AVAILABILITY

All datasets generated for this study are included in the manuscript/**Supplementary Files**.

ETHICS STATEMENT

Written informed consent was obtained from the individual(s) for the publication of any potentially identifiable images or data included in this article.

AUTHOR CONTRIBUTIONS

SY, MC, and DX designed the experiments. SY, PW, JW, and JY carried out the experiments. CJ and HL gave advice on experimental design and data analysis. SY, PW, and JW wrote and revised the paper. MC and DX edited the article.

FUNDING

This work was supported by grants from the National Natural Science Foundation, China (81601408, 31570941, 81870237, and 31270993), Shandong Natural Science Foundation for Young Scholars, China (ZR2019QH012 and ZR2016HQ12), Shandong Medical and Health Science and Technology Development Program (2018WS091), and Weifang Science and Technology Development Program, China (2019GX031, 2019YX020, and 2017YX019).

SUPPLEMENTARY MATERIAL

The Supplementary Material for this article can be found online at: https://www.frontiersin.org/articles/10.3389/fimmu.2019.02218/full#supplementary-material

REFERENCES

1. Catrina AI, Joshua V, Klareskog L, Malmstrom V. Mechanisms involved in triggering rheumatoid arthritis. *Immunol Rev*. (2016) 269:162–74. doi: 10.1111/imr.12379
2. Meier FM, Frerix M, Hermann W, Muller-Ladner U. Current immunotherapy in rheumatoid arthritis. *Immunotherapy*. (2013) 5:955–74. doi: 10.2217/imt.13.94
3. Turesson C. Extra-articular rheumatoid arthritis. *Curr Opin Rheumatol*. (2013) 25:360–6. doi: 10.1097/BOR.0b013e32835f693f
4. Scott DL, Wolfe F, Huizinga TW. Rheumatoid arthritis. *Lancet*. (2010) 376:1094–108. doi: 10.1016/S0140-6736(10)60826-4
5. Marques-Rocha JL, Samblas M, Milagro FI, Bressan J, Martinez JA, Marti A. Noncoding RNAs, cytokines, and inflammation-related diseases. *FASEB J*. (2015) 29:3595–611. doi: 10.1096/fj.14-260323
6. Fitzgerald KA, Caffrey DR. Long noncoding RNAs in innate and adaptive immunity. *Curr Opin Immunol*. (2014) 26:140–6. doi: 10.1016/j.coi.2013.12.001
7. Li M, Guan H. Noncoding RNAs Regulating NF-kappaB Signaling. *Adv Exp Med Biol*. (2016) 927:317–36. doi: 10.1007/978-981-10-1498-7_12
8. Lu MC, Yu HC, Yu CL, Huang HB, Koo M, Tung CH, et al. Increased expression of long noncoding RNAs LOC100652951 and LOC100506036 in T cells from patients with rheumatoid arthritis facilitates the inflammatory responses. *Immunol Res*. (2016) 64:576–83. doi: 10.1007/s12026-015-8756-8
9. Mao X, Su Z, Mookhtiar AK. Long non-coding RNA: a versatile regulator of the nuclear factor-kappaB signalling circuit. *Immunology*. (2017) 150:379–88. doi: 10.1111/imm.12698
10. Zhang Y, Xu YZ, Sun N, Liu JH, Chen FF, Guan XL, et al. Long noncoding RNA expression profile in fibroblast-like synoviocytes from patients with rheumatoid arthritis. *Arthritis Res Ther*. (2016) 18:227. doi: 10.1186/s13075-016-1129-4
11. Mousavi MJ, Jamshidi A, Chopra A, Aslani S, Akhlaghi M, Mahmoudi M. Implications of the noncoding RNAs in rheumatoid arthritis pathogenesis. *J Cell Physiol*. (2018) 234:335–47. doi: 10.1002/jcp.26911
12. Yuan M, Wang S, Yu L, Qu B, Xu L, Liu L, et al. Long noncoding RNA profiling revealed differentially expressed lncRNAs associated with disease activity in PBMCs from patients with rheumatoid arthritis. *PLoS ONE*. (2017) 12:e0186795. doi: 10.1371/journal.pone.0186795
13. Jiang H, Ma R, Zou S, Wang Y, Li Z, Li W. Reconstruction and analysis of the lncRNA-miRNA-mRNA network based on competitive endogenous RNA reveal functional lncRNAs in rheumatoid arthritis. *Mol Biosyst*. (2017) 13:1182–92. doi: 10.1039/C7MB00094D
14. Hur K, Kim SH, Kim JM. Potential implications of long noncoding RNAs in autoimmune diseases. *Immune Netw*. (2019) 19:e4. doi: 10.4110/in.2019.19.e4
15. Xu D, Jiang Y, Yang L, Hou X, Wang J, Gu W, et al. Long noncoding RNAs expression profile and functional networks in rheumatoid arthritis. *Oncotarget*. (2017) 8:95280–92. doi: 10.18632/oncotarget.20036
16. Xu D, Song M, Chai C, Wang J, Jin C, Wang X, et al. Exosome-encapsulated miR-6089 regulates inflammatory response via targeting TLR4. *J Cell Physiol*. (2018) 234:1502–11. doi: 10.1002/jcp.27014
17. Huang X, Xiao R, Pan S, Yang X, Yuan W, Tu Z, et al. Uncovering the roles of long non-coding RNAs in cancer stem cells. *J Hematol Oncol*. (2017) 10:62. doi: 10.1186/s13045-017-0428-9
18. Gao Y, Li S, Zhang Z, Yu X, Zheng J. The role of long non-coding RNAs in the pathogenesis of RA, SLE, and SS. *Front Med*. (2018) 5:193. doi: 10.3389/fmed.2018.00193
19. Lai NS, Koo M, Yu CL, Lu MC. Immunopathogenesis of systemic lupus erythematosus and rheumatoid arthritis: the role of aberrant expression of non-coding RNAs in T cells. *Clin Exp Immunol*. (2017) 187:327–36. doi: 10.1111/cei.12903
20. Liang J, Chen W, Lin J. LncRNA: an all-rounder in rheumatoid arthritis. *J Transl Int Med*. (2019) 7:3–9. doi: 10.2478/jtim-2019-0002
21. Mo BY, Guo XH, Yang MR, Liu F, Bi X, Liu Y, et al. Long non-coding RNA GAPLINC promotes tumor-like biologic behaviors of fibroblast-like synoviocytes as microRNA sponging in rheumatoid arthritis patients. *Front Immunol*. (2018) 9:702. doi: 10.3389/fimmu.2018.00702
22. Abdollahzadeh R, Daraei A, Mansoori Y, Sepahvand M, Amoli MM, Tavakkoly-Bazzaz J. Competing endogenous RNA (ceRNA) cross talk and language in ceRNA regulatory networks: a new look at hallmarks of breast cancer. *J Cell Physiol*. (2019) 234:10080–100. doi: 10.1002/jcp.27941
23. Chan JJ, Tay Y. Noncoding RNA: RNA regulatory networks in cancer. *Int J Mol Sci*. (2018) 19:E1310. doi: 10.3390/ijms19051310
24. He L, Chen Y, Hao S, Qian J. Uncovering novel landscape of cardiovascular diseases and therapeutic targets for cardioprotection via long noncoding RNA-miRNA-mRNA axes. *Epigenomics*. (2018) 10:661–71. doi: 10.2217/epi-2017-0176
25. Ye Y, Gao X, Yang N. LncRNA ZFAS1 promotes cell migration and invasion of fibroblast-like synoviocytes by suppression of miR-27a in rheumatoid arthritis. *Hum Cell*. (2018) 31:14–21. doi: 10.1007/s13577-017-0179-5
26. Bhatelia K, Singh K, Singh R. TLRs: linking inflammation and breast cancer. *Cell Signal*. (2014) 26:2350–7. doi: 10.1016/j.cellsig.2014.07.035
27. Carmody RJ, Chen YH. Nuclear factor-kappaB: activation and regulation during toll-like receptor signaling. *Cell Mol Immunol*. (2007) 4:31–41.
28. Andreakos E, Sacre S, Foxwell BM, Feldmann M. The toll-like receptor-nuclear factor kappaB pathway in rheumatoid arthritis. *Front Biosci*. (2005) 10:2478–88. doi: 10.2741/1712
29. Miao CG, Yang YY, He X, Li XF, Huang C, Huang Y, et al. Wnt signaling pathway in rheumatoid arthritis, with special emphasis on the different roles in synovial inflammation and bone remodeling. *Cell Signal*. (2013) 25:2069–78. doi: 10.1016/j.cellsig.2013.04.002
30. Sujitha S, Rasool M. MicroRNAs and bioactive compounds on TLR/MAPK signaling in rheumatoid arthritis. *Clin Chim Acta*. (2017) 473:106–15. doi: 10.1016/j.cca.2017.08.021
31. Wang Y, Zheng F, Gao G, Yan S, Zhang L, Wang L, et al. MiR-548a-3p regulates inflammatory response via TLR4/NF-kappaB signaling pathway in rheumatoid arthritis. *J Cell Biochem*. (2018) 120:1133–40. doi: 10.1002/jcb.26659
32. Xu D, Yan S, Wang H, Gu B, Sun K, Yang X, et al. IL-29 Enhances LPS/TLR4-mediated inflammation in rheumatoid arthritis. *Cell Physiol Biochem*. (2015) 37:27–34. doi: 10.1159/000430330
33. Saber T, Veale DJ, Balogh E, McCormick J, NicAnUltaigh S, Connolly M, et al. Toll-like receptor 2 induced angiogenesis and invasion is mediated through the Tie2 signalling pathway in rheumatoid arthritis. *PLoS ONE*. (2011) 6:e23540. doi: 10.1371/journal.pone.0023540
34. McGarry T, Veale DJ, Gao W, Orr C, Fearon U, Connolly M. Toll-like receptor 2 (TLR2) induces migration and invasive mechanisms in rheumatoid arthritis. *Arthritis Res Ther*. (2015) 17:153. doi: 10.1186/s13075-015-0664-8
35. Mathy NW, Chen XM. Long non-coding RNAs (lncRNAs) and their transcriptional control of inflammatory responses. *J Biol Chem*. (2017) 292:12375–82. doi: 10.1074/jbc.R116.760884
36. Wang S, Li X, Zhao RC. Transcriptome analysis of long noncoding RNAs in toll-like receptor 3-activated mesenchymal stem cells. *Stem Cells Int*. (2016) 2016:6205485. doi: 10.1155/2016/6205485
37. Yu L, Qu H, Yu Y, Li W, Zhao Y, Qiu G. LncRNA-PCAT1 targeting miR-145-5p promotes TLR4-associated osteogenic differentiation of adipose-derived stem cells. *J Cell Mol Med*. (2018) 22:6134–47. doi: 10.1111/jcmm.13892
38. Fan H, Lv Z, Gan L, Ning C, Li Z, Yang M, et al. A novel lncRNA regulates the toll-like receptor signaling pathway and related immune function by stabilizing FOS mRNA as a competitive endogenous RNA. *Front Immunol*. (2019) 10:838. doi: 10.3389/fimmu.2019.00838
39. Ji TT, Wang YK, Zhu YC, Gao CP, Li XY, Li J, et al. Long noncoding RNA Gm6135 functions as a competitive endogenous RNA to regulate toll-like receptor 4 expression by sponging miR-203–3p in diabetic nephropathy. *J Cell Physiol*. (2019) 234:6633–41. doi: 10.1002/jcp.27412
40. Li Z, Li X, Du X, Zhang H, Wu Z, Ren K, et al. The interaction between lncRNA SNHG1 and miR-140 in regulating growth and tumorigenesis via TLR4/NF-kappaB pathway in cholangiocarcinoma. *Oncol Res*. (2019) 27:663–72. doi: 10.3727/096504018X15420741307616
41. Wei M, Li L, Zhang Y, Zhang ZJ, Liu HL, Bao HG. LncRNA X inactive specific transcript contributes to neuropathic pain development by sponging miR-154-5p via inducing toll-like receptor 5 in CCI rat models. *J Cell Biochem*. (2018) 120:1271–81. doi: 10.1002/jcb.27088
42. Siebert S, Tsoukas A, Robertson J, McInnes I. Cytokines as therapeutic targets in rheumatoid arthritis and other inflammatory diseases. *Pharmacol Rev*. (2015) 67:280–309. doi: 10.1124/pr.114.009639

43. Thompson C, Davies R, Choy E. Anti cytokine therapy in chronic inflammatory arthritis. *Cytokine*. (2016) 86:92–9. doi: 10.1016/j.cyto.2016.07.015
44. Cai L, Chen WN, Li R, Hu CM, Lei C, Li CM. Therapeutic effect of acetazolamide, an aquaporin 1 inhibitor, on adjuvant-induced arthritis in rats by inhibiting NF-kappaB signal pathway. *Immunopharmacol Immunotoxicol*. (2018) 40:117–25. doi: 10.1080/08923973.2017.1417998
45. Xia ZB, Meng FR, Fang YX, Wu X, Zhang CW, Liu Y, et al. Inhibition of NF-kappaB signaling pathway induces apoptosis and suppresses proliferation and angiogenesis of human fibroblast-like synovial cells in rheumatoid arthritis. *Medicine*. (2018) 97:e10920. doi: 10.1097/MD.0000000000010920

Conflict of Interest Statement: The authors declare that the research was conducted in the absence of any commercial or financial relationships that could be construed as a potential conflict of interest.

Advantages of publishing in Frontiers

OPEN ACCESS
Articles are free to read for greatest visibility and readership

FAST PUBLICATION
Around 90 days from submission to decision

HIGH QUALITY PEER-REVIEW
Rigorous, collaborative, and constructive peer-review

TRANSPARENT PEER-REVIEW
Editors and reviewers acknowledged by name on published articles

Frontiers
Avenue du Tribunal-Fédéral 34
1005 Lausanne | Switzerland

Visit us: www.frontiersin.org
Contact us: info@frontiersin.org | +41 21 510 17 00

REPRODUCIBILITY OF RESEARCH
Support open data and methods to enhance research reproducibility

DIGITAL PUBLISHING
Articles designed for optimal readership across devices

FOLLOW US
@frontiersin

IMPACT METRICS
Advanced article metrics track visibility across digital media

EXTENSIVE PROMOTION
Marketing and promotion of impactful research

LOOP RESEARCH NETWORK
Our network increases your article's readership